

Antileishmanial and antitrypanosomal compounds from *Achillea fragrantissima*



Dissertation zur Erlangung des
naturwissenschaftlichen Doktorgrades der Julius-
Maximilians-Universität Würzburg

vorgelegt von

Joseph Skaf

aus Homs

Würzburg 2018

Eingereicht bei der Fakultät für Chemie und Pharmazie am

Gutachter der schriftlichen Arbeit

1. Gutachter: _____

2. Gutachter: _____

Prüfer des öffentlichen Promotionskolloquiums

1. Prüfer: _____

2. Prüfer: _____

3. Prüfer: _____

Datum des öffentlichen Promotionskolloquiums

Doktorurkunde ausgehändigt am

Die vorliegende Dissertation wurde von Dezember 2013 bis September 2017 am
Institut für Pharmazie und Lebensmittelchemie der Universität Würzburg unter
Anleitung von

Frau Prof. Dr. Ulrike Holzgrabe

angefertigt.

Ihr möchte ich besonders für die freundliche Aufnahme in Ihren Arbeitskreis und
Ihre Unterstützung und Hilfe in jeder Phase der Erstellung dieser Dissertation
danken.

Danksagung

Ich möchte den folgenden Kooperationspartnern für die Unterstützung und Zusammenarbeit danken: Prof. Dr. Omar Hamarsheh, Yesid Ramirez, Prof. Dr. August Stich, Antje Fuss, Prof. Dr. Petra Högger, Dr. Tobias A. Ölschläger und Srikanth Balasubramanian.

Als nächstes danke ich Prof. Dr. Christoph Sotriffer und den Assistenten im ersten Semester für die gemeinsame Zeit bei der Betreuung der Studenten im Labor für anorganische Chemie.

Außerdem möchte ich meinem gesamten Arbeitskreis für die angenehme Arbeitsatmosphäre und Hilfsbereitschaft danken: Dr. Johannes Wiest, Daniela, Huma, Dr. Ludwig Höllein, Dr. Jens Schmidt, Dr. Amal yassin, Nora, Liana, Paul, Dr. Regina Messerer, Dr. Anna Lehmann, Dr. Florian Seufert, Flo, Antonio, Patrick, Nicolas, Markus, Christine H., Nic, Nina, Jonas U., Jonas W., Christine E., Christiane, Alex, Ruben, Klaus, Anja, Frau Möhler und Frau Ebner.

Weiterhin bedanke ich mich für die finanzielle Unterstützung der Paul + Maria Kremer-Stiftung sowie des Deutschen Akademischen Austauschdiensts (DAAD).

Meiner Frau Nairmeen und meinem Sohn Michael danke ich für ihre Liebe und ihren Rückhalt.

Meiner Familie

Table of Contents

1. Introduction	1
1.1 <i>Trypanosomiasis – African sleeping sickness.....</i>	4
1.1.1 Historical background.....	4
1.1.2 Course of infection and pathology	5
1.1.3 Life cycle and transmission of <i>Trypanosoma brucei</i>	6
1.1.4 Diagnosis and treatment.....	7
1.2 <i>Leishmaniasis.....</i>	8
1.2.1 Historical background.....	8
1.2.2 Course of infection and pathology	9
1.2.3 Life cycle and transmission.....	10
1.2.4 Diagnosis and treatment.....	11
1.3 <i>The genus Achillea</i>	14
1.4 <i>Achillea fragrantissima.....</i>	16
1.5 <i>References:</i>	18
2. Aim of the work	23
3. Results and discussion	24
3.1 <i>Bio-assay fractionation</i>	25
3.2 <i>Identification of isolated compounds.....</i>	26
3.2.1 Identification of isolated sesquiterpene lactones	26
3.2.2 Identification of isolated Flavonoids.....	29
3.2.3 Identification of isolated alkamides	31
3.3 <i>Bio-evaluation of the isolated compounds</i>	38
3.4 <i>Study of structure-activity relationship (SAR) of alkamides</i>	40
3.5 <i>Synthesis and bio-evaluation of compounds 41 and 42.....</i>	46
3.6 <i>Physicochemical properties of compounds 26 and 27 by means of Sirius T3. 49</i>	
3.6.1 Determination of pKa values of compounds 26 and 27.	49

CONTENTS

3.6.2 Determination of log P values for compounds 26 and 27.....	50
3.6.3 Determination of kinetic and intrinsic solubility of compounds 26 and 27. 50	
3.7 <i>References</i>	52
4. Side project	58
4.1 <i>References</i>	63
5. Summary	64
6. Zusammenfassung	67
7. Experimental	70
7.1 <i>General</i>	70
7.2 <i>Preliminary investigations</i>	71
7.3 <i>Plant material</i>	72
7.4 <i>Extraction and Isolation</i>	72
7.5 <i>Characterization of plant isolated compounds</i>	74
7.6 <i>Biological assays</i>	83
7.6.1 <i>Anti-trypanosomal assay</i>	83
7.6.2 <i>Cytotoxicity assay</i>	84
7.6.3 <i>In vivo toxicity assay (Galleria mellonella larvae)</i>	84
7.7 <i>Synthesis and characterization of compounds 14- 40</i>	85
7.7.1 <i>General procedure A for synthesis of compounds 14 –19 and 22- 40</i> .85	
7.7.2 <i>General procedure B for synthesis of compounds 20 and 21.</i>	85
7.7.3 <i>Purification of synthesized compounds 14 - 40</i>	86
7.8 <i>Synthesis and characterization of compounds 41 and 42.</i>	105
7.9 <i>Synthesis and characterization of the compounds of the side project.</i> ..	109
7.10 <i>References</i>	113
8. Appendix: NMR Spectral data of all compounds included in this thesis.	
114	

List of figures

Fig. 1 Artemisinin	2
Fig. 2 Life cycle of African trypanosomiasis (Public domain, CDC).	6
Fig. 3 Structures of available antitrypanosomal drugs.	8
Fig. 4 Life cycle of Leishmanian parasite (Public domain, CDC).	11
Fig. 5 Structures of some important antileishmanial drugs.	13
Fig. 6 Structures of some characteristic substituents from genus <i>Achillea</i>	15
Fig. 7 <i>Achillea fragrantissima</i> cultivated in the Botanical garden, University of Würzburg. Photo: Author.	16
Fig. 8 Sesquiterpene lactones and flavonoids from <i>A. fragrantissima</i>	17
Fig. 9 Chemical structure of isolated chrysosplenol D.	24
Fig. 10 Preparation and bio-evaluation of extracts from <i>A. fragrantissima</i>	25
Fig. 11 Bioassay-guided fractionation of the DCM extract of <i>A. fragrantissima</i> . .	26
Fig. 12 Chemical structures of isolated sesquiterpene lactones.	29
Fig. 13 Chemical structures of isolated flavonoids.	30
Fig. 14 Chemical structures of isolated alkamides.	33
Fig. 15 Structure, ¹ H- ¹ H COSY and HMBC correlations for 13	34
Fig. 16 ¹ H Spectrum of compound 13	35
Fig. 17 ¹ H- ¹ H COSY Spectrum of compound 13	36
Fig. 18 HMBC Spectrum of compound 13	37
Fig. 19 Modified regions in Pellitorine 10 for SAR study.	40
Fig. 20 Survival rates of the larvae for compound 26 and 27.	45
Fig. 21 Structure of phenoxyethylbenzamide hit compound 1	46
Fig. 22 Structure of compound 42	46
Fig. 23 ESI-MS data of ring-opened lactone M1-GSH-Adduct.	60
Fig. 24 Structure of M1-GSH-adduct.	60
Fig. 25 ¹ H NMR spectrum of M1-GSH-adduct in D ₂ O.	61
Fig. 26 Overlay of ¹ H NMR spectra of M1-GSH-adduct, M1 and glutathione in D ₂ O.	61
Fig. 27 ¹ H ¹ H-COSY of M1-GSH-adduct in D ₂ O.	62
Fig. 28 Fractionation of dichloromethane extract of <i>A. fragrantissima</i> by means of flash chromatography.	72

List of tables

Table 1 Bio-evaluation of isolated compounds38
Table 2 Anti-trypanosomal activity, cytotoxicity, and selectivity indices of
compounds **14- 40**.....41
Table 3 Physicochemical properties of compounds 26 and 27.51

1. Introduction

Neglected tropical diseases (NTDs), such as leishmaniasis, sleeping sickness as well as Chagas disease and malaria, which are caused by diversity of unicellular eukaryotic parasitic pathogens, are a major global health problem [1] affecting and threatening more than one billion people worldwide [2], especially in low-income populations in developing regions of Africa, India and South America. It costs the developing economies billions of dollars yearly [3]. Although these infections threaten considerable number of world population, only few medicines characterized by poor efficacy and serious adverse effects are currently available. In addition, resistance has been already reported to increase. Hence, there is urgent need to substitute the old medications with new effective ones [4-5].

Nature is a rich source of drugs which are active towards many microorganisms [6]. One of the most prominent antibiotics from nature is penicillin isolated from *Penicillium notatum* in the late 1920ies and active against a broad variety of gram-positive and gram-negative bacteria. Its invention was the starting point of the search for antibiotics in fungi, plants and many other sources providing most of the antibiotic classes currently available for the treatment of infections [7]. However, scientists throughout the world are still looking for new antibiotics from nature, as can be read in the comprehensive review by Saleem [8]. Even though, a countless number of natural products with activity towards various microorganisms are reported each year, almost all of them do not find their way into *in vivo* studies and finally into preclinical development [8].

Discovering new antiprotozoal lead structures is nowadays achieved by either high-throughput screening (HTS) of large libraries of available natural or chemically synthesized compounds, or by bioassay-guided fractionation of natural extracts [4]. A lead structure can be defined as a biologically active compound responsible for deriving a series of compounds by chemical modifications in order to achieve optimal therapeutic activity and toxicity [9]. In the last decades plant and microbial extracts have been widely considered as prominent resources of antiparasitic compounds or lead structures [10].

INTRODUCTION

Artemisinin (Nobel Prize Award 2015) (Fig. 1), a sesquiterpene lactone from *Artemisia annua*, quinine from the bark of the cinchona tree, are examples of antimalarial natural products [4, 11]. Avermectins, macrocyclic lactone derivatives, fermentation products by *Streptomyces avermitilis*, are a series of natural drugs with potent anthelmintic and insecticidal properties [12].

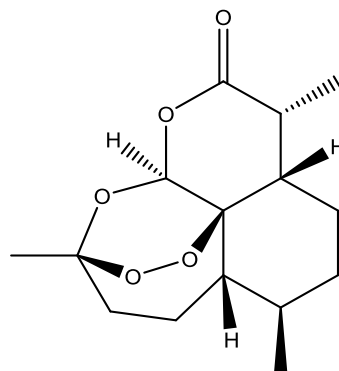


Fig. 1 Artemisinin

Plant-derived compounds have a long history of clinical use, better patient tolerance and acceptance. To date, 35,000-70,000 plant species have been screened for their medicinal use [6].

The candidate plants for investigation have been usually selected on the basis of information about their known usage in traditional medicine. On the one hand this approach helps in suggesting the supposed targeted biological activities and on the other hand, the active compounds isolated from such plants are supposed to be safer as the ones isolated from plant species with unknown medicinal applications [10].

After isolation and characterization of the natural active compounds, many challenges related to unique chemical features of the natural products face usually the medicinal chemists, as they start synthesizing a library, in order to improve the efficacy, reduce the toxicity, improve the chemical and physical properties such as solubility and lipophilicity and the pharmacokinetic properties such as absorption, distribution, and bioavailability [10-11].

The unique chemical features are usually represented with higher number of chiral centers as well as increased steric complexity, in addition to higher number of oxygen atoms such as in sesquiterpene lactones and flavonoids [10]. Moreover, a lot of natural products suffer from chemically reactive groups which are able to covalently bind especially to SH groups of cysteine residues of proteins and/or glutathione, resulting in non-selectivity because cysteins are ubiquitous. Michael systems, such as enones and catechols, which are easily oxidized to ortho-quinones, again being enones, are prone to such reactions and

INTRODUCTION

can be found e.g. in the structures of sesquiterpene lactones, flavonoids, alkalamides, iridoides, coumarines, quinones, and xanthonones [4]. Such compounds are not drug-like due to their unselective affinity to many targets and to their toxicity. This problem has recently been addressed by Baell et al. [13] and it is the central point of the PAINS concept [4].

An impressive example of optimization of natural compounds has been reported by the Holzgrabe group, who has found antileishmanial activity in the extract from *Valeriana walichii* [5]. Applying bioassay-guided fractionation resulted in the isolation of the highly active caffeic acid ester of borneol. For improvement of activity and decrease of toxicity, a medium sized library of caffeic acid ester analogues was synthesized, which resulted in an antileishmanial compounds active towards *L. major* promastigotes and amastigotes as well as *L. donovani* promastigotes and did not exhibit toxicity because the reactive moieties of the originally isolated compound were eliminated [14]. Consequently, the most active compounds were tested in both an *L. major* and *L. donovani* mouse model and showed very good *in vivo* activity [15].

1.1 Trypanosomiasis – African sleeping sickness

1.1.1 Historical background

In the middle ages, only a few written reports proof the occurrence of trypanosomiasis in Africa. One of these first historical records was by the Arabian geographer Abu Abdallah Yaqut (1179–1229), who talked about a village in the “Country of Gold” (Wangara, west Africa), whose “inhabitants and even their dogs were just skin and bones and asleep”. The Arabian historian Ibn Khaldun (1332–1406) reported the death of Sultan Mari Jata, emperor of Mali, from an illness corresponding to human trypanomiasis [16].

Sleeping sickness first records in the early modern times came from ship doctors and medical officers who worked for slave-trade companies. The disease caused increased losses prompting ship owners and slave traders to press doctors to find a remedy. The first accurate medical report of sleeping sickness was published in 1734 by the English naval surgeon John Aktins who described only the neurological symptoms in the late stage of the disease. Thomas Winterbottom, the English physician, published in 1803 a report describing the swollen lymph nodes along the back of the neck in the early stage of the sickness.[16] Trypanosoma were discovered for the first time in 1841 in trout blood by Valentine, and then in 1842 by Remark in pike fish as well as in many other fresh water fishes [17]. In 1852, the Scottish explorer David Livingstone reported that the disease is caused by the bite of Tsetse fly. In 1895, the Scottish pathologist and microbiologist David Bruce discovered *T. brucei* being the cause of cattle trypanosomiasis. However, the first observation of trypanosomes in human blood was achieved by the British Colonial surgeon Robert Michael Forde in 1901 when he examined a steamboat captain in The Gambia. He thought that these organisms are worms. Few months later in 1902 the English physician Joseph Everett Dutton could identify them as Trypanosomes and he proposed the name *Trypanosoma gambiense*. The second human pathogenic trypanosome species, *T. rhodesiense* was discovered in 1910 by the parasitologists John William Watson Stephens and Harold Benjamin Fantham [16].

The World Health Organization (WHO) reported three major *T.b.* epidemics, the first was between 1896 and 1906, the second in the 1920s and the third in the 1970s [18-19]. The WHO report of January 2017 estimates the number of actual cases to be below 20,000 with a further 65 million people at risk of infection [3].

1.1.2 Course of infection and pathology

Many *Trypanosoma* species are known; some of them can affect humans and cause fatal infections if left not treated [20].

Trypanosoma brucei gambiense is transmitted to humans by Tsetse fly (*Glossina palpalis*), distributed in West Africa, and is responsible for chronic human African trypanosomiasis (HAT) or sleeping sickness.

Trypanosoma brucei rhodensiense, is transmitted to humans by *Glossina morsitans*, which is widely distributed in Eastern African countries, and it causes acute sleeping sickness [20-21].

Trypanosoma cruzi is zoonotic parasite mainly transmitted to humans by the bite of *Rhodnius prolixus* and could also be transmitted to human through contaminated blood transfusion to cause American trypanosomiasis or Chagas disease, found in South and Central America [22-23].

Trypanosoma can also infect animals e.g. *s trypanosoma vivax* which can infect cattle [24] and *Trypanosoma equiperdum* which infects mainly horses [25].

The course of infection is characterized by two stages of illness. The first stage, called hemolymphatic stage lasts 1 to 3 weeks and is characterized by a peripheral extracellular infection associated with non-specific clinical symptoms, such as fever, headaches and joint pains. Progression into the second-stage occurs after a mean of 300–500 days in *gambiense* HAT, while in *rhodesiense* HAT brain invasion is estimated to take place after 3 weeks to 2 months of infection [18]. During the second stage of infection the trypanosomes could pass through the blood-brain barrier (BBB) into the central nervous system causing

severe symptoms including mental impairment, fever, headache and chronic encephalopathy. This is followed by somnolence and death if left untreated [26-27].

1.1.3 Life cycle and transmission of *Trypanosoma brucei*

As can be seen in Fig. 2, the infection in mammalian host starts by the injection of metacyclic trypomastigotes into mammalian bloodstream by tsetse fly bite. The injected metacyclic trypomastigotes transform consequently into bloodstream trypomastigotes, which start to multiply by binary fission and are transferred via lymphatic system to invade various body fluids [28]. The tsetse fly becomes infected as it ingests the bloodstream trypomastigotes during a blood meal on an infected mammalian host. In 3 to 5 weeks the parasite multiplies in the digestive system of the fly and undergoes morphological changes, followed by migration into the fly’s salivary glands, where it transforms to epimastigotes and then eventually to infective metacyclic trypomastigotes [28].

Sleeping Sickness, African (African trypanosomiasis)
(Trypanosoma brucei gambiense)
(Trypanosoma brucei rhodesiense)

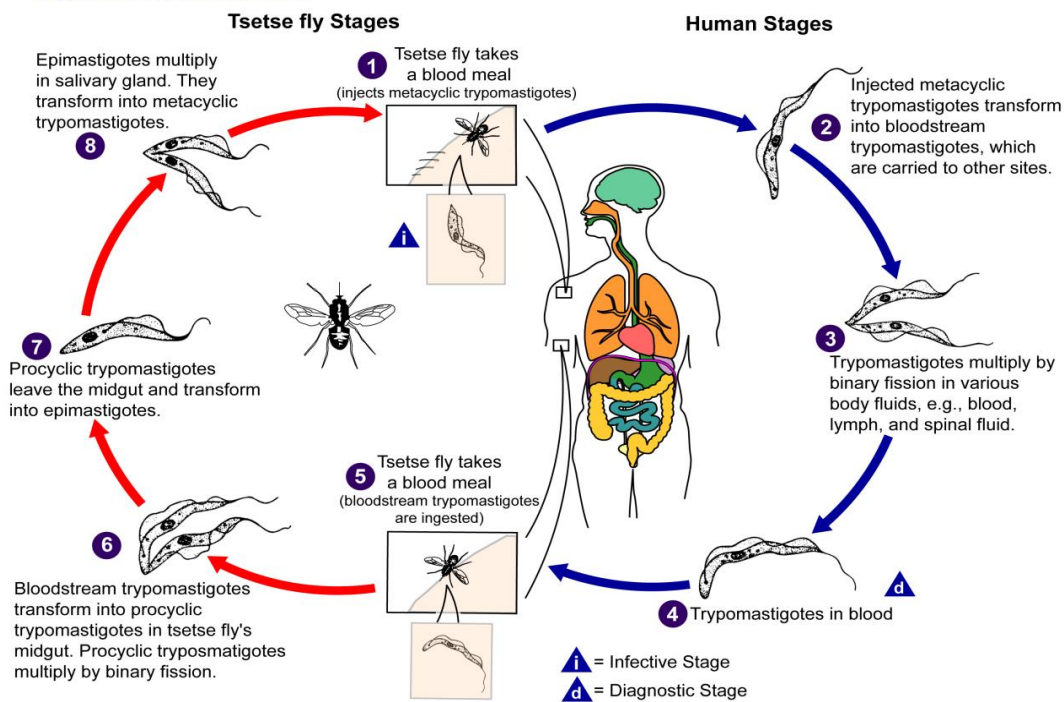


Fig. 2 Life cycle of African trypanosomiasis (Public domain, CDC).

1.1.4 Diagnosis and treatment

Early diagnosis of the infection is difficult, because of the lack in the specific clinical symptoms, especially in the first stage of the disease and the lack of sensitivity of the parasitological methods available [3]. Diagnosis of trypanosomiasis is usually done by microscopic detection of the parasite in the blood, lymph, cerebrospinal fluid (CSF) or any other body fluid. Only the presence or the absence of the parasite in the CSF can determine the stage of the disease, which is crucial for selection of the appropriate treatment [28].

Currently available treatments of trypanosomiasis (Fig. 3) depend on both the subspecies of the parasite and the stage of infection. During the first stage, pentamidine is the drug of choice to treat *T.b. gambiense*, while suramine is used against *T.b. rhodesiense*. Both medicines are not able to cross the BBB; therefore, they are ineffective in the second stage of the disease. In addition, they are associated with significant side effects such as gastrointestinal discomfort, pancreatitis, nephro- and hepatotoxicity [26, 29].

In the late stage of the infection, three therapeutic options are available. Firstly, melarsoprol, an organo-arsenic compound, is effective against both subspecies. It has, however, many undesirable side effects and can lead to fatal encephalopathic syndromes (3% to 10%) [18, 26]. Eflornithine is a second therapeutic option, which possesses less toxicity than melarsoprol. Unfortunately, it is only effective against *T.b. gambiense*. Both medications are administered intravenously, which is a problem in developing countries without a suitable health care system. Nowadays, the WHO recommends using the NECT, nifurtimox and eflornithine combination therapy, because it simplifies the treatment regime of eflornithine by reducing the treatment period and the number of daily doses. However, this combination is not effective against *T.b. rhodesiense* [26, 29].

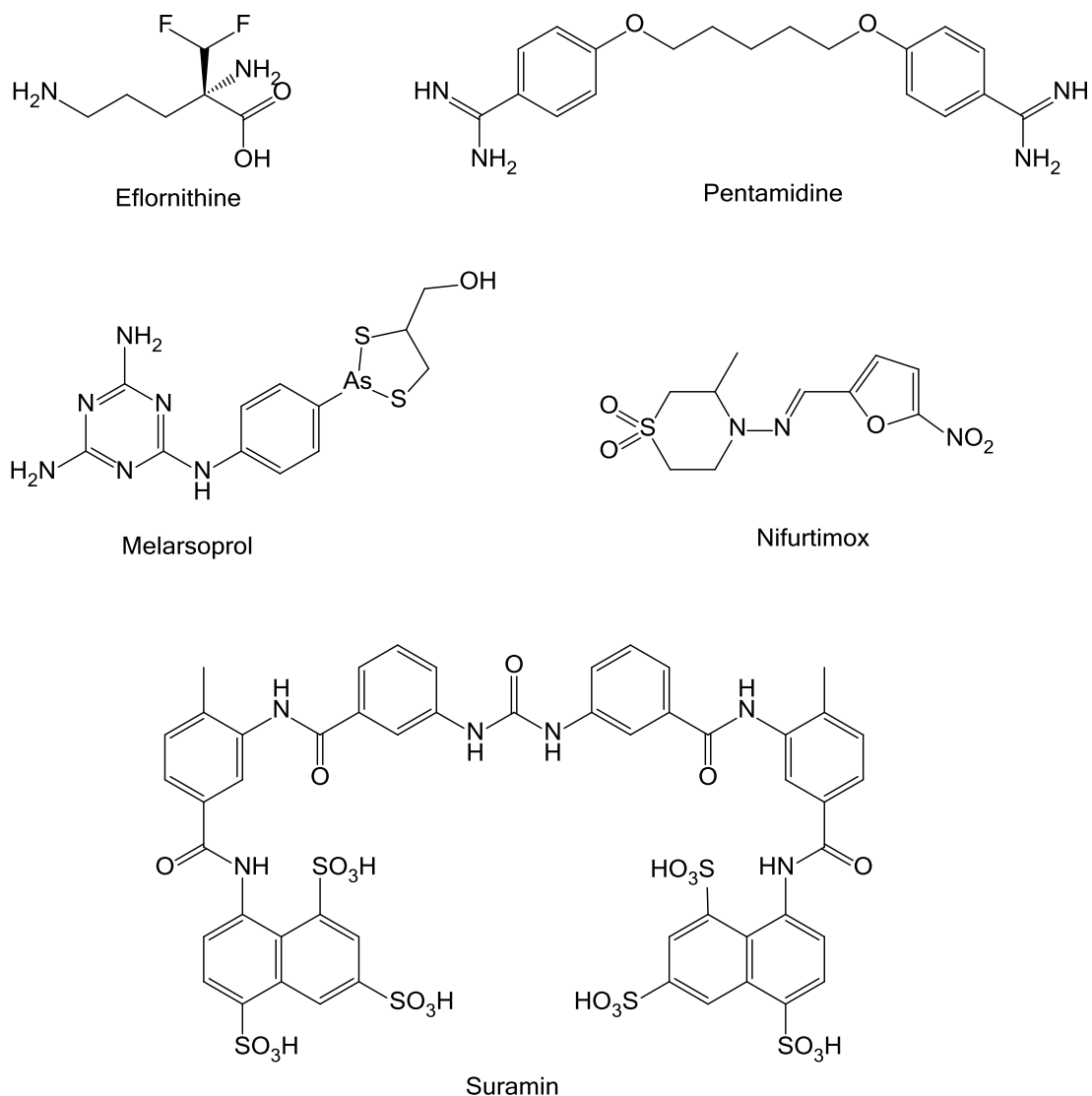


Fig. 3 Structures of available antitrypanosomal drugs.

1.2 Leishmaniasis

1.2.1 Historical background

Historically, leishmaniasis was reported for the first time in the 19th century as a disease which causes unexplained fever. Later in 1903 the explorer Marc Leishman observed unknown bodies in the spleen of a dead British soldier and incorrectly explained it as degenerated trypanosomes, while the identification of the pathogen of visceral leishmaniasis was achieved by the Irish medical officer

Charles Donovan, who had also reported unknown bodies in the spleen of the patients combined with similar symptoms. The Indian species of *Leishmania*, causing visceral Leishmaniasis, was called *L. donovani* to his honors [30]. Currently, 29 species of genus *Leishmania* are identified and classified depending on genetic and biochemical characterizations. Leishmaniasis is nowadays endemic in all continents except Antarctica and Oceania and is regarded as the third-most-common parasitic disease after schistosomiasis and malaria [31]. The WHO estimates, in its update of April 2017, 700 000 to 1 million new cases causing 20 000 to 30 000 deaths to be occurred annually [32].

1.2.2 Course of infection and pathology

Leishmaniasis is transmitted by the bite of an infected female sand-fly, belonging to the genera *Phlebotomus*. The disease is differentiated into three clinical syndromes: visceral leishmaniasis (VL, also known as kala-azar); cutaneous leishmaniasis (CL); and mucocutaneous leishmaniasis (MCL). The most common form of the disease is CL, while VL is the lethal form of the disease [33].

Visceral leishmaniasis, also called *Kala-Azar* or black disease, is caused by *L. donovani* and *L. infantum*. The disease is widely distributed in Asia, along the Mediterranean coast, and in Africa and South America and it infects between 0.2 and 0.4 million people annually. *L. donovani* targets people in all ages, whereas *L. infantum* targets mainly children up to 3 years of age [31]. The disease is fatal if not treated and characterized with protracted fever, severe weight loss, hepatomegaly, splenomegaly, anemia and possible dark colored skin [34]. The progression of the disease is slow and the symptoms can appear within weeks to years after the initial infection [31]. A possible late complication of VL is Post-kala-azar dermal leishmaniasis (PKDL), which manifests as a skin rash on the face, trunk and limbs [35].

Cutaneous leishmaniasis (CL) or Oriental sore [34] is caused mainly by *L. major* and it infects 0.7 – 1.2 million people annually worldwide [10]. The clinical manifestations of CL are one or more indolent skin ulcers which vary in size from

a few millimetres to centimetres in diameter. Healing occurs spontaneously over months/years and leaves usually permanent scars on the skin [36].

The CL form develops in 1-10 % of the cases the MCL form. About 35.000 new cases are yearly reported in areas of Peru, Bolivia and Brazil and it is caused usually by *L. braziliensis*, *L. panamensis* and *L. amazonensis* [31]. MCL is similar to CL but it attacks additionally the respiratory mucosa as well as the soft tissues of the nose and the mouth resulting in progressive destruction of the nasal mucosa, as well as the soft and hard palate, and eventually the nasal septum [34].

1.2.3 Life cycle and transmission

As it can be seen in Fig. 4, the leishmanial protozoan differentiates during its life cycle into two morphological types: an extracellular 15-20 μm long flagellated promastigotes in the sand fly and 3-5 μm long obligate intracellular non-flagellated amastigotes in the mammalian host. During a blood meal promastigotes are injected by an infected sand fly into the mammalian host. The promastigotes are phagocytosed by macrophages and other mononuclear phagocytic cells where they transform into amastigotes. Amastigotes multiply by simple division inside the cells and then disseminate into blood and lymph system to infect other cells after disruption of the host cells. During another blood meal the sand fly ingests infected macrophages. Amastigotes migrate in the midgut and transform into flagellated promastigotes which multiply in the guts of the sand fly to infect eventually another mammalian host [31].

Leishmaniasis

(*Leishmania spp.*)

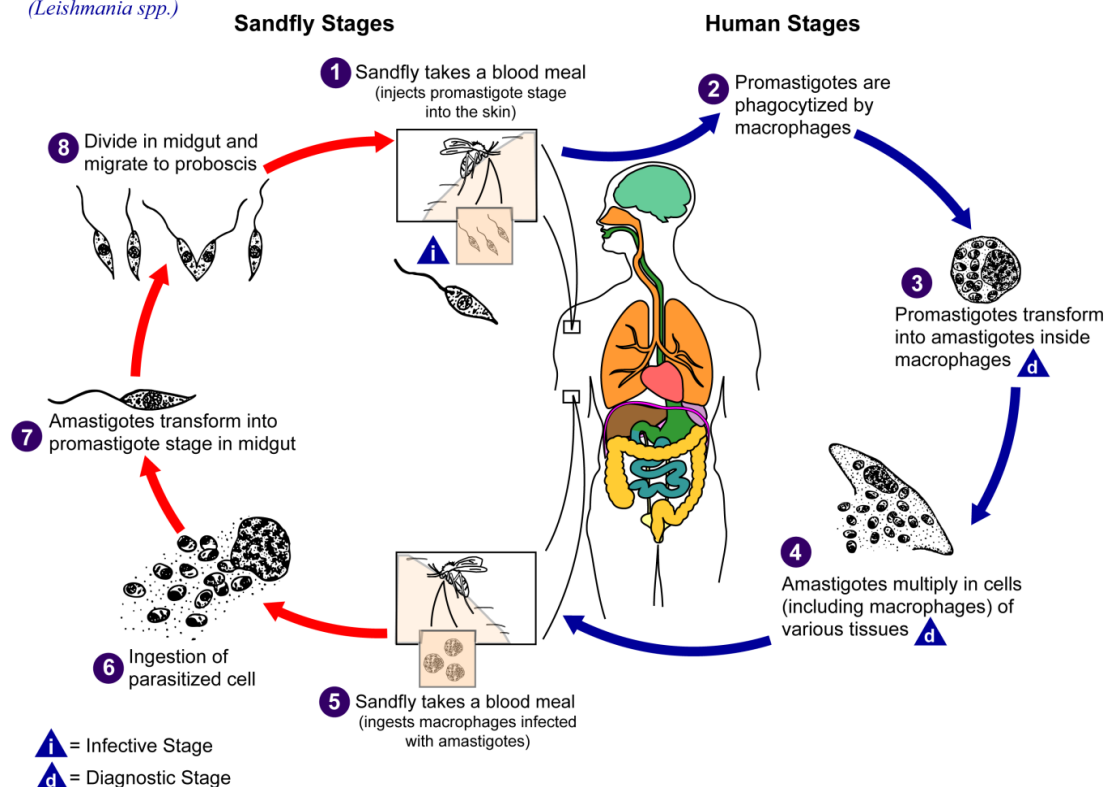


Fig. 4 Life cycle of Leishmanian parasite (Public domain, CDC).

1.2.4 Diagnosis and treatment

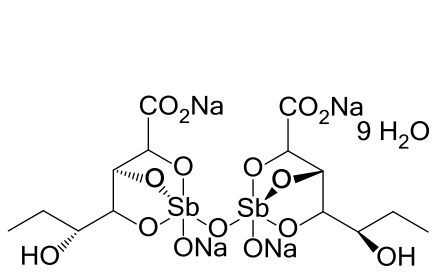
In VL the diagnosis usually performed by combining clinical signs and the parasitological and serological tests. However, examining tissue aspirates from bone marrow, spleen and lymph nodes under microscope can confirm the diagnosis. In the case of CL and MCL, the clinical symptoms beside the parasitological tests can confirm the diagnosis [32].

The treatment of the disease depends on the form of the parasite and the regional factor. As recommended by the WHO the treatment regime must follow the national and regional guidelines to avoid drug resistance [32]. From the 1940s pentavalent antimonials constituted the standard medications for treatment of leishmaniasis, but the potential toxicity and severe side effects (nephrotoxicity and cardiotoxicity) as well as the increasing resistance led to substitute this group with Amphotericin B, a macrolide antibiotic, which is administered intravenously

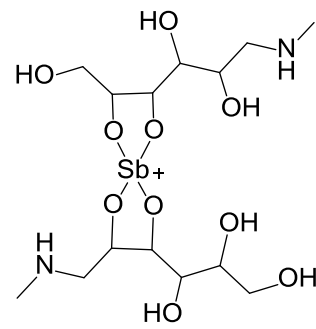
INTRODUCTION

and also shows severe side effects such as nausea, vomiting, rigors, fever, hypertension or hypotension, and hypoxia and toxicity like nephrotoxicity [37]. Moreover, it requires careful and slow intravenous administration [38]. Discovering miltefosine in 1980s was considered as an essential advance in the treatment of all forms of leishmaniasis, as it could be pharmaceutically formulated for oral administration, in addition to its potential efficacy, reduced toxicity and side effects compared to its precursors. Although mild hepatotoxicity and nephrotoxicity as well as teratogenicity were observed, miltefosine is still recommended as the drug of first choice for the treatment of childhood VL [38]. Other medications are also in use such as the lipid formulations of Amphotericin B, which provide better bioavailability of the drug on one side and reduced hospitalization period as well as toxicity [38-39]. The aminoglycoside antibiotic Paromomycine is used topically for CL and IV for VL. Pentamidine, aromatic diamidine, shows high toxicity and reduced efficacy because of increasing resistance. Finally, Sitamquine, an 8-amino-quinoline, is a promising antileishmanial drug that it showed satisfactory efficacy against different species of *Leishmania* [38]. Structures of some important antileishmanial drugs are shown in Fig. 5.

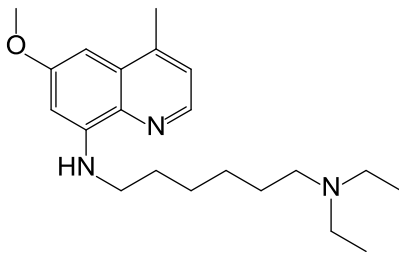
INTRODUCTION



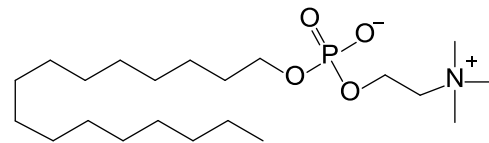
Stibocluconate



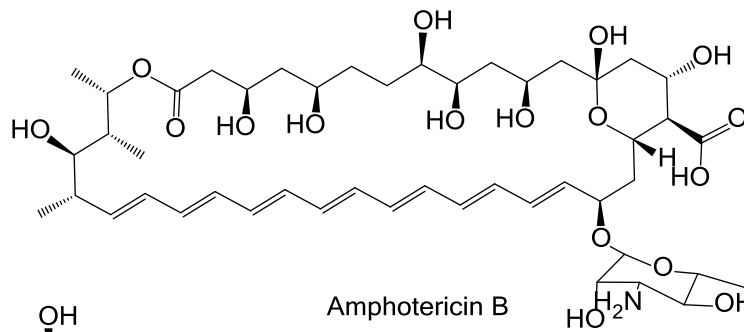
Meglumine antimonate



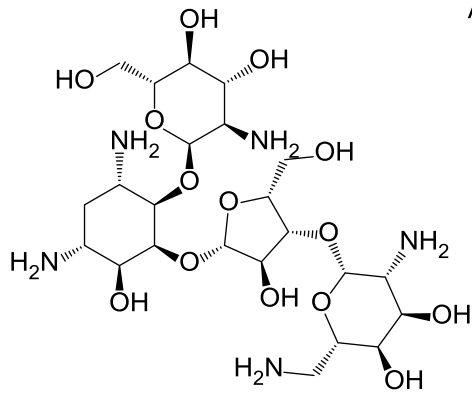
Sitamaquine



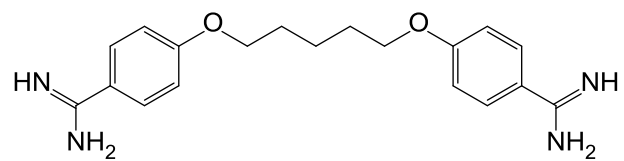
Miltefosine



Amphotericin B



Paromomycine



Pentamidine

Fig. 5 Structures of some important antileishmanial drugs.

1.3 The genus *Achillea*

The genus *Achillea* from the *Asteraceae* family, the largest family of the vascular plants, comprises about 115 different species spread worldwide, especially in North America, Southeast Europe and Southwest Asia [40]. The plants from genus *Achillea* have common morphological properties such as hairy aromatic leaves and flat clusters of small flowers on the top of the stem [41]. The name of *Achillea* is referred to the Achilles in the literary Trojan War of the Iliad who used yarrow (*A. millefolium*) to treat the wounds of the injured soldiers [41].

From phytochemical point of view, the plants belonging to genus *Achillea* are rich with sesquiterpene lactones and flavonoids [42] as well as with fatty and amino acids derivatives and alkaloids [41]. As the species of genus *Achillea* spread throughout the world, they are known to be within the oldest medicinal plants that have traditionally been used for pharmaceutical purposes [43]. The first antispasmodic flavonoids, cynaroside and cosmosiin were isolated from *A. millefolium* as well the first natural proazulene, achillicin was identified from the genus *Achillea* [41]. Some nitrogen containing compounds were also reported to be found in the aerial parts of *Achillea* species including proline, stachydrine, betonicine, betaine and choline [41]. *Achillea* plants are rich with essential oils [44]. Essential oils from genus *Achillea* are reported to possess antimicrobial and antiprotozoal properties. For example, the essential oil from *A. clavennae* exhibited broad antibacterial spectrum against different pathogens such as *Klebsiella pneumoniae* and penicillins-resistant *Streptococcus pneumoniae*. Eucalyptol and camphor are two major components of the essential oils with reported antibacterial activity [45]. Moreover, the essential oil from the leaves and flowers of *A. millefolium* exhibited potential antileishmanial activity [46].

Additionally, crude extracts from genus *Achillea* have been reported to exhibit antibacterial and antiprotozoal properties. The methanolic extract of *A. damascena* (complete plant) possessed activity against variety of microorganisms such as *Staphylococcus aureus*, *Proteus* species, *Shigella dysenteriae*, *Candida albicans*, *Salmonella enteritidis*, and *Streptococcus faecalis* [45].

INTRODUCTION

Furthermore, there are many reports about antiprotozoal activity of extracts from *Achillea* plants. For instance, the dichloromethane extract of the flowering aerial parts of *A. ptarmica* has been reported to possess significant antitrypanosomal activity attributed to its content of alkaloids such as pellitorine [47]. Structures of some characteristic substituents from genus *Achillea* are represented in Fig. 6.

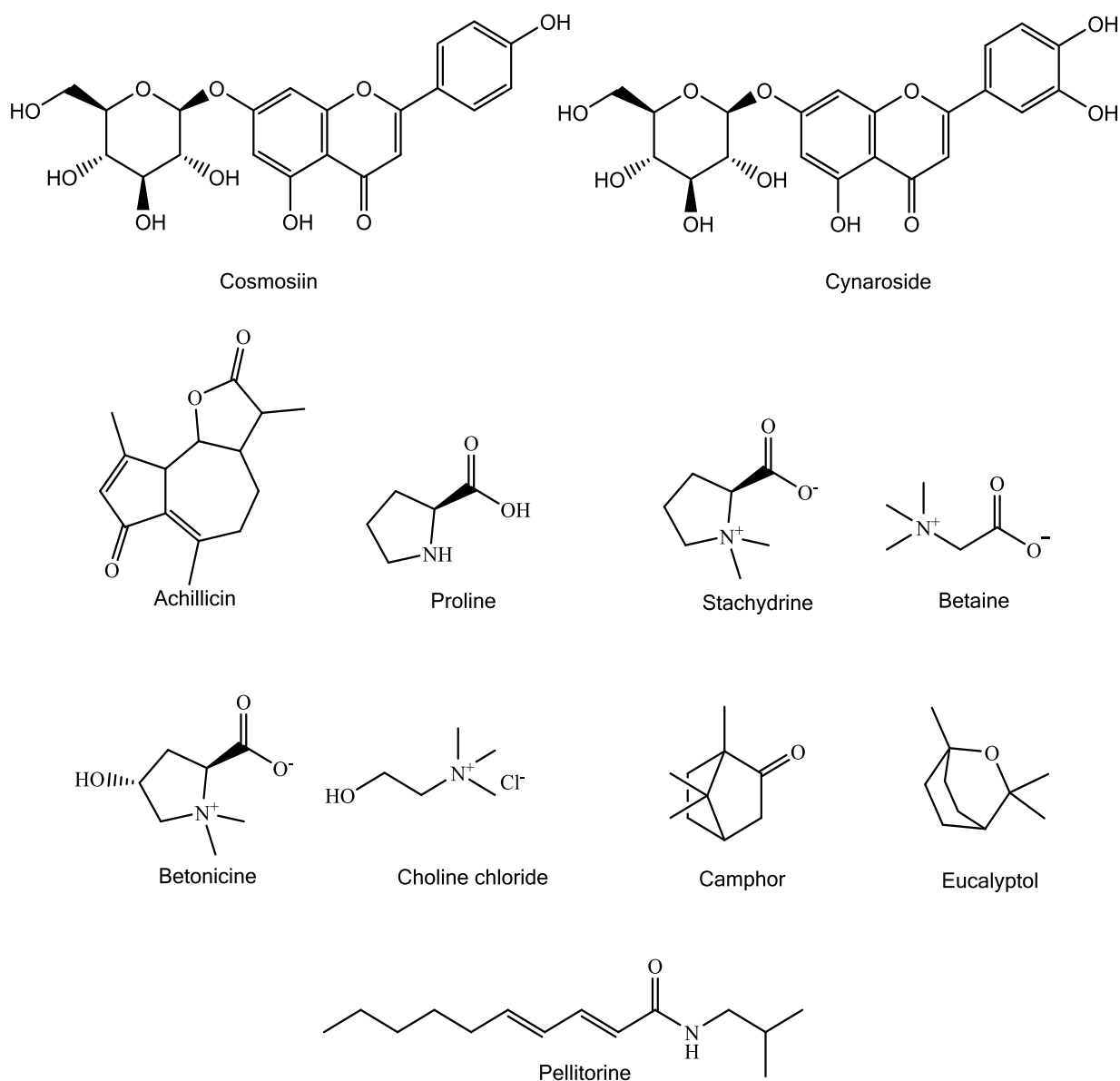


Fig. 6 Structures of some characteristic substituents from genus *Achillea*.

1.4 *Achillea fragrantissima*

Achillea fragrantissima (Fig. 7), Qaysum (Arabic name), is a desert plant and belongs to the genus *Achillea* from the *Asteraceae* family. *A. fragrantissima* is a shrubby white-wooly herb that grows up to one meter in height and it has a pleasant aroma, because of its high content of essential oils [42, 48]. The plant is common in Libya, Egypt, Palestine, Syria, Saudi Arabia, and Iraq [33].

Previous phytochemical studies of *A. fragrantissima* showed that the plant is rich with volatile oils, tannins, monoterpene ketones, fatty acids such as lauric, myristic, palmitic, stearic, linoleic, linolenic, and oleic [42] as well as with sesquiterpene lactones [42] such as Achillolide A and B [48] (Fig. 8). Many flavonoids were also identified from *A. fragrantissima* such as cirsimaritin, chrysosplenol D, cirsiol, and isovitexin [42, 49] (Fig. 8).

Since many years *A. fragrantissima* has been used in traditional medicine in the Middle East region for the treatment of respiratory diseases and gastrointestinal disturbances [50]. Bedouins use the plant for the preparing anti-diuretic drinks for the treatment of stomach ailments and various infections, e.g. of the urinary tract [29, 51]. Moreover, the volatile oil of the flowers is reported to exhibit wide spectrum antimicrobial activity [42]. The flavonoid cirsiol, isolated from *A. fragrantissima*, caused relaxation of contracted rats' smooth muscles, which was explained by inhibition of transmembrane Ca^{2+} influx [33, 42]. A bioassay-guided fractionation of an ethanolic extract of the aerial parts of *A. fragrantissima* led to the isolation of several α -glucosidase inhibitors (Antidiabetic drugs) among them were chrysosplenol D and isovitexin [49]. Additionally, many



Fig. 7 *Achillea fragrantissima* cultivated in the Botanical garden, University of Würzburg. Photo: Author.

INTRODUCTION

other medicinal properties of *A. fragrantissima* were reported such as using it to treat fever, headache and weakness as well as poliomyelitis-1 (POLIO) virus [42]. Furthermore, the leaves of the plant have been reported to show strong cytotoxic activity against two types of melanoma cell lines [33].

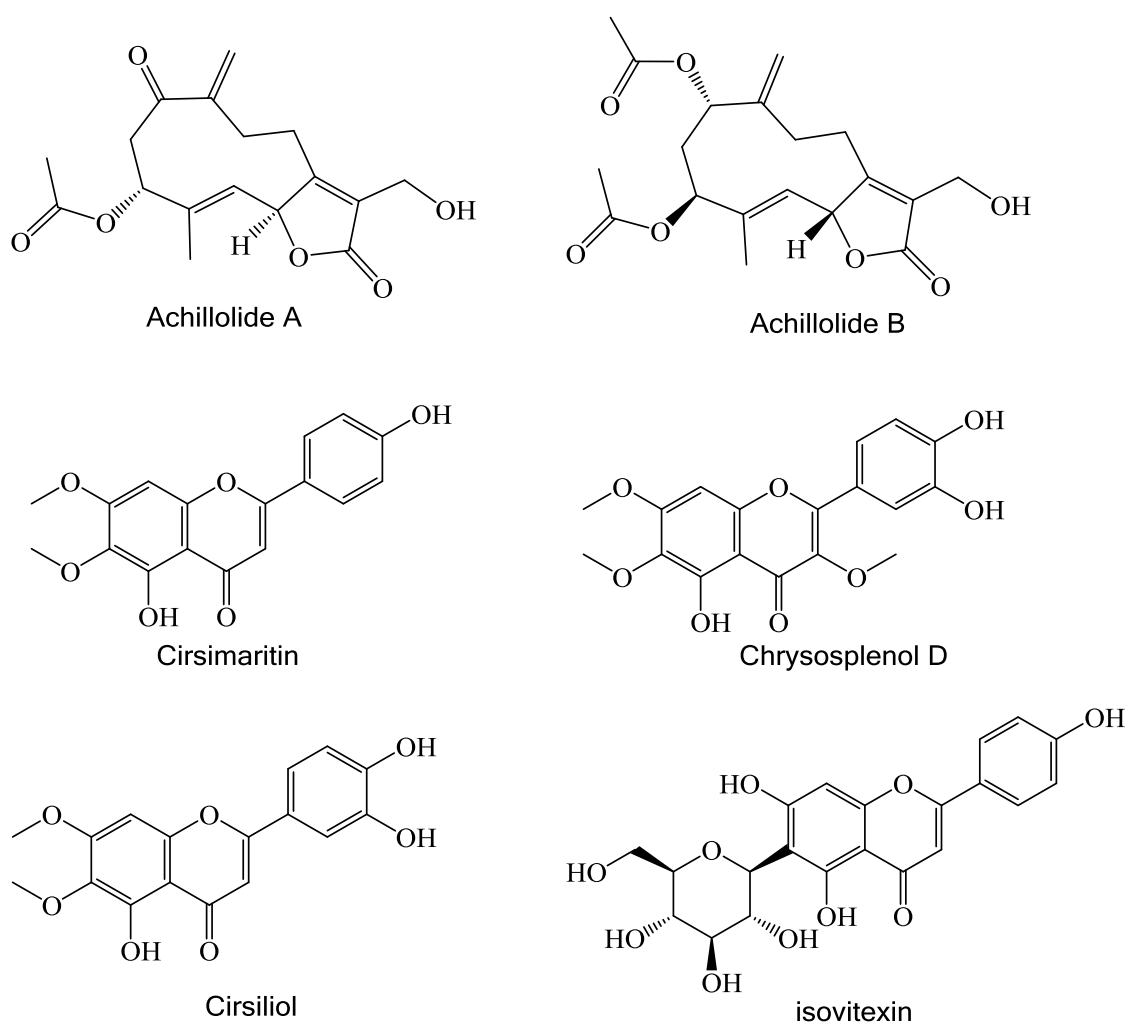


Fig. 8 Sesquiterpene lactones and flavonoids from *A. fragrantissima*.

1.5 References:

1. Acharya, A. S.; Kaur, R.; Goel, A. D., Neglected tropical diseases—Challenges and opportunities in India. *Indian J Med Specialities* **2017**, *8* (3), 102-108.
2. Peeling, R. W.; Boeras, D. I.; Nkengasong, J., Re-imagining the future of diagnosis of Neglected Tropical Diseases. *Comput Struct Biotechnol J* **2017**, *15* (Supplement C), 271-274.
3. World Health Org. Neglected tropical diseases http://www.who.int/neglected_diseases/diseases/en/ (Accessed 10 Oct 2017).
4. Glaser, J.; Holzgrabe, U., Focus on PAINS: false friends in the quest for selective anti-protozoal lead structures from Nature? *MedChemComm* **2016**, *7* (2), 214-223.
5. Ponte-Sucre, A.; Bruhn, H.; Schirmeister, T.; Cecil, A.; Albert, C. R.; Buechold, C.; Tischer, M.; Schlesinger, S.; Goebel, T.; Fuss, A.; Mathein, D.; Merget, B.; Sottriffer, C. A.; Stich, A.; Krohne, G.; Engstler, M.; Bringmann, G.; Holzgrabe, U., Anti-trypanosomal activities and structural chemical properties of selected compound classes. *Parasitol Res* **2015**, *114* (2), 501-12.
6. Veeresham, C., Natural products derived from plants as a source of drugs. *J Adv Pharm Technol Res* **2012**, *3* (4), 200-201.
7. Bennett, J. W.; Chung, K.-T., Alexander Fleming and the discovery of penicillin. In *Adv Appl Microbiol*, Academic Press: 2001; Vol. 49, pp 163-184.
8. Saleem, M., Natural Products as Antimicrobial Agents—an Update. In *Novel Antimicrobial Agents and Strategies*, Wiley-VCH Verlag GmbH & Co. KGaA: 2014; pp 219-294.
9. Sharma, V.; Sharma, P. C.; Kumar, V., A mini review on pyridoacridines: Prospective lead compounds in medicinal chemistry. *J Adv Res* **2015**, *6* (1), 63-71.
10. Katiyar, C.; Gupta, A.; Kanjilal, S.; Katiyar, S., Drug discovery from plant sources: An integrated approach. *Ayu* **2012**, *33* (1), 10-19.
11. Balunas, M. J.; Kinghorn, A. D., Drug discovery from medicinal plants. *Life Sci J* **2005**, *78* (5), 431-441.

12. Yates, D. M.; Portillo, V.; Wolstenholme, A. J., The avermectin receptors of *Haemonchus contortus* and *Caenorhabditis elegans*. *Int J Parasitol* **2003**, *33* (11), 1183-1193.
13. Baell, J.; Walters, M. A., Chemistry: Chemical con artists foil drug discovery. *Nature* **2014**, *513* (7519), 481-3.
14. Glaser, J.; Schultheis, M.; Hazra, S.; Hazra, B.; Moll, H.; Schurigt, U.; Holzgrabe, U., Antileishmanial lead structures from nature: analysis of structure-activity relationships of a compound library derived from caffeic Acid bornyl ester. *Molecules* **2014**, *19* (2), 1394-410.
15. Masic, A.; Valencia Hernandez, A. M.; Hazra, S.; Glaser, J.; Holzgrabe, U.; Hazra, B.; Schurigt, U., Cinnamic Acid Bornyl Ester Derivatives from *Valeriana wallichii* Exhibit Antileishmanial In Vivo Activity in *Leishmania major*-Infected BALB/c Mice. *PLoS One* **2015**, *10* (11), e0142386.
16. Steverding, D., The history of African trypanosomiasis. *Parasites & Vectors* **2008**, *1*, 3.
17. Tobey, E. N., Trypanosomata and trypanosomiasis : (A Summary.). *J Med Res* **1906**, *15* (1), 117-145.
18. World Health Org. Trypanosomiasis, human African sleeping sickness. <http://www.who.int/mediacentre/factsheets/fs259/en/> (Accessed 23. July 2017).
19. Stich, A.; Ponte-Sucre, A.; Holzgrabe, U., Do we need new drugs against human African trypanosomiasis? *Lancet Infect Dis* **2013**, *13* (9), 733-734.
20. Schmidt, I.; Pradel, G.; Sologub, L.; Golzmann, A.; Ngwa, C. J.; Kucharski, A.; Schirmeister, T.; Holzgrabe, U., Bistacrine derivatives as new potent antimalarials. *Bioorg Med Chem* **2016**, *24* (16), 3636-3642.
21. Barrett, M. P.; Burchmore, R. J. S.; Stich, A.; Lazzari, J. O.; Frasch, A. C.; Cazzulo, J. J.; Krishna, S., The trypanosomiases. *The Lancet* **2003**, *362* (9394), 1469-1480.
22. Vianna Martins, A.; Patrícia Gomes, A.; de Mendonça, E. G.; Rangel Fietto, J. L.; Alberto Santana, L.; de Almeida Oliveira, M. G.; Geller, M.; Freitas Santos, R. d.; Roger Vitorino, R.; Siqueira-Batista, R., Biology of *Trypanosoma cruzi*: An update. *Infectio* **2012**, *16* (1), 45-58.

23. Salem, M. M.; Werbovets, K. A., Natural products from plants as drug candidates and lead compounds against leishmaniasis and trypanosomiasis. *Curr Med Chem* **2006**, *13* (21), 2571-98.
24. Garcia, H. A.; Ramírez, O. J.; Rodrigues, C. M. F.; Sánchez, R. G.; Bethencourt, A. M.; Del M. Pérez, G.; Minervino, A. H. H.; Rodrigues, A. C.; Teixeira, M. M. G., Trypanosoma vivax in water buffalo of the Venezuelan Llanos: An unusual outbreak of wasting disease in an endemic area of typically asymptomatic infections. *Vet Parasitol* **2016**, *230* (Supplement C), 49-55.
25. Suganuma, K.; Yamasaki, S.; Molefe, N. I.; Musinguzi, P. S.; Davaasuren, B.; Mossaad, E.; Narantsatsral, S.; Battur, B.; Battsetseg, B.; Inoue, N., The establishment of in vitro culture and drug screening systems for a newly isolated strain of Trypanosoma equiperdum. *Int J Parasitol Drugs Drug Resist* **2017**, *7* (2), 200-205.
26. Sykes, M. L.; Baell, J. B.; Kaiser, M.; Chatelain, E.; Moawad, S. R.; Ganame, D.; Ioset, J. R.; Avery, V. M., Identification of compounds with anti-proliferative activity against Trypanosoma brucei brucei strain 427 by a whole cell viability based HTS campaign. *PLoS Negl Trop Dis* **2012**, *6* (11), e1896.
27. Masand, V. H.; El-Sayed, N. N. E.; Mahajan, D. T.; Mercader, A. G.; Alafeefy, A. M.; Shibi, I. G., QSAR modeling for anti-human African trypanosomiasis activity of substituted 2-Phenylimidazopyridines. *J Mol Struct* **2017**, *1130*, 711-718.
28. Brun, R.; Blum, J.; Chappuis, F.; Burri, C., Human African trypanosomiasis. *The Lancet* **2010**, *375* (9709), 148-159.
29. Skaf, J.; Hamarsheh, O.; Berninger, M.; Balasubramanian, S.; Oelschlaeger, T. A.; Holzgrabe, U., Improving anti-trypanosomal activity of alkaloids isolated from Achillea fragrantissima. *Fitoterapia* **2018**, *125*, 191-198.
30. Glaser, J. Antileishmanial compounds from Nature - Elucidation of the active principles of an extract from Valeriana wallichii rhizomes. PhD thesis, University of Würzburg, Würzburg, 2015.
31. Zulfiqar, B.; Shelper, T. B.; Avery, V. M., Leishmaniasis drug discovery: recent progress and challenges in assay development. *Drug Discov Today* **2017**, *22* (10), 1516-1531.

32. World Health Org. Leishmaniasis. <http://www.who.int/mediacentre/factsheets/fs375/en/> (Accessed 24 Oct 2017).
33. Awad, B. M.; Habib, E. S.; Ibrahim, A. K.; Wanas, A. S.; Radwan, M. M.; Helal, M. A.; ElSohly, M. A.; Ahmed, S. A., Cytotoxic activity evaluation and molecular docking study of phenolic derivatives from *Achillea fragrantissima* (Forssk.) growing in Egypt. *Med Chem Res* **2017**, 26 (9), 2065-2073.
34. Glaser, J. Antileishmanial Compounds from Nature- Elucidation of the Active Principles of an Extract From *Valeriana Wallichii* Rhizomes. University of Würzburg, 2015.
35. Boelaert, M.; Sundar, S., 47 - Leishmaniasis A2 - Farrar, Jeremy. In *Manson's Tropical Infectious Diseases (Twenty-Third Edition)*, Hotez, P. J.; Junghanss, T.; Kang, G.; Laloo, D.; White, N. J., Eds. W.B. Saunders: London, 2014; pp 631-651.e4.
36. Reithinger, R.; Dujardin, J.-C.; Louzir, H.; Pirmez, C.; Alexander, B.; Brooker, S., Cutaneous leishmaniasis. *Lancet Infect Dis* **2007**, 7 (9), 581-596.
37. Balslev, U.; Nielsen, T. L., Adverse effects associated with intravenous pentamidine isethionate as treatment of *Pneumocystis carinii* pneumonia in AIDS patients. *Dan Med Bull* **1992**, 39 (4), 366-8.
38. Freitas-Junior, L. H.; Chatelain, E.; Kim, H. A.; Siqueira-Neto, J. L., Visceral leishmaniasis treatment: What do we have, what do we need and how to deliver it? *Int J Parasitol Drugs Drug Resist* **2012**, 2 (Supplement C), 11-19.
39. Pace, D., Leishmaniasis. *J Infect* **2014**, 69 (Supplement 1), S10-S18.
40. el-Shazly, A. M.; Hafez, S. S.; Wink, M., Comparative study of the essential oils and extracts of *Achillea fragrantissima* (Forssk.) Sch. Bip. and *Achillea santolina* L. (Asteraceae) from Egypt. *Pharmazie* **2004**, 59 (3), 226-30.
41. Saeidnia, S.; Gohari, A. R.; Mokhber-Dezfuli, N.; Kiuchi, F., A review on phytochemistry and medicinal properties of the genus *Achillea*. *DARU : Journal of Faculty of Pharmacy, Tehran University of Medical Sciences* **2011**, 19 (3), 173-186.
42. Abdel-Rahman, R. F.; Alqasoumi, S. I.; El-Desoky, A. H.; Soliman, G. A.; Paré, P. W.; Hegazy, M. E. F., Evaluation of the anti-inflammatory, analgesic and anti-ulcerogenic potentials of *Achillea fragrantissima* (Forssk.). *S Afr J Bot* **2015**, 98 (Supplement C), 122-127.

INTRODUCTION

43. Alsohaili, S.; Al-fawwaz, A., Composition and antimicrobial activity of *Achillea frangantissima* essential oil using food model media. *Eur Sci J* **2014**, *10*, 1857-7881.
44. Rezaei, F.; Jamei, R.; Heidari, R.; Maleki, R., Chemical composition and antioxidant activity of oil from wild *Achillea setacea* and *A. vermicularis*. *Int J Food Prop* **2017**, *20* (7), 1522-1531.
45. Si, X.-T.; Zhang, M.; Qing, S.; Kiyota, H., Chemical Constituents of the Plants in the Genus *Achillea*. *Chem Biodivers* **2007**, *38*.
46. O Santos, A.; C Santin, A.; U Yamaguchi, M.; E R Cortez, L.; Ueda-Nakamura, T.; P Dias-Filho, B.; Nakamura, C., Antileishmanial activity of an essential oil from the leaves and flowers of *Achillea millefolium*. *Ann Trop Med Parasitol* **2010**, *104*, 475-83.
47. Althaus, J.; Kaiser, M.; Brun, R.; Schmidt, T., Antiprotozoal Activity of *Achillea ptarmica* (Asteraceae) and Its Main Alkamide Constituents. *Molecules* **2014**, *19*, 6428-38.
48. Segal, R.; Dor, A.; Duddeck, H.; Snatzke, G.; Rosenbaum, D.; Kajtár, M., The sesquiterpene lactones from *achillea fragrantissima*, I. Achillolide A and B, two novel germacranolides. *Tetrahedron* **1987**, *43* (18), 4125-4132.
49. Ezzat, S.; Salama, M., A new α -glucosidase inhibitor from *Achillea fragrantissima* (Forssk.) Sch. Bip. growing in Egypt. *Nat Prod Res* **2014**, *28*.
50. Elmann, A.; Mordechay, S.; Erlank, H.; Telerman, A.; Rindner, M.; Ofir, R., Anti-neuroinflammatory effects of the extract of *Achillea fragrantissima*. *BMC Complement Altern Med* **2011**, *11*, 98.
51. El-Ashmawy, I. M.; Al-Wabel, N. A.; Bayad, A. E., *Achillea fragrantissima*, rich in flavonoids and tannins, potentiates the activity of diminazine aceturate against *Trypanosoma evansi* in rats. *Asian Pac J Trop Med* **2016**, *9* (3), 228-34.

2. Aim of the work

Leishmaniasis and trypanosomiasis are two of the most dangerous neglected tropical diseases affecting millions of people worldwide, especially the poor populations in the tropical and subtropical regions. Current antileishmanial and antitrypanosomal drugs are mostly old and have severe undesirable side effects in addition to a reported growing resistance against them. Thus, the discovery of new therapeutic agents against these diseases is nowadays an urgent need. The fact that the drug discovery of antimalarial drugs relied mainly on natural resources is a strong motivation to investigate plant extracts in order to discover new natural lead compounds targeting such protozoal diseases.

As a preliminary screening of a dichloromethane extract of the aerial parts *Achillea fragrantissima* exhibited antileishmanial activity, the aim of this study was to discover new antileishmanial and/or antitrypanosomal compounds from *Achellia fragrantissima*.

Hence the objectives of this study project were:

- (1) Growing the plant from seeds.
- (2) Isolation of antileishmanial/antitrypanosomal compounds, structure elucidation and characterization of the biological, chemical and physicochemical properties.
- (3) Synthesis of a compound library – structurally related to the most active compound – in order to analyze the structure-activity relationships and to improve the antileishmanial and/or antitrypanosomal activity.
- (4) Characterization of the physicochemical properties which are important for pharmacokinetics and improvement of these properties for in vivo studies.

3. Results and discussion

Some preliminary investigations of a dichloromethane extract of *A. fragrantissima*, brought from Palestine, using the corresponding *Alamar-Blue* assay [1] revealed a potential antileishmanial activity. For this reason, the extract was fractionated by means of flash chromatography followed by preparative HPLC yielding four antileishmanial active compounds. The chemical structure of one of these compounds was assigned to chrysosplenol D, a flavonoid carries three methoxy and three hydroxyl substitutions (Fig 9). Unfortunately, the chemical structures of the other three compounds could not be elucidated because of their small amounts and insufficient purity or a possible contamination during the biological testing. Moreover, additional investigations could not be performed at that time as the whole provided amount of the extract has been already consumed and it was difficult to obtain additional amounts of the extract from the provider in Palestine. Thus, the plant had to be grown from the seeds.

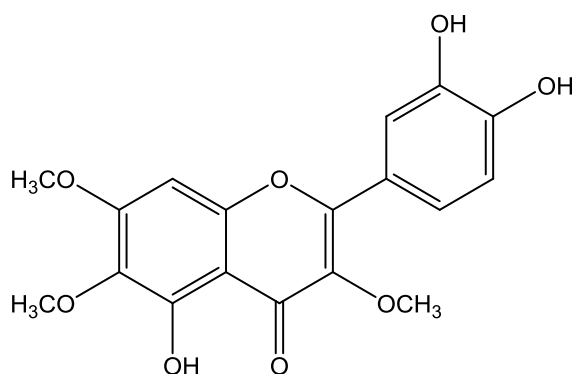


Fig. 9 Chemical structure of isolated chrysosplenol D.

Therefore, seeds of *A. fragrantissima* were collected in Homs, Syria, and planted in a greenhouse of the botanical garden of the University of Würzburg. The fully-grown plants were harvested in summer and dried in shadow yielding 700 gr of plant material. The plants were then divided into aerial parts and roots, powdered and extracted using dichloromethane and water as extraction solvents and dried *in vacuo* yielding a dichloromethane and a water extract of the aerial parts as well for the roots, which were bio-evaluated against *Trypanosoma brucei* showing an activity with IC_{50} value < 10 mg/mL for the dichloromethane

RESULTS AND DISCUSSION

extract of the aerial parts, while the dichloromethane extract of the roots and the water extracts of the aerial parts and the roots were considered inactive (Fig. 10).

The antileishmanial bio-evaluation became difficult at University of Würzburg due to the end of DFG-funded “Sonderforschungsbereich 630”. Therefore, and to save time the biological tests were performed against *Trypanosoma brucei brucei* TC221.

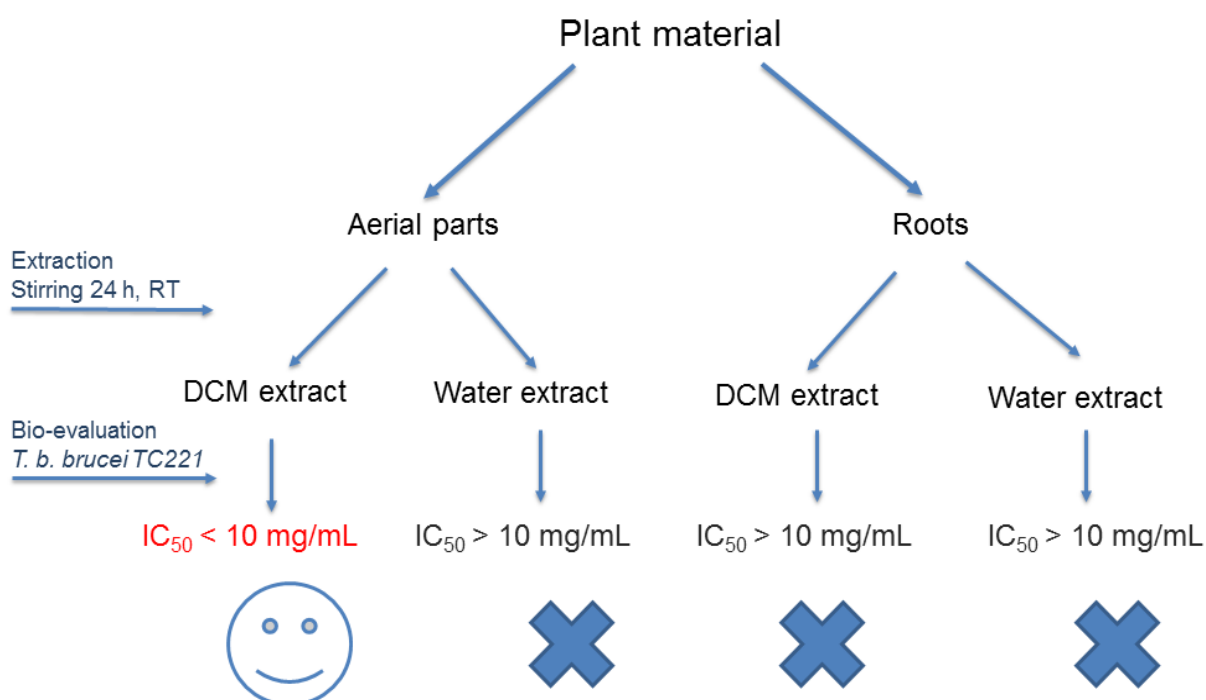


Fig. 10 Preparation and bio-evaluation of extracts from *A. fragrantissima*.

3.1 Bio-assay fractionation

Since a substantial anti-infective activity was found in the dichloromethane extract of the aerial parts ($IC_{50} < 10$ mg/mL), the extract was fractionated by means of flash chromatography to obtain 7 fractions. These fractions were again tested against *T.b. brucei*. The active fractions 2 to 7 were further fractionated, each resulting in 13 compounds. Isolated compounds were identified and characterized using NMR, MS, and IR techniques and subsequently evaluated

for their antitrypanosomal activity. Fig. 11 shows the entire scheme of fractionation.

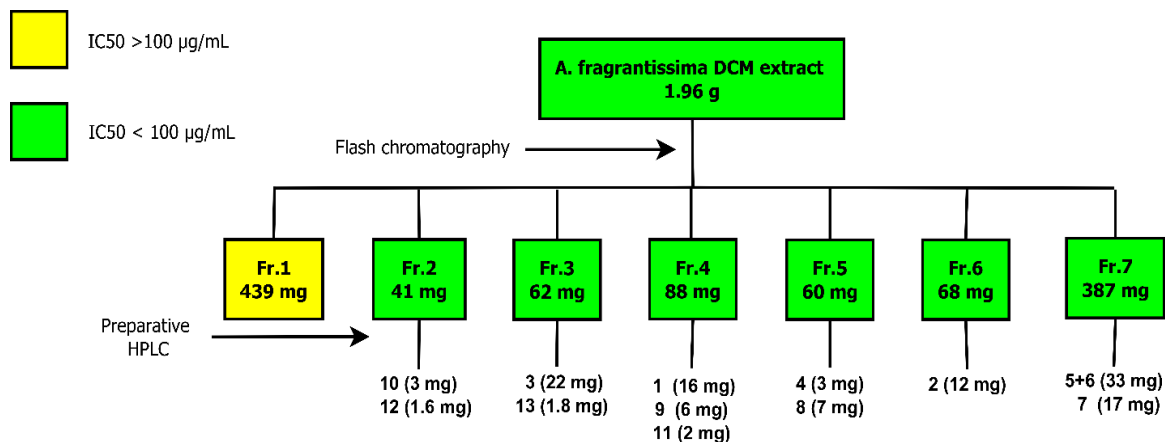


Fig. 11 Bioassay-guided fractionation of the DCM extract of *A. fragrantissima*.

3.2 Identification of isolated compounds

Three groups of natural products were found in the dichloromethane extract of the aerial parts of *A. fragrantissima*: seven sesquiterpene lactones **1-7**, two flavonoids **8** and **9**, and four alkaloids **10-13** including a novel alkaloid **13**.

3.2.1 Identification of isolated sesquiterpene lactones

Compound **1**, a sesquiterpene lactone, has been previously reported to be found in the aerial parts of *A. fragrantissima* [2-3]. This compound was isolated from fraction **4** as colorless crystals. The ESI-MS analysis recorded a molecular peak at $m/z = 363.00$ matching the chemical formula: $C_{19}H_{22}O_7$. The IR spectrum showed a strong band at 1752 cm^{-1} indicating a γ -lactone ring and other carbonyl functions at 1722 cm^{-1} and 1666 cm^{-1} regarding the carbonyl of the acetyl functions and the carbonyl of the enone group at C-1, respectively. The ^{13}C -NMR spectrum showed a signal at 199.9 ppm indicating a ketone carbonyl group at C-1. A CH_2 signal at 125.9 ppm with its corresponding ^1H signals at 5.96 and 5.81

RESULTS AND DISCUSSION

ppm indicate an exo-methylene moiety to be present at C-10 forming a conjugated enone Michael system with the carbonyl group at C-1.

Compound **2** was isolated as colorless oil from fraction **6**. It has been assigned to be Achillolide A, a sesquiterpene lactone, which was previously isolated and identified from *A. fragrantissima* [2-3]. The ESI-MS presents a molecular peak at $m/z = 320.95$ matching the suggested chemical formula: $C_{17}H_{20}O_6$ revealing a loss of acetyl group in comparison with **1**. The IR spectrum showed absorption bands for hydroxyl group at 3446 cm^{-1} and carbonyl functions at 1741 and 1670 cm^{-1} . The ^1H - and ^{13}C -NMR spectra were similar to the ones of **1** but with a hydroxyl group instead of the acetyl moiety was connected to C-13.

Compound **3** was isolated as white solid substance from fraction **3**. This compound is a sesquiterpene lactone, which has never been reported being found in *A. fragrantissima* but in *A. afra* [4]. The ESI-MS presents a molecular peak at $m/z = 349.00$ matching the chemical formula: $C_{19}H_{24}O_6$. The NMR spectra indicated a sesquiterpene lactone with similar skeleton as in compounds **1** and **2**. The ^{13}C -NMR spectrum showed no signal around 200 ppm indicating the absence of the ketone carbonyl group at C-1. The ^1H and ^{13}C signals of the exo-methylene group were also not detected comparing with the spectrums of **1** and **2**. The ^1H spectrum presented a methyl moiety at 1.64 ppm which is connected to C-10 instead of the exo-methylene group. This is confirmed using HMBC data.

Compound **4** was isolated in a small amount as colorless oil from fraction **5**. This compound has previously been reported isolated and characterized from *A. luoviciana* [5]. The ESI-MS showed a molecular peak at $m/z = 381.00$ matching the chemical formula: $C_{19}H_{24}O_8$, indicating the presence of additional two oxygens compared to **3**, hinted to the existence of a hydroperoxide moiety that was assigned to be at C-1. The IR spectra showed a strong absorption band for carbonyl groups at 1731 cm^{-1} .

Compounds **5** and **6** have been isolated from fraction **7** as white amorphous substance. They were assigned to be a mixture of two epimeric lactones, with a different configuration of the hydroxyl group at the carbon C-1.

RESULTS AND DISCUSSION

The ESI-MS showed a molecular peak at $m/z = 323.00$ matching the chemical formula: $C_{17}H_{22}O_6$. The IR spectrum reveals a broad absorption band at 3403 cm^{-1} corresponding to the hydroxyl groups and a strong band at 1719 cm^{-1} for the carbonyl groups. This epimeric mixture has been isolated before from *A. fragrantissima* [3] and from *A. judacia* [6].

Sesquiterpene lactone **7** has been isolated as crystals from fraction **7**. The ESI-MS data showed a molecular peak at $m/z = 323.00$ matching the chemical formula: $C_{19}H_{24}O_8$. IR spectrum showed an absorption band at 3317 cm^{-1} for the hydroxyl group and strong bands at 1743 cm^{-1} , 1717 cm^{-1} , and 1671 cm^{-1} for the carbonyl groups. The ^1H and ^{13}C NMR spectra indicated that the structure of **7** to be different from those of **5** and **6** with the absence of the exo-methylene group and the emergence of a double bond between C-9 and C-10. Sesquiterpene lactone **7** is a known constituent of *A. fragrantissima* [3].

The spectral data of all isolated sesquiterpene lactones **1-7** were in accordance with their respective literature. For structural formulae see Fig. 12.

Among all isolated sesquiterpene lactones only compound **2**, achillolide A, has been previously reported to exhibit biological activities while no biological activities were investigated for compounds **1**, **3**, **4**, **5+6**, and **7**. Achillolide A was reported to provide protection of the astrocytes against oxidation stress and that was explained by reducing intracellular reactive oxygene [7]. Moreover, achillolide A is known to inhibit the activation of microglial cells which release neurotoxic and proinflammatory mediators during the neuroinflammatory process [8].

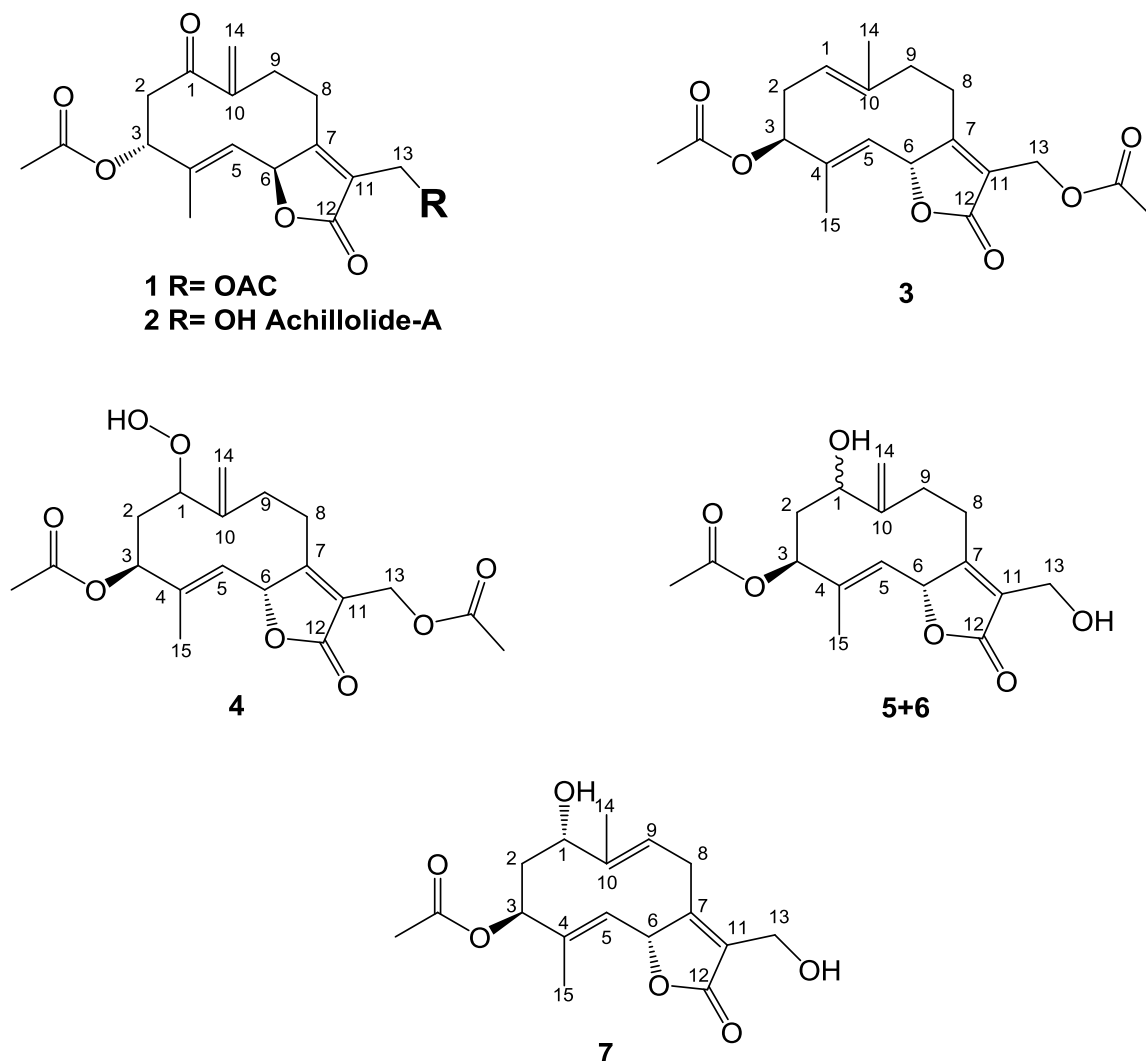


Fig. 12 Chemical structures of isolated sesquiterpene lactones.

3.2.2 Identification of isolated Flavonoids

Compound **8** was assigned to chryso splenol D, a flavonoid previously isolated from *A. fragrantissima* [9] and from *Sphaeranthus amaranthoides* [10]. Chryso splenol D has been isolated from fraction **5** as amorphous yellow powder. ESI-MS showed a molecular peak at $m/z = 360.95$ matching the chemical formula: $C_{18}H_{16}O_8$. The IR spectrum showed an absorption band at 3367 cm^{-1} indicating the presence of hydroxyl group and a band at 1652 cm^{-1} for the carbonyl group. The $^1\text{H-NMR}$ spectrum revealed four signals each integrates 1 in the aromatic range indicating four aromatic protons and three signals each integrates 3 in the range of 3.80 ppm to 4.00 ppm indicating three methoxy groups to be present in the structure.

RESULTS AND DISCUSSION

From fraction **4** another flavonoid, chryso splenetin **9** [11], was as well isolated as yellow amorphous substance. ESI-MS showed a molecular peak at $m/z = 374.95$ matching the chemical formula: $C_{19}H_{18}O_8$. IR spectrum showed an absorption band at 3241 cm^{-1} for hydroxyl groups and a band at 1650 cm^{-1} for carbonyl groups. The ^1H - and ^{13}C -NMR spectra showed similar structure as in **8** but with the difference that chryso splenol-D has a hydroxyl group at C-3', whereas chryso splenetin carries a methoxy group. The spectral data of isolated flavonoids **8** and **9** were in accordance with their respective literature. For structural formulae see Fig. 13.

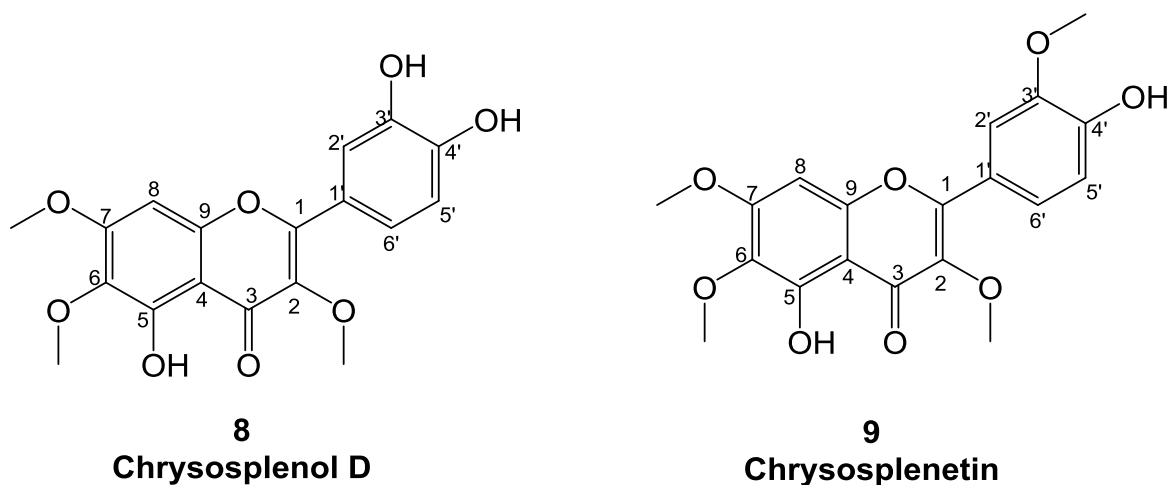


Fig. 13 Chemical structures of isolated flavonoids.

Isolated flavonoids are known to have variety of biological effects. Chryso splenol D (**8**) was reported to show high toxicity against human breast, skin, and cervical cancer cell lines [12]. Additionally, it displayed potential cytotoxic activity against breast cancer cell line MCF7 and human liver cancer cell line HepG2 with IC_{50} values of $8.32\text{ }\mu\text{g/mL}$ and $20.8\text{ }\mu\text{g/mL}$, respectively [13]. Moreover, it was reported having the ability to reduce the immune-activated production of major mediators of angiogenesis, namely NO, PGE2 and cytokines which play a crucial role in growth of tumours and formation of metastasis [14]. Moreover, Chryso splenol D is also known to inhibit inflammation *in vitro* and *in vivo* [15] and to exhibit as well antibacterial activity too, that it could inhibit the

RESULTS AND DISCUSSION

growth of *Clostridium perfringens* which infect mainly poultry [16]. Additionally, it exhibited activity against *Escherichia coli*, *Bacillus subtilis*, *Micrococcus tetragenus* and *Pseudomonas florescence* [17]. Chrysosplenol D has been reported for its vascular relaxation activity as well [18]. Chrysosplenol D (**8**) and chrysosplenetin (**9**) were reported to induce apoptosis-like morphological changes and to have potent preferential cytotoxic activity on PANC-1 human pancreatic cancer cells [19]. Both flavonoids revealed antimalarial activity as well [20]. Chrysosplenol D and Chrysosplenetin were reported to potentiate the activity of berberine, a weak antibacterial alkaloid, against a resistance strain of *Staphylococcus aureus*, which was ascribed to the inhibition of an *S. aureus* multidrug resistance pump. Both flavonoids were earlier reported to potentiate the activity of artemisinin against *Plasmodium falciparum* [21]. Chrysosplenetin could significantly increase the rat plasma level and the antimalarial activity of artemisinin [22]. Moreover, Chrysosplenetin has been reported having anticholinesterase effect with 80% inhibition at a concentration of 0.1 mg/mL and IC₅₀ value of 27.14 µg/mL [23]. Additionally, chrysosplenetin exhibited activity against enterovirus 17 (EV17) with low cytotoxicity having an IC₅₀ value of about 0.02 µM [24].

3.2.3 Identification of isolated alkamides

Alkamides group has been previously never isolated from *A. fragrantissima*, while in this study four alkamides including Pellitorine (**10**) and the new alkamide **13** were isolated and identified.

Compound **10**, Pellitorine, an alkamide that has been previously reported to be found in the roots of *piper nigrum* [25], roots of *Cissampelos glaberrima* [26], and the aerial parts of *A. ptarmica* [27]. The ESI-MS showed a molecular peak at $m/z = 224.05$ matching the chemical formula: C₁₄H₂₅NO. The IR spectrum showed a sharp absorption band at 3296 cm⁻¹ indicating the presence of a secondary amine and a band at 1654 cm⁻¹ for the carbonyl group of the amide. The NMR spectra revealed α , β -unsaturated conjugated system. The coupling constant of 15.1 for both double bonds confirms their *trans* configuration. Pellitorine **10** was reported to exhibit antiprotozoal activity against

RESULTS AND DISCUSSION

P. falciparum with IC_{50} of 14.6 μ M and against *T.b. rhodesiense* with IC_{50} of 24.0 μ M [27]. Moreover, it was reported to possess antibacterial [28] and antifungal [29] activities. Pellitorine is also known to inhibit α -glycosidase enzyme *in vitro*, which is important for carbohydrate digestion [30]. Moreover, pellitorine was reported to have therapeutic effects for vascular inflammatory diseases attributed to its protection of the vascular barrier integrity by inhibiting hyperpermeability, expression of cellular adhesion molecules (CAMs), and adhesion and migration of leukocytes [31]. Additionally, pellitorine has been reported having antithrombotic properties *in vitro* and *in vivo*, that it prolonged activated partial thromboplastin time (aPTT) and prothrombin time (PT) and it could inhibit the activity of thrombin and activated factor X (FXa) and it elicited anticoagulant effect in mouse [32]. Furthermore, pellitorine was considered as a potential anticancer lead compound as it exhibited strong cytotoxic activity against HL-60 and MCT-7 cell lines [25]. Notably, pellitorine showed good gut permeation and rapidly permeates the BBB once it is in the blood, indicating a possible role in the treatment of central nervous system diseases [33]. This property is e.g. important for the treatment of the CNS infections such as the second stage of trypanosomiasis [34].

Compound **11**, an alkamide, isolated before from different plants from genus achillea such as *A. ptarmica* [27] and *A. dracunculus* [35-36]. The ESI-MS showed a molecular peak at $m/z = 242.00$ matching the chemical formula: $C_{16}H_{19}NO$. The compound was isolated from fraction 4 as yellow amorphous powder. In the 1H -NMR spectrum four proton signals in the range of 6.00 ppm to 7.20 ppm can be seen. These protons constitute two conjugated double bonds exactly as the conjugated system in pellitorine with coupling constants of $J^{H2-H3} = 14.8$ and $J^{H4-H5} = 15.2$ confirming the *trans* configurations of the double bonds. This compound has a piperidine substitution at the amide head instead of isobutylamine in pellitorine. The ^{13}C -NMR spectrum reveals four signals in the range of 66 ppm to 78 ppm indicating four alkyne carbons to be located at the end of the aliphatic chain. Compound **11** is reported to possess antiprotozoal activity [27]. It has been found to inhibit effectively cytochrome p450 enzymes that it showed dose-dependent inhibitory effect on Cyp3Ar with IC_{50} value of 3.3 μ M [35]. Alkamide **11** was as well reported to inhibit the biosynthesis of the

RESULTS AND DISCUSSION

melanin pigments in B16 mouse melanoma cells via inhibiting α -melanocyte-stimulating hormone (α -MSH) [36].

Compound **12** has been isolated from fraction 2 as yellow oil. The ESI-MS showed a molecular peak at $m/z = 222.10$ matching the chemical formula: $C_{16}H_{17}NO$. The substance was reported to be isolated from the aerial parts of *A. ptarmica* [27] and *Asarum sieboldii* [37]. The 1H and ^{13}C -NMR data showed that it has similar skeleton as pellitorine but containing a third double bond be located at C-8, which was confirmed by means of COSY and HMBC data. Alkamide **12** showed antiprotozoal activity against *T.b. rhodesiense* with IC_{50} of $9.1 \mu M$ [27]. Moreover, compound **12** was reported having significant peroxisome proliferator-activated receptor (PPAR) transactivational effects [37]. Activation of PPAR improves hyperglycaemia and hyperlipidaemia in obese and diabetic animals by a reduction in hepatic and peripheral insulin resistance [38].

The spectral data of isolated Alkamides **10-12** were in accordance with their respective literature. For structural formulae see Fig. 14.

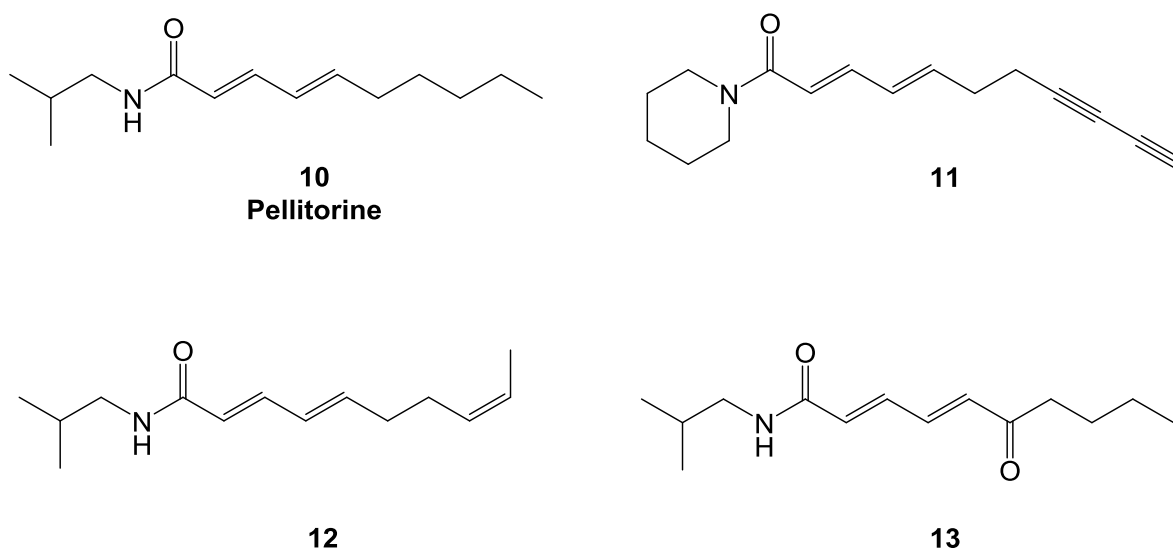


Fig. 14 Chemical structures of isolated alkamides.

The new compound **13** (Fig. 15) was isolated from fraction 3 as a white solid substance. The 1H NMR data (Fig. 16) point to the structure of an alkamide

RESULTS AND DISCUSSION

which is similar to the known Pellitorine (**10**) (Fig. 14). The MS-data (m/z : 238.10) hinted to an additional oxygen atom. The ^{13}C -NMR spectrum displays a signal at $\delta = 202.83$ ppm which is not visible in DEPT, indicating the presence of a ketone group. The ^1H NMR spectrum (Fig. 16) and the COSY diagram (Fig. 17) point to a conjugated diene moiety at $\delta = 7.25$ ppm (m, 2H, H-3, 4), 6.51 ppm (d, $J = 14.9$ Hz, 1H, H-5), and 6.44 ppm (d, $J = 14.5$ Hz, 1H, H-2). The coupling constants of 14.9 Hz and 14.5 Hz indicate a *trans*-configuration of the protons of each double bond. Furthermore, the analysis of the HMBC data (Fig. 18) confirms the position of the carbonyl carbon $\delta = 202.83$ ppm being at C-6. Fig. 14 shows the ^1H - ^1H COSY and HMBC correlations for **13**. The IR spectrum shows one sharp band at 3358 cm^{-1} indicating a secondary amine and two bands at 1658 cm^{-1} (m) and 1632 cm^{-1} (s) indicating two carbonyl groups corresponding to the amide group at position 1 and the ketone group at position 6, respectively. Therefore, the structure was assigned to (2*E*,4*E*)-*N*-isobutyl-6-oxodeca-2,4-dienamide [39].

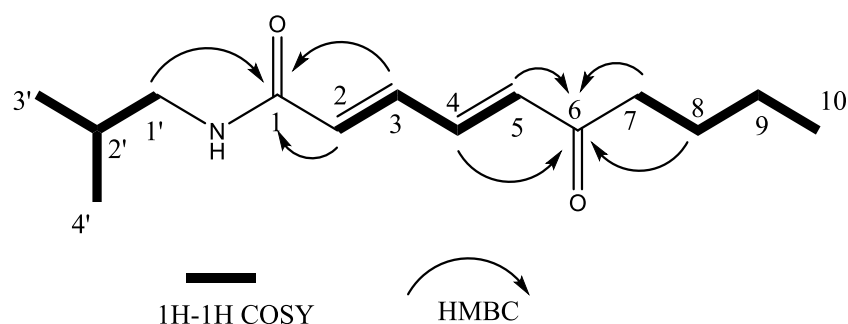


Fig. 15 Structure, ^1H - ^1H COSY and HMBC correlations for **13**.

RESULTS AND DISCUSSION

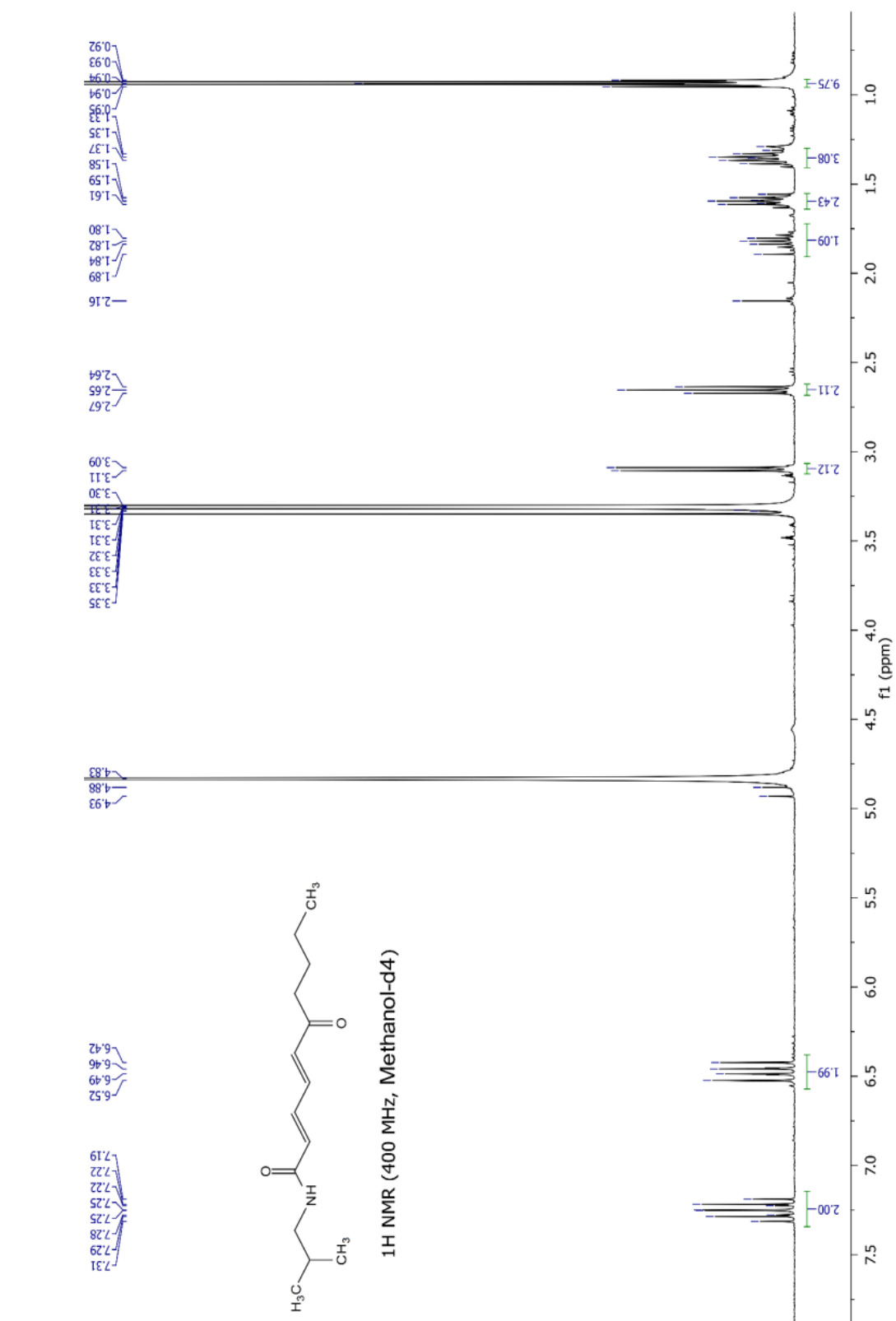


Fig. 16 ¹H Spectrum of compound 13.

RESULTS AND DISCUSSION

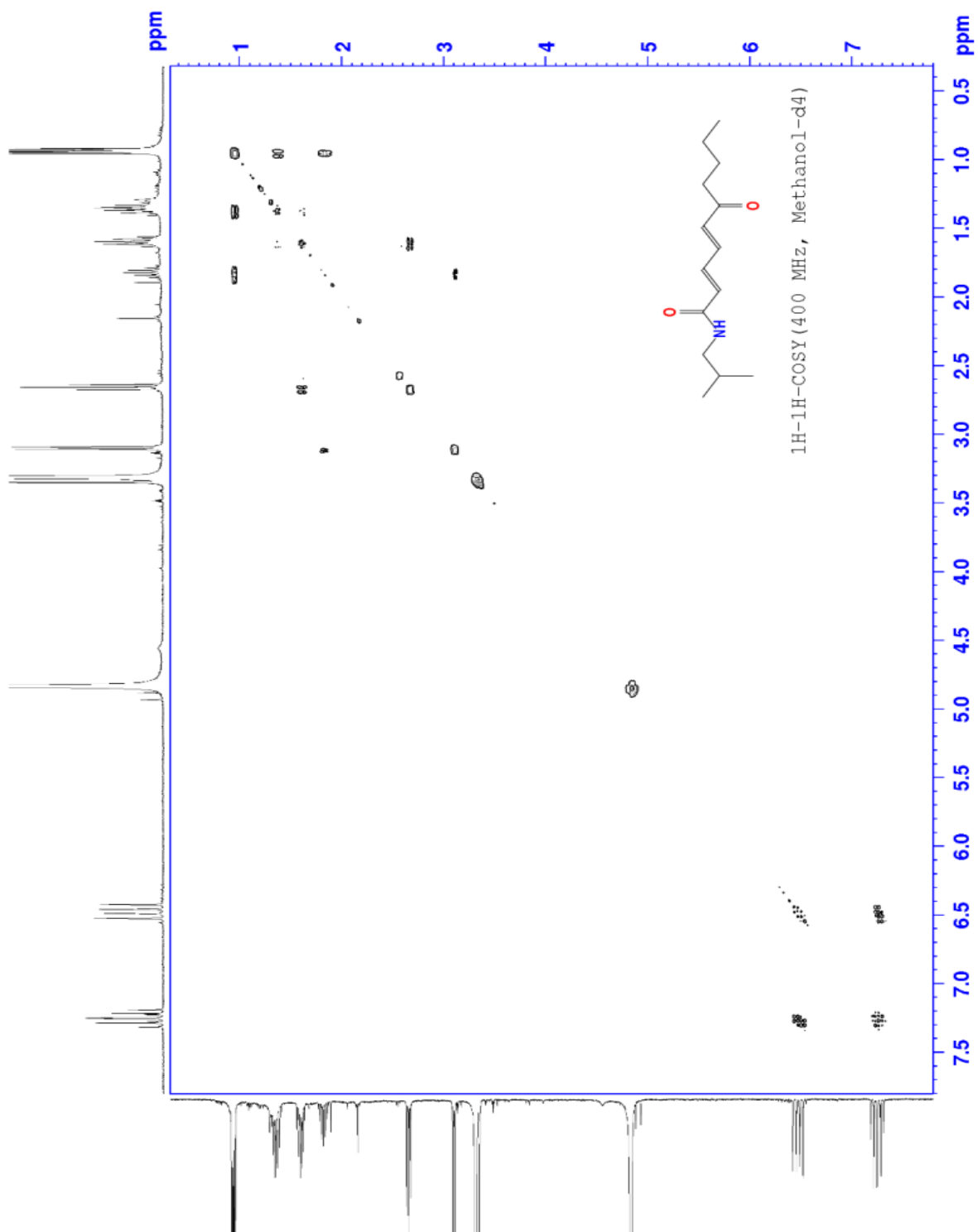


Fig. 17 ^1H - ^1H COSY Spectrum of compound **13**.

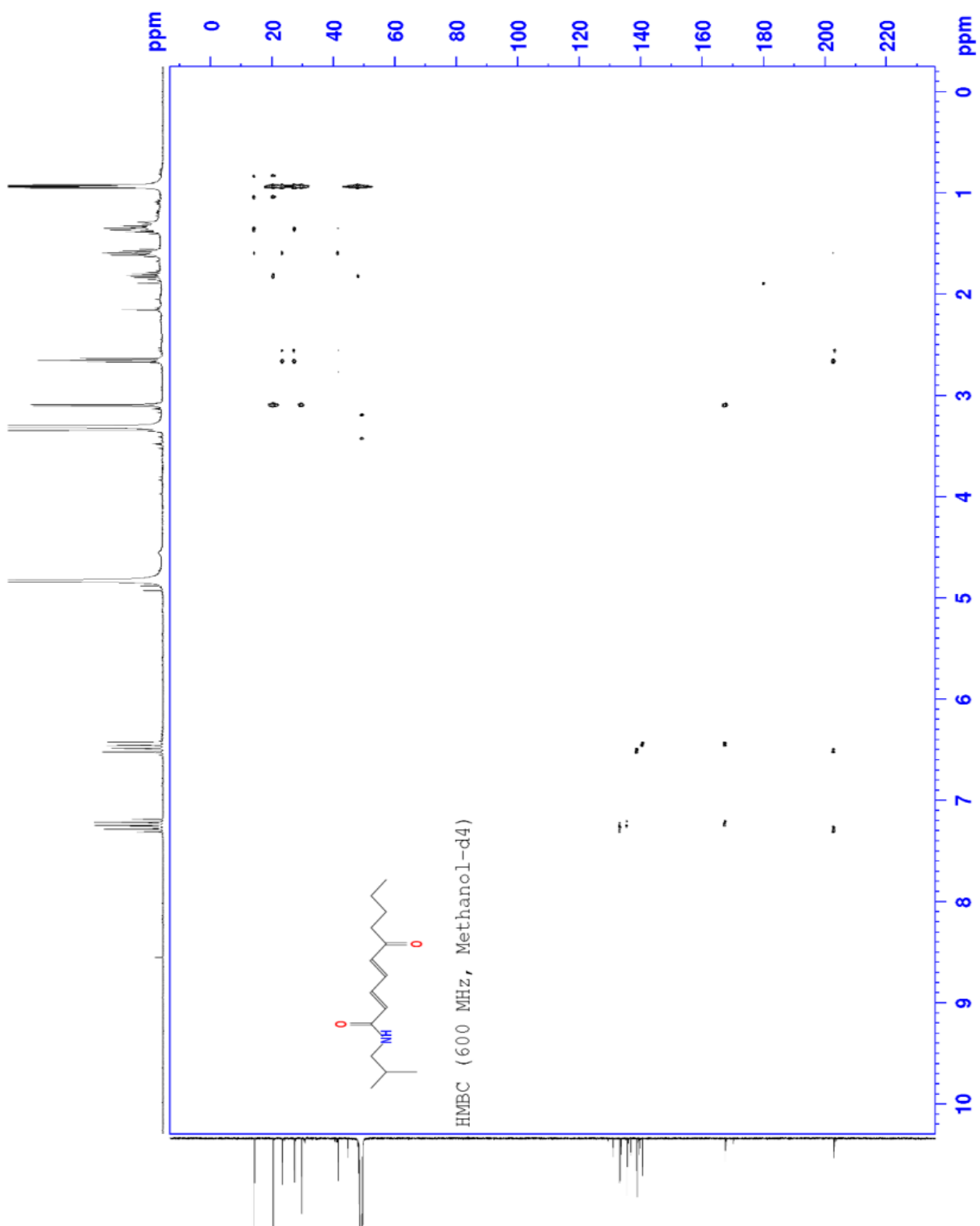


Fig. 18 HMBC Spectrum of compound 13.

3.3 Bio-evaluation of the isolated compounds

All isolated compounds were subjected to the evaluation of their *in vitro* activity against *T.b brucei* using the corresponding *Alamar-Blue* assay and pentamidine as a reference compound [40]. The biological data of all isolated compounds are reported in Table 1.

Table 1 Bio-evaluation of isolated compounds.

Compound	Chemical group	IC ₅₀ [μ M] <i>T.b. brucei</i>
1	Sesquiterpene lactones	3.03 \pm 0.06
2	Sesquiterpene lactones	10.97 \pm 0.47
3	Sesquiterpene lactones	10.97 \pm 0.11
4	Sesquiterpene lactones	27.03 \pm 0.13
5+6	Sesquiterpene lactones	60.92 \pm 0.76
7	Sesquiterpene lactones	>80
8	Flavonoids	30.35 \pm 0.23
9	Flavonoids	47.27 \pm 0.39
10	Alkamides	30.76 \pm 0.08
11	Alkamides	31.05 \pm 0.13
12	Alkamides	36.98 \pm 0.64
13	Alkamides	40.37 \pm 0.21
Pentamidine	Dibenzamidine	0.007 \pm 0.00

Sesquiterpene lactones **1**, **2**, **3**, and **4**, were quite active with IC₅₀ values between 3 and 27 μ M. The epimeric mixture of **5** and **6** showed weak activity only, whereas compound **7** was not active at all. Inspecting structures of the active sesquiterpene lactones revealed that the combination of two acetoxy groups and an enone Michael system is important for the activity of **1**. In absence

RESULTS AND DISCUSSION

of either the Michael system (cf. **3** and **4**), or of the acetoxy group at C-13 (see **2**, **5**, and **6**) and of both the Michael system and the acetoxy group the activity is substantially reduced or completely lost as in **7**.

This is the first study on the anti-trypanosomal activity of these particular sesquiterpene lactones. However, sesquiterpene lactones are widely known to exhibit antiprotozoal activity [41-42]. Their biological activity is usually accompanied with cytotoxicity and can mostly be explained by a reactive Michael system being prone to show the PAINS problem [43]. Since this structural feature determines both anti-trypanosomal and cytotoxic activity [41], we did not consider the sesquiterpene lactones for further investigations or synthetic optimizations.

The isolated flavonoids chrysosplenol-D **8** and chrysosplenetine **9** represented moderate activities with two-digit micromolar antitrypanosomal activity. Both flavonoids were never reported for their anti-trypanosomal activity. However, flavonoids are generally known to exhibit anti-protozoal activity [44] in addition to various other bioactivities [45]. They are also well known as strong antioxidants being able to effectively protect against radical toxicity. This is due to the catechol moiety which can be easily oxidized to the quinones which often present in flavonoids. However, quinones deliberately react with the nucleophilic thiol residues in proteins resulting in cytotoxicity [46].

Pellitorine **10** and the alkamides **11**, **12**, and **13** exhibited anti-trypanosomal activity with an IC₅₀ range of 30 to 40 μM. Of note, pellitorine **10** as well as **11** and **12** were previously isolated from *A. ptarmica* [27] and reported to have anti-trypanosomal activity against *T.b rhodesiense*.

3.4 Study of structure-activity relationship (SAR) of alkamides

Whereas flavonoids and sesquiterpene lactones are widely known to have a variety of biological effects [47-48] due to reactive moieties and their SARs as anti-protozoal agents were explored previously [41, 44], the anti-trypanosomal activity of alkamides remains almost unknown. Hence, a library of 27 alkamides was synthesized and subjected to biological testing in order to improve the antitrypanosomal activity and to derive SAR. The compounds were varied at three key regions of the structure, namely the amide head, the central core, and the aliphatic chain (Fig 19) [39].

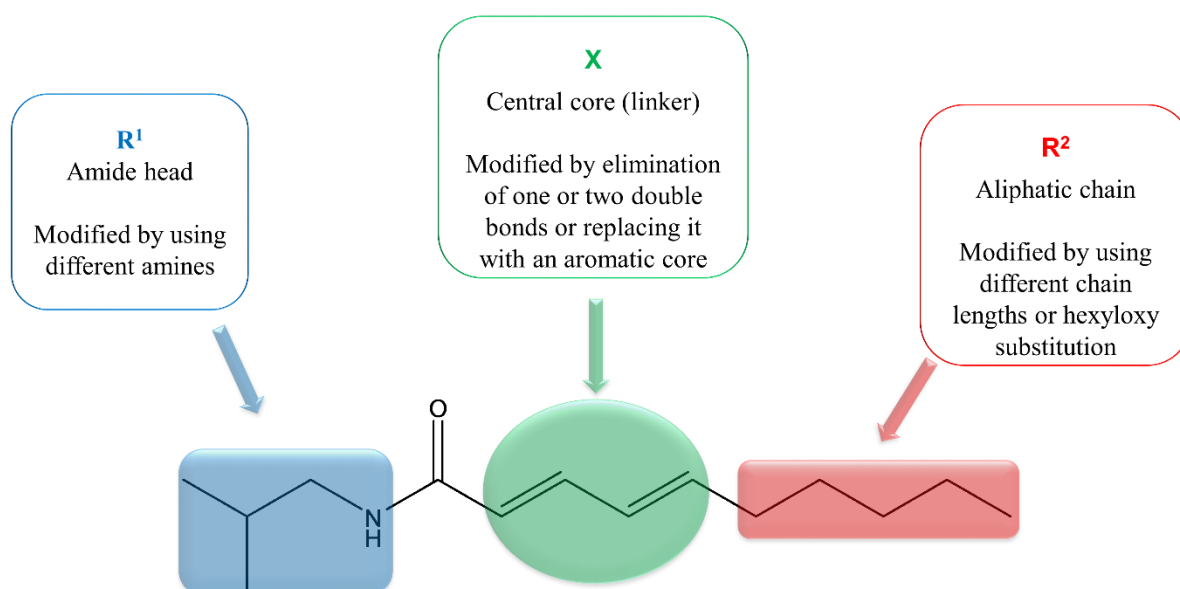
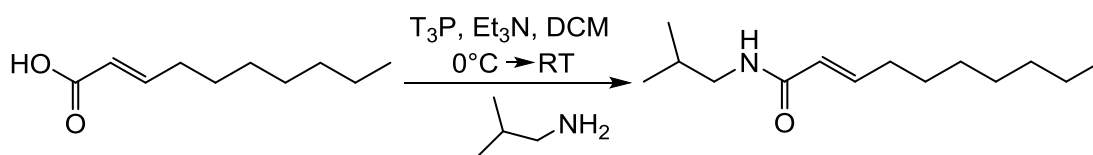
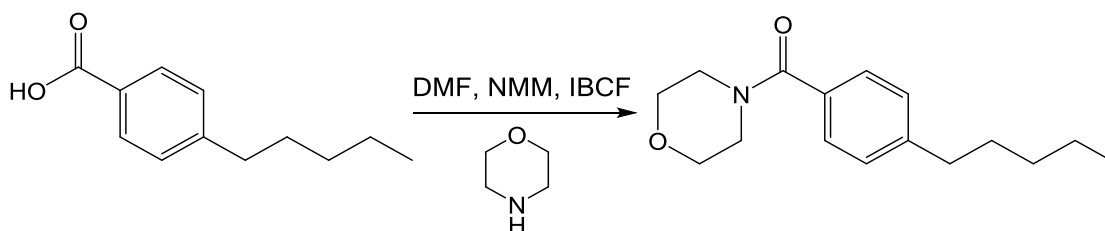


Fig. 19 Modified regions in Pellitorine 10 for SAR study.

The amides were prepared using general procedures by coupling of a carboxylic acid and an amine in DCM under nitrogen atmosphere using propylphosphonic anhydride as coupling reagent and triethylamine as a base for preparation of compounds **14 -19** and **22 – 40** (Scheme 1) or in DMF under argone atmosphere using *i*-butyl chloroformiate (IBCF) as coupling reagent and *N*-Methylmorpholine (NMM) as a base for preparation of compounds **20** and **21** (Scheme 2).



Scheme 1 General procedure A for Synthesis of compound **16**.



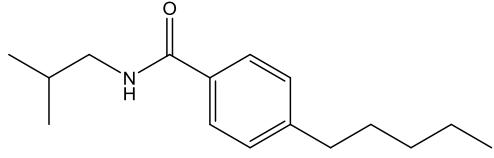
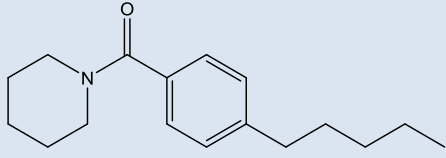
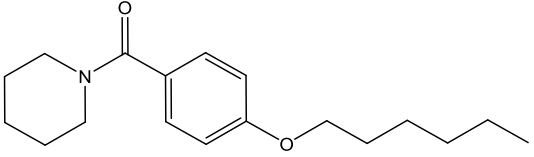
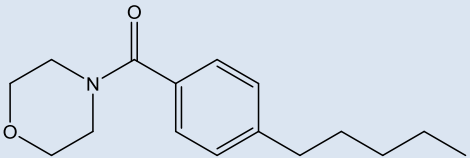
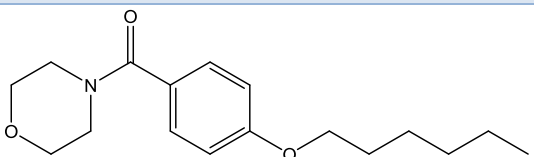
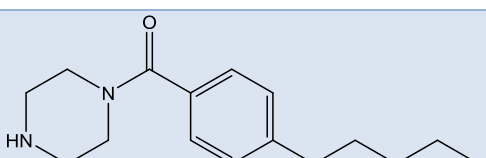
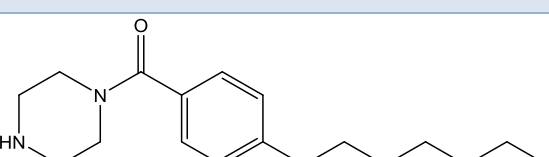
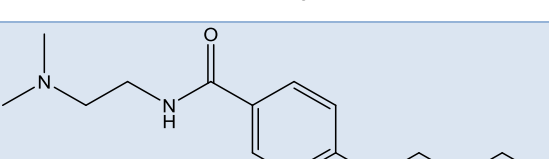
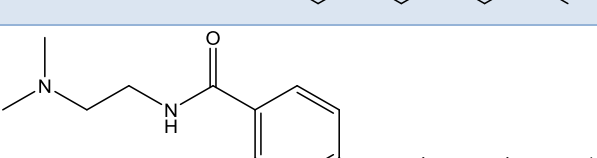
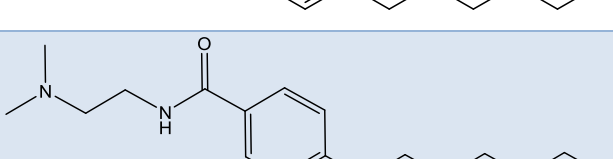
Scheme 2 General procedure B for Synthesis of compound **20**.

All 27 compounds were biologically assessed for anti-trypanosomal activity against *T.b. brucei* and for cytotoxicity against macrophages J774.1. Selectivity indices were calculated as the ratio of IC₅₀ against macrophages J774.1 and the IC₅₀ against *T.b. brucei*. The biological data are summarized in Table 2.

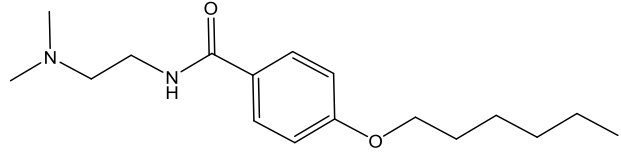
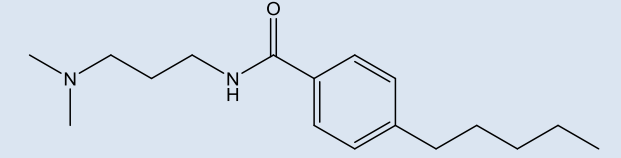
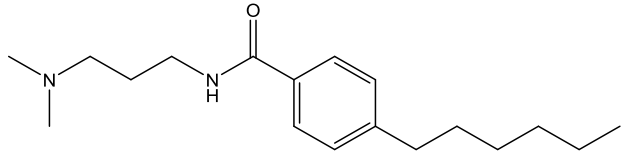
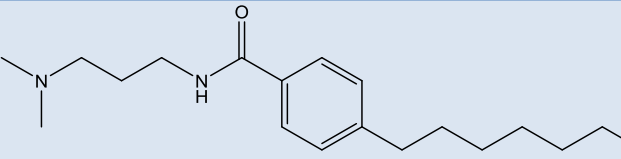
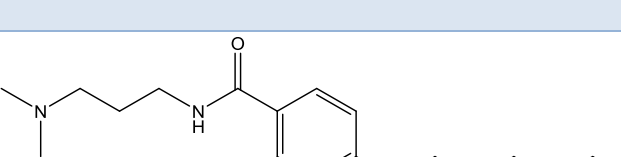
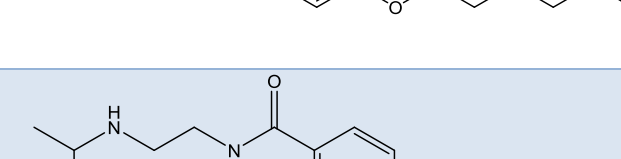
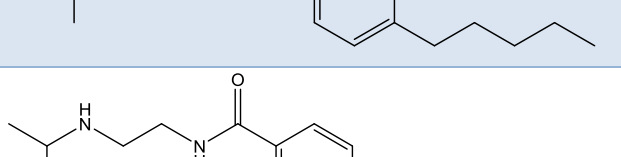
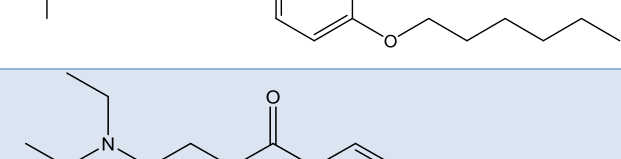
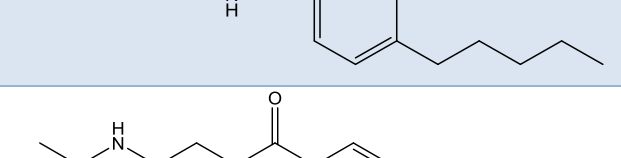
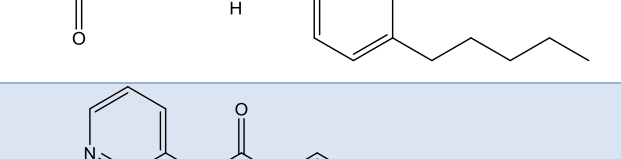
Table 2 Anti-trypanosomal activity, cytotoxicity, and selectivity indices of compounds **14-40**.

Compound	Chemical structure	IC ₅₀ [μM] <i>T.b. brucei</i>	IC ₅₀ [μM] J 774.1	Sel. Index ^a
14		>40	>100	-
15		>40	>100	-
16		36.64 ± 0.08	>100	>2.7

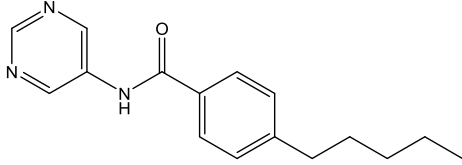
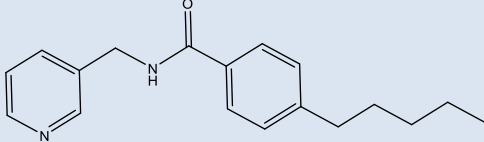
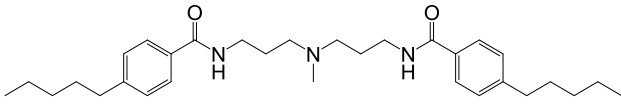
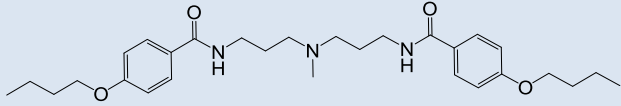
RESULTS AND DISCUSSION

17		34.37 ± 0.10	>100	>2.9
18		30.73 ± 0.03	>100	>3.3
19		19.82 ± 0.07	81.5	4.1
20		>40	-	-
21		>40	-	-
22		3.90 ± 0.01	93.9	24.1
23		2.16 ± 0.02	48.6	22.5
24		3.11 ± 0.01	49.5	15.9
25		3.24 ± 0.02	29.5	9.1
26		0.72 ± 0.00	14.4	20.1

RESULTS AND DISCUSSION

27		0.72 ± 0.00	32.9	45.7
28		3.74 ± 0.01	48.6	13
29		3.31 ± 0.24	18.2	5.5
30		2.94 ± 0.02	23.5	8
31		3.01 ± 0.01	23.8	7.9
32		3.36 ± 0.01	44.7	13.3
33		3.41 ± 0.06	19.1	5.6
34		3.89 ± 0.01	50.2	12.9
35		31.74 ± 0.29	>100	>3.2
36		20.77 ± 0.07	49.8	2.4

RESULTS AND DISCUSSION

37		32.49 ± 0.07	48.7	1.5
38		13.61 ± 0.1	19.1	1.4
39		0.48 ± 0.00	5.1	10.6
40		0.71 ± 0.00	4.8	6.8
^a Sel. Index = (IC ₅₀ against microphages J744.1) / (IC ₅₀ against <i>T.b. brucei</i>)				

Comparing the IC₅₀ values of the compounds differing in length of the aliphatic chain (R²) revealed the importance of the number of C atoms for the activity. Compound **14**, having a terminal methyl group, was found to be inactive (IC₅₀ > 40 μM), while both Pellitorine **10** and the alkamide **16** having a pentyl chain were found to be active at a concentration level of approx. 30 μM. The presence of one or two double bonds at positions 1 and/or 2, or an aromatic system, respectively, in the linker region X is also essential for the activity. Compound **15**, having a completely saturated chain, was found to be inactive.

Compounds possessing a basic amine moiety in region R¹, i.e. **22** - **34**, were highly potent anti-trypanosomal substances with IC₅₀ values in the range of 0.72 to 3.90 μM. Compounds **26** and **27**, having heptyl and hexyloxy chains, respectively, in region R² possess the highest activities in the submicromolar concentration range along with the highest selectivity indices of 20.1 and 45.6, respectively. Interestingly, compounds carrying a morpholine at R¹ were found to be inactive; compound **35** having an acetamide moiety has a moderate activity and a low cytotoxicity, whereas compounds **36** – **38** bearing aromatic heterocyclic amines have a moderate activity, but a remarkable cytotoxicity and thus, low selectivity indices. The two bis-amino compounds **39** and **40** exhibited

RESULTS AND DISCUSSION

high activities in the submicromolar concentration range but again a high cytotoxicity was observed [39].

The toxicity of the most active compounds **26** and **27** was assessed using *Galleria mellonella* larvae as an *in vivo* model. The greater wax moth *Galleria mellonella* larvae have been increasingly used as an *in vivo* model for assessing the toxicity and efficacy of antimicrobial agents and studying microbial infections [49-50]. Their ability to survive at physiological temperatures (30 °C or 37 °C), low maintenance costs, easy handling, and absence of any ethical concerns are some of the most important advantages of using these larvae for toxicity evaluation and pharmacokinetics studies [51]. The survival rates of the larvae are represented in Fig. 20, demonstrating that none of the tested concentration levels (1.25 – 20 mM) of both compounds induced toxic effects on the individuals. Also, the occurrence of few deaths observed with the tested concentration levels was not statistically significant, whereas methanol treatment (positive control) significantly led to death of the larvae ($p < 0.0001$). Because of the apparent absence of an *in vivo* toxicity and the relatively high trypanocidal activity, **26** and **27** can be regarded as promising lead compounds [39].

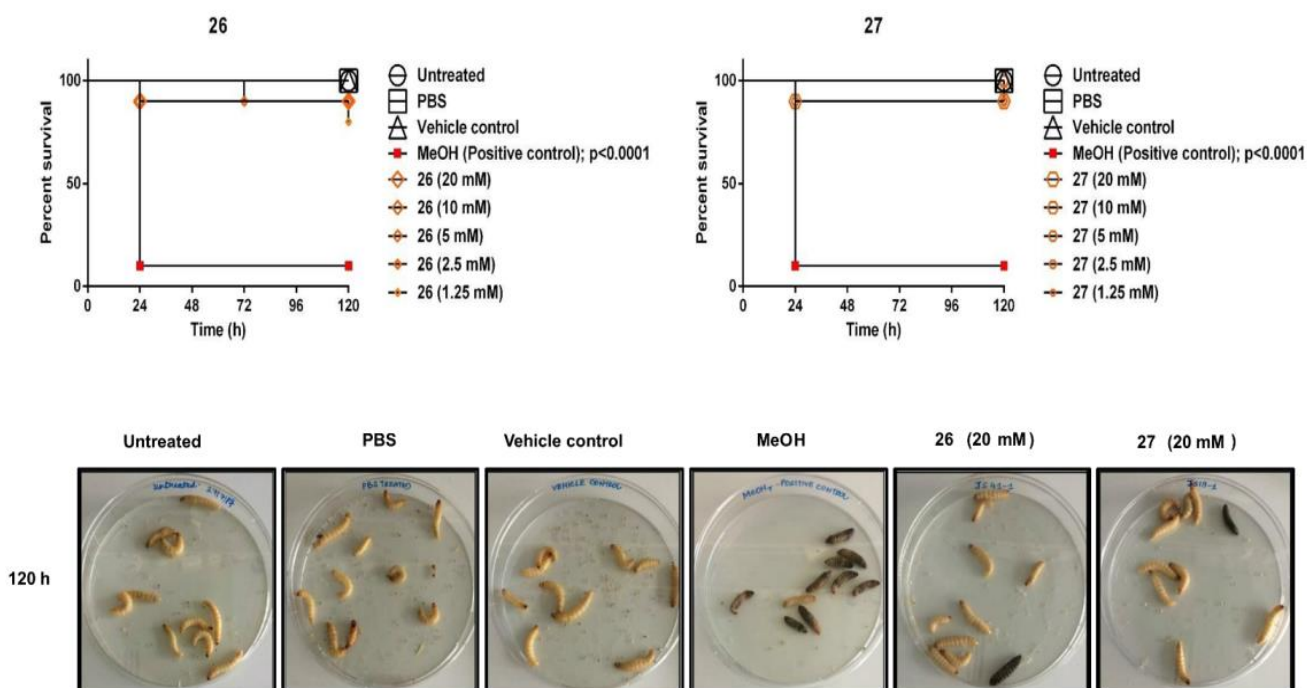


Fig. 20 Survival rates of the larvae for compound 26 and 27.

3.5 Synthesis and bio-evaluation of compounds 41 and 42.

A high throughput screening (HTS) of 87,926 compounds against *Trypanosoma brucei* was reported by Avery and co-workers [34]. This huge work led to a number of novel antitrypanosomal lead compounds exhibiting potent activities with low micromolar IC_{50} values and low cytotoxicity. These hit compounds included phenoxyethylbenzamide hit compound 1 (Fig. 21) exhibiting an IC_{50} value of 1.15 μM and possessing an amide head with 3-methylpiperidyl moiety and an aromatic core.

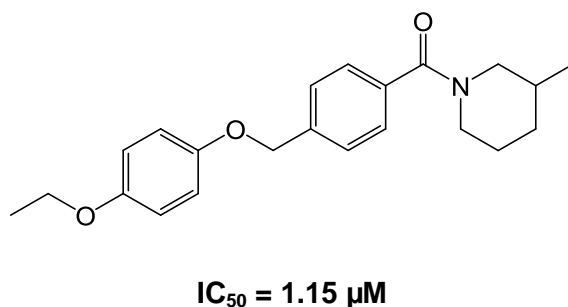


Fig. 21 Structure of phenoxyethylbenzamide hit compound 1.

Further investigations on this compound performed by Manos-Turvey and co-workers [52] led to increase the activity to submicromolar concentration ($IC_{50} = 0.49 \mu M$) by replacing the 3-methylpiperidyl moiety at the amide head with 2-methylpiperidyl moiety (compound 42) (Fig. 22)

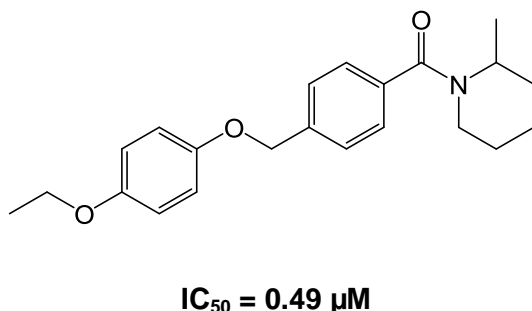


Fig. 22 Structure of compound 42.

The question arose whether the inclusion of *N,N*-Dimethylethylenediamine moiety at the amide head, which stimulated the potent activities of compounds

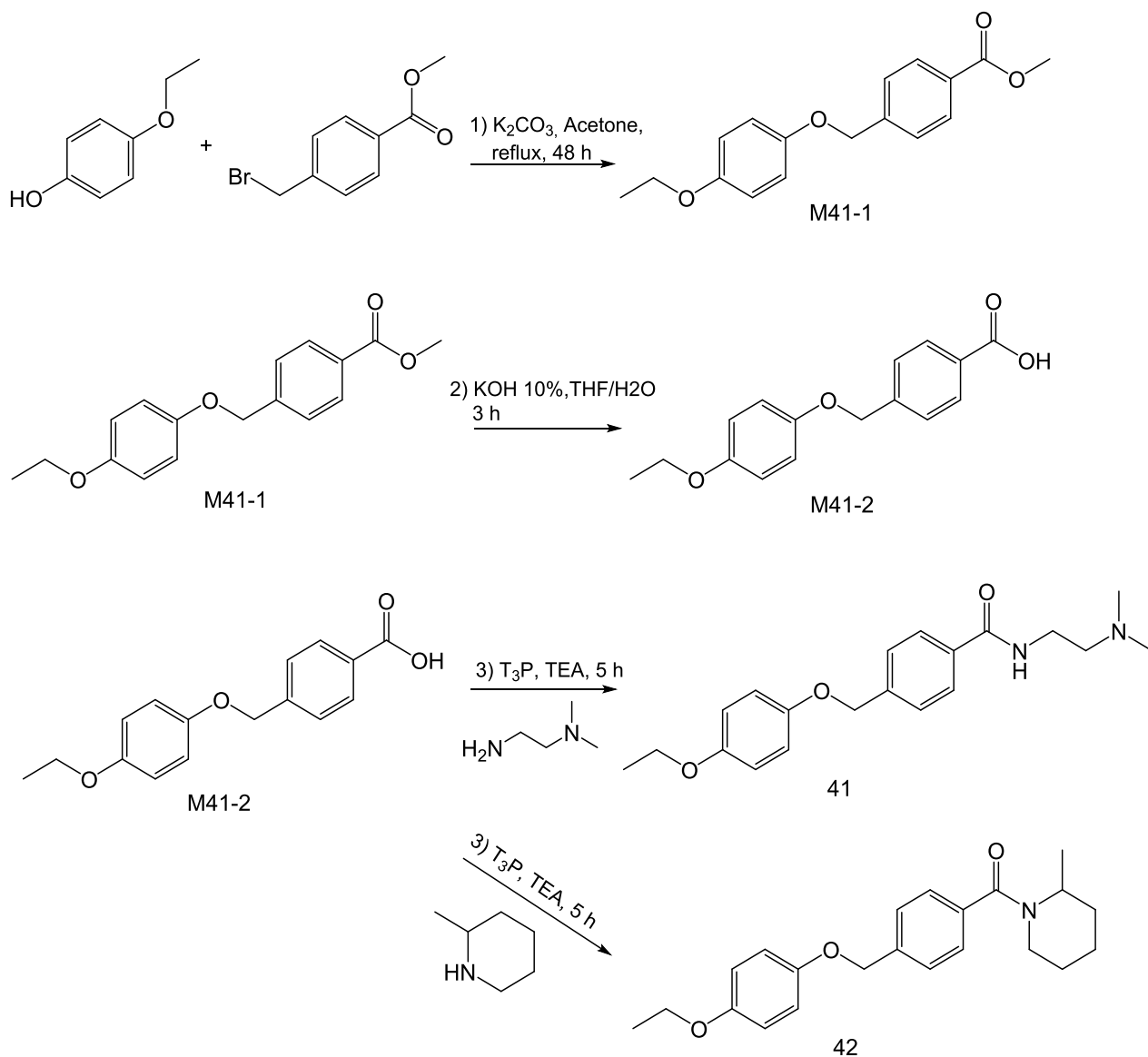
RESULTS AND DISCUSSION

24-26, could influence the activity of the phoxymethylbenzamide hit compounds.

Therefore, compounds **41** having *N,N*-Dimethylethylenediamine moiety and **42** having 2-methylpiperidyl moiety (Scheme 3) were synthesized and bio-evaluated against *T. b brucei* (TC221), in order to compare their antitrypanosomal activities.

Synthesis procedure began from methyl 4-(bromomethyl)benzoate, which was reacted with 4-ethoxyphenol in the presence of K_2CO_3 , affording compound **M41-1** which was purified by recrystallization from ethanol. Base hydrolysis of compound **M41-1** (ester) afforded the free acid **M41-2**, which was purified after precipitation by acidification (HCl 1 M), followed by washing with cold water and cold ethanol. Synthesis of **41** and **24** was performed by coupling of the carboxylic acid **M41-1** with the corresponding amines using propylphosphonic anhydride (T_3P) as coupling reagent and triethylamine as base under argon atmosphere (General procedure A). Purification of compounds **41** and **42** was done by means of flash chromatography. Synthesis is represented in scheme 3.

RESULTS AND DISCUSSION



Scheme. 3. Synthesis pathway of compounds **41** and **42**.

The compounds **41** and **42** were subjected for biological testing against *T. b brucei* exhibiting potent activities and IC_{50} values of 3.45 μM for **41** and 0.42 μM for **42**. Although compound **41** revealed a potent antitrypanosomal activity, its activity is still less than the activity of the reported compound **42**.

3.6 Physicochemical properties of compounds 26 and 27 by means of Sirius T3.

Physicochemical parameters such as pKa and log P values as well intrinsic and kinetic solubility are essential for the development process of a new medicine. They are especially important for calculating the applied doses for *in vivo* studies by determination of solubility limits for the free acids and bases as well as for the salts as the substance could dissociate or precipitate under specific *in vivo* conditions [53].

3.6.1 Determination of pKa values of compounds 26 and 27.

Since both the partition between lipid and water and the equilibrium (thermodynamic) solubility of an active agent depend on its ionization state at certain pH value, the determination of its pKa value is of great importance. pKa can be determined with Sirius T3 using either UV- or pH-metric methods.

- UV-metric assay

This method requires that the drug should have a chromophore and at least one ionizable group in the pH range of 2 to 12, which is in spatial proximity to the chromophore.

The change in the ionization state of a compound by titration over the given pH range results in different molar extinction coefficients and can be determined by UV absorption changes depending on the pKa value.

- pH-metric assay

The change of the electrochemical potential and thus the change of the concentration of H⁺ ions in the analyzed solution by addition of an acid or a base is determined with a pH electrode. The equivalence point and thus the pKa value can be determined by the fast change in the pH or the voltage per volume addition [53-54].

The pKa values of compounds **26** and **27** were determined using pH-metric assay. As both compounds are bases, the titrations were done from low to high pH range (2-12). The experiments were performed by dissolving the test

RESULTS AND DISCUSSION

substances in ISA-water (ionic strength adjusted water, KCl 0.15 M). The solution was acidified with 0.5 M HCl to pH 2 and the titration was done with 0.5 M KOH solution till a pH value of 12. The pKa values for compounds **26** and **27** were found to be 7.91 and 8.45, respectively.

3.6.2 Determination of log P values for compounds **26** and **27**

The measurement of the log P value on the Sirius T3 is based on aqueous potentiometric titration. In this approach the corresponding compound is titrated for pKa in the presence of a water-immiscible solvent (typically octanol). Because of the partition of the neutral form mainly of the tested compound into the octanol phase, the measured pKa (p_oKa) value will be shifted. By comparing the p_oKa with the measured aqueous pKa value, the degree of shift can be determined and thus the amount of compound partitioning into the octanol phase can be deduced and a log P value reported [53].

To determine the log P values of compounds **26** and **27**, the p_oKa values of both compounds were measured by pH-metric titration using different ratios of octanol and ISA-water. The titrations were performed from low to high pH range (2-12) with 0.5 M KOH solution giving the log P values of 3.49 for **26** and 3.76 for **27** which is reasonably drug-like.

3.6.3 Determination of kinetic and intrinsic solubility of compounds **26** and **27**.

Intrinsic solubility is the equilibrium solubility of the free acid or free base form of an ionisable compound at a pH where it is fully un-ionised. **Equilibrium solubility** is the concentration of compound in a saturated solution when excess solid is present, and solution and solid are at equilibrium. **Kinetic Solubility** is the concentration of a compound in solution when an induced precipitate first appears. **Supersaturated solutions** contain excess neutral species in solution, which will carry on precipitating until the system reaches equilibrium [54].

RESULTS AND DISCUSSION

The solubility of compounds **26** and **27** was determined by means of the Sirius T3. Compounds were dissolved by adjusting the pH of the solution with measured volume of an acid titrant (0.5 M HCl) until the sample completely dissolved in its ionized form. The solutions of ionized solutes were back titrated toward precipitation by adding measured aliquots of base titrant (0.5 M KOH). The exact point of the first precipitation was recorded by the UV probe. The concentration of the sample at the point of initial precipitation called kinetic solubility.

Once precipitation is detected the rate of pH change with the time is closely monitored. The action of a compound precipitating from a supersaturated solution or dissolving into a subsaturated solution causes reproducible gradients of pH change. These gradients are monitored, whilst small amounts of strong acid (0.5 M HCl) and strong base (0.5 M KOH) are added alternately to cause the sample to fluctuate between a supersaturated and subsaturated state. By careful monitoring of these rates of pH change, the equilibrium conditions can be determined and hence an intrinsic solubility can be calculated [54]. Solubility values as well pKa and log P values of compounds **26** and **27** are reported in table 3.

Table 3 Physicochemical properties of compounds 26 and 27.

	Compound 26	Compound 27
pKa value	7.91	8.45
Kinetic solubility	1.013 mM (RSD = 11.6%)	0.90 mM (RSD = 9.9%)
Intrinsic solubility	0.41 mM (RSD = 9.6%)	0.45 mM (RSD = 7.8%)
Log P value	3.49	3.76

3.7 References

1. Bringmann, G.; Thomale, K.; Bischof, S.; Schneider, C.; Schultheis, M.; Schwarz, T.; Moll, H.; Schurigt, U., A novel *Leishmania major* amastigote assay in 96-well format for rapid drug screening and its use for discovery and evaluation of a new class of leishmanicidal quinolinium salts. *Antimicrob Agents Chemother* **2013**, *57* (7), 3003-11.
2. Segal, R.; Dor, A.; Duddeck, H.; Snatzke, G.; Rosenbaum, D.; Kajtár, M., The sesquiterpene lactones from achillea fragrantissima, I. Achillolide A and B, two novel germacranolides. *Tetrahedron* **1987**, *43* (18), 4125-4132.
3. Abdel-Mogib, M.; Jakupovic, J.; Dawidar, A. M.; Metwally, M. A.; Abou-Elzahab, M., Glaucolides from *Achillea fragrantissima*. *Phytochemistry* **1989**, *28* (12), 3528-3530.
4. Jakupovic, J.; Klemeyer, H.; Bohlmann, F.; Graven, E. H., Glaucolides and guaianolides from *Artemisia afra*. *Phytochemistry* **1988**, *27* (4), 1129-1133.
5. Jakupovic, J.; Tan, R. X.; Bohlmann, F.; Boldt, P. E.; Jia, Z. J., Sesquiterpene lactones from *Artemisia ludoviciana*. *Phytochemistry* **1991**, *30* (5), 1573-1577.
6. Khafagy, S. M.; El-Din, A. A. S.; Jakupovic, J.; Zdero, C.; Bohlmann, F., Glaucolide-like sesquiterpene lactones from *Artemisia judaica*. *Phytochemistry* **1988**, *27* (4), 1125-1128.
7. Elmann, A.; Telerman, A.; Erlank, H.; Ofir, R.; Kashman, Y.; Beit-Yannai, E., Achillolide A Protects Astrocytes against Oxidative Stress by Reducing Intracellular Reactive Oxygen Species and Interfering with Cell Signaling. *Molecules* **2016**, *21* (3).
8. Elmann, A.; Telerman, A.; Mordechay, S.; Erlank, H.; Rindner, M.; Kashman, Y.; Ofir, R., Downregulation of microglial activation by achillolide A. *Planta Med* **2015**, *81* (3), 215-21.
9. Ezzat, S.; Salama, M., A new α -glucosidase inhibitor from *Achillea fragrantissima* (Forssk.) Sch. Bip. growing in Egypt. *Nat Prod Res* **2014**, *28*.
10. Gayatri, S.; Suresh, R.; Reddy, C. U. M.; Chitra, K., Isolation and Characterization of Chemopreventive Agent from *Sphaeranthus amaranthoides* Burm F. *Pharmacognosy Research* **2016**, *8* (1), 61-65.

RESULTS AND DISCUSSION

11. Ferreira, J. F. S.; Luthria, D. L.; Sasaki, T.; Heyerick, A., Flavonoids from *Artemisia annua* L. as Antioxidants and Their Potential Synergism with Artemisinin against Malaria and Cancer. *Molecules* **2010**, *15* (5).
12. Amina, M.; Alam, P.; Parvez, M. K.; Al-Musayeib, N. M.; Al-Hwaity, S. A.; Al-Rashidi, N. S.; Al-Dosari, M. S., Isolation and validated HPTLC analysis of four cytotoxic compounds, including a new sesquiterpene from aerial parts of *Plectranthus cylindraceus*. *Nat Prod Res* **2017**, 1-6.
13. Awad, B. M.; Habib, E. S.; Ibrahim, A. K.; Wanas, A. S.; Radwan, M. M.; Helal, M. A.; ElSohly, M. A.; Ahmed, S. A., Cytotoxic activity evaluation and molecular docking study of phenolic derivatives from *Achillea fragrantissima* (Forssk.) growing in Egypt. *Med Chem Res* **2017**, *26* (9), 2065-2073.
14. Zhu, X. X.; Yang, L.; Li, Y. J.; Zhang, D.; Chen, Y.; Kostecka, P.; Kmonickova, E.; Zidek, Z., Effects of sesquiterpene, flavonoid and coumarin types of compounds from *Artemisia annua* L. on production of mediators of angiogenesis. *Pharmacol Rep* **2013**, *65* (2), 410-20.
15. Li, Y. J.; Guo, Y.; Yang, Q.; Weng, X. G.; Yang, L.; Wang, Y. J.; Chen, Y.; Zhang, D.; Li, Q.; Liu, X. C.; Kan, X. X.; Chen, X.; Zhu, X. X.; Kmoniekova, E.; Zidek, Z., Flavonoids casticin and chrysosplenol D from *Artemisia annua* L. inhibit inflammation in vitro and in vivo. *Toxicol Appl Pharmacol* **2015**, *286* (3), 151-8.
16. Ivarsen, E.; Frette, X. C.; Christensen, K. B.; Christensen, L. P.; Engberg, R. M.; Grevsen, K.; Kjaer, A., Bioassay-Guided Chromatographic Isolation and Identification of Antibacterial Compounds from *Artemisia annua* L. That Inhibit *Clostridium perfringens* Growth. *J AOAC Int* **2014**, *97* (5), 1282-90.
17. Ling, T. J.; Ling, W. W.; Chen, Y. J.; Wan, X. C.; Xia, T.; Du, X. F.; Zhang, Z. Z., Antiseptic activity and phenolic constituents of the aerial parts of *Vitex negundo* var. *cannabifolia*. *Molecules* **2010**, *15* (11), 8469-77.
18. Okuyama, E.; Suzumura, K.; Yamazaki, M., Pharmacologically Active Components of *Vitidis Fructus* (*Vitex rotundifolia*). : I. The Components Having Vascular Relaxation Effects. *J Nat Med* **1998**, *52* (3), 218-225.
19. Awale, S.; Linn, T. Z.; Li, F.; Tezuka, Y.; Myint, A.; Tomida, A.; Yamori, T.; Esumi, H.; Kadota, S., Identification of chrysosplenetin from *Vitex negundo* as a potential cytotoxic agent against PANC-1 and a panel of 39 human cancer cell lines (JFCR-39). *Phytother Res* **2011**, *25* (12), 1770-5.

RESULTS AND DISCUSSION

20. Liu, K. C.; Yang, S. L.; Roberts, M. F.; Elford, B. C.; Phillipson, J. D., Antimalarial activity of *Artemisia annua* flavonoids from whole plants and cell cultures. *Plant Cell Rep* **1992**, *11* (12), 637-40.
21. Stermitz, F. R.; Scriven, L. N.; Tegos, G.; Lewis, K., Two flavonols from *Artemisia annua* which potentiate the activity of berberine and norfloxacin against a resistant strain of *Staphylococcus aureus*. *Planta Med* **2002**, *68* (12), 1140-1.
22. Ma, L.; Wei, S.; Yang, B.; Ma, W.; Wu, X.; Ji, H.; Sui, H.; Chen, J., Chryso-splenetin inhibits artemisinin efflux in P-gp-over-expressing Caco-2 cells and reverses P-gp/MDR1 mRNA up-regulated expression induced by artemisinin in mouse small intestine. *Pharm Biol* **2017**, *55* (1), 374-380.
23. Chougouo, R. D. K.; Nguekeu, Y. M. M.; Dzoyem, J. P.; Awouafack, M. D.; Kouamouo, J.; Tane, P.; McGaw, L. J.; Eloff, J. N., Anti-inflammatory and acetylcholinesterase activity of extract, fractions and five compounds isolated from the leaves and twigs of *Artemisia annua* growing in Cameroon. *SpringerPlus* **2016**, *5* (1), 1525.
24. Zhu, Q. C.; Wang, Y.; Liu, Y. P.; Zhang, R. Q.; Li, X.; Su, W. H.; Long, F.; Luo, X. D.; Peng, T., Inhibition of enterovirus 71 replication by chryso-splenetin and penduletin. *Eur J Pharm Sci* **2011**, *44* (3), 392-8.
25. Ee, G. C.; Lim, C. M.; Rahmani, M.; Shaari, K.; Bong, C. F., Pellitorine, a potential anti-cancer lead compound against HL6 and MCT-7 cell lines and microbial transformation of piperine from *Piper Nigrum*. *Molecules* **2010**, *15* (4), 2398-404.
26. Rosario, S. L.; da Silva, A. J.; Parente, J. P., Alkamides from *Cissampelos glaberrima*. *Planta Med* **1996**, *62* (4), 376-7.
27. Althaus, J. B.; Kaiser, M.; Brun, R.; Schmidt, T. J., Antiprotozoal activity of *Achillea ptarmica* (Asteraceae) and its main alkamide constituents. *Molecules* **2014**, *19* (5), 6428-38.
28. Srinivasa Reddy, P.; Jamil, K.; Madhusudhan, P.; Anjani, G.; Das, B., Antibacterial Activity of Isolates from *Piper longum* and *Taxus baccata*. *Pharm Biol* **2001**, *39* (3), 236-238.
29. Navickiene, H. M. D.; Alécio, A. C.; Kato, M. J.; Bolzani, V. d. S.; Young, M. C. M.; Cavalheiro, A. J.; Furlan, M., Antifungal amides from *Piper hispidum* and *Piper tuberculatum*. *Phytochemistry* **2000**, *55* (6), 621-626.

RESULTS AND DISCUSSION

30. Pullela, S. V.; Tiwari, A. K.; Vanka, U. S.; Vummenthula, A.; Tatipaka, H. B.; Dasari, K. R.; Khan, I. A.; Janaswamy, M. R., HPLC assisted chemobiological standardization of α -glucosidase-I enzyme inhibitory constituents from Piper longum Linn-An Indian medicinal plant. *J Ethnopharmacol* **2006**, *108* (3), 445-449.
31. Lee, W.; Ku, S.-K.; Min, B.-W.; Lee, S.; Jee, J.-G.; Kim, J. A.; Bae, J.-S., Vascular barrier protective effects of pellitorine in LPS-induced inflammation in vitro and in vivo. *Fitoterapia* **2014**, *92* (Supplement C), 177-187.
32. Ku, S.-K.; Lee, I.-C.; Kim, J. A.; Bae, J.-S., Antithrombotic activities of pellitorine in vitro and in vivo. *Fitoterapia* **2013**, *91* (Supplement C), 1-8.
33. Veryser, L.; Bracke, N.; Wynendaele, E.; Joshi, T.; Tatke, P.; Taevernier, L.; De Spiegeleer, B., Quantitative In Vitro and In Vivo Evaluation of Intestinal and Blood-Brain Barrier Transport Kinetics of the Plant N-Alkylamide Pellitorine. *Biomed Res Int* **2016**, *2016*, 5497402.
34. Sykes, M. L.; Baell, J. B.; Kaiser, M.; Chatelain, E.; Moawad, S. R.; Ganame, D.; Ioset, J. R.; Avery, V. M., Identification of compounds with anti-proliferative activity against Trypanosoma brucei brucei strain 427 by a whole cell viability based HTS campaign. *PLoS Negl Trop Dis* **2012**, *6* (11), e1896.
35. Brahmi, Z.; Katho, T.; Hatsumata, R.; Hiroi, A.; Miyakawa, N.; Yakou, E.; Sugaya, K.; Onose, J.-i.; Abe, N., Effective Cytochrome P450 (CYP) Inhibitors Isolated from Tarragon (*Artemisia dracunculoides*). *Biosci Biotechnol Biochem* **2012**, *76* (5), 1028-1031.
36. Yamada, M.; Nakamura, K.; Watabe, T.; Ohno, O.; Kawagoshi, M.; Maru, N.; Uotsu, N.; Chiba, T.; Yamaguchi, K.; Uemura, D., Melanin biosynthesis inhibitors from Tarragon *Artemisia dracunculoides*. *Biosci Biotechnol Biochem* **2011**, *75* (8), 1628-30.
37. Quang, T. H.; Ngan, N. T. T.; Minh, C. V.; Kiem, P. V.; Tai, B. H.; Thao, N. P.; Song, S. B.; Kim, Y. H., Anti-inflammatory and PPAR transactivational effects of secondary metabolites from the roots of *Asarum sieboldii*. *Bioorg Med Chem Lett* **2012**, *22* (7), 2527-2533.
38. Sakamoto, J.; Kimura, H.; Moriyama, S.; Odaka, H.; Momose, Y.; Sugiyama, Y.; Sawada, H., Activation of human peroxisome proliferator-activated receptor (PPAR) subtypes by pioglitazone. *Biochem Biophys Res Commun* **2000**, *278* (3), 704-11.

RESULTS AND DISCUSSION

39. Skaf, J.; Hamarsheh, O.; Berninger, M.; Balasubramanian, S.; Oelschlaeger, T. A.; Holzgrabe, U., Improving anti-trypanosomal activity of alkamides isolated from *Achillea fragrantissima*. *Fitoterapia* **2018**, *125*, 191-198.
40. Ráz, B.; Iten, M.; Grether-Bühler, Y.; Kaminsky, R.; Brun, R., The Alamar Blue® assay to determine drug sensitivity of African trypanosomes (*T.b. rhodesiense* and *T.b. gambiense*) in vitro. *Acta Tropica* **1997**, *68* (2), 139-147.
41. Zimmermann, S.; Fouche, G.; De Mieri, M.; Yoshimoto, Y.; Usuki, T.; Nthambeleni, R.; Parkinson, C. J.; van der Westhuyzen, C.; Kaiser, M.; Hamburger, M.; Adams, M., Structure-activity relationship study of sesquiterpene lactones and their semi-synthetic amino derivatives as potential antitrypanosomal products. *Molecules* **2014**, *19* (3), 3523-38.
42. Julianti, T.; Hata, Y.; Zimmermann, S.; Kaiser, M.; Hamburger, M.; Adams, M., Antitrypanosomal sesquiterpene lactones from *Saussurea costus*. *Fitoterapia* **2011**, *82* (7), 955-9.
43. Glaser, J.; Holzgrabe, U., Focus on PAINS: false friends in the quest for selective anti-protozoal lead structures from Nature? *MedChemComm* **2016**, *7* (2), 214-223.
44. Tasdemir, D.; Kaiser, M.; Brun, R.; Yardley, V.; Schmidt, T. J.; Tosun, F.; Rüedi, P., Antitrypanosomal and Antileishmanial Activities of Flavonoids and Their Analogues: In Vitro, In Vivo, Structure-Activity Relationship, and Quantitative Structure-Activity Relationship Studies. *Antimicrob Agents Chemother* **2006**, *50* (4), 1352-1364.
45. Robak, J.; Gryglewski, R. J., Bioactivity of flavonoids. *Pol J Pharmacol* **1996**, *48* (6), 555-64.
46. Lemmens, K. J.; Vrolijk, M. F.; Bouwman, F. G.; van der Vijgh, W. J.; Bast, A.; Haenen, G. R., The minor structural difference between the antioxidants quercetin and 4'-O-methylquercetin has a major impact on their selective thiol toxicity. *Int J Mol Sci* **2014**, *15* (5), 7475-84.
47. Agrawal, A. D., Pharmacological Activities of Flavonoids: A Review. *Int J of Pharm Sci Nanotech* **2011**, *4* (2), 1394-1398.
48. Chadwick, M.; Trewin, H.; Gawthrop, F.; Wagstaff, C., Sesquiterpenoids lactones: benefits to plants and people. *Int J Mol Sci* **2013**, *14* (6), 12780-805.

RESULTS AND DISCUSSION

49. Gibreel, T. M.; Upton, M., Synthetic epidermicin NI01 can protect *Galleria mellonella* larvae from infection with *Staphylococcus aureus*. *J Antimicrob Chemother.* **2013**, 68 (10), 2269-2273.
50. Aparecida Procópio Gomes, L.; Alves Figueiredo, L. M.; Luiza do Rosário Palma, A.; Corrêa Geraldo, B. M.; Isler Castro, K. C.; Ruano de Oliveira Fugisaki, L.; Olavo Cardoso Jorge, A.; Dias de Oliveira, L.; Campos Junqueira, J., *Punica granatum* L. (Pomegranate) Extract: In Vivo Study of Antimicrobial Activity against *Porphyromonas gingivalis* in *Galleria mellonella* Model. *Scientific World* **2016**, 2016, 8626987.
51. Tsai, C. J.-Y.; Loh, J. M. S.; Proft, T., *Galleria mellonella* infection models for the study of bacterial diseases and for antimicrobial drug testing. *Virulence* **2016**, 7 (3), 214-229.
52. Manos-Turvey, A.; Watson, E. E.; Sykes, M. L.; Jones, A. J.; Baell, J. B.; Kaiser, M.; Avery, V. M.; Payne, R. J., Synthesis and evaluation of phenoxyethylbenzamide analogues as anti-trypanosomal agents. *MedChemComm* **2015**, 6 (3), 403-406.
53. Hiltensperger, G. Entwicklung neuer Wirkstoffe zur Behandlung der afrikanischen Schlafkrankheit. PhD Thesis, University of Würzburg, 2013.
54. Sirius T3 Instruction Manual. Revision 1.0, East Sussex, 2009.

4. Side project

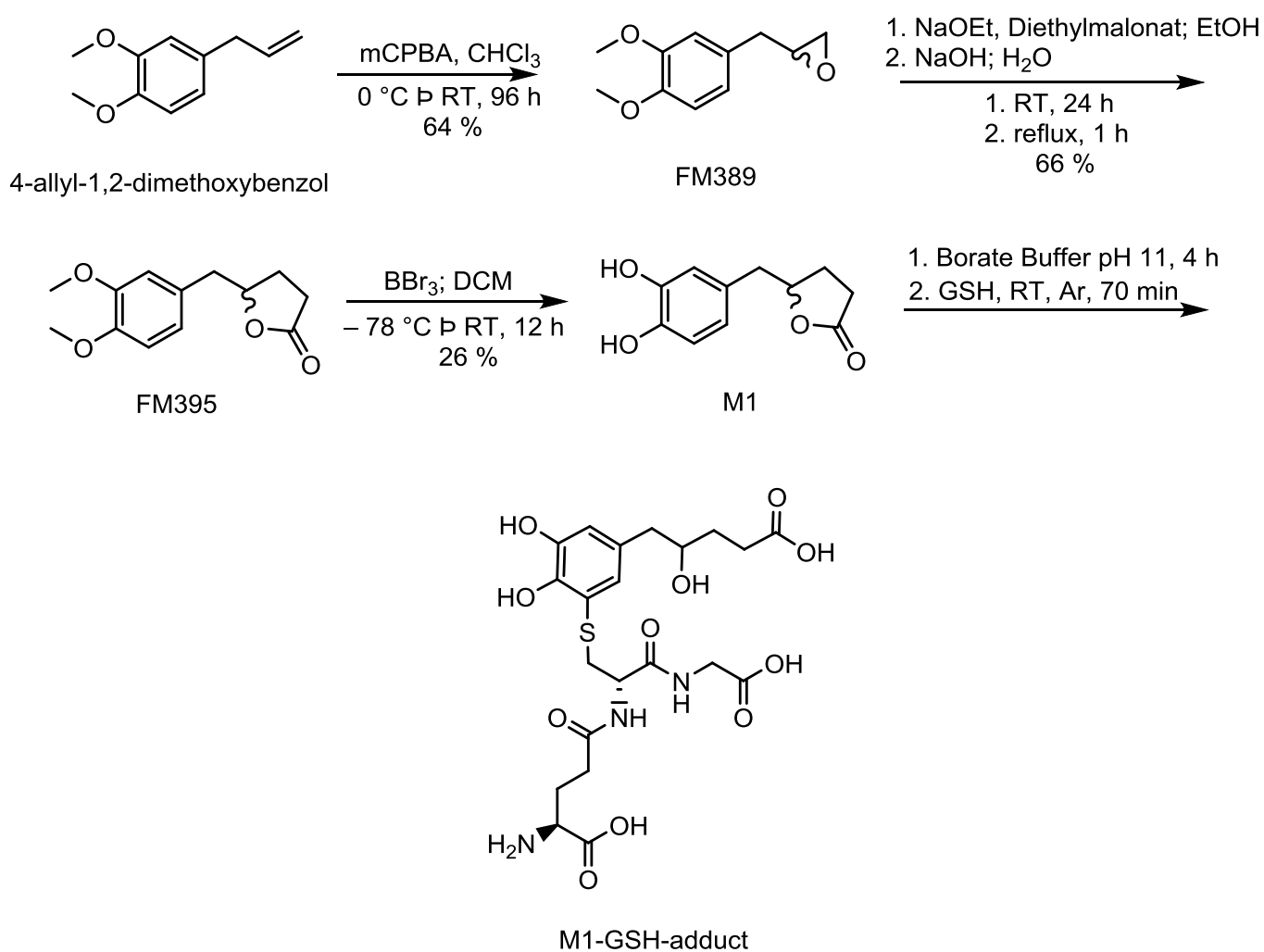
Synthesis of ring-opened lactone **M1**-GSH-Adduct: N^5 -((2*R*)-3-((4-carboxy-2-hydroxybutyl)-2,3-dihydroxyphenyl)thio-1-((carboxymethyl)amino)-1-oxopropan-2-yl)-*L*-glutamine

The cysteinyl leukotrienes, leukotriene C4, leukotriene D4 and leukotriene E4, are arachidonic acid derivatives modified by glutathione, Cys-Gly or Cys. Activated mast cells release cysteinyl leukotrienes, which produce inflammatory reactions. The biological effects of the cysteinyl leukotrienes are mediated by two G protein-coupled receptors (GPCRs), CysLT1 and CysLT2. A CysLT1 selective antagonist, montelukast, is nowadays one of the treatments of asthma [1-2]. Therefore, synthesis and biological testing of glutathione adducts is interesting and under investigation in this project.

Interestingly, **M1** was detected in plasma samples as a microbial metabolite after intake of maritime pine bark extract (Pycnogenol) [3]. The compound **M1** is not originally found in the pine bark extract but generated by intestinal microbial from catechin units and it attracted interest because it has a higher bioactivity e.g. regarding the inhibition of nitrite generation as an index for NO production, than its metabolic precursor catechin [3]. Moreover, *in vitro* and *in vivo* studies showed that **M1** is predominantly metabolized into glutathione conjugates which were rapidly formed and revealed prolonged presence within the cells [3]. The bioactivity of the **M1**-glutathione conjugates and the potential anti-inflammatory effects of **M1** require investigation. Therefore, synthesis of a similar glutathione adduct was performed.

Synthesis of compound **M1** (Scheme 4) was performed according to [4]. In the first step the double bond of the starting compound (4-allyl-1,2-dimethoxybenzol) reacted with *meta*-chloroperbenzoic acid (mCPBA) and was converted to the epoxide **FM389**. Next, the diethyl malonate acted as a nucleophile which attacked the epoxide and opened its ring. Subsequently, saponification took place. The resulting carboxylic function was decarboxylated to give the intermediate compound **FM395**. In the last step a typical demethylation was carried out using boron tribromide. As next, the synthesis of the ring-opened

lactone **M1-GSH-Adduct** (Scheme 4) was performed according to references [5-6]. Under basic conditions (borate buffer pH 11), the lactone ring of **M1** was opened and its catechol group could be oxidized into the corresponding o-quinone, which could then react with the nucleophilic thiol group of glutathione forming the desired glutathione adduct. The product was purified by means of preparative HPLC.



Scheme. 4. Synthesis pathway of ring-opened lactone M1-GSH-Adduct.

The ESI-MS data (positive mode) showed a molecular peak at $m/z = 532.16$ (Fig. 23) matching the molecular mass of the targeted adduct.

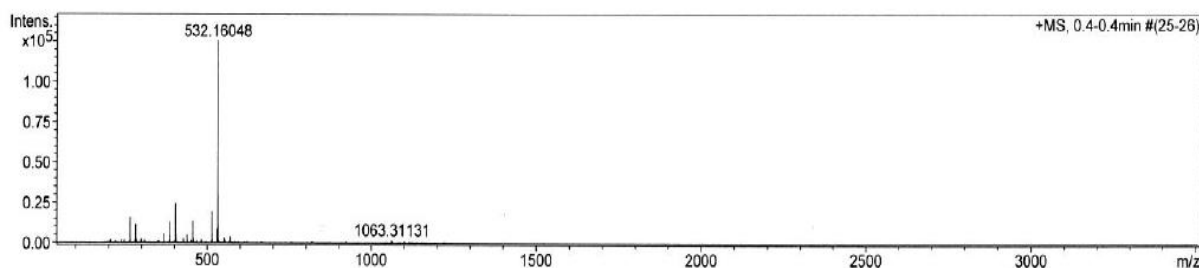


Fig. 23 ESI-MS data of ring-opened lactone M1-GSH-Adduct.

The ^1H NMR spectrum (Fig. 25) confirmed the binding of the sulfur in position 3 proposed in M \ddot{u} lek et al. [3]. In the aromatic region two proton signals “x,” “y” (doublets at 6.93 ppm/1.4 Hz and 6.84 ppm/1.8 Hz) were detected. The coupling constants indicated a coupling in meta-position of the protons, therefore the sulfur binded at position 3 at the phenyl ring (Fig. 24). An overlay of the ^1H NMR spectra of M1-GSH-adduct (Fig. 26), M1 and glutathione proved unambiguously the binding via the sulfur, because of strong low field shift of signal “g” and a weak high field shift of signal “f” of the glutathione rest in the adduct.

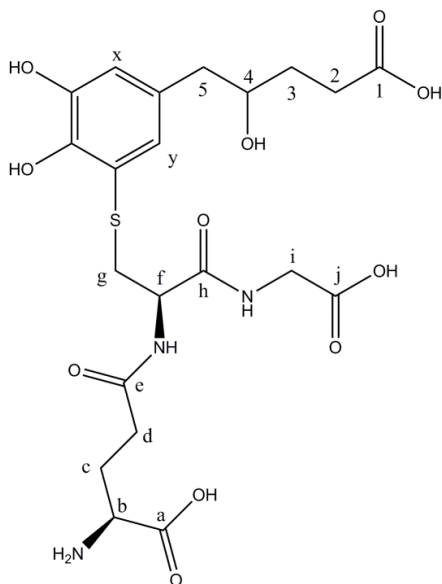


Fig. 24 Structure of M1-GSH-adduct.

The opening of the lactone ring in M1 was confirmed by integration of the proton signals, overlay with the original M1 ^1H NMR spectrum (Fig. 25) and signal assignment by ^1H ^1H -COSY NMR spectrum (Fig. 27).

The ^1H ^1H -COSY spectrum (Fig. 27) indicated the following cross peaks: signal 2 with 3, signal 3 with 2/4, signal 4 with 3/5 and signal 5 with 4. In combination of the integrals of the proton signal 2 (2H), signal 3 (2H), signal 4 (1H) and signal 5 (2H) the opening of the lactone can

be unambiguously confirmed.

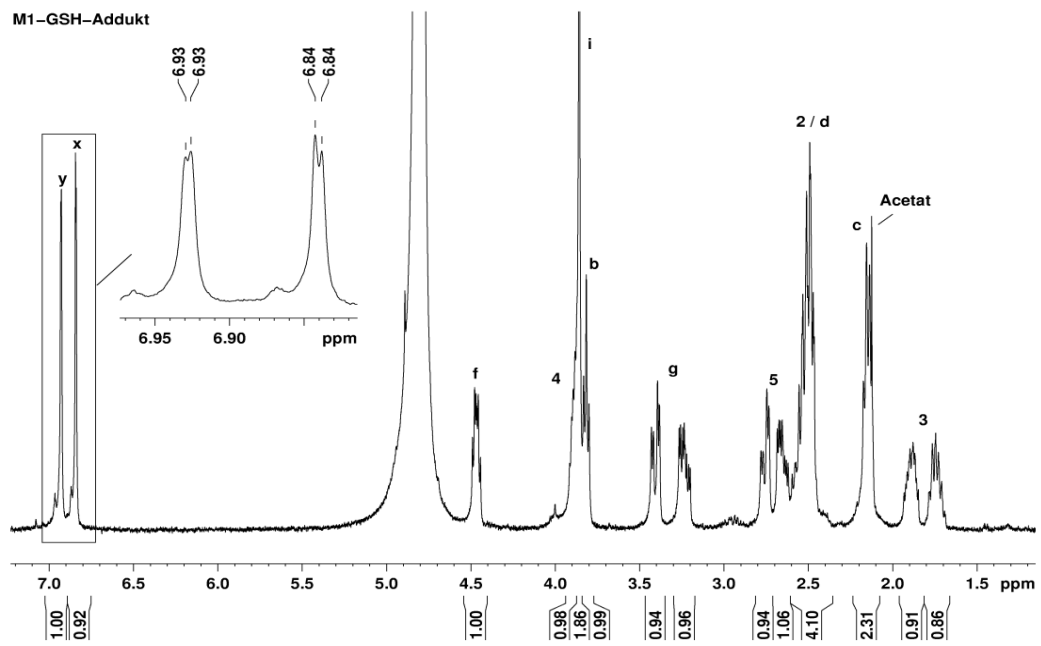


Fig. 25 ¹H NMR spectrum of M1-GSH-adduct in D₂O.

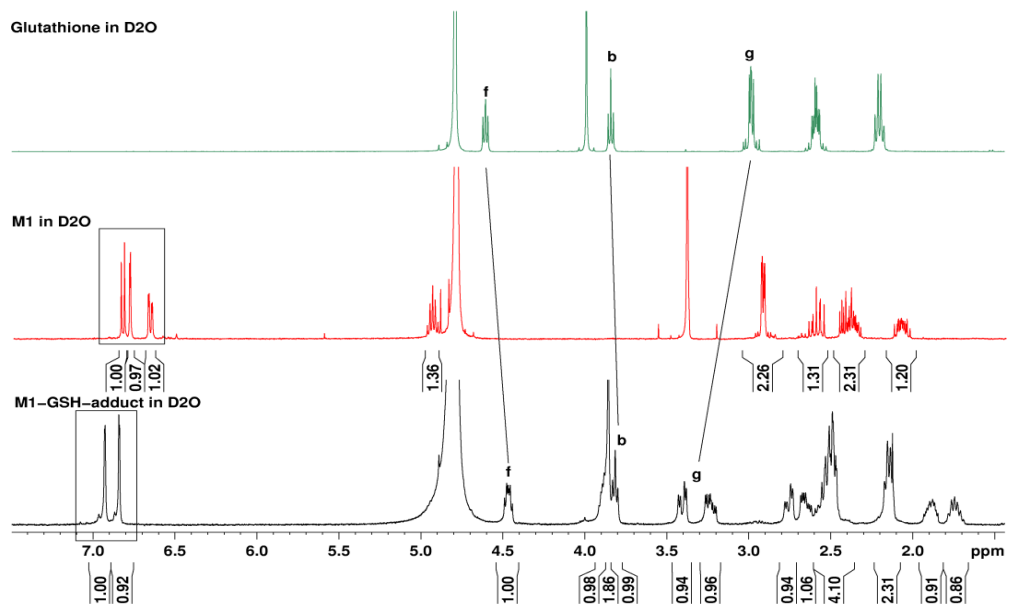


Fig. 26 Overlay of ¹H NMR spectra of M1-GSH-adduct, M1 and glutathione in D₂O.

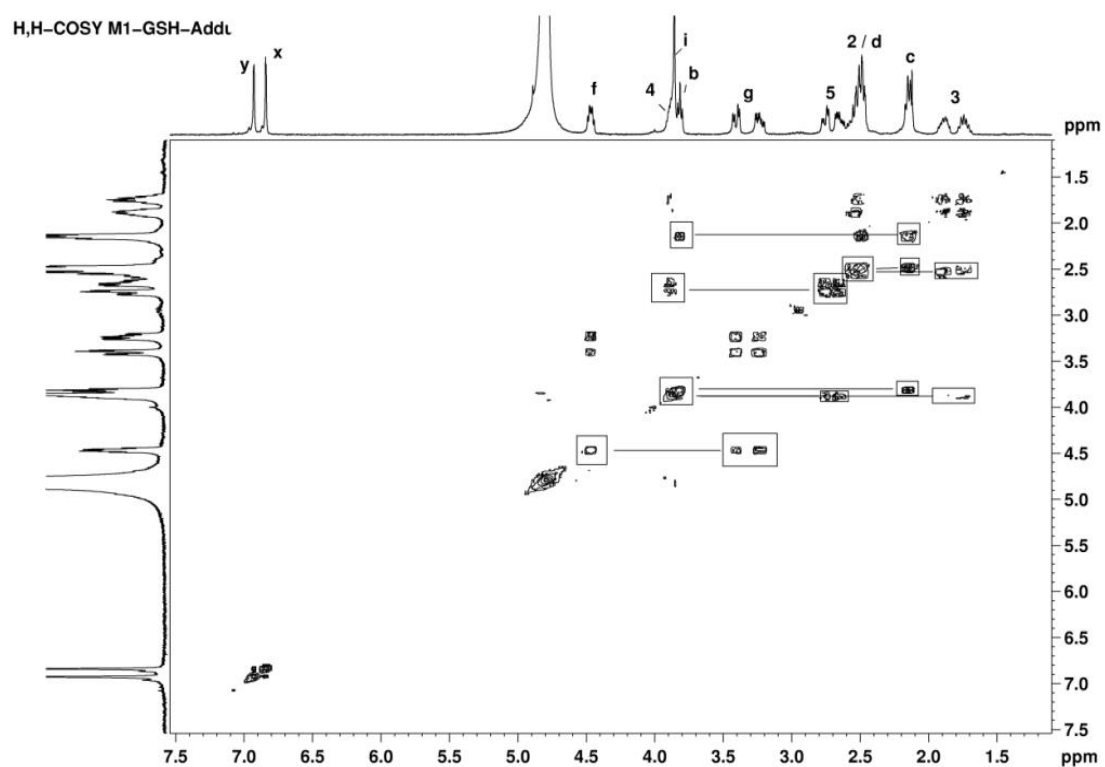


Fig. 27 ^1H ^1H -COSY of M1-GSH-adduct in D_2O .

The successful synthesis of the open-lactone-ring M1-Glutathione adduct was achieved and the structure was confirmed by NMR and LC-ESI-MS.

4.1 References

1. Brink, C.; Dahlen, S. E.; Drazen, J.; Evans, J. F.; Hay, D. W.; Nicosia, S.; Serhan, C. N.; Shimizu, T.; Yokomizo, T., International Union of Pharmacology XXXVII. Nomenclature for leukotriene and lipoxin receptors. *Pharmacol Rev* **2003**, *55* (1), 195-227.
2. Evans, J. F., Cysteinyl leukotriene receptors. *Prostaglandins Other Lipid Mediat* **2002**, *68-69*, 587-97.
3. Múlek, M.; Fekete, A.; Wiest, J.; Holzgrabe, U.; Mueller, M. J.; Högger, P., Profiling a gut microbiota-generated catechin metabolite's fate in human blood cells using a metabolomic approach. *J Pharm Biomed Anal* **2015**, *114* (Supplement C), 71-81.
4. Matz, F. Entwicklung von vif–Elongin-C–Interaktionsinhibitoren als neuartige HIV–Therapeutika. PhD Thesis, University of Würzburg, Würzburg, 2013.
5. Davoine, C.; Douki, T.; Iacazio, G.; Montillet, J. L.; Triantaphylides, C., Conjugation of keto fatty acids to glutathione in plant tissues. Characterization and quantification by HPLC-tandem mass spectrometry. *Anal Chem* **2005**, *77* (22), 7366-72.
6. Salazar, P.; Martín, M.; González-Mora, J. In *Polydopamine-modified surfaces in biosensor applications*, 2016; pp 385-396.

5. Summary

Leishmaniasis and trypanosomiasis are two of the most dangerous neglected protozoal diseases that occur mainly in tropical and subtropical regions worldwide affecting and threatening millions among the poor people. Nowadays, only few antileishmanial and antitrypanosomal drugs are available and characterized with severe side effects and a growing resistance against them. Therefore, discovering new antileishmanial and antitrypanosomal drugs is a pressing need.

The use of extracts and compounds from natural plants has a long history in the treatment of various protozoal diseases. For example, artemisinin (Nobel Prize, 2015) from traditional Chinese plant *Artemisia annua* is an effective medicine to combat multidrug resistant malaria.

This PhD thesis is dealing with the bioassay-guided fractionation of a dichloromethane extract of the aerial parts of *Achillea fragrantissima* with the aim of isolation and structure isolation of the antileishmanial and/or antitrypanosomal principles in the plant.

A preliminary screening of a dichloromethane extract of the aerial parts *Achillea fragrantissima* exhibited antileishmanial activity. Subsequently, the extract was subjected to a bioassay-guided fractionation disclosing the flavonoid Chrysofenol D to be one active ingredient.

As the preliminary investigations consumed the whole provided amount of the extract, the plant had to be grown from the seed in order to obtain enough plant material for extracts preparation. Bio-evaluation against *Trypanosoma brucei* of the dichloromethane extract of the aerial parts of *A. fragrantissima* exhibited a substantial antitrypanosomal activity ($IC_{50} < 10$ mg/mL). The fractionation of this extract by means of flash chromatography and subsequently preparative HPLC resulted in isolation and identification of three groups of natural products having an antitrypanosomal activity, namely seven sesquiterpene lactones including Achillolide

SUMMARY

A (2), two flavonoids chrysofenol D (8) and chrysofenetin (9), and four alkaloids including pellitorine (10) and the novel alkaloid 13.

Bioevaluation of isolated compounds revealed that sesquiterpene lactones are the most active principles in the plant. Structures and Bio-evaluation data are represented in Fig. S1.

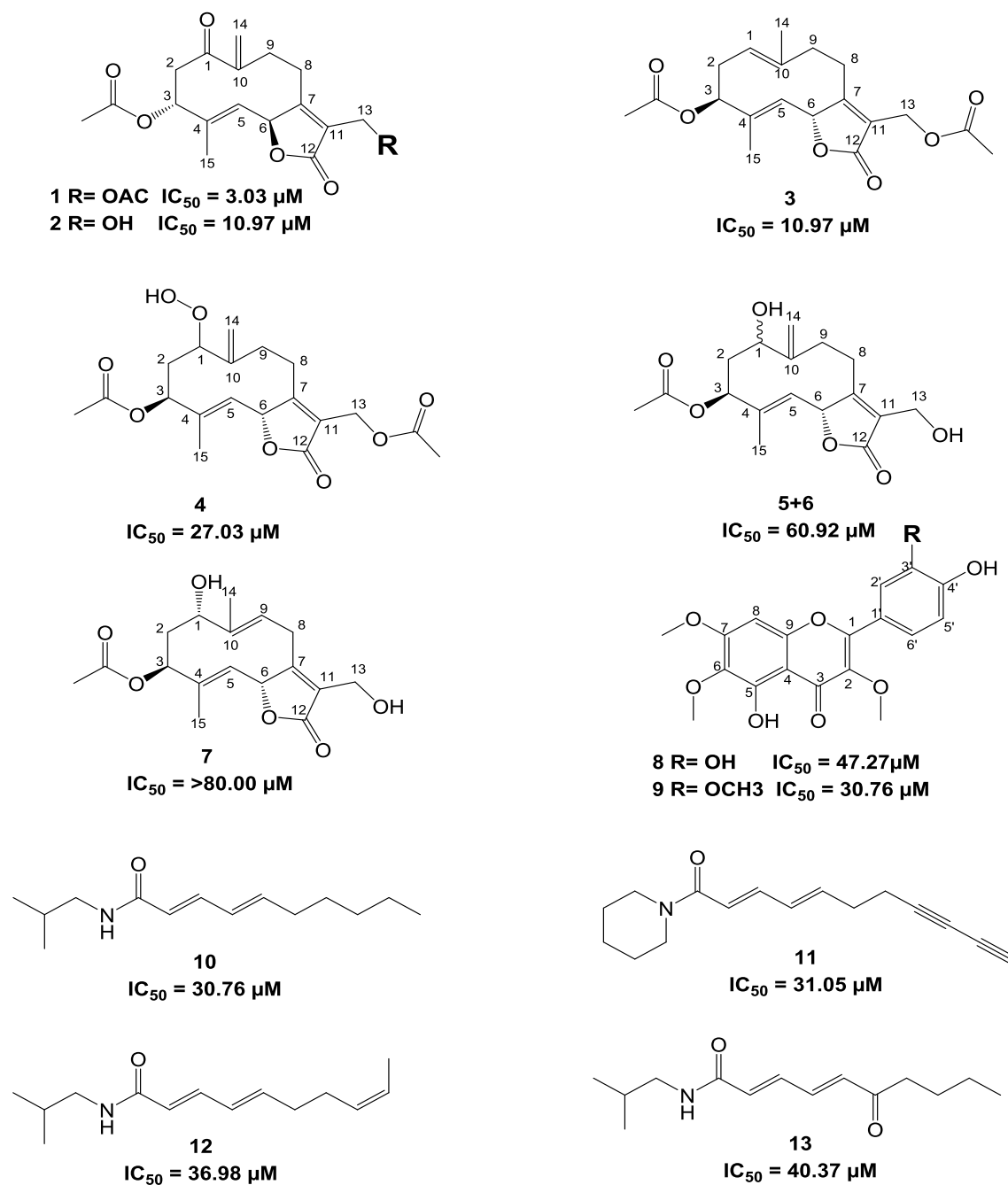


Fig. S1. Structures and bio-evaluation of isolated compounds.

SUMMARY

The antiprotozoal activities of sesquiterpene lactones and flavonoids were previously explored, whereas the activity of alkamides was almost unknown. Therefore, the structure of the alkamide **10** (pellitorine) was used as a scaffold for the synthesis of a compound library in order to derive structure-activity relationship (SAR). The compounds were varied at three key regions of the structure, namely the amide head, the central core, and the aliphatic chain.

With regard to antitrypanosomal activity, compounds bearing a basic amine moiety exhibited highly potent activities ranging from 0.72 to 3.90 μM . Compounds **26** and **27** (Fig. S2), having heptyl and hexyloxy chains, respectively, possessed the highest activities in the submicromolar concentration range along with the highest selectivity indices of 20.1 and 45.6. Notably, compounds **26** and **27** showed no toxicity in an *in vivo* model utilizing *Galleria mellonella* in concentrations up to 20 mM. These compounds can be regarded as new leads. However, further work has to be performed to elucidate the mode of action of these compounds.

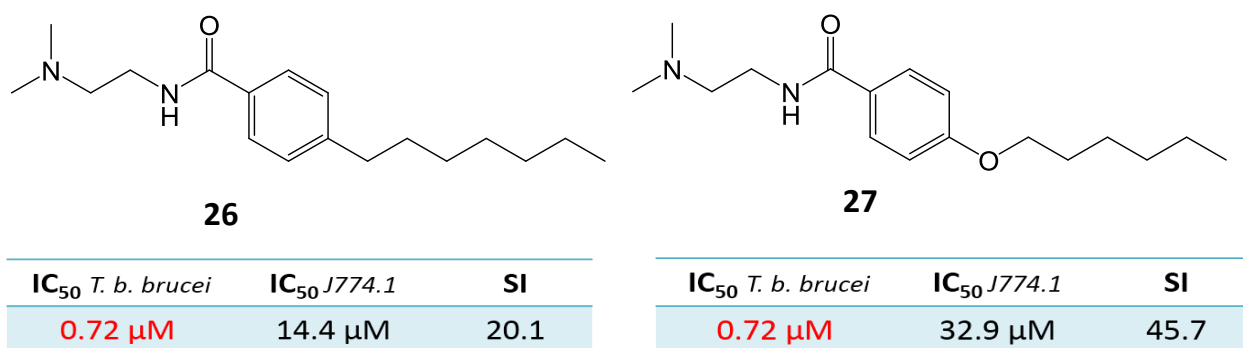


Fig. S2. Antitrypanosomal activity, cytotoxicity, and selectivity indices of compound **26** and **27**.

6. Zusammenfassung

Leishmaniose und die Schlafkrankheit sind zwei lebensgefährliche und vernachlässigte Protozoen-Erkrankungen, die hauptsächlich in tropischen und subtropischen Regionen weltweit auftreten und Millionen von armen Menschen bedrohen. Heutzutage gibt es nur wenige Arzneistoffe gegen Leishmanien und Trypanosomen. Die Wirkstoffe zeichnen sich durch schwere Nebenwirkungen und eine wachsende Unwirksamkeit auf Grund von Resistenzen aus. Daher ist die Entwicklung neuer Arzneistoffe gegen Leishmanien und Trypanosomen dringend nötig.

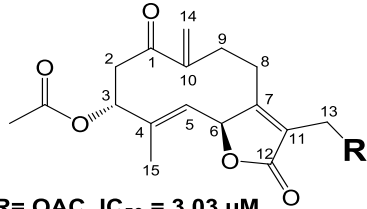
Die Verwendung von Extrakten und Verbindungen aus natürlichen Pflanzen hat eine lange Geschichte in der Behandlung von verschiedenen Protozoenerkrankungen. Zum Beispiel ist Artemisinin (Nobelpreis, 2015) aus der traditionellen chinesischen Pflanze *Artemisia annua* ein wirksamer Arzneistoff gegen multiresistente Malariaerreger.

Diese Dissertation beschäftigt sich mit der aktivitätsgeleiteten Fraktionierung eines Dichlormethanextrakts aus den oberirdischen Teilen von *Achillea fragrantissima* mit dem Ziel der Isolierung und Strukturaufklärung der anti-leishmanialen und/oder anti-trypanosomalen Verbindungen der Pflanze. Die vorläufige Testung eines Dichlormethanextrakts der oberirdischen Teile *Achillea fragrantissima* hatte Aktivität gegen Leishmanien gezeigt. Deshalb wurde der Extrakt aktivitätsgeleitet fraktioniert und das Flavonoid Chrysoptanol D als ein aktiver Bestandteil entdeckt.

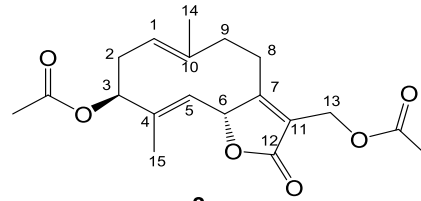
Da die Voruntersuchungen die gesamte bereitgestellte Menge des Extraktes verbraucht hatte, musste die Pflanze aus dem Samen gezogen werden, um genügend Pflanzenmaterial für die Extrahierungsherstellung zu erhalten. Biologische Testung des Dichlormethanextrakts der oberirdischen Teile von *A. fragrantissima* zeigte eine gute antitrypanosomale Aktivität ($IC_{50} < 10 \text{ mg/mL}$). Die Fraktionierung dieses Extrakts mittels Flash-Chromatographie und anschließender präparativer HPLC führte zur Isolierung und Identifizierung von drei Gruppen natürlicher Produkte

ZUSAMMENFASSUNG

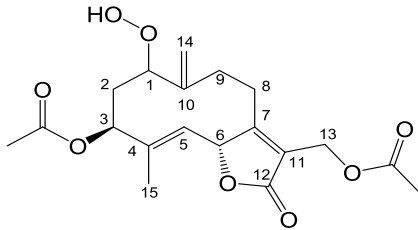
mit antitrypanosomaler Aktivität, nämlich sieben Sesquiterpenlactonen, einschließlich Achillolid A (**2**), zwei Flavonoiden Chrysosplenol D (**8**) und Chrysospletinetin (**9**) und vier Alkamide einschließlich Pellitorin (**10**) und das neue Alkamid **13**. Die biologische Testung der isolierten Verbindungen ergab, dass die Sesquiterpenlactone die aktivsten Verbindungen in der Pflanze sind. Die Strukturen und die Testergebnisse sind in Abb.S1 gezeigt.



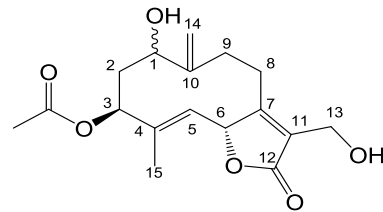
1 R= OAC $IC_{50} = 3.03 \mu M$
2 R= OH $IC_{50} = 10.97 \mu M$



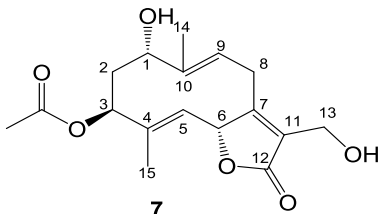
3
 $IC_{50} = 10.97 \mu M$



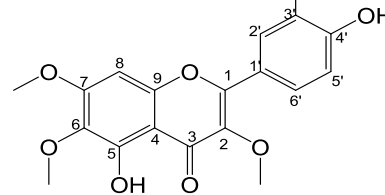
4
 $IC_{50} = 27.03 \mu M$



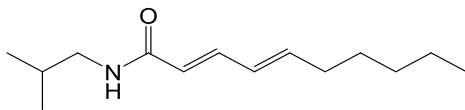
5+6
 $IC_{50} = 60.92 \mu M$



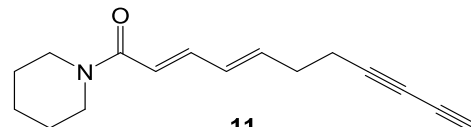
7
 $IC_{50} = >80.00 \mu M$



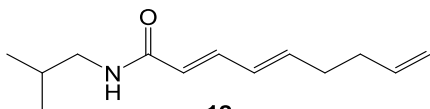
8 R= OH $IC_{50} = 47.27 \mu M$
9 R= OCH₃ $IC_{50} = 30.76 \mu M$



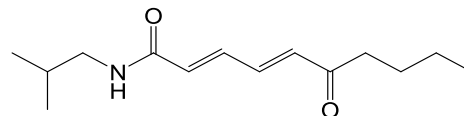
10
 $IC_{50} = 30.76 \mu M$



11
 $IC_{50} = 31.05 \mu M$



12
 $IC_{50} = 36.98 \mu M$



13
 $IC_{50} = 40.37 \mu M$

Abb. S1 Strukturen und biologische Bewertung der isolierten Substanzen.

ZUSAMMENFASSUNG

Die antiprotozoalen Aktivitäten der Sesquiterpenlactone und Flavonoide wurden bereits untersucht, während die Aktivität von Alkamiden nahezu unbekannt war. Daher wurde die Struktur des Alkamids **10** (Pellitorin) als Grundgerüst für die Synthese einer Substanzbibliothek verwendet, um Struktur-Wirkungs-Beziehungen zu analysieren. Die Verbindungen wurden an drei Schlüsselregionen der Struktur variiert, nämlich dem Amidkopf, dem zentralen Kern und der aliphatischen Kette. Im Hinblick auf die antitrypanosomale Aktivität zeigten Verbindungen, die eine basische Amingruppe trugen, hohe Aktivitäten im Bereich von 0,72 bis 3,90 μM .

Die Verbindungen **26** und **27** (Abb. S2) mit Heptyl- bzw. Hexyloxyketten besaßen die besten Aktivitäten im submikromolaren Konzentrationsbereich zusammen mit den höchsten Selektivitätsindizes von 20.1 und 45.6. Zudem zeigten die Verbindungen **26** und **27** in einem In-vivo-Modell der *Galleria mellonella* keine Toxizität in Konzentrationen von bis zu 20 mM. Diese Verbindungen können als neue Leitverbindungen angesehen werden. Es müssen jedoch weitere Experimente durchgeführt werden, um die Wirkungsweise dieser Verbindungen aufzuklären.

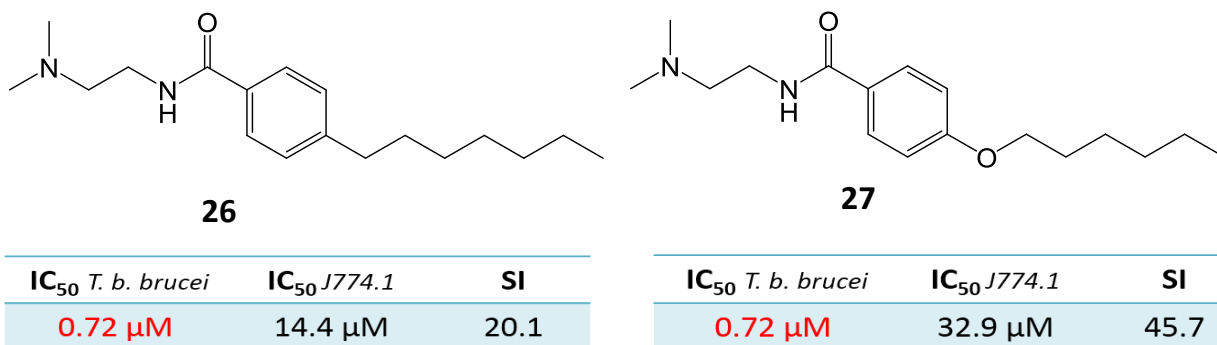


Abb. S2 Antitrypanosomale Aktivitäten, Zytotoxizitäten und die Selektivitätsindizes der Verbindungen **26** und **27**.

7. Experimental

7.1 General

All starting materials and reagents were purchased from Sigma Aldrich, Schnelldorf, Germany, and TCI Chemicals, Eschborn, Germany. NMR spectra were recorded on a Bruker Avance 400 Ultra Shield™ spectrometer (Bruker Biospin, Ettlingen, Germany) and a Bruker DMX 600 (Bruker, Karlsruhe, Germany) instrument which were calibrated using the residual undeuterated solvent as an internal reference (DMSO-*d*6: ¹H 2.50 ppm, ¹³C 39.5 ppm; methanol-*d*4: ¹H 3.31 ppm and 4.78 ppm, ¹³C 49.0 ppm, Chloroform-*d*1: ¹H 7.24 ppm, ¹³C 77.2 ppm, Deuterium Oxide: ¹H 4.79 ppm, Toluene-*d*8: ¹H 2.09, 6.98 ppm, 7.00, and 7.09 ppm, ¹³C 20.4, 125.5, 128.3, and 129.2 ppm). Coupling constants (*J*) are given in Hertz.

For determining the purity and the retention times of all compounds, analytical HPLC was conducted on a Shimadzu system (Hilden, Germany) equipped with a DGU-20A3R degassing unit, a LC20AB liquid chromatograph, and a SPD20A UV/Vis detector. The stationary phase was a Synergi fusion-RP (150 x 4.6 mm, 4 μm) column (Phenomenex, Aschaffenburg, Germany). The following gradient elution was applied: solvent A: water with 0.1% formic acid, solvent B: MeOH with 0.1% formic acid. Solvent A from 0% to 100% in 13 min, then 100% A for 5 min, from 100% to 5% A in 1 min, and 5% for 4 min. The flow rate was set to 1.0 mL/min. UV detection was performed at 254 nm. ESI mass spectral data were acquired on a Shimadzu LCMS-2020 instrument (Hilden, Germany). IR spectra were recorded on a Jasco FT/IR-6100 spectrometer with an ATR unit (Groß-Umstadt, Germany) at room temperature. Flash column chromatography was performed on an Interchim Puri-Flash 430 instrument (Ultra Performance Flash Purification) connected to an Interchim Flash ELSD (Montluçon, France). Preparative HPLC was performed using an Agilent 1100 preparative HPLC instrument (Waldbronn, Germany) and a fraction collector and multiple wavelength detector. *Galleria mellonella* at the final larval stage were purchased from Mouse Live Bait (Balk, The Netherlands) [1]. The

physicochemical properties were measured on Sirius T3 device (Sirius Analytical, East Sussex, UK).

7.2 Preliminary investigations

Initially, a dichloromethane extract (0.89 gr) of *A. fragrantissima* collected in Palestine was screened using the corresponding *Alamar-Blue* assay [2] revealing a substantial anti-leishmanial activity. Therefore, the extract was fractionated by means of flash chromatography using a linear gradient of chloroform: solvent A and methanol: solvent B (B% from 0% to 100% in 25 min) yielding 17 fractions, which were bio-evaluated against leishmania presenting fraction 11 to be the most active fraction. Subsequently, Fraction 11 was subfractionated using preparative HPLC and Nucleosil C18, 250 mm × 10 mm, 5 µm column (Macherey-Nagel, Düren, Deutschland) applying the following gradient: solvent A: water, solvent B: acetonitrile, 10% B (2 min), 30% B (3 min), 100% B (25 min), 80% B (33 min), 40% B (37 min), 10% B (38 min); flow rate: 2.4 mL/min yielding 20 fractions. Biological assessment of these fractions revealed four active fractions; fraction 12 (RT: 13.49 min, 1.5 mg), fraction 15 (RT: 17.32 min, 1.8 mg), fraction 19 (RT: 20.54 min, 1.0 mg), and fraction 20 (RT: 21.56 min, 0.4 mg). The active fractions were subjected to structure elucidation by means of NMR, MS, and IR. The chemical structure of one active compound could be assigned to chrysosplenol D, whereas the structures of the other three compounds could not be elucidated because of their small amounts and insufficient purity.

As the preliminary investigations consumed the whole provided amount of the first DCM extract of *A. fragrantissima* and because it was not possible due to political reasons at that time to obtain more of the extract or the plants from Palestine, the plant had to be grown from the seeds.

7.3 Plant material

Seeds of *Achillea fragrantissima* were obtained from a suburb near Homs, Syria. 100 seeds were planted in spring in a greenhouse of the botanical garden of the university of Würzburg. The fully-grown plants were collected in summer and dried at room temperature in shade for 20 days until constant weight (harvest approx.700 g). The identity of the seeds and the grown plants was verified by Dr. Hildebrandt and Dr. Vogg at the botanical garden, University of Würzburg [1].

7.4 Extraction and Isolation

The aerial parts of *A. fragrantissima* were powdered using a laboratory grinder. The pulverized plant material (100 g) was extracted for 24 hours at room temperature with dichloromethane by stirring. The extract was filtered, followed by complete drying *in vacuo* to give a crude residue (1.96%; *w/w*). Fractionation of the extract was performed using flash chromatography using hexane A, ethyl acetate B, and methanol C as solvents applying the following elution system: 70% A + 30% B (15 min), 100% B (55 min), 100% B (65 min), 100% C (85 min) yielding 7 major fractions (Fig. 30).

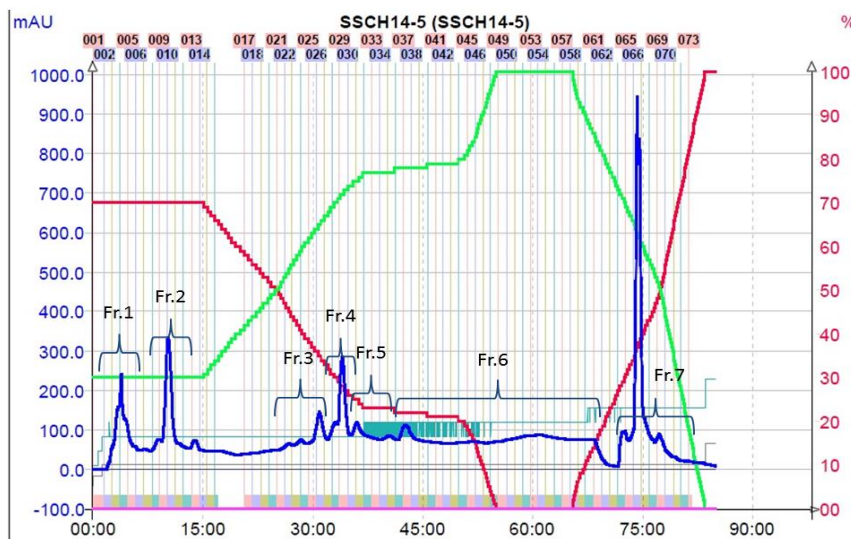


Fig. 28 Fractionation of dichloromethane extract of *A. fragrantissima* by means of flash chromatography.

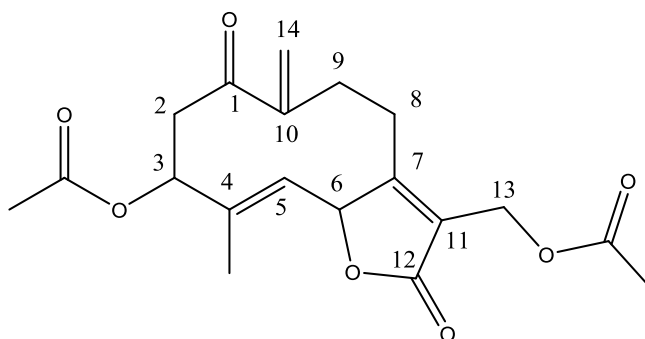
EXPERIMENTAL

After bio-evaluation of each fraction *in vitro* against *T.b brucei* using the *Alamar-Blue* assay [3]. The active fractions (F2- F7) ($IC_{50} < 10$ mg/mL) were sub-fractionated by means of preparative HPLC using a semi-preparative Synergy 4 μ m MAX-RP 80A column 150 x 10 mm (Phenomenex, Aschaffenburg, Germany). The following gradient was applied: solvent A: water, solvent B: acetonitrile; 10% B (2 min), 30% B (3 min), 100% B (25 min), 10% B (27 min). Fractionation of fraction 2 led to the isolation of Pellitorine **10** (RT: 22.19 min, 3.0 mg) and compound **12** (RT: 20.13 min, 1.6 mg). From fraction 3 compound **3** (RT: 17.77 min, 22.0 mg) and compound **13** (RT: 17.03 min, 1.8 mg) were isolated. Fraction 4 contained three compounds, compound **1** (RT: 14.83 min, 16.0 mg), compound **9** (RT: 16.67 min, 6.0 mg), and compound **11** (RT: 18.62 min, 2.0 mg). Fractionation of fraction 5 resulted in isolation of compound **4** (RT: 12.70 min, 3.0 mg) and compound **8** (RT: 14.14 min, 7.0 mg). Fraction 6 contained compound 2 (RT: 11.09 min, 12 mg). From fraction 7 three compounds were isolated, compounds **5** and **6** as mixture (RT: 8.68 min, 33 mg) and compound **7** (RT: 9.05 min, 17 mg). The structures of all isolated compounds were elucidated by means of NMR, infrared (IR), and mass spectroscopy (MS).

EXPERIMENTAL

7.5 Characterization of plant isolated compounds

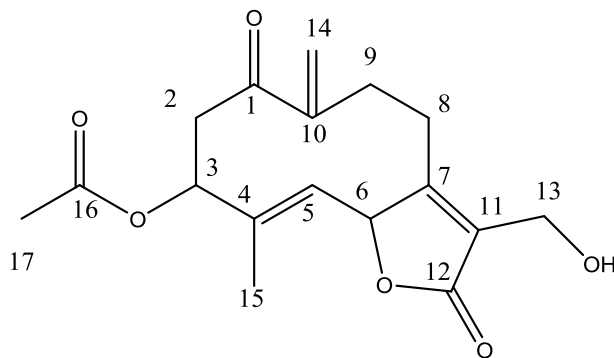
(E)-(9-Acetoxy-10-methyl-6-methylene-2,7-dioxo-2,4,5,6,7,8,9,11a-octahydrocyclodeca[b]furan-3-yl)methyl acetate; 1



Compound **1** was isolated from fraction 4 as colorless crystals; Purity (HPLC-UV) 89%; Retention time (HPLC): 8.60 min; Chemical formula: $C_{19}H_{22}O_7$; **IR (ATR), $\tilde{\nu}$ [cm⁻¹]:**1752, 1722, 1666, 1370, 1217, 1010, 941; **ESI-MS** (m/z): 363.0 ([M+H]⁺, found), 363.14 ([M+H]⁺, calculated); **¹H-NMR** (Methanol-d₄, δ [ppm], J [Hz]): 5.96 (d, $J = 1.1$, 1H, H-14a), 5.81 (d, $J = 1.8$, 1H, 14b), 5.52-5.62 (m, 2H, H-6, 3), 4.80-4.91 (m, 3H, H-5, 13), 3.73 (dd, $J = 13.3, 8.5$, 1H, H-2b), 3.02 (m, 1H, H-8a), 2.94 (m, 1H, H-9b), 2.70 (dd, $J = 13.3, 9.5$, H-2a), 2.35 (m, 1H, H-8b), 2.21 (m, 1H, H-9a), 2.09 (d, $J = 0.6$, 6H, H-17, 19), 1.79 (d, $J = 1.2$, 3H, H-15); **¹³C-NMR** (Methanol-d₄, δ [ppm]): 199.9, 174.2, 171.6, 171.0, 170.2, 149.4, 138.1, 127.1, 125.9, 124.1, 80.5, 76.6, 56.0, 44.2, 33.1, 24.4, 20.2, 20.0, 10.2.

EXPERIMENTAL

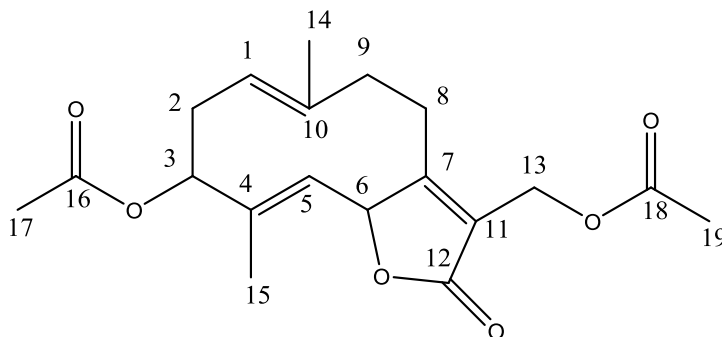
(E)-3-(Hydroxymethyl)-10-methyl-6-methylene-2,7-dioxo-2,4,5,6,7,8,9,11a-octahydrocyclodeca[b]furan-9-yl acetate; 2



Compound **2** was isolated from fraction 6 as a colorless oil; Purity (HPLC-UV) 97%; Retention time (HPLC): 7.80 min; Chemical formula: $C_{17}H_{20}O_6$; **IR (ATR), $\tilde{\nu}$ [cm⁻¹]:** 3446, 2932, 1741, 1670, 1237, 1013; **ESI-MS** (m/z): 320.95 ([M+H]⁺, found), 321.13 ([M+H]⁺, calculated); **¹H-NMR** (Methanol-d₄, δ [ppm], J [Hz]): 5.94 (d, J = 1.0, 1H, H-14b), 5.82 (d, J = 1.7, 1H, 14a), 5.48- 5.62 (m, 2H H-3,6), 4.87 (d, J = 10.1, 1H, H-5), 4.33 (m, 2H, H-13), 3.74 (dd, J = 13.4, 8.5, 2H, H-2b), 2.86- 3.06 (m, 2H, H-9b, 8b), 2.67 (dd, J = 13.4, 9.4, 1H, H-2a), 2.45 (m, 1H, H-9a), 2.14 (m, 1H, H-8a), 2.10 (s, 3H, H-17), 1.78 (d, J = 1.2, 3H, H-15); **¹³C-NMR** (Methanol-d₄, δ [ppm]): 200.5, 175.6, 171.6, 168.6, 150.1, 138.0, 128.6, 128.3, 126.5, 80.8, 77.3, 54.7, 44.9, 34.0, 24.8, 20.8, 10.8.

EXPERIMENTAL

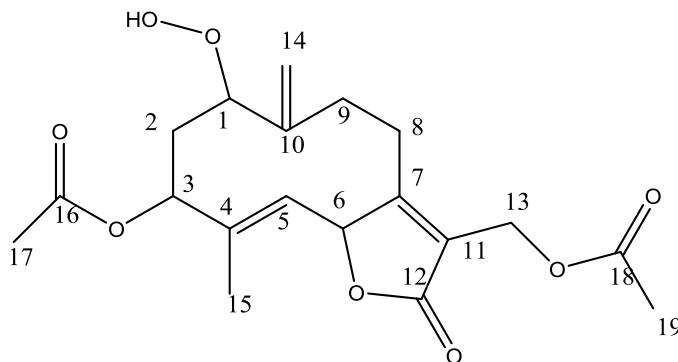
((6Z,10E)-9-Acetoxy-6,10-dimethyl-2-oxo-2,4,5,8,9,11a-hexahydrocyclodeca[b]furan-3-yl)methyl acetate; **3**



Compound **3** was isolated from fraction 3 as a white solid substance; Purity (HPLC-UV) 80%; Retention time (HPLC): 9.78 min; Chemical formula: $C_{19}H_{24}O_6$; **ESI-MS** (m/z): 349.05 ($[M+H]^+$, found), 349.16 ($[M+H]^+$, calculated); **1H -NMR** (Methanol- d_4 , δ [ppm], J [Hz]): 5.72 (d, $J = 10.3$, 1H, H-6), 5.13 (m, 1H, H-3), 4.74-4.91 (m, 3H, H-1, 13), 4.50 (m, 1H, H-5), 3.05 (dd, $J = 13.8, 7.7$, 1H, H-8b), 2.56 (m, 1H, H-9b), 2.37-2.49 (m, 2H, H-2), 2.43 (m, 1H, H-8a), 2.26 (m, 1H, H-9a), 2.09 (s, 3H, H-17), 2.06 (s, 3H, H-19) 1.75 (d, $J = 1.1$, 3H, H-15), 1.64 (s, 3H, H-14); **^{13}C -NMR** (Methanol- d_4 , δ [ppm]): 174.8, 172.8, 172.0, 139.5, 138.9, 125.9, 125.8, 123.5, 82.2, 79.8, 56.4, 41.2, 32.2, 26.7, 20.9, 20.6, 16.3, 11.8.

EXPERIMENTAL

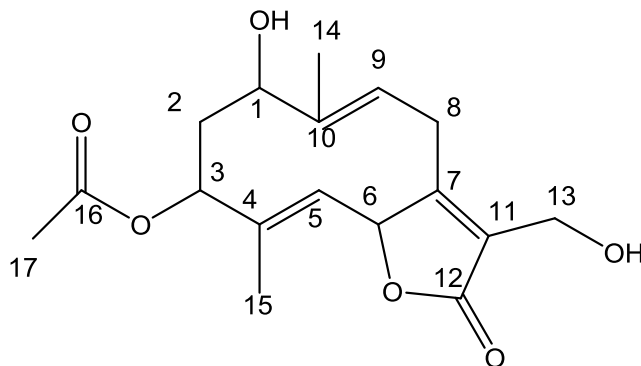
(E)-(9-Acetoxy-7-hydroperoxy-10-methyl-6-methylene-2-oxo-2,4,5,6,7,8,9,11a-octahydrocyclodeca[b]furan-3-yl)methyl acetate; 4



Compound **4** was isolated from fraction **5** as a colorless oil; Purity (HPLC-UV) 85%; Retention time (HPLC): 8.12 min; Chemical formula: C₁₉H₂₄O₈; **IR (ATR), $\tilde{\nu}$ [cm⁻¹]:** 2940, 1731, 1367, 1225, 1023, 911; **ESI-MS** (m/z): 349.05 ([M+H]⁺, found), 349.16 ([M+H]⁺, calculated); **¹H-NMR** (Methanol-d₄, δ [ppm], *J* [Hz]): 5.68 (d, *J* = 10.2, 1H, H-6), 5.31 (d, *J* = 1.5, 1H, 14b), 5.03-5.23 (m, 3H, H-14a, 3,5), 4.82 (m, 2H, H-13), 4.22 (m, 1H, H-1), 3.32 (m, 1H, H-8b), 2.69 (m, 1H, H-9b), 2.46 (m, H-8a), 2.27 (m, H-2b), 2.08 (s, H-17), 2.06 (s, H-19), 2.02 (m, H-2a), 1.97 (m, H-9a), 1.79 (s, H-15); **¹³C-NMR** (Methanol-d₄, δ [ppm]): 174.8, 172.2, 171.6, 171.3, 148.9, 141.2, 124.2, 123.6, 116.5, 88.5, 81.3, 77.6, 56.1, 34.9, 26.5, 24.8, 20.9, 20.6, 11.7.

EXPERIMENTAL

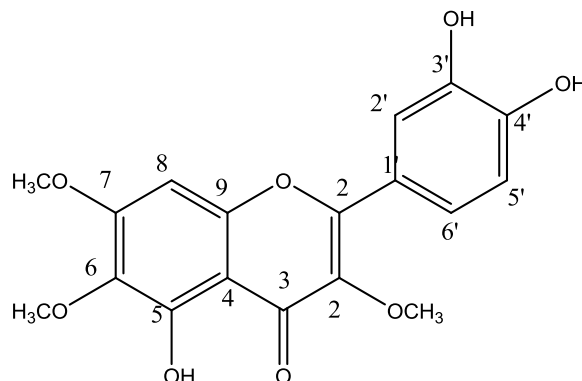
(5*Z*,10*E*)-7-Hydroxy-3-(hydroxymethyl)-6,10-dimethyl-2-oxo-2,4,7,8,9,11a-hexahydrocyclodeca[b]furan-9-yl acetate; **7**



Compound **7** was isolated from fraction 7 as white crystals; Purity (HPLC-UV) 94%; Retention time (HPLC): 7.57 min; Chemical formula: C₁₇H₂₂O₆; **IR (ATR), $\tilde{\nu}$ [cm⁻¹]:** 3317, 2940, 1743, 1717, 1671, 1267, 1008, 967; **ESI-MS** (m/z): 323.00 ([M+H]⁺, found), 323.14 ([M+H]⁺, calculated); **¹H-NMR** (Methanol-d₄, δ [ppm], *J* [Hz]): 5.66 (d, *J* = 10.8, 1H, H-6), 5.20 (m, 1H, H-9), 4.89-4.96 (m, 2H, H-3,5), 4.27-4.40 (m, 3H, H-1, 13), 3.38 (m, 1H, H-8b), 3.04 (t, *J* = 12.3, 1H, H-8a), 2.16 (m, 1H, H-2b), 2.05 (s, 3H, H-17), 1.98 (m, 1H, H-2a), 1.95 (s, 3H, H-15), 1.74 (s, 3H, H-14); **¹³C-NMR** (Methanol-d₄, δ [ppm]): 175.7, 171.9, 166.7, 138.2, 137.8, 127.4, 126.8, 125.6, 81.8, 77.5, 65.9, 54.9, 34.1, 26.6, 20.9, 17.1, 11.4.

EXPERIMENTAL

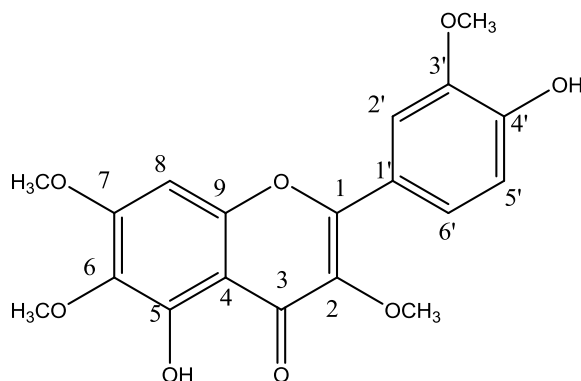
2-(3,4-Dihydroxyphenyl)-5-hydroxy-3,6,7-trimethoxy-4H-chromen-4-one; **8**



Compound **8** was isolated from fraction 5 as a yellow solid substance; Purity (HPLC-UV) 97%; Retention time (HPLC): 9.64 min; Chemical formula: $C_{18}H_{16}O_8$; **IR (ATR)**, $\tilde{\nu}$ [cm^{-1}]: 3367, 2932, 1733, 1652, 1593, 1457, 1355, 1278, 1004; **ESI-MS** (m/z): 361.10 ($[M+H]^+$, found), 361.09 ($[M+H]^+$, calculated); **1H -NMR** (Methanol- d_4 , δ [ppm], J [Hz]): 7.66 (d, $J = 1.7$, 1H, H-2'), 7.56 (dd, $J = 8.4, 1.5$, 1H, H-6'), 6.91 (d, $J = 8.4$, 1H, H-5'), 6.75 (d, $J = 1.4$, 1H, H-8), 3.96 (s, 3H, 7-OCH₃), 3.83 (s, 3H, 3-OCH₃), 3.81 (s, 3H, 6-OCH₃); **^{13}C -NMR** (Methanol- d_4 , δ [ppm]): 180.2, 160.6, 158.5, 154, 153.4, 150.1, 146.5, 139.5, 133.3, 122.8, 122.3, 116.6, 116.4, 107.2, 91.9, 61, 60.5, 56.9.

EXPERIMENTAL

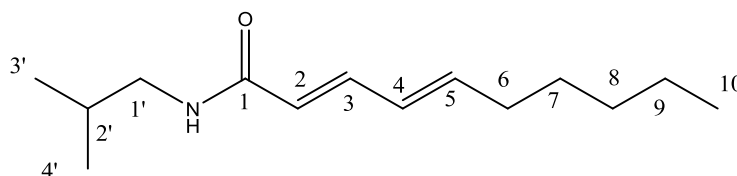
5-Hydroxy-2-(4-hydroxy-3-methoxyphenyl)-3,6,7-trimethoxy-4H-chromen-4-one; **9**



Compound **9** was isolated from fraction 4 as a yellow Solid substance; Purity (HPLC-UV) 95%; Retention time (HPLC): 10.18 min; Chemical formula: $C_{19}H_{18}O_8$; **IR (ATR)**, $\tilde{\nu}$ [cm^{-1}]: 3241, 2936, 1650, 1589, 1512, 1460, 1428, 1343, 1272, 1159, 801; **ESI-MS** (m/z): 374.95($[M+H]^+$, found), 375.1 ($[M+H]^+$, calculated); **1H -NMR** (Methanol- d_4 , δ [ppm], J [Hz]): 7.75 (d, $J = 2.1$, 1H, H-2'), 7.69 (dd, $J = 8.5, 2.1$, 1H, H-6'), 6.95 (d, $J = 8.5$, 1H, H-5'), 6.80 (s, 1H, H-8), 3.98 (s, 3H, 7-OCH₃), 3.95 (s, 3H, 3'-OCH₃), 3.84 (s, 3H, 6-OCH₃), 3.82 (s, 3H, 3-OCH₃); **^{13}C -NMR** (Methanol- d_4 , δ [ppm]): 180.31, 160.73, 158.3, 154, 153.4, 151.3, 149, 139.6, 133.3, 123.9, 122.7, 116.6, 112.8, 107.3, 92.1, 61, 60.6, 57.1, 56.6 .

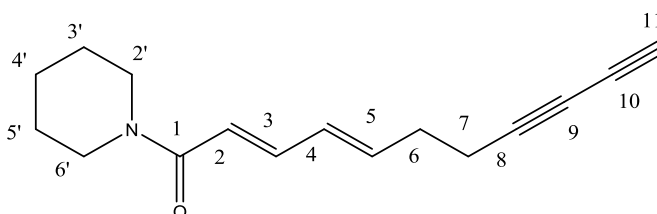
EXPERIMENTAL

(2E,4E)-N-Isobutyldeca-2,4-dienamide (*Pellitorine*); **10**



Compound **10** was isolated from fraction 2 as a white solid substance; Purity (HPLC-UV) 99%; Retention time (HPLC): 11.06 min; Chemical formula: C₁₄H₂₅NO; **IR (ATR), $\tilde{\nu}$ [cm⁻¹]:** 2959, 2951, 2925, 2867, 1654, 1616, 1545, 1253, 992; **ESI-MS** (m/z): 224.05 ([M+H]⁺, found), 224.20 ([M+H]⁺, calculated); **¹H-NMR** (Methanol-d₄, δ [ppm], *J* [Hz]): 7.11 (dd, *J* = 15.1, 10.7, 1H, H-3), 6.20 (ddd, *J* = 15.1, 10.7, 0.6, 1H, H-4), 6.10 (m, 1H, H-5), 5.92 (d, *J* = 15.1, 1H, H-2), 3.06 (d, *J* = 6.9, 1H, H-1'), 2.17 (m, 2H, H-6), 1.79 (m, 1H, H-2'), 1.44 (m, 2H, H-7), 1.33 (m, 4H, H-8, 9), 0.89-0.93 (m, 9H, H-3',4, 10); **¹³C-NMR** (Methanol-d₄, δ [ppm]): 169.2, 144.0, 142.1, 129.8, 123.01, 48.0, 33.9, 32.5, 29.7, 29.7, 23.5, 20.5, 14.3.

(2E,4E)-1-(Piperidin-1-yl)undeca-2,4-dien-8,10-diyn-1-one; **11**

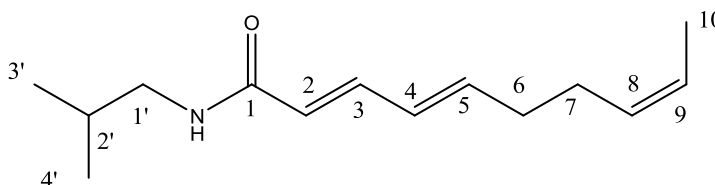


Compound **11** was isolated from fraction 4 as a yellow solid substance; Purity (HPLC-UV) 84%; Retention time (HPLC): 10.06 min; Chemical formula: C₁₆H₁₉NO; **IR (ATR), $\tilde{\nu}$ [cm⁻¹]:** 2927, 1586, 1441, 1253, 996 ; **ESI-MS** (m/z): 242.0 ([M+H]⁺, found), 242.15 ([M+H]⁺, calculated); **¹H-NMR** (Methanol-d₄, δ [ppm], *J* [Hz]): 7.16 (dd, *J* = 14.8, 10.9, 1H, H-3), 6.52 (d, *J* = 14.8, 1H, H-2), 6.38 (dd, *J* = 15.2, 10.9,

EXPERIMENTAL

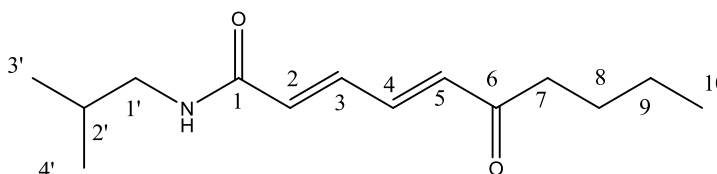
1H, H-4), 6.1 (m, 1H, H-5), 3.6 (m, 4H, H-2',6'), 2.55 (s, H-11), 2.4 (m, 4H, H-6, 7), 1.70 (m, 2H, H-4'), 1.60 (m, 4H, H-3',5'). ¹³C NMR δ: 167.7, 143.8, 131.5, 120.7, 77.3, 68.9, 66.8, 66.3, 48.1, 44.5, 32.4, 32.4, 27.8, 26.8, 25.5, 19.2.

(2E,4E,8Z)-N-Isobutyldeca-2,4,8-trienamide, 12



Compound **12** was isolated from fraction 2 as a yellow oil; Purity (HPLC-UV) 97%; Retention time (HPLC): 10.71 min; Chemical formula: C₁₄H₂₃NO; **ESI-MS** (m/z): 222.10 ([M+H]⁺, found), 222.18 ([M+H]⁺, calculated); **¹H-NMR** (Methanol-d₄, δ [ppm], *J* [Hz]): 7.10 (dd, *J* = 15.1, 10.6, 1H, H-3), 6.21 (dd, *J* = 15.1, 10.6, 1H, H-4), 6.10 (m, 1H, H-5), 5.93 (d, *J* = 15.1, 1H, H-2), 5.47 (m, 1H, H-9), 5.39 (m, 1H, H-8) 3.06 (d, *J* = 6.9, 2H, H-1'), 2.21 (m, 2H, H-6,7), 1.79 (m, 1H, H-2'), 1.60 (m, 3H, H-10), 0.92 (m, 6H, H-3',4'). ¹³C NMR δ: 169.1, 143.2, 142.0, 130.4, 130.0, 125.4, 123.2, 48.0, 33.8, 29.7, 27.2, 20.4, 12.8.

(2E,4E)-N-Isobutyl-6-oxodeca-2,4-dienamide; 13



Compound **13** was isolated from fraction 3 as a white solid substance; Purity (HPLC-UV) 93%; Retention time (HPLC): 9.85 min; Chemical formula: C₁₄H₂₃NO₂; **IR (ATR), $\tilde{\nu}$ [cm⁻¹]:** 3358, 2920, 2850, 1658, 1632; **ESI-MS** (m/z): 238.10 ([M+H]⁺, found), 238.18 ([M+H]⁺, calculated); **¹H-NMR** (Methanol-*d*₄, δ [ppm], *J* [Hz]): 7.25 (m, 2H, H-3, 4), 6.51 (d, *J*=14.9, 1H, H-5), 6.44 (d, *J* = 14.5, 1H, H-2), 3.1 (d, *J* =

6.9, 2H, H-1'), 2.66 (t, 2H, $J = 7.3$, H-7), 1.82 (m, 1H, H-2'), 1.59 (m, 2H, H-8), 1.35 (m, 2H, H-9), 0.94 (m, 9H, H-10, 3', 4'); $^{13}\text{C-NMR}$ (Methanol- d_4 , δ [ppm]): 202.8, 167.4, 140.6, 138.7, 135.5, 133.2, 48.1, 41.5, 29.7, 27.3, 23.3, 20.5, 14.2.

7.6 Biological assays

7.6.1 Anti-trypanosomal assay

The aim of this test is the investigation of the metabolism-inhibiting effect of the test substances against trypomastigote forms of trypanosoma. In principle the test is performed by incubation of different concentrations of the test substances with the cultivated Trypanosomes and then adding a reduction sensitive indicator, *Alamar Blue*. As next the absorption will be photometrically measured after total 72 h. The increase of absorption is a direct proportional to the metabolic activity of the cells. The absence of the metabolic activity can be considered as an evidence of the cytotoxic effect of the test substances. Trypanosomes show an exponential growth rate, so that the number of the cells will be doubled every eight hours.

The fractions, the extracts as well as isolated and synthesized compounds were tested towards trypanosoma according to Rüz et al. [3]. Trypomastigote forms of *T.b. brucei* laboratory strain TC221 were cultivated in Balz medium. A defined number of parasites (10^4 trypanosomes per mL) was tested in 96-well plates against different concentrations of the test substances in a final volume of 200 μL (1% DMSO in Balz medium). Positive (trypanosomes added to culture medium) and negative controls (test substance without trypanosomes) were run with each plate. The plates were incubated at 37 °C in an atmosphere of 5% CO_2 . After 24 h additional 20 μL of *Alamar-Blue* was added to each well. A reading was done at 48 h. Any effect of the test substances was quantified as IC_{50} values by linear interpolation of three different measurements. The activity of the test substances was measured by light absorption using MR 700 microplate reader (Dynatech Engineering Ltd, Willenhall, UK) at a wavelength of 550 nm with a reference wavelength of 630 nm.

7.6.2 Cytotoxicity assay

The experiments were carried out according to Hiltensperger et al. [4]. The macrophage cell line J774.1 was maintained in complete Click RPMI medium. For the experimental procedures, cells were detached from the flasks using a rubber scraper and cell densities were adjusted to having 2×10^4 cells per mL. J774.1 macrophages were seeded into 96-well plates and were incubated (37 °C, 5% CO₂, 95% humidity) overnight to allow attachment and recovery. A set of increasing concentrations (1, 2.5, 5, 10, 25, 50, 75 and 100 µM) of the tested compounds (125 µL) and complete RPMI medium were transferred into the cell culture plates and allowed to incubate for 24 h. After adding 10 µL of the cell proliferation reagent WST-1, incubation was continued at the same conditions. The plates were read after 30 min and 2 h, respectively, at $\lambda = 440$ nm. Control experiments to evaluate the effect of cell density, incubation time, and DMSO concentration were performed. Absorbance in the absence of any compounds was set as 100% of growth control.

7.6.3 In vivo toxicity assay (*Galleria mellonella* larvae)

Toxicity assessment in *Galleria mellonella* was performed as described previously by Gibreel and Upton [5] with minor modifications. Larvae were used immediately upon arrival for toxicity evaluation experiments and were considered healthy if they were clear in color and free of any spots or pigmentation (weighing approximately 200 - 250 mg). Solutions of the test substances **26** and **27** having concentrations ranging from 1.25 – 20 mM were prepared in endotoxin-free PBS + 10% DMSO (vehicle). 20 µl of test substance was injected in the last left pro-leg of a larvae using insulin syringes (BD Micro-Fine™ + Demi). Ten larvae per group were used. Four control groups were included in the experiment: one group received no injection, one group was injected 20 µl of endotoxin-free PBS, one group was injected 20 µl of vehicle control, and one group received 20 µl methanol as positive control. All groups of larvae were incubated in the absence of light at 37 °C in Petri dishes. Larval survival rates were recorded every 24 h for 120 h. Larvae not

EXPERIMENTAL

responding to touch were scored dead and vice versa. Finally, Kaplan-Meier survival curves were generated with GraphPad Prism v 6.04 and statistical significance of the curves was evaluated using the Log-rank (Mantel-Cox) and Gehan-Breslow-Wilcoxon test utilizing the software; $p < 0.05$, statistically significant.

7.7 Synthesis and characterization of compounds 14- 40.

7.7.1 General procedure A for synthesis of compounds 14 –19 and 22-40.

To a mixture of 1 equiv. of the corresponding carboxylic acid, 4 equiv. of triethylamine, 1 equiv. of the corresponding amine in dichloromethane (10 mL), and 1 equiv. of propylphosphonic anhydride solution ($T_{3P}^{\text{®}}$) was slowly added at 0 °C under Argon atmosphere. The reaction mixture was allowed to warm to RT and was stirred for 5 h. The reaction was diluted with dichloromethane (20 mL) and saturated aqueous NaCl solution (30 mL). The aqueous layer was extracted 3 times with dichloromethane (90 mL). The combined organic layers were dried over Na_2SO_4 . The solvent was removed *in vacuo*.

7.7.2 General procedure B for synthesis of compounds 20 and 21.

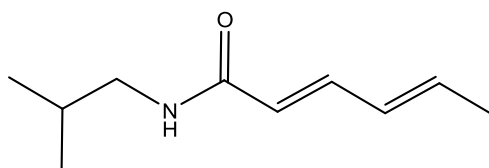
1 equiv. of the corresponding carboxylic acid and 5 equiv. of 4-methylmorpholine (NMM) were dissolved in abs. dimethylformamide (10 mL) at RT under Argon atmosphere. After cooling to 0 °C, 4 equiv. of i-butyl chloroformate were added and the mixture was stirred for 1 h. Then, 4 equiv. of the corresponding amine were added, and the mixture was stirred for additional 2 h at RT. The solvent was removed *in vacuo*, and 20 mL of water were added. The aqueous solution was extracted 3 times with ethyl acetate (150 mL). The combined organic layers were dried over Na_2SO_4 . The solvent was removed *in vacuo*.

EXPERIMENTAL

7.7.3 Purification of synthesized compounds 14 - 40.

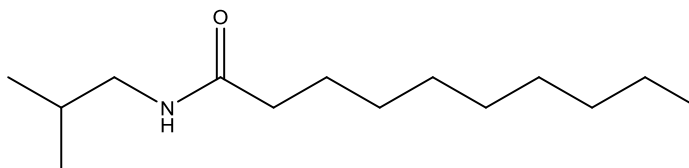
The purification of all synthesized compounds **14** - **40** was performed by means of flash chromatography using a mixture of cyclohexane and ethyl acetate (70 : 30) as solvent system over 20 min for compounds **14** – **19** (Method A), and dichloromethane and methanol gradient (100 : 0 to 85 : 15) over 35 min for compounds **20** – **40** (Method B).

(2E,4E)-N-Isobutylhexa-2,4-dienamide; **14**



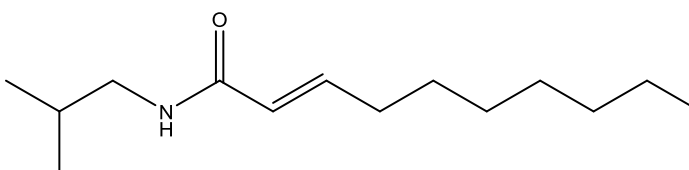
1.0 eq. (112 mg, 1.0 mmol) (2E,4E)-hexa-2,4-dienoic acid was reacted with 1.0 eq. (318 mg, 0.60 mL, 1.0 mmol) propylphosphonic anhydride solution (T3P[®]), 4 eq. triethylamine (101 mg, 0.60 mL, 4.0 mmol) and 1.0 eq (73 mg, 0.10 mL, 1 mmol) isobutyl amine according to general procedure A, The product was purified by means of flash chromatography using Method A to afford the desired amide **14** (157 mg, 0.94 mmol).

White solid; Yield 94%; Purity (HPLC-UV) 99%; Retention time (HPLC): 9.20 min; Chemical formula: C₁₀H₁₇NO; **IR (ATR), $\tilde{\nu}$ [cm⁻¹]:** 3307, 2959, 2871, 1654; **ESI-MS (m/z):** 168.05 ([M+H]⁺, found), 168.13 ([M+H]⁺, calculated); **¹H-NMR (Methanol-*d*₄, δ [ppm], *J* [Hz]):** 7.10 (dd, *J* = 15.1, 10.6 1H), 6.22 (m, 1H), 6.11 (m, 1H), 5.91 (dd, *J* = 15.1, 0.6, 1H), 3.06 (d, *J* = 6.9, 2H), 1.81 (m, 4H), 0.92 (d, *J* = 6.9, 6H); **¹³C-NMR (Methanol-*d*₄, δ [ppm]):** 169.2, 142.0, 131.1, 122.8, 48.0, 29., 20.5, 18.6.

***N*-Isobutylundecanamide; 15**

1.0 eq. (172 mg, 1.0 mmol) decanoic acid was reacted with 1.0 eq. (318 mg, 0.60 mL, 1.0 mmol) propylphosphonic anhydride solution (T3P[®]), 4 eq. triethylamine (101 mg, 0.60 mL, 4.0 mmol) and 1.0 eq (73 mg, 0.10 mL, 1 mmol) isobutyl amine according to general procedure A, The product was purified by means of flash chromatography (ELSD detector) using Method A to afford the desired amide **15** (218 mg, 0.96 mmol).

White solid; Yield 96%; Chemical formula: C₁₄H₂₉NO; **IR (ATR), $\tilde{\nu}$ [cm⁻¹]:** 3305, 2953, 2913, 2848, 1641, 1552; **ESI-MS** (m/z): 228.10 ([M+H]⁺, found), 228.23 ([M+H]⁺, calculated); **¹H-NMR** (Methanol-*d*₄, δ [ppm], *J* [Hz]): 2.98 (d, *J* = 6.9, 2H), 2.18 (t, *J* = 7.2, 2H), 1.76 (m, 1H), 1.60 (m, 2H), 1.30 (m, 12H), 0.90 (m, 9H); **¹³C-NMR** (Methanol-*d*₄, δ [ppm]): 176.3, 47.9, 37.2, 33.0, 30.6, 30.4, 30.3, 30.3, 29.6, 27.1, 23.7, 20.4, 14.4.

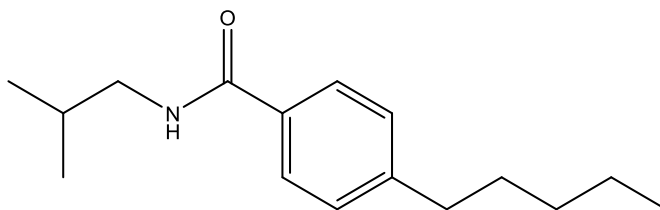
***(E)*-N-Isobutyldec-2-enamide; 16**

1.0 eq. (170 mg, 1.0 mmol) (*E*)-Dec-2-enoic acid was reacted with 1.0 eq. (318 mg, 0.60 mL, 1.0 mmol) propylphosphonic anhydride solution (T3P[®]), 4 eq. triethylamine (101 mg, 0.60 mL, 4.0 mmol) and 1.0 eq (73 mg, 0.10 mL, 1 mmol) isobutyl amine according to general procedure A, The product was purified by means of flash chromatography using Method A to afford the desired amide **16** (203 mg, 0.90 mmol).

EXPERIMENTAL

White solid; Yield 90%; Purity (HPLC-UV) 98%; Retention time (HPLC): 11.05 min; Chemical formula: C₁₄H₂₇NO; **IR (ATR), $\tilde{\nu}$ [cm⁻¹]:** 3296, 2954, 2920, 2851, 1666, 1622, 1547, 1465, 1337, 975; **ESI-MS** (m/z): 226.10 ([M+H]⁺, found), 226.21 ([M+H]⁺, calculated); **¹H-NMR** (Methanol-*d*₄, δ [ppm], *J* [Hz]): 6.76 (m, 1H), 5.93 (m, 1H), 3.05 (d, *J* = 6.9, 2H), 2.19 (m, 2H), 1.79 (m, 1H), 1.47 (m, 2H), 1.32 (m, 8H), 0.91 (m, 9H); **¹³C-NMR** (Methanol-*d*₄, δ [ppm]): 168.8, 145.6, 124.7, 47.9, 33.0, 32.9, 30.2, 30.1, 29.7, 29.4, 23.6, 20.5, 14.4.

***N*-Isobutyl-4-pentylbenzamide; 17**

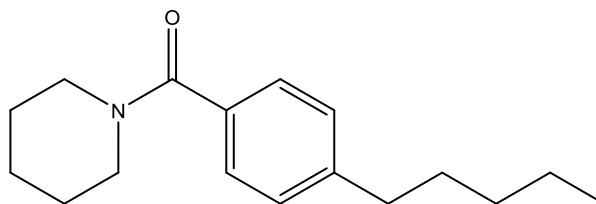


1.0 eq. (192 mg, 1.0 mmol) 4-Pentylbenzoic acid was reacted with 1.0 eq. (318 mg, 0.60 mL, 1.0 mmol) propylphosphonic anhydride solution (T3P[®]), 4 eq. triethylamine (101 mg, 0.60 mL, 4.0 mmol) and 1.0 eq (73 mg, 0.10 mL, 1 mmol) isobutyl amine according to general procedure A, The product was purified by means of flash chromatography using Method A to afford the desired amide **17** (212 mg, 0.86 mmol).

White solid; Yield 86%; Purity (HPLC-UV) 99%; Retention time (HPLC): 11.28 min; Chemical formula: C₁₆H₂₅NO; **IR (ATR), $\tilde{\nu}$ [cm⁻¹]:** 3311, 2955, 2925, 2869, 1634, 1534; **ESI-MS** (m/z): 248.05 ([M+H]⁺, found), 248.20 ([M+H]⁺, calculated); **¹H-NMR** (Methanol-*d*₄, δ [ppm], *J* [Hz]): 7.72 (m, 2H), 7.27 (m, 2H), 3.18 (d, *J* = 7.1, 2H), 2.66 (t, *J* = 7.6, 2H), 1.92 (m, 1H), 1.64 (m, 2H), 1.34 (m, 4H), 0.96 (d, *J* = 6.7, 6H), 0.90 (t, *J* = 7, 3H); **¹³C-NMR** (Methanol-*d*₄, δ [ppm]): 170.4, 148.1, 133.3, 129.5, 128.3, 48.3, 36.7, 32.5, 32.1, 29.7, 23.5, 20.5, 14.3.

EXPERIMENTAL

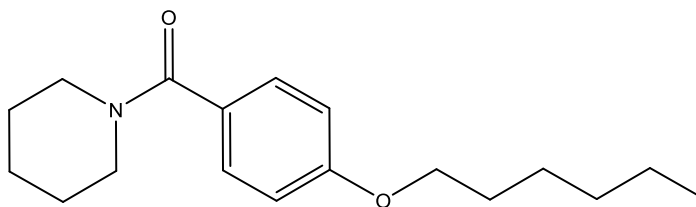
(4-Pentylphenyl)(piperidin-1-yl)methanone; **18**



1.0 eq. (192 mg, 1.0 mmol) 4-Pentylbenzoic acid was reacted with 1.0 eq. (318 mg, 0.60 mL, 1.0 mmol) propylphosphonic anhydride solution (T3P[®]), 4 eq. triethylamine (101 mg, 0.60 mL, 4.0 mmol) and 1.0 eq (85 mg, 0.10 mL, 1 mmol) piperidine according to general procedure A, The product was purified by means of flash chromatography using Method A to afford the desired amide **18** (225 mg, 0.86 mmol).

Colorless oil; Yield 87%; Purity (HPLC-UV) 99%; Retention time (HPLC): 11.57 min; Chemical formula: C₁₇H₂₅NO; **IR (ATR), $\tilde{\nu}$ [cm⁻¹]:** 2928, 2854, 1627, 1426, 1272; **ESI-MS** (m/z): 260.05 ([M+H]⁺, found), 260.20 ([M+H]⁺, calculated); **¹H-NMR** (Methanol-*d*₄, δ [ppm], *J* [Hz]): 7.29 (m, 4H), 3.54 (m, 4H), 2.65 (t, *J* = 7.6, 2H), 1.64 (m, 8H), 1.35 (m, 4H), 0.91 (t, *J* = 7.0, 3H); **¹³C-NMR** (Methanol-*d*₄, δ [ppm]): 172.6, 146.2, 134.7, 129.6, 127.8, 50.0, 44.3, 36.7, 32.5, 32.2, 27.9, 26.7, 25.4, 23.5, 14.3.

(4-(Hexyloxy)phenyl)(piperidin-1-yl)methanone; **19**



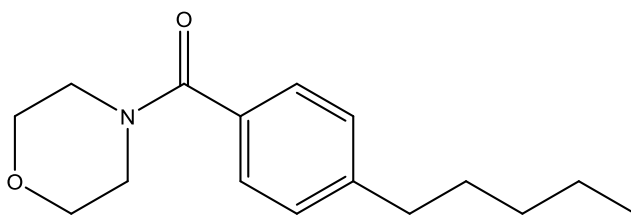
1.0 eq. (222 mg, 1.0 mmol) 4-(hexyloxy)benzoic acid was reacted with 1.0 eq. (318 mg, 0.60 mL, 1.0 mmol) propylphosphonic anhydride solution (T3P[®]), 4 eq. triethylamine (101 mg, 0.60 mL, 4.0 mmol) and 1.0 eq (85 mg, 0.10 mL, 1 mmol) piperidine according to general procedure A, The product was purified by means of

EXPERIMENTAL

flash chromatography using Method A to afford the desired amide **18** (265 mg, 0.92 mmol).

Colorless oil; Yield 92%; Purity (HPLC-UV) 99%; Retention time (HPLC): 11.41 min; Chemical formula: $C_{18}H_{27}NO_2$; **IR (ATR), $\tilde{\nu}$ [cm⁻¹]:** 2930, 2854, 1605, 1424, 1242, 998, 837; **ESI-MS (m/z):** 290.10 ([M+H]⁺, found), 290.21 ([M+H]⁺, calculated); **¹H-NMR (Methanol-*d*₄, δ [ppm], *J* [Hz]):** 7.34 (m, 2H), 6.96 (m, 2H), 4.01 (t, *J* = 6.5, 2H), 3.84 – 3.35 (m, 4H), 1.85 – 1.44 (m, 10H), 1.37 (m, 4H), 0.92 (m, 3H).; **¹³C-NMR (Methanol-*d*₄, δ [ppm]):** 172.5, 161.9, 129.8, 128.9, 115.3, 69.1, 50.2, 44.5, 32.7, 30.2, 27.4, 26.8, 25.5, 23.6, 14.3.

Morpholino(4-pentylphenyl)methanone; **20**

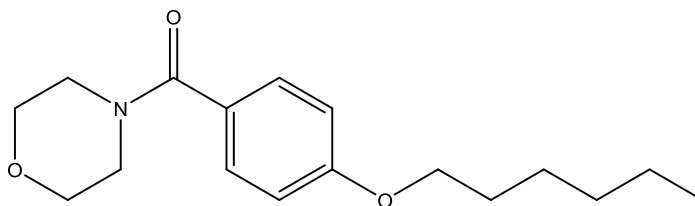


1.0 eq. (192 mg, 1.0 mmol) 4-Pentylbenzoic acid was reacted with 4 eq. (546 mg, 0.52 mL, 4.0 mmol) *i*-butyl chloroformate, 5 eq. (505 mg, 0.55 mL, 5.0 mmol) 4-methylmorpholine (NMM) and 4 eq. (348 mg, 0.35 mL, 4.0 mmol) Morpholine according to general procedure B, The product was purified by means of flash chromatography using Method B to afford the desired amide **20** (204 mg, 0.78 mmol).

Colorless oil; Yield 78%; Purity (HPLC-UV) 97%; Retention time (HPLC): 10.59 min; Chemical formula: $C_{16}H_{23}NO_2$; **IR (ATR), $\tilde{\nu}$ [cm⁻¹]:** 2925, 2854, 1630, 1422, 1276, 1112, 1010, 839; **ESI-MS (m/z):** 262.05 ([M+H]⁺, found), 262.18 ([M+H]⁺, calculated); **¹H-NMR (Methanol-*d*₄, δ [ppm], *J* [Hz]):** 7.34 (m, 2H), 7.29 (m, 2H), 3.68 (m, 8H), 2.65 (t, *J* = 7.2, 2H), 1.64 (m, 2H), 1.35 (m, 4H), 0.91 (t, *J* = 7, 3H); **¹³C-NMR (Methanol-*d*₄, δ [ppm]):** 172.8, 146.6, 133.7, 129.6, 128.3, 67.7, 43.9, 36.6, 23.5, 32.1.

EXPERIMENTAL

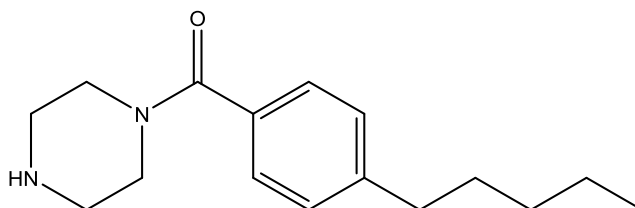
(4-(Hexyloxy)phenyl)(morpholino)methanone; 21



1.0 eq. (222 mg, 1.0 mmol) 4-(hexyloxy)benzoic acid was reacted with 4 eq. (546 mg, 0.52 mL, 4.0 mmol) *i*-butyl chloroformate, 5 eq. (505 mg, 0.55 mL, 5.0 mmol) 4-methylmorpholine (NMM) and 4 eq. (348 mg, 0.35 mL, 4.0 mmol) Morpholine according to general procedure B. The product was purified by means of flash chromatography using Method B to afford the desired amide **20** (235 mg, 0.81 mmol).

Colorless oil; Yield 81%; Purity (HPLC-UV) 99%; Retention time (HPLC): 10.87 min; Chemical formula: C₁₇H₂₅NO₃; **IR (ATR), $\tilde{\nu}$ [cm⁻¹]:** 2924, 2856, 1605, 1422, 1242, 1004, 836; **ESI-MS (m/z):** 292.15 ([M+H]⁺, found), 292.19 ([M+H]⁺, calculated); **¹H-NMR (DMSO, δ [ppm], J [Hz]):** 7.35 (d, J = 8.5, 2H), 6.96 (d, J = 8.4, 2H), 3.99 (t, J = 6.5, 2H), 3.58, (m, 4 H), 3.48 (m, 4H), 1.71, (m, 2H), 1.41 (m, 2H), 1.31 (m, 4H), 0.88 (t, J = 6.7, 3H); **¹³C-NMR (DMSO, δ [ppm]):** 168.9, 159.6, 129.0, 127.7, 114.0, 67.54, 66.0, 43.8, 30.9, 28.5, 25.1, 22.0, 13.8.

(4-Pentylcyclohexyl)(piperazin-1-yl)methanone; 22



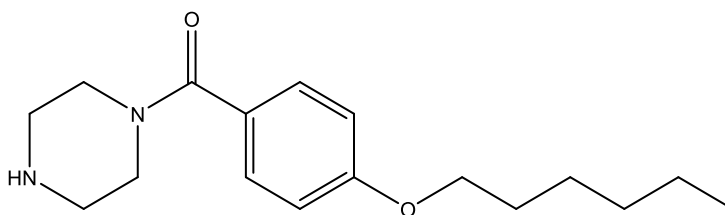
1.0 eq. (192 mg, 1.0 mmol) 4-pentylbenzoic acid was reacted with 1.0 eq. (318 mg, 0.60 mL, 1.0 mmol) propylphosphonic anhydride solution (T3P[®]), 4 eq. triethylamine (101 mg, 0.60 mL, 4.0 mmol) and 1.0 eq (86 mg, 1 mmol) piperazine according to

EXPERIMENTAL

general procedure A, The product was purified by means of flash chromatography using Method B to afford the desired amide **22** (172 mg, 0.66 mmol).

Colorless oil; Yield 66%; Purity (HPLC-UV) 99%; Retention time (HPLC): 7.70 min; Chemical formula: C₁₆H₂₄N₂O; **IR (ATR), $\tilde{\nu}$ [cm⁻¹]:** 3277, 2926, 1428, 1273, 1116, 1014, 830; **ESI-MS (m/z):** 261.05 ([M+H]⁺, found), 261.19 ([M+H]⁺, calculated); **¹H-NMR (Methanol-*d*₄, δ [ppm], *J* [Hz]):** 7.32 (m, 4H), 3.48 (m, 4H), 2.87 (m, 4H), 2.66 (t, *J* = 7.6, 2H), 1.64 (m, 2H), 1.34 (m, 4H), 0.91 (t, *J* = 7, 3H); **¹³C-NMR (Methanol-*d*₄, δ [ppm]):** 172.8, 146.6, 133.8, 129.7, 128.18, 46.2, 43.7, 36.6, 32.5, 32.2, 14.3.

(4-(Hexyloxy)phenyl)(piperazin-1-yl)methanone; **23**

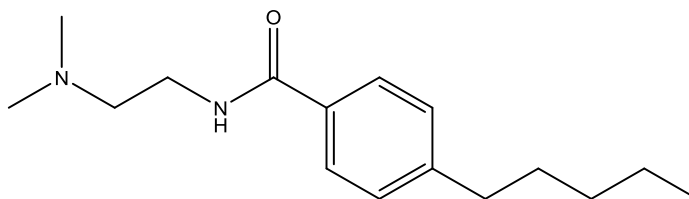


1.0 eq. (222 mg, 1.0 mmol) 4-(hexyloxy)benzoic acid was reacted with 1.0 eq. (318 mg, 0.60 mL, 1.0 mmol) propylphosphonic anhydride solution (T3P[®]), 4 eq. triethylamine (101 mg, 0.60 mL, 4.0 mmol) and 1.0 eq (86 mg, 1 mmol) piperazine according to general procedure A, The product was purified by means of flash chromatography using Method B to afford the desired amide **23** (209 mg, 0.72 mmol).

Yellowish oil; Yield 72%; Purity (HPLC-UV) 99%; Retention time (HPLC): 7.97 min; Chemical formula: C₁₇H₂₆N₂O₂; **IR (ATR), $\tilde{\nu}$ [cm⁻¹]:** 3280, 2926, 2857, 1604, 1428, 1242, 1172, 1005, 836; **ESI-MS (m/z):** 291.05 ([M+H]⁺, found), 291.20 ([M+H]⁺, calculated); **¹H-NMR (Chloroform-*d*₁, δ [ppm], *J* [Hz]):** 7.30 (m, 2H), 6.87 (m, 2H), 3.94 (t, *J* = 6.6, 2H), 3.65 (m, 4H), 2.84 (m, 4H), 1.75 (m, 2H), 1.43 (m, 2H), 1.30 (m, 4H), 0.88 (m, 3H).; **¹³C-NMR (Chloroform-*d*₁, δ [ppm]):** 170.6, 160.5, 126.2, 127.8, 114.4, 68.3, 46.4, 45.9, 31.7, 29.3, 25.8, 22.7, 14.2.

EXPERIMENTAL

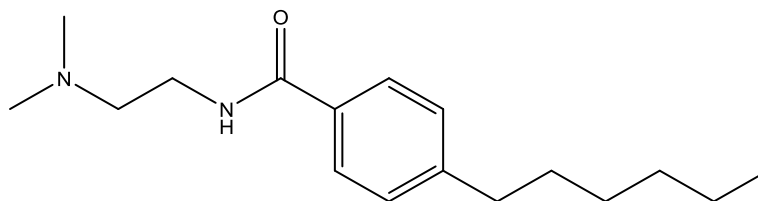
N-2-(Dimethylamino)ethyl-4-pentylbenzamide; **24**



1.0 eq. (192 mg, 1.0 mmol) 4-Pentylbenzoic acid was reacted with 1.0 eq. (318 mg, 0.60 mL, 1.0 mmol) propylphosphonic anhydride solution (T3P[®]), 4 eq. triethylamine (101 mg, 0.60 mL, 4.0 mmol) and 1.0 eq (88 mg, 0.11 mL, 1 mmol) *N,N*-Dimethylethylenediamine according to general procedure A, The product was purified by means of flash chromatography using Method B to afford the desired amide **24** (191 mg, 0.73 mmol).

Colorless oil; Yield 73%; Purity (HPLC-UV) 99%; Retention time (HPLC): 8.08 min; Chemical formula: C₁₆H₂₆N₂O; **IR (ATR), $\tilde{\nu}$ [cm⁻¹]:** 3314, 2927, 2857, 1635, 1541, 1504, 1457, 1303, 1187, 853; **ESI-MS** (m/z): 263.10 ([M+H]⁺, found), 263.21 ([M+H]⁺, calculated); **¹H-NMR** (Methanol-*d*₄, δ [ppm], *J* [Hz]): 7.76 (m, 2H), 7.25 (m, 2H), 3.52 (t, *J* = 6.8, 2H), 2.61 (m, 4H), 2.32 (s, 6H), 1.62 (m, 2H), 1.33 (m, 4H), 0.89 (t, *J* = 7, 3H); **¹³C-NMR** (Methanol-*d*₄, δ [ppm]): 170.0, 148.1, 132.8, 129.5, 128.3, 59.2, 45.4, 38.3, 36.6, 32.5, 32.0, 23.5, 14.3.

N-2-(Dimethylamino)ethyl-4-hexylbenzamide; **25**



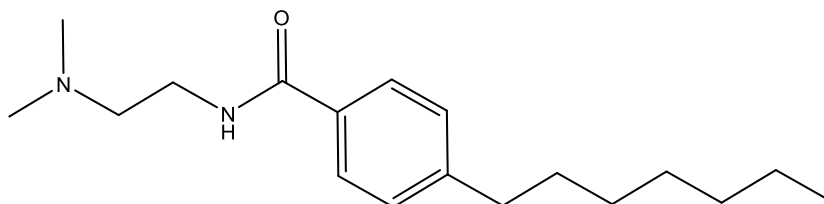
1.0 eq. (206 mg, 1.0 mmol) 4-hexylbenzoic acid was reacted with 1.0 eq. (318 mg, 0.60 mL, 1.0 mmol) propylphosphonic anhydride solution (T3P[®]), 4 eq. triethylamine (101 mg, 0.60 mL, 4.0 mmol) and 1.0 eq (88 mg, 0.11 mL, 1 mmol) *N,N*-Dimethylethylenediamine according to general procedure A, The product was

EXPERIMENTAL

purified by means of flash chromatography using Method B to afford the desired amide **25** (229 mg, 0.83 mmol).

Colorless oil; Yield 83%; Purity (HPLC-UV) 98%; Retention time (HPLC): 8.50 min; Chemical formula: C₁₇H₂₈N₂O; **IR (ATR), $\tilde{\nu}$ [cm⁻¹]:** 3319, 2926, 2856, 1635, 1541, 1504, 1458, 1303, 846; **ESI-MS (m/z):** 277.05 ([M+H]⁺, found), 277.22 ([M+H]⁺, calculated); **¹H-NMR (Methanol-*d*₄, δ [ppm], *J* [Hz]):** 7.75 (m, 2H), 7.26 (m, 2H), 3.53 (t, *J* = 6.8, 2H), 2.63 (m, 4H), 2.35 (s, 6H), 1.62 (m, 2H), 1.31 (m, 6H), 0.89 (m, 3H); **¹³C-NMR (Methanol-*d*₄, δ [ppm]):** 170.1, 148.2, 132.8, 129.5, 128.3, 59.2, 45.4, 38.3, 36.7, 32.8, 32.3, 29.9, 23.6, 14.3.

***N*-(2-(Dimethylamino)ethyl)-4-heptylbenzamide; 26**

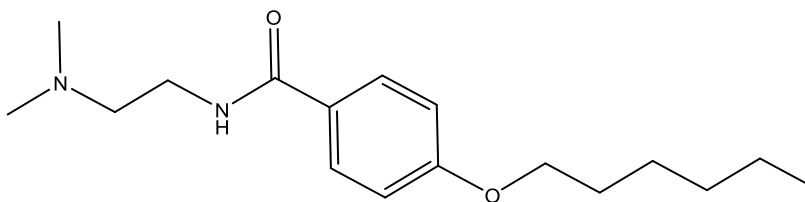


1.0 eq. (220 mg, 1.0 mmol) 4-heptylbenzoic acid was reacted with 1.0 eq. (318 mg, 0.60 mL, 1.0 mmol) propylphosphonic anhydride solution (T3P[®]), 4 eq. triethylamine (101 mg, 0.60 mL, 4.0 mmol) and 1.0 eq (88 mg, 0.11 mL, 1 mmol) *N,N*-Dimethylethylenediamine according to general procedure A, The product was purified by means of flash chromatography using Method B to afford the desired amide **26** (212 mg, 0.73 mmol).

Colorless oil; Yield 73%; Purity (HPLC-UV) 99%; Retention time (HPLC): 8.91 min; Chemical formula: C₁₈H₃₀N₂O; **IR (ATR), $\tilde{\nu}$ [cm⁻¹]:** 3332, 2925, 2855, 1636, 1541, 1504, 1457, 1303, 1187, 850; **ESI-MS (m/z):** 291.10 ([M+H]⁺, found), 291.24 ([M+H]⁺, calculated); **¹H-NMR (Methanol-*d*₄, δ [ppm], *J* [Hz]):** 7.75 (m, 2H), 7.26 (m, 2H), 3.51 (t, *J* = 6.8, 2H), 2.65 (t, *J* = 7.2, 2H), 2.56 (t, *J* = 6.8, 2H), 2.30 (s, 6H), 1.62 (m, 2H), 1.32 (m, 8H), 0.89 (t, *J* = 7, 3H); **¹³C-NMR (Methanol-*d*₄, δ [ppm]):** 170.1, 148.1, 132.9, 129.5, 128.3, 59.2, 45.5, 38.4, 36.7, 32.9, 32.4, 30.2, 30.2, 23.6, 14.4.

EXPERIMENTAL

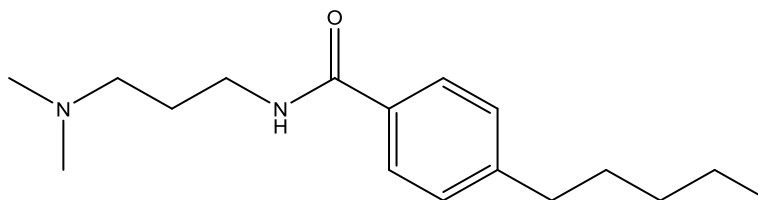
N-(2-(Dimethylamino)ethyl)-4-(hexyloxy)benzamide; **27**



1.0 eq. (222 mg, 1.0 mmol) 4-(hexyloxy)benzoic acid was reacted with 1.0 eq. (318 mg, 0.60 mL, 1.0 mmol) propylphosphonic anhydride solution (T3P[®]), 4 eq. triethylamine (101 mg, 0.60 mL, 4.0 mmol) and 1.0 eq (88 mg, 0.11 mL, 1 mmol) *N,N*-Dimethylethylenediamine according to general procedure A, The product was purified by means of flash chromatography using Method B to afford the desired amide **27** (237 mg, 0.81 mmol).

White solid; Yield 81%; Purity (HPLC-UV) 99%; Retention time (HPLC): 8.35 min; Chemical formula: C₁₇H₂₈N₂O₂; **IR (ATR), $\tilde{\nu}$ [cm⁻¹]:** 3316, 2938, 2869, 1630, 1607, 1294, 1252, 1176, 1022, 845; **ESI-MS** (m/z): 293.05 ([M+H]⁺, found), 293.22 ([M+H]⁺, calculated); **¹H-NMR** (Methanol-*d*₄, δ [ppm], *J* [Hz]): 7.79 (m, 2H), 6.69 (m, 2H), 4.02 (t, *J* = 6.4, 2H), 3.51 (t, *J* = 6.8, 2H), 2.58 (t, *J* = 6.8 Hz, 2H), 2.32 (s, 3H), 1.78 (m, , 2H), 1.48 (m, 2H), 1.44 – 1.28 (m, 4H), 1.05 – 0.80 (m, 3H); **¹³C-NMR** (Methanol-*d*₄, δ [ppm]): 169.8, 163.4, 130.1, 127.4, 115.1, 69.2, 59.3, 45.4, 38.4, 32.7, 30.2, 26.8, 23.6, 14.3.

N-(3-(Dimethylamino)propyl)-4-pentylbenzamide; **28**



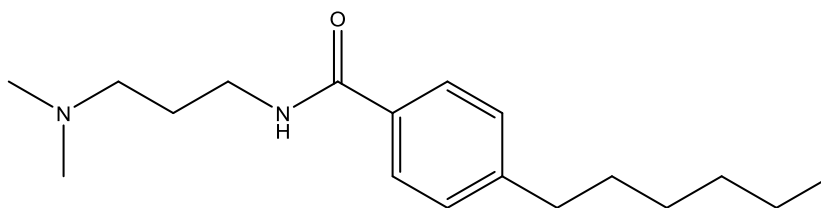
1.0 eq. (192 mg, 1.0 mmol) 4-Pentylbenzoic acid was reacted with 1.0 eq. (318 mg, 0.60 mL, 1.0 mmol) propylphosphonic anhydride solution (T3P[®]), 4 eq. triethylamine (101 mg, 0.60 mL, 4.0 mmol) and 1.0 eq (102 mg, 0.13 mL, 1 mmol) *N,N*-Dimethyl-

EXPERIMENTAL

1,3-diaminopropane according to general procedure A, The product was purified by means of flash chromatography using Method B to afford the desired amide **28** (188 mg, 0.68 mmol).

Colorless oil; Yield 68%; Purity (HPLC-UV) 99%; Retention time (HPLC): 8.14 min; Chemical formula: C₁₇H₂₈N₂O; **IR (ATR), $\tilde{\nu}$ [cm⁻¹]:** 3353, 2927, 1624, 1549, 1467, 1311, 854; **ESI-MS (m/z):** 277.05 ([M+H]⁺, found), 277.22 ([M+H]⁺, calculated); **¹H-NMR (Methanol-*d*₄, δ [ppm], *J* [Hz]):** 7.79 (m, 2H), 7.29 (m, 2H), 3.49 (t, *J* = 6.6, 2H), 3.18 (m, 2H), 2.90 (s, 6H), 2.66 (t, *J* = 7.6, 2H), 2.06 (m, 2H), 1.63 (m, 2H), 1.32 (m, 4H), 0.89 (t, *J* = 7, 3H); **¹³C-NMR (Methanol-*d*₄, δ [ppm]):** 170.8, 148.6, 132.3, 129.6, 128.3, 56.7, 43.6, 37.5, 36.6, 32.4, 32.0, 26.1, 23.4, 14.3.

***N*-3-(Dimethylamino)propyl-4-hexylbenzamide; 29**



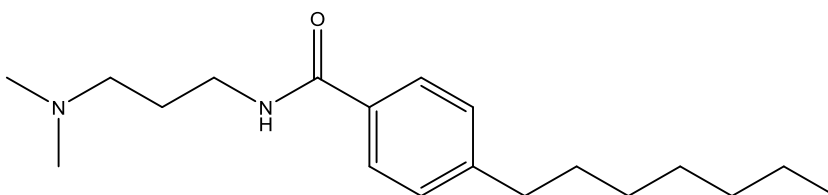
1.0 eq. (206 mg, 1.0 mmol) 4-hexylbenzoic acid was reacted with 1.0 eq. (318 mg, 0.60 mL, 1.0 mmol) propylphosphonic anhydride solution (T3P[®]), 4 eq. triethylamine (101 mg, 0.60 mL, 4.0 mmol) and 1.0 eq (102 mg, 0.13 mL, 1 mmol) *N,N*-Dimethyl-1,3-diaminopropane according to general procedure A, The product was purified by means of flash chromatography using Method B to afford the desired amide **29** (200 mg, 0.69 mmol).

Colorless oil; Yield 69%; Purity (HPLC-UV) 98%; Retention time (HPLC): 8.58 min; Chemical formula: C₁₈H₃₀N₂O; **IR (ATR), $\tilde{\nu}$ [cm⁻¹]:** 3316, 2926, 2856, 1634, 1541, 1504, 1459, 1303, 845; **ESI-MS (m/z):** 291.10 ([M+H]⁺, found), 291.24 ([M+H]⁺, calculated); **¹H-NMR (DMSO, δ [ppm], *J* [Hz]):** 8.44 (t, *J* = 5.5, NH), 7.75 (m, 2H), 7.25 (m, 2H), 3.27 (m, 2H), 2.60 (t, *J* = 7.6, 2H), 2.34 (t, *J* = 7.2, 2H), 2.19 (s, 6H), 1.67 (m, 2H), 1.56 (m, 2H), 1.26 (m, 6H), 0.84 (m, 3H); **¹³C-NMR (DMSO, δ [ppm]):**

EXPERIMENTAL

165.9, 145.5, 132.0, 128.0, 127.0, 56.6, 44.7, 37.9, 34.8, 31.0, 30.6, 28.2, 26.7, 21.9, 13.8.

N-3-(Dimethylamino)propyl-4-heptylbenzamide; **30**

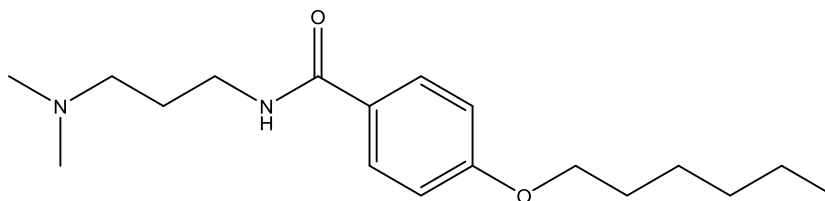


1.0 eq. (220 mg, 1.0 mmol) 4-heptylbenzoic acid was reacted with 1.0 eq. (318 mg, 0.60 mL, 1.0 mmol) propylphosphonic anhydride solution (T3P[®]), 4 eq. triethylamine (101 mg, 0.60 mL, 4.0 mmol) and 1.0 eq (102 mg, 0.13 mL, 1 mmol) *N,N*-Dimethyl-1,3-diaminopropane according to general procedure A, The product was purified by means of flash chromatography using Method B to afford the desired amide **30** (283 mg, 0.93 mmol).

Colorless oil; Yield 93%; Purity (HPLC-UV) 99%; Retention time (HPLC): 8.95 min; Chemical formula: C₁₉H₃₂N₂O; **IR (ATR), $\tilde{\nu}$ [cm⁻¹]:** 3336, 2922, 2852, 1625, 1547, 1467, 1312, 1182, 938, 852; **ESI-MS (m/z):** 305.05 ([M+H]⁺, found), 305.25 ([M+H]⁺, calculated); **¹H-NMR (Methanol-*d*₄, δ [ppm], *J* [Hz]):** 7.78 (m, 2H), 7.28 (m, 2H), 3.49 (t, *J* = 6.6, 2H), 3.15 (m, 2H), 2.87 (s, 6H), 2.67 (t, *J* = 7.6, 2H), 2.04 (m, 2H), 1.63 (m, 2H), 1.32 (m, 8H), 0.89 (t, *J* = 7.0, 3H); **¹³C-NMR (Methanol-*d*₄, δ [ppm]):** 169.3, 147.1, 131.0, 128.2, 127.0, 55.4, 42.2, 36.1, 35.3, 31.5, 31.0, 28.8, 24.9, 22.2, 13.0.

EXPERIMENTAL

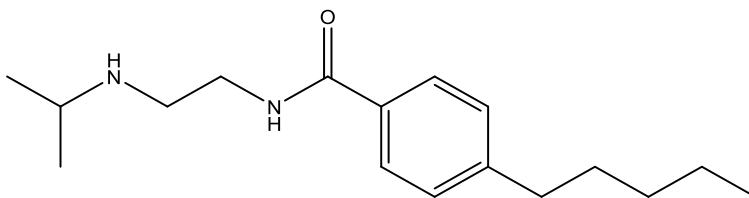
N-(3-(Dimethylamino)propyl)-4-(hexyloxy)benzamide; **31**



1.0 eq. (222 mg, 1.0 mmol) 4-(hexyloxy)benzoic acid was reacted with 1.0 eq. (318 mg, 0.60 mL, 1.0 mmol) propylphosphonic anhydride solution (T3P[®]), 4 eq. triethylamine (101 mg, 0.60 mL, 4.0 mmol) and 1.0 eq (102 mg, 0.13 mL, 1 mmol) *N,N*-Dimethyl-1,3-diaminopropane according to general procedure A, The product was purified by means of flash chromatography using Method B to afford the desired amide **31** (239 mg, 0.78 mmol).

White solid; Yield 78%; Purity (HPLC-UV) 93%; Retention time (HPLC): 8.43 min; Chemical formula: C₁₈H₃₀N₂O₂; **IR (ATR), $\tilde{\nu}$ [cm⁻¹]:** 3325, 2938, 2847, 2760, 1608, 1506, 1254, 1178, 846; **ESI-MS (m/z):** 307.05 ([M+H]⁺, found), 307.23 ([M+H]⁺, calculated); **¹H-NMR (Methanol-*d*₄, δ [ppm], *J* [Hz]):** 7.77 (m, 2H), 6.95 (m, 2H), 4.01 (t, *J* = 6.5, 2H), 3.39 (t, *J* = 7, 2H), 2.41 (m, 2H), 2.26 (s, 3H), 1.77 (m, 4H), 1.48 (m, 2H), 1.36 (m, 4H), 0.91 (m, 3H); **¹³C-NMR (Methanol-*d*₄, δ [ppm]):** 169.7, 163.3, 130.0, 127.9, 115.1, 69.2, 58.1, 45.4, 39.2, 32.7, 30.2, 28.1, 26.8, 23.6, 14.3.

N-(2-(Isopropylamino)ethyl)-4-pentylbenzamide; **32**



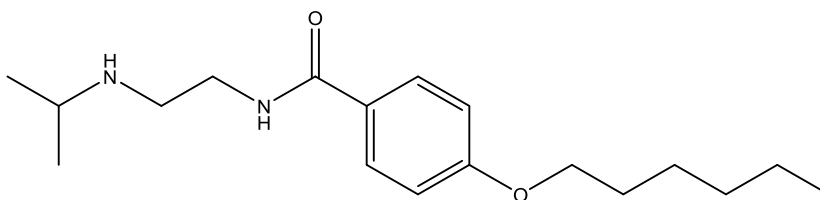
1.0 eq. (192 mg, 1.0 mmol) 4-Pentylbenzoic acid was reacted with 1.0 eq. (318 mg, 0.60 mL, 1.0 mmol) propylphosphonic anhydride solution (T3P[®]), 4 eq. triethylamine (101 mg, 0.60 mL, 4.0 mmol) and 1.0 eq (102 mg, 0.13 mL, 1 mmol) *N*-

EXPERIMENTAL

Isopropylethylenediamine according to general procedure A, The product was purified by means of flash chromatography using Method B to afford the desired amide 32 (254 mg, 0.92 mmol).

White solid; Yield 92%; Purity (HPLC-UV) 100%; Retention time (HPLC): 8.11 min; Chemical formula: $C_{17}H_{28}N_2O$; **IR (ATR), $\tilde{\nu}$ [cm^{-1}]**: 3313, 2980, 2692, 1638, 1540, 1314, 848; **ESI-MS (m/z)**: 277.10 ($[M+H]^+$, found), 277.22 ($[M+H]^+$, calculated); **1H -NMR (Methanol- d_4 , δ [ppm], J [Hz])**: 7.82 (d, $J = 8.3$, 2H), 7.30 (d, $J = 8.3$, 2H), 3.71 (t, $J = 6.0$, 2H), 3.45 (m, 1H), 3.26 (t, $J = 6.0$, 2H), 2.67 (t, $J = 7.2$, 2H), 1.64 (m, 2H), 1.32 (m, 10H), 0.90 (t, $J = 7.0$, 3H); **^{13}C -NMR (Methanol- d_4 , δ [ppm])**: 169.7, 147.4, 130.6, 128.2, 127.2, 50.6, 44.8, 36.5, 35.3, 31.1, 30.6, 22.1, 17.7, 12.9.

4-(Hexyloxy)-*N*-(2-(isopropylamino)ethyl)benzamide; 33



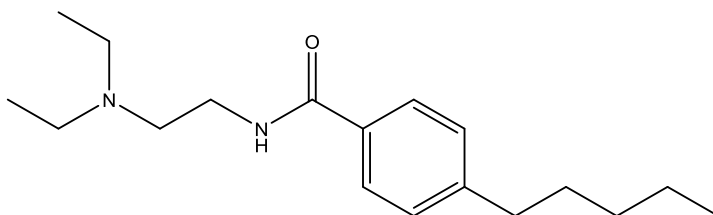
1.0 eq. (222 mg, 1.0 mmol) 4-(hexyloxy)benzoic acid was reacted with 1.0 eq. (318 mg, 0.60 mL, 1.0 mmol) propylphosphonic anhydride solution (T3P[®]), 4 eq. triethylamine (101 mg, 0.60 mL, 4.0 mmol) and 1.0 eq (102 mg, 0.13 mL, 1 mmol) *N*-Isopropylethylenediamine according to general procedure A, The product was purified by means of flash chromatography using Method B to afford the desired amide 33 (242 mg, 0.79 mmol).

White solid; Yield 79%; Purity (HPLC-UV) 99%; Retention time (HPLC): 8.35 min; Chemical formula: $C_{18}H_{30}N_2O_2$; **IR (ATR), $\tilde{\nu}$ [cm^{-1}]**: 3319, 2935, 2869, 1608, 1509, 1388, 1251, 1012, 846; **ESI-MS (m/z)**: 307.10 ($[M+H]^+$, found), 307.23 ($[M+H]^+$, calculated); **1H -NMR (Methanol- d_4 , δ [ppm], J [Hz])**: 7.84 (d, $J = 8.6$, 2H), 6.95 (d, $J = 8.6$, 2H), 4.00 (t, $J = 6.3$, 2H), 3.63 (d, $J = 5.9$, 2H), 3.21 (m, 1H), 3.08 (t, $J = 5.9$, 2H), 1.76 (m, 2H), 1.46 (m, 2H), 1.32 (m, 2H), 1.25 (d, $J = 6.4$, 2H), 0.90 (t, $J = 6.0$,

EXPERIMENTAL

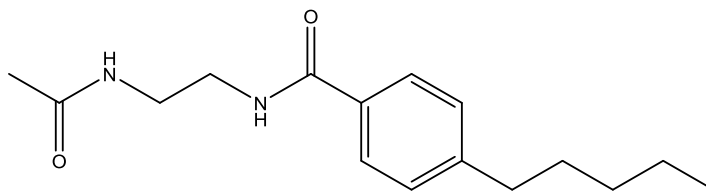
3H); $^{13}\text{C-NMR}$ (Methanol- d_4 , δ [ppm]): 170.1, 163.4, 130.3, 126.9, 115.1, 69.1, 50.9, 46.1, 38.8, 32.7, 30.2, 26.7, 23.6, 20.2, 14.4.

N-(2-(Diethylamino)ethyl)-4-pentylbenzamide; **34**



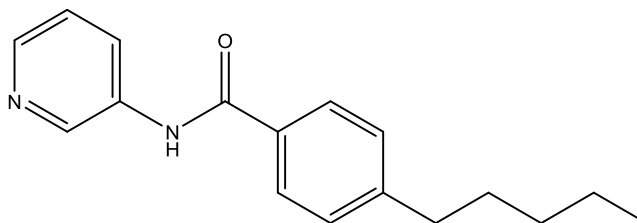
1.0 eq. (192 mg, 1.0 mmol) 4-Pentylbenzoic acid was reacted with 1.0 eq. (318 mg, 0.60 mL, 1.0 mmol) propylphosphonic anhydride solution (T3P[®]), 4 eq. triethylamine (101 mg, 0.60 mL, 4.0 mmol) and 1.0 eq (116 mg, 0.14 mL, 1 mmol) *N,N*-Diethylethylenediamine according to general procedure A, The product was purified by means of flash chromatography using Method B to afford the desired amide **34** (264 mg, 0.91 mmol).

Colorless oil; Yield 91%; Purity (HPLC-UV) 99%; Retention time (HPLC): 8.16 min; Chemical formula: $\text{C}_{18}\text{H}_{30}\text{N}_2\text{O}$; **IR (ATR), $\tilde{\nu}$ [cm $^{-1}$]**: 3274, 2928, 2857, 1636, 1540, 1504, 1294, 855; **ESI-MS (m/z)**: 291.10 ($[\text{M}+\text{H}]^+$, found), 291.24 ($[\text{M}+\text{H}]^+$, calculated); **$^1\text{H-NMR}$** (Methanol- d_4 , δ [ppm], J [Hz]): 7.76 (m, 2H), 7.28 (m, 2H), 3.60 (t, $J = 6.8$, 2H), 2.97 (t, $J = 6.8$, 2H), 2.91 (m, 4H), 2.66 (t, $J = 7.6$, 2H), 1.64 (m, 2H), 1.33 (m, 4H), 1.19 (t, $J = 7.2$, 6H), 0.90 (t, $J = 7.0$, 2H); **$^{13}\text{C-NMR}$** (Methanol- d_4 , δ [ppm]): 169.21, 147.1, 131.1, 128.2, 126.9, 51.4, 36.1, 35.3, 31.1, 30.7, 22.1, 12.9, 9.2.

***N*-(2-Acetamidoethyl)-4-pentylbenzamide; 35**

1.0 eq. (192 mg, 1.0 mmol) 4-Pentylbenzoic acid was reacted with 1.0 eq. (318 mg, 0.60 mL, 1.0 mmol) propylphosphonic anhydride solution (T3P[®]), 4 eq. triethylamine (101 mg, 0.60 mL, 4.0 mmol) and 1.0 eq (102 mg, 0.10 mL, 1 mmol) *N*-(2-Aminoethyl)acetamide according to general procedure A, The product was purified by means of flash chromatography using Method B to afford the desired amide **35** (240 mg, 0.87 mmol).

White solid; Yield 87%; Purity (HPLC-UV) 99%; Retention time (HPLC): 12.89 min; Chemical formula: C₁₆H₂₄N₂O₂; **IR (ATR), $\tilde{\nu}$ [cm⁻¹]:** 3302, 2926, 2852, 1631, 1553, 1289, 1239, 917, 844; **ESI-MS** (m/z): 277.10 ([M+H]⁺, found), 277.19 ([M+H]⁺, calculated); **¹H-NMR** (Methanol-*d*₄, δ [ppm], *J* [Hz]): 7.73 (m, 2H), 7.26 (m, 2H), 3.48 (m, 2H), 3.39 (m, 2H), 2.66 (t, *J* = 7.6, 2H), 1.64 (m, 2H), 1.33 (m, 4H), 0.90 (t, *J* = 7.0, 3H); **¹³C-NMR** (Methanol-*d*₄, δ [ppm]): 173.8, 170.5, 148.3, 132.9, 129.5, 128.3, 40.8, 40.1, 36.6, 32.5, 22.5, 14.3.

4-Pentyl-*N*-(pyridin-3-yl)benzamide; 36

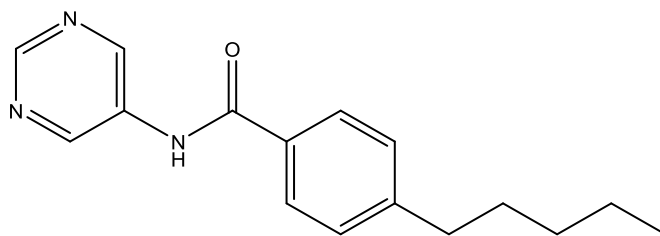
1.0 eq. (192 mg, 1.0 mmol) 4-Pentylbenzoic acid was reacted with 1.0 eq. (318 mg, 0.60 mL, 1.0 mmol) propylphosphonic anhydride solution (T3P[®]), 4 eq. triethylamine (101 mg, 0.60 mL, 4.0 mmol) and 1.0 eq (95 mg, 1 mmol) 3-Pyridineamine

EXPERIMENTAL

according to general procedure A, The product was purified by means of flash chromatography using Method B to afford the desired amide **36** (225 mg, 0.84 mmol).

White solid; Yield 84%; Purity (HPLC-UV) 99%; Retention time (HPLC): 13.01 min; Chemical formula: C₁₇H₂₀N₂O; **IR (ATR), $\tilde{\nu}$ [cm⁻¹]:** 3229, 3040, 2924, 2855, 1668, 1583, 1539, 1416, 1283, 858; **ESI-MS** (m/z): 269.05 ([M+H]⁺, found), 269.16 ([M+H]⁺, calculated); **¹H-NMR** (Methanol-*d*₄, δ [ppm], *J* [Hz]): 9.59 (d, *J* = 2.0, 1H), 8.79 (dd, *J* = 8.7, 0.9, 1H), 8.60 (d, *J* = 5.6, 1H), 8.09 (dd, *J* = 8.6, 5.7, 1H), 7.96 (d, *J* = 8.2, 2H), 7.38 (d, *J* = 8.2, 2H), 2.72 (t, *J* = 7.7, 2H), 1.67 (m, 2H), 1.36 (m, 4H), 0.91 (t, *J* = 6.8, 1H); **¹³C-NMR** (Methanol-*d*₄, δ [ppm]): 168.7, 149.9, 141.1, 137.4, 137.2, 133.3, 131.8, 129.9, 129.1, 128.7, 36.7, 32.5, 32.0, 23.5, 14.3.

4-Pentyl-*N*-(pyrimidin-5-yl)benzamide; **37**



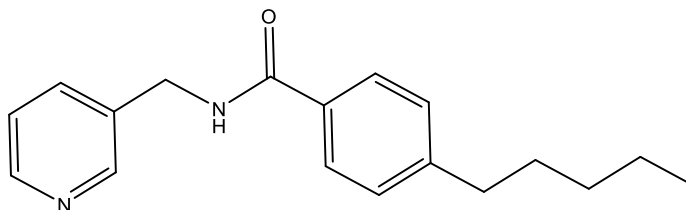
1.0 eq. (192 mg, 1.0 mmol) 4-Pentylbenzoic acid was reacted with 1.0 eq. (318 mg, 0.60 mL, 1.0 mmol) propylphosphonic anhydride solution (T3P[®]), 4 eq. triethylamine (101 mg, 0.60 mL, 4.0 mmol) and 1.0 eq (108 mg, 0.11 mL, 1 mmol) 5-Aminopyrimidine according to general procedure A, The product was purified by means of flash chromatography using Method B to afford the desired amide **37** (156 mg, 0.58 mmol).

Brown solid; Yield 58%; Purity (HPLC-UV) 98%; Retention time (HPLC): 10.89 min; Chemical formula: C₁₆H₁₉N₃O; **IR (ATR), $\tilde{\nu}$ [cm⁻¹]:** 3318, 3030, 2929, 2856, 1628, 1547, 1451, 1304, 1023, 856; **ESI-MS** (m/z): 270.05 ([M+H]⁺, found), 270.16 ([M+H]⁺, calculated); **¹H-NMR** (Methanol-*d*₄, δ [ppm], *J* [Hz]): 9.56 (s, 2H), 9.18 (s,

EXPERIMENTAL

1H), 7.95 (m, 2H), 7.37 (d, $J = 8.4$, 1H), 2.70 (t, $J = 7.6$, 2H), 1.66 (m, 2H), 1.35 (m, 4H), 0.89 (m, 3H); $^{13}\text{C-NMR}$ (Methanol- d_4 , δ [ppm]): 168.8, 149.8, 149.7, 148.8, 131.6, 129.8, 129.1, 36.7, 32.5, 32.0, 23.5, 14.3.

4-Pentyl-*N*-(pyridin-3-ylmethyl)benzamide; **38**

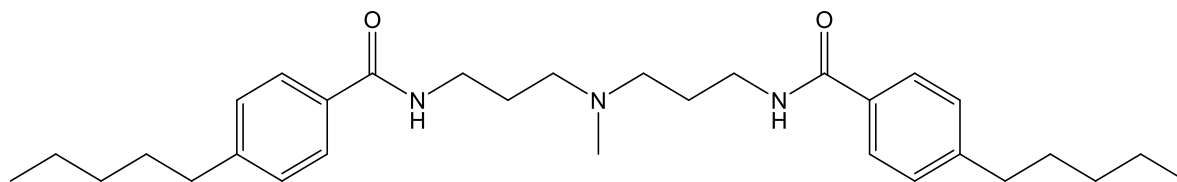


1.0 eq. (192 mg, 1.0 mmol) 4-Pentylbenzoic acid was reacted with 1.0 eq. (318 mg, 0.60 mL, 1.0 mmol) propylphosphonic anhydride solution (T3P[®]), 4 eq. triethylamine (101 mg, 0.60 mL, 4.0 mmol) and 1.0 eq (108 mg, 0.11 mL, 1 mmol) 3-Picolylamine according to general procedure A, The product was purified by means of flash chromatography using Method B to afford the desired amide **38** (231 mg, 0.82 mmol).

White solid; Yield 82%; Purity (HPLC-UV) 99%; Retention time (HPLC): 9.72 min; Chemical formula: $\text{C}_{18}\text{H}_{22}\text{N}_2\text{O}$; IR (ATR), $\tilde{\nu}$ [cm^{-1}]: 3318, 3030, 2929, 2856, 1628, 1547, 1451, 1304, 1023, 856; ESI-MS (m/z): 283.05 ($[\text{M}+\text{H}]^+$, found), 283.18 ($[\text{M}+\text{H}]^+$, calculated); $^1\text{H-NMR}$ (Methanol- d_4 , δ [ppm], J [Hz]): 8.55 (m, 1H), 8.42 (dd, $J = 4.9, 1.6$, 1H), 7.83 (m, 1H), 7.76 (m, 2H), 7.39 (m, 2H), 7.27 (m, 2H), 4.59 (s, 2H), 2.65 (t, $J = 7.2$, 2H), 1.63 (m, 2H), 1.33 (m, 4H), 0.89 (t, $J = 7.0$, 3H); $^{13}\text{C-NMR}$ (Methanol- d_4 , δ [ppm]): 170.2, 149.4, 148.7, 148.5, 137.9, 136.9, 132.6, 129.6, 128.4, 125.2, 41.9, 36.7, 32.5, 32.0, 23.5, 14.3.

EXPERIMENTAL

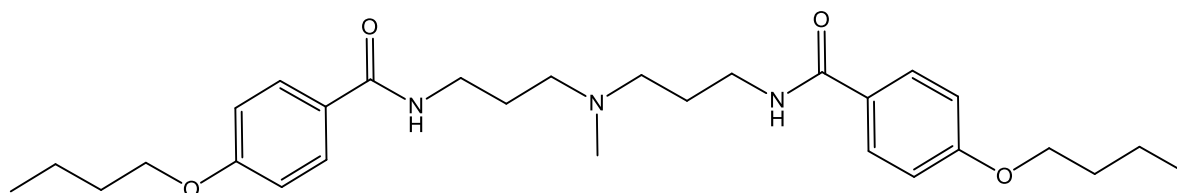
N,N-((Methylazanediyl)bis(propane-3,1-diyl))bis(4-pentylbenzamide); **39**



2.0 eq. (385 mg, 2.0 mmol) 4-Pentylbenzoic acid was reacted for 16 h with 2.0 eq. (636 mg, 1.20 mL, 2.0 mmol) propylphosphonic anhydride solution (T3P[®]), 4 eq. triethylamine (101 mg, 0.60 mL, 4.0 mmol) and 1.0 eq (145 mg, 0.16 mL, 1 mmol) 3,3'-Diamino-*N*-methyl dipropylamine according to general procedure A, The product was purified by means of flash chromatography using Method B to afford the desired amide **39** (420 mg, 0.85 mmol).

White solid; Yield 85%; Purity (HPLC-UV) 100%; Retention time (HPLC): 9.57 min; Chemical formula: C₃₁H₄₇N₃O₂; **IR (ATR), $\tilde{\nu}$ [cm⁻¹]:** 3422, 3312, 2925, 2677, 1632, 1540, 1294, 1007, 854; **ESI-MS (m/z):** 494.25 ([M+H]⁺, found), 494.37 ([M+H]⁺, calculated); **¹H-NMR (Methanol-*d*₄, δ [ppm], *J* [Hz]):** 7.75 (m, 4H), 7.25 (d, *J* = 8.4, 4H), 3.50 (t, *J* = 6.5, 4H), 3.16 (m, 4H), 2.85 (s, 3H), 2.65 (t, *J* = 7.2, 2H), 2.06 (m, 4H), 1.63 (m, 4H), 1.33 (m, 8H), 0.90 (t, *J* = 7.0, 6H); **¹³C-NMR (Methanol-*d*₄, δ [ppm]):** 170.71, 148.5, 132.4, 129.6, 128.4, 55.4, 40.3, 37.6, 36.7, 32.5, 32.1, 26.0, 23.5.

N,N-((Methylazanediyl)bis(propane-3,1-diyl))bis(4-butoxybenzamide); **40**



2.0 eq. (388 mg, 2.0 mmol) 4-butoxybenzoic acid was reacted for 18 h with 2.0 eq. (636 mg, 1.20 mL, 2.0 mmol) propylphosphonic anhydride solution (T3P[®]), 4 eq. triethylamine (101 mg, 0.60 mL, 4.0 mmol) and 1.0 eq (145 mg, 0.16 mL, 1 mmol)

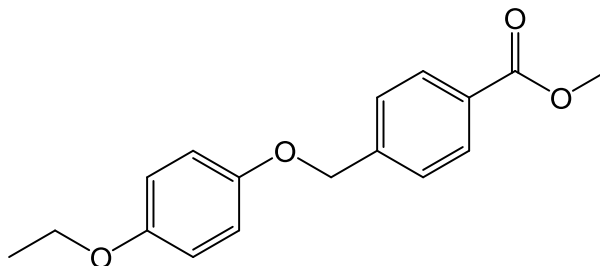
EXPERIMENTAL

3,3'-Diamino-*N*-methyldipropylamine according to general procedure A, The product was purified by means of flash chromatography using Method B to afford the desired amide **40** (452 mg, 0.91 mmol).

White solid; Yield 91%; Purity (HPLC-UV) 100%; Retention time (HPLC): 9.10 min; Chemical formula: C₂₉H₄₃N₃O₄; **IR (ATR), $\tilde{\nu}$ [cm⁻¹]:** 3316, 2954, 2886, 1631, 1505, 1249, 1176, 835; **ESI-MS (m/z):** 498.15 ([M+H]⁺, found), 498.33 ([M+H]⁺, calculated); **¹H-NMR (Methanol-*d*₄, δ [ppm], *J* [Hz]):** 7.75 (m, 4H), 6.92 (m, 4H), 3.99 (t, *J* = 6.4, 4H), 3.40 (t, *J* = 6.9, 4H), 2.53 (m, 4H), 2.31 (s, 3H), 1.76 (m, 8H), 1.49 (m, 4H), 0.98 (t, *J* = 7.4, 6H); **¹³C-NMR (Methanol-*d*₄, δ [ppm]):** 169.8, 163.3, 130.0, 127.9, 115.3, 68.9, 56.3, 42.1, 39.2, 32.3, 27.6, 20.2, 14.1.

7.8 Synthesis and characterization of compounds 41 and 42.

Methyl 4-((4-ethoxyphenoxy)methyl)benzoate; **M41-1**

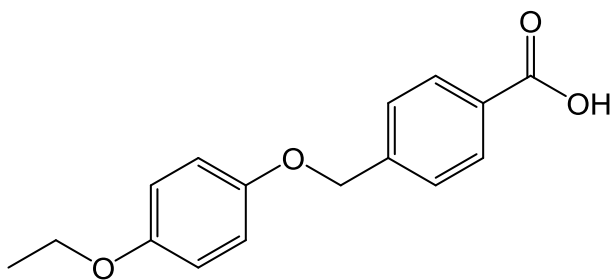


1 g (7.2 mmol) of 4-ethoxyphenol was dissolved in acetone (50 ml) followed by adding K₂CO₃ (1.2 g, 8.7 mmol) and methyl 4-(bromomethyl)benzoate (1.6 g, 7.2 mmol) to the stirred solution. The reaction was heated and refluxed for 48 hours. After that the solvent was removed *in vacuo* and the residue was dissolved in dichloromethane (100 mL) and washed with water three times (3 x 50 mL) and filtered over water-free sodium sulfate. Solvent was removed *in vacuo*. The compound was purified by recrystallization from methanol (150 mL) to yield 1.7 g (84%) of **M41-1**.

EXPERIMENTAL

Colorless crystals; Yield 84%; Purity (HPLC-UV) 99%; Retention time (HPLC): 11.04 min; Chemical formula: $C_{17}H_{18}O_4$; **ESI-MS** (m/z): 287.00 ($[M+H]^+$, found), 287.12 ($[M+H]^+$, calculated); **IR (ATR), $\tilde{\nu}$ [cm^{-1}]**: 2974, 1723, 1110, 1025; **1H -NMR** (DMSO- d_6 , δ [ppm], J [Hz]): δ 7.97 (d, $J = 8.4$ Hz, 1H), 7.57 (d, $J = 8.4$ Hz, 1H), 6.93 (m, 1H), 6.84 (m, 1H), 5.13 (s, 1H), 3.94 (q, $J = 7.0$ Hz, 1H), 1.28 (t, $J = 7.0$ Hz, 2H). **^{13}C -NMR** (DMSO- d_6 , δ [ppm]): δ 166.0, 152.8, 151.9, 142.9, 129.2, 128.8, 127.3, 115.7, 115.2, 68.9, 63.2, 52.1, 14.7.

4-((4-Ethoxyphenoxy)methyl)benzoic acid; M41-2

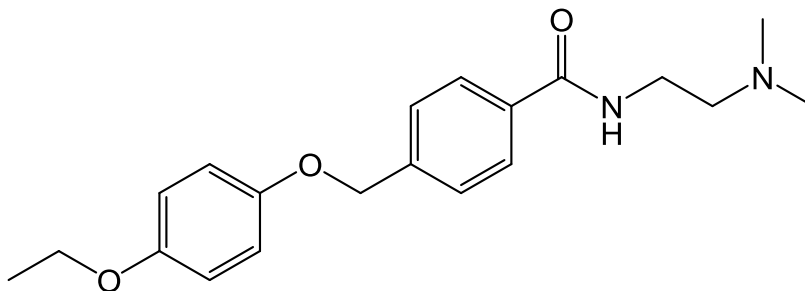


1 g (3.5 mmol) of **M41-1** was dissolved in 8 mL tetrahydrofuran (THF) followed by adding of 2M aqueous KOH (8.0 mL) to the solution. Water was added to make the volume up to 23 mL. The reaction was stirred for 24 hours. The organic solvent was removed *in vacuo*. The aqueous phase was then acidified to pH 1 by 1M HCl solution to precipitate the desired compound. As next, the precipitate was filtered and washed with cold water followed by cold ethanol affording 720 mg (76 %) of **M41-2**.

White solid; Yield 76%; Purity (HPLC-UV) 98%; Retention time (HPLC): 10.42 min; Chemical formula: $C_{16}H_{16}O_4$; **IR (ATR), $\tilde{\nu}$ [cm^{-1}]**: 2979, 2868, 1676, 1508, 1288, 1223; **1H -NMR** (DMSO- d_6 , δ [ppm], J [Hz]): δ 7.94 (d, $J = 8.4$ Hz, 2H), 7.52 (d, $J = 8.4$ Hz, 2H), 6.93 (m, 2H), 6.84 (m, 2H), 5.11 (s, 4H), 3.94 (q, $J = 7.0$ Hz, 4H), 1.28 (t, $J = 7.0$ Hz, 6H); **^{13}C -NMR** (DMSO- d_6 , δ [ppm]): δ 167.6, 153.2, 152.5, 142.6, 129.8, 127.6, 116.2, 115.7, 69.5, 63.7, 15.2.

EXPERIMENTAL

N-(2-(Dimethylamino)ethyl)-4-((4-ethoxyphenoxy)methyl)benzamide; **41**

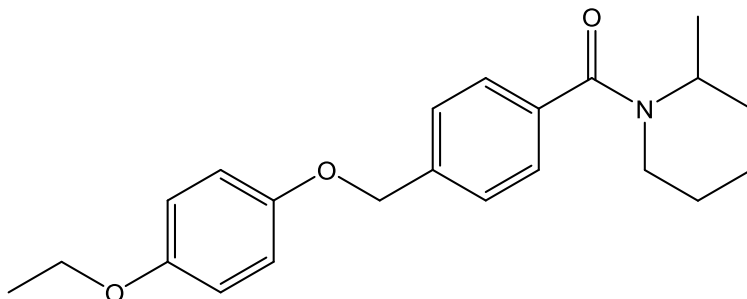


1.0 eq. (272 mg, 1.0 mmol) **M41-2** was reacted with 1.0 eq. (318 mg, 0.60 mL, 1.0 mmol) propylphosphonic anhydride solution (T3P[®]), 4 eq. triethylamine (101 mg, 0.60 mL, 4.0 mmol) and 1.0 eq. (88 mg, 0.11 mL, 1 mmol) *N,N*-Dimethylethylenediamine according to general procedure A, The product was purified by means of flash chromatography using Method B to afford the desired amide **41** (72 mg, 0.42 mmol).

White solid; Yield 42%; Purity (HPLC-UV) 99%; Retention time (HPLC): 7.58 min; Chemical formula: C₂₀H₂₆N₂O₃; IR (ATR), $\tilde{\nu}$ [cm⁻¹]: 3260, 2976, 2926, 1634, 1508; ESI-MS (m/z): 343.05 ([M+H]⁺, found), 343.20 ([M+H]⁺, calculated); ¹H-NMR (Chloroform-*d*, δ [ppm], *J* [Hz]): δ 7.85 (d, *J* = 8.4 Hz, 2H), 7.47 (d, *J* = 8.4 Hz, 2H), 7.02 – 6.67 (m, 4H), 5.05 (s, 2H), 3.97 (q, *J* = 7.0 Hz, 2H), 3.60 (m, 2H), 2.69 (t, *J* = 5.7 Hz, 2H), 2.40 (s, 6H), 1.38 (t, *J* = 7.0 Hz, 3H). ¹³C-NMR (Chloroform-*d*, δ [ppm]): δ 167.2, 153.4, 152.5, 140.9, 133.7, 127.4, 127.2, 115.8, 115.4, 70.0, 63.9, 57.9, 44.8, 36.6, 14.9

EXPERIMENTAL

(4-((4-Ethoxyphenoxy)methyl)phenyl)(2-methylpiperidin-1-yl)methanone; **42**



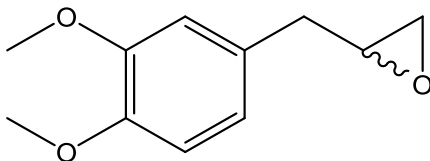
1.0 eq. (272 mg, 1.0 mmol) **M41-2** was reacted with 1.0 eq. (318 mg, 0.60 mL, 1.0 mmol) propylphosphonic anhydride solution (T3P[®]), 4 eq. triethylamine (101 mg, 0.60 mL, 4.0 mmol) and 1.0 eq. (99 mg, 0.12 mL, 1 mmol) 2-Methylpiperidine according to general procedure A, The product was purified by means of flash chromatography using Method B to afford the desired amide **42** (304 mg, 0.42 mmol).

White solid; Yield 86%; Purity (HPLC-UV) 99%; Retention time (HPLC): 10.89 min; Chemical formula: C₂₂H₂₇NO₃; **IR (ATR), $\tilde{\nu}$ [cm⁻¹]:** 3260, 2976, 1617, 1506, 1428, 1231; **ESI-MS** (m/z): 354.05 ([M+H]⁺, found), 354.20 ([M+H]⁺, calculated); **¹H-NMR** (Toluene-*d*₈, δ [ppm], *J* [Hz]): δ 7.32 (m, 2H), 7.20 (m, 2H), 6.79 (m, 2H), 6.72 (m, 2H), 4.68 (s, 2H), 4.50 (br. s, 1H), 3.97 (br. s, 1H), 3.63 (q, *J* = 7.0 Hz, 2H), 2.64 (m, 1H), 1.20- 1.50 (m, 6H), 1.16 (t, *J* = 7.0 Hz, 3H), 0.97 (d, *J* = 7.0 Hz, 3H). **¹³C-NMR** (Toluene-*d*₈, δ [ppm]): δ 169.6, 154.1, 153.4, 139.0, 137.5, 127.3, 116.1, 115.7, 70.3, 63.7, 47.0, 39.9, 30.4, 26.3, 19.3, 15.8, 15.0.

EXPERIMENTAL

7.9 Synthesis and characterization of the compounds of the side project

2-(3,4-Dimethoxybenzyl)oxiran; FM389



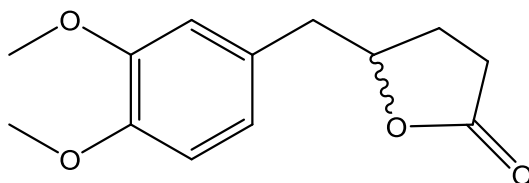
1.0 eq. 4-allyl-1,2-dimethoxybenzol (13.4 g, 75.0 mmol) was dissolved in chloroform, cooled to 0 °C, 1.0 eq. *meta*-chloroperbenzoic acid (13.3 g, 77.0 mmol) was added and the reaction mixture stirred for 96 hours at room temperature.

It was then added to saturated aqueous sodium hydrogen carbonate solution and extracted 3X with dichloromethane. The combined organic phases were dried over sodium sulfate and the solvent removed *in vacuo*. The resulting crude product is purified by column chromatography using Petrolether/Ethylacetat 9:1 as solvent system yielding 8.62 g, 44.1 mmol (57%) of **FM389**.

Chemical formula: C₁₁H₁₄O₃.

¹H-NMR: (Chloroform-*d*, δ [ppm], *J* [Hz]): δ 6.78 (m, 3 H), 3.86 (s, 3 H), 3.84 (s, 3 H), 3.11 (m, 1 H), 2.79 (m, 3 H), 2.52 (m, 1 H).

5-(3,4-Dimethoxybenzyl)dihydrofuran-2(3H)-on; FM395



9.0 eq. Sodium ethanolate (7.62 g, 141 mmol) was dissolved in ethanol and 10.0 eq. Diethyl malonate (246 g, 164 154 mmol) was added to the solution and it was stirred at room temperature for 1 hour. Subsequently, a solution of 1.0 eq. Epoxide (3.00 g, 15.4 mmol) in ethanol was slowly added to the reaction mixture and stirred for a

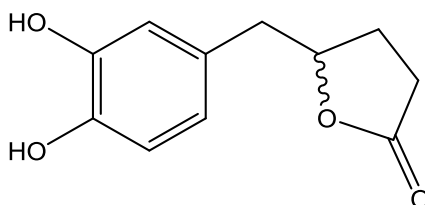
EXPERIMENTAL

further 24 hours. Aqueous sodium hydroxide solution (3 M, 50 eq.) was added and heated to boiling for one hour and then stirred at room temperature for a further 2 hours. The reaction mixture was concentrated *in vacuo*. The residue was washed with diethyl ether and the aqueous phase was acidified with hydrochloric acid to pH 1. This was then extracted 3 x with dichloromethane and dried over sodium sulfate. The solvent was removed *in vacuo*. The resulting crude product is purified by column chromatography using Petrolether/Ethylacetat 4:1 as solvent system yielding 2.7 g, 10.7 mmol (69 %) of FM395.

Chemical formula: C₁₃H₁₆O₄.

¹H-NMR: (Chloroform-*d*, δ [ppm], *J* [Hz]): δ 6.77 (m, 3 H), 4.71 (m, 1 H), 3.86 (s, 3 H), 3.85 (s, 3 H), 2.91 (dd, *J* = 14.2, 6.0, 1 H), 2.83 (dd, *J* = 14.2, 6.0, 1 H), 2.48 – 2.18 (m, 3 H), 1.99 – 1.87 (m, 1 H).

5-(3,4-Dihydroxybenzyl)dihydrofuran-2(3H)-on; M1



1.0 eq. (2.0 g, 8.5 mmol) ether component **FM395** was presented in dichloromethane and cooled to -78 °C using dry ice. Subsequently, 3 eq. (6.4 g, 25.5 mmol) boron tribromide was dropwise added with constant stirring at -78 °C for 1 hour. The reaction mixture was heated overnight to room temperature. As next, the reaction mixture was mixed with water and extracted 3 x with dichloromethane. The combined organic phases were washed with saturated aqueous sodium chloride solution and then dried over sodium sulfate. The solid was filtered and the filtrate was dried *in vacuo*. The resulting crude product was purified by column chromatography using Petrolether / Ethylacetat 1:1 as solvent system yielding 430 mg, 1.9 mmol (22%) of **M1**.

EXPERIMENTAL

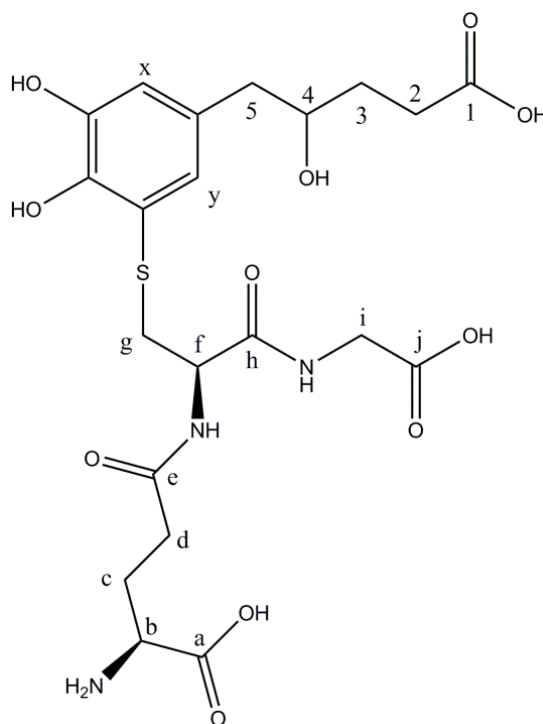
Chemical formula: C₁₁H₁₂O₄.

IR (ATR), $\tilde{\nu}$ [cm⁻¹]: 3300, 2921, 1722, 1709, 1598, 1518, 1468.

¹H-NMR (methanol-*d*₄, δ [ppm], *J* [Hz]): δ 6.69 (m, 2 H), 6.56 (dd, *J* = 8.0, 2.1, 1H), 4.73 (m, 1 H), 2.88 (dd, *J* = 14.1, 6.1 Hz, 1H), 2.79 (dd, *J* = 14.1, 6.1 Hz, 1H), 2.48 (m, 1 H), 2.18 – 2.38 (m, 2 H), 1.96 (m, 1 H).

The ¹H-NMR spectra of compounds **FM389**, **FM395** and **M1** are in accordance with their corresponding literature [6].

N⁵-((2*R*)-3-((4-Carboxy-2-hydroxybutyl)-2,3-dihydroxyphenyl)thio-1-((carboxymethyl)amino)-1-oxopropan-2-yl)-L-glutamine; ring-opened lactone M1-GSH-Adduct



The synthesis of the ring-opened lactone M1-GSH-Adduct was performed by first oxidizing 0.05 mmol of the substrate M1 under basic conditions (2 mL borate buffer 0.5 M, pH=11) and stirring at room temperature for four hours. The colour of the solution changed from light yellow to dark red, which confirms the oxidation of the

EXPERIMENTAL

catechol group to the corresponding *o*-quinone group. The elucidation of the structure with NMR also confirmed that an opening of the lactone- ring occurred.

0.5 mmol glutathione was dissolved in 3 mL 0.5 M borate buffer, pH=11. The dark-red colored solution of M1 was added dropwise to the glutathione solution under argon conditions with continuous stirring. The reaction was stopped after 70 min by adding 1M HCl dropwise in order to adjust the pH of the mixture to 4.5. The mixture was evaporated *in vacuo* at 30°C, the residue was reconstituted in 1 mL of water and fractionated using the preparative HPLC system and a semi preparative column (Phenomenex, Synergy 4 μ m MAX-RP 80A; 150 x 10 mm), 90% acetic acid 0.2% and 10% acetonitrile as eluents, using a gradient elution by increasing the acetonitrile from 10 to 40% in 15 min. The injection volume was 60 μ L. The flow rate was 3 ml/min. The main peak at retention time of 6.4 min was collected under nitrogen flushing of the collector, then directly moved into 5 plastic tubes under argon. The organic phase was removed under a gentle stream of nitrogen and the residual water was removed by lyophilisation. The dried product was a white solid, which was stored at -80°C till analyses. 0.164 mg of the substance was used for LC-ESI-MS analyses and approximately 1 mg was dissolved into 300 μ L D₂O for the NMR measurement. The sample was dissolved in 300 μ L D₂O from Deutero GmbH (Kastellaun, Germany) and filled in a Shigemi tube for D₂O.

Chemical formula: C₂₁H₂₉N₃O₁₁S.

White solid; **ESI-MS** (m/z): 532.16 ([M+H]⁺, found), 532.16 ([M+H]⁺, calculated); **¹H-NMR** (D₂O, δ [ppm], *J* [Hz]): δ 6.94 (d, *J* = 1.4, H-y, 1H), 6.85 (d, *J* = 1.8, H-x, 1H), 4.48 (m, H-f, 1H), 3.85 (m, H-4, i, b, 4H), 3.41 (m, H-g₁, 1H), 3.24 (m, H-g₂, 1H), 2.77 (m, H-5₁, 1H), 2.66 (m, H-5₂, 1H), 2.53 (m, H-2, d, 4H), 2.16 (m, H-c, 2H), 1.88 (m, 3a, 1H), 1.75 (m, 3b, 1H).

7.10 References

1. Skaf, J.; Hamarsheh, O.; Berninger, M.; Balasubramanian, S.; Oelschlaeger, T. A.; Holzgrabe, U., Improving anti-trypanosomal activity of alkamides isolated from *Achillea fragrantissima*. *Fitoterapia* **2018**, *125*, 191-198.
2. Bringmann, G.; Thomale, K.; Bischof, S.; Schneider, C.; Schultheis, M.; Schwarz, T.; Moll, H.; Schurigt, U., A novel *Leishmania major* amastigote assay in 96-well format for rapid drug screening and its use for discovery and evaluation of a new class of leishmanicidal quinolinium salts. *Antimicrob Agents Chemother* **2013**, *57* (7), 3003-11.
3. Rätz, B.; Iten, M.; Grether-Bühler, Y.; Kaminsky, R.; Brun, R., The Alamar Blue® assay to determine drug sensitivity of African trypanosomes (*T.b. rhodesiense* and *T.b. gambiense*) in vitro. *Acta Tropica* **1997**, *68* (2), 139-147.
4. Hiltensperger, G.; Hecht, N.; Kaiser, M.; Rybak, J. C.; Hoerst, A.; Dannenbauer, N.; Muller-Buschbaum, K.; Bruhn, H.; Esch, H.; Lehmann, L.; Meinel, L.; Holzgrabe, U., Quinolone Amides as Antitrypanosomal Lead Compounds with In Vivo Activity. *Antimicrob Agents Chemother* **2016**, *60* (8), 4442-52.
5. Gibreel, T. M.; Upton, M., Synthetic epidermicin NI01 can protect *Galleria mellonella* larvae from infection with *Staphylococcus aureus*. *J Antimicrob Chemother.* **2013**, *68* (10), 2269-2273.
6. Matz, F. Entwicklung von vif–Elongin-C–Interaktionsinhibitoren als neuartige HIV–Therapeutika. PhD Thesis, University of Würzburg, Würzburg, 2013.

8. Appendix: NMR Spectral data of all compounds included in this thesis.

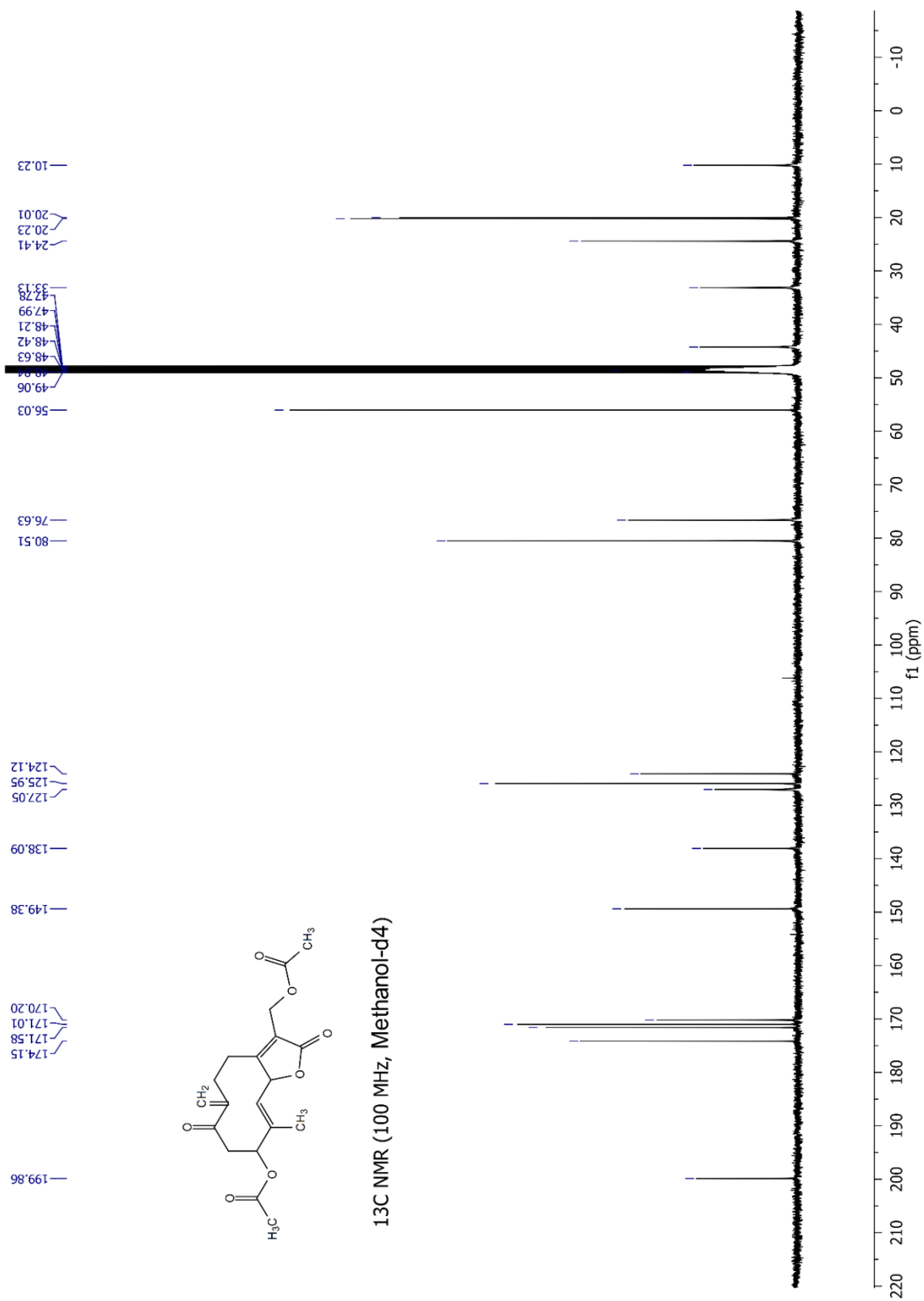
Fig. A 1 ^1H Spectrum of compound 1.....	117
Fig. A 2 ^{13}C Spectrum of compound 1.....	118
Fig. A 3 ^1H Spectrum of compound 2.....	119
Fig. A 4 ^{13}C Spectrum of compound 2.....	120
Fig. A 5 ^1H Spectrum of compound 3.....	121
Fig. A 6 ^{13}C Spectrum of compound 3.....	122
Fig. A 7 ^1H Spectrum of compound 4.....	123
Fig. A 8 ^{13}C Spectrum of compound 4.....	124
Fig. A 9 ^1H Spectrum of compounds 5+6.....	125
Fig. A 10 ^{13}C Spectrum of compounds 5+6.....	126
Fig. A 11 ^1H Spectrum of compound 7.....	127
Fig. A 12 ^{13}C Spectrum of compound 7.....	128
Fig. A 13 ^1H Spectrum of compound 8.....	129
Fig. A 14 ^{13}C Spectrum of compound 8.....	130
Fig. A 15 ^1H Spectrum of compound 9.....	131
Fig. A 16 ^{13}C Spectrum of compound 9.....	132
Fig. A 17 ^1H Spectrum of compound 10.....	133
Fig. A 18 ^{13}C Spectrum of compound 10.....	134
Fig. A 19 ^1H Spectrum of compound 11.....	135
Fig. A 20 ^{13}C Spectrum of compound 11.....	136
Fig. A 21 ^1H Spectrum of compound 12.....	137
Fig. A 22 ^{13}C Spectrum of compound 12.....	138
Fig. A 23 ^1H Spectrum of compound 13.....	139
Fig. A 24 ^{13}C Spectrum of compound 13.....	140
Fig. A 25 DEPT Spectrum of compound 13.....	141
Fig. A 26 ^1H ^1H COSY Spectrum of compound 13.....	142
Fig. A 27 HSQC Spectrum of compound 13.....	143
Fig. A 28 HMBC Spectrum of compound 13.....	144
Fig. A 29 ^1H Spectrum of compound 14.....	145

APPENDIX

Fig. A 30 ^{13}C Spectrum of compound 14.	146
Fig. A 31 ^1H Spectrum of compound 15.....	147
Fig. A 32 ^{13}C Spectrum of compound 15.	148
Fig. A 33 ^1H Spectrum of compound 16.....	149
Fig. A 34 ^{13}C Spectrum of compound 16.	150
Fig. A 35 ^1H Spectrum of compound 17.....	151
Fig. A 36 ^{13}C Spectrum of compound 17.	152
Fig. A 37 ^1H Spectrum of compound 18.....	153
Fig. A 38 ^{13}C Spectrum of compound 18.	154
Fig. A 39 ^1H Spectrum of compound 19.....	155
Fig. A 40 ^{13}C Spectrum of compound 19.	156
Fig. A 41 ^1H Spectrum of compound 20.....	157
Fig. A 42 ^{13}C Spectrum of compound 20.	158
Fig. A 43 ^1H Spectrum of compound 21.....	159
Fig. A 44 ^{13}C Spectrum of compound 21.	160
Fig. A 45 ^1H Spectrum of compound 22.....	161
Fig. A 46 ^{13}C Spectrum of compound 22.	162
Fig. A 47 ^1H Spectrum of compound 23.....	163
Fig. A 48 ^{13}C Spectrum of compound 23.	164
Fig. A 49 ^1H Spectrum of compound 24.....	165
Fig. A 50 ^{13}C Spectrum of compound 24.	166
Fig. A 51 ^1H Spectrum of compound 25.....	167
Fig. A 52 ^{13}C Spectrum of compound 25.	168
Fig. A 53 ^1H Spectrum of compound 26.....	169
Fig. A 54 ^{13}C Spectrum of compound 26.	170
Fig. A 55 ^1H Spectrum of compound 27.....	171
Fig. A 56 ^{13}C Spectrum of compound 27.	172
Fig. A 57 ^1H Spectrum of compound 28.....	173
Fig. A 58 ^{13}C Spectrum of compound 28.	174
Fig. A 59 ^1H Spectrum of compound 29.....	175
Fig. A 60 ^{13}C Spectrum of compound 29.	176

APPENDIX

Fig. A 61 ^1H Spectrum of compound 30.....	177
Fig. A 62 ^{13}C Spectrum of compound 30.....	178
Fig. A 63 ^1H Spectrum of compound 31.....	179
Fig. A 64 ^{13}C Spectrum of compound 31.....	180
Fig. A 65 ^1H Spectrum of compound 32.....	181
Fig. A 66 ^{13}C Spectrum of compound 32.....	182
Fig. A 67 ^1H Spectrum of compound 33.....	183
Fig. A 68 ^{13}C Spectrum of compound 33.....	184
Fig. A 69 ^1H Spectrum of compound 34.....	185
Fig. A 70 ^{13}C Spectrum of compound 34.....	186
Fig. A 71 ^1H Spectrum of compound 35.....	187
Fig. A 72 ^{13}C Spectrum of compound 35.....	188
Fig. A 73 ^1H Spectrum of compound 36.....	189
Fig. A 74 ^{13}C Spectrum of compound 36.....	190
Fig. A 75 ^1H Spectrum of compound 37.....	191
Fig. A 76 ^{13}C Spectrum of compound 37.....	192
Fig. A 77 ^1H Spectrum of compound 38.....	193
Fig. A 78 ^{13}C Spectrum of compound 38.....	194
Fig. A 79 ^1H Spectrum of compound 39.....	195
Fig. A 80 ^{13}C Spectrum of compound 39.....	196
Fig. A 81 ^1H Spectrum of compound 40.....	197
Fig. A 82 ^{13}C Spectrum of compound 40.....	198
Fig. A 83 ^1H Spectrum of compound 41.....	199
Fig. A 84 ^{13}C Spectrum of compound 41.....	200
Fig. A 85 ^1H Spectrum of compound 42.....	201
Fig. A 86 ^{13}C Spectrum of compound 42.....	202
Fig. A 87 ^1H Spectrum of compound M1.....	203
Fig. A 88 ^1H Spectrum of ring-opened lactone M1-GSH-Adduct.....	204

Fig. A 2 ¹³C Spectrum of compound 1.

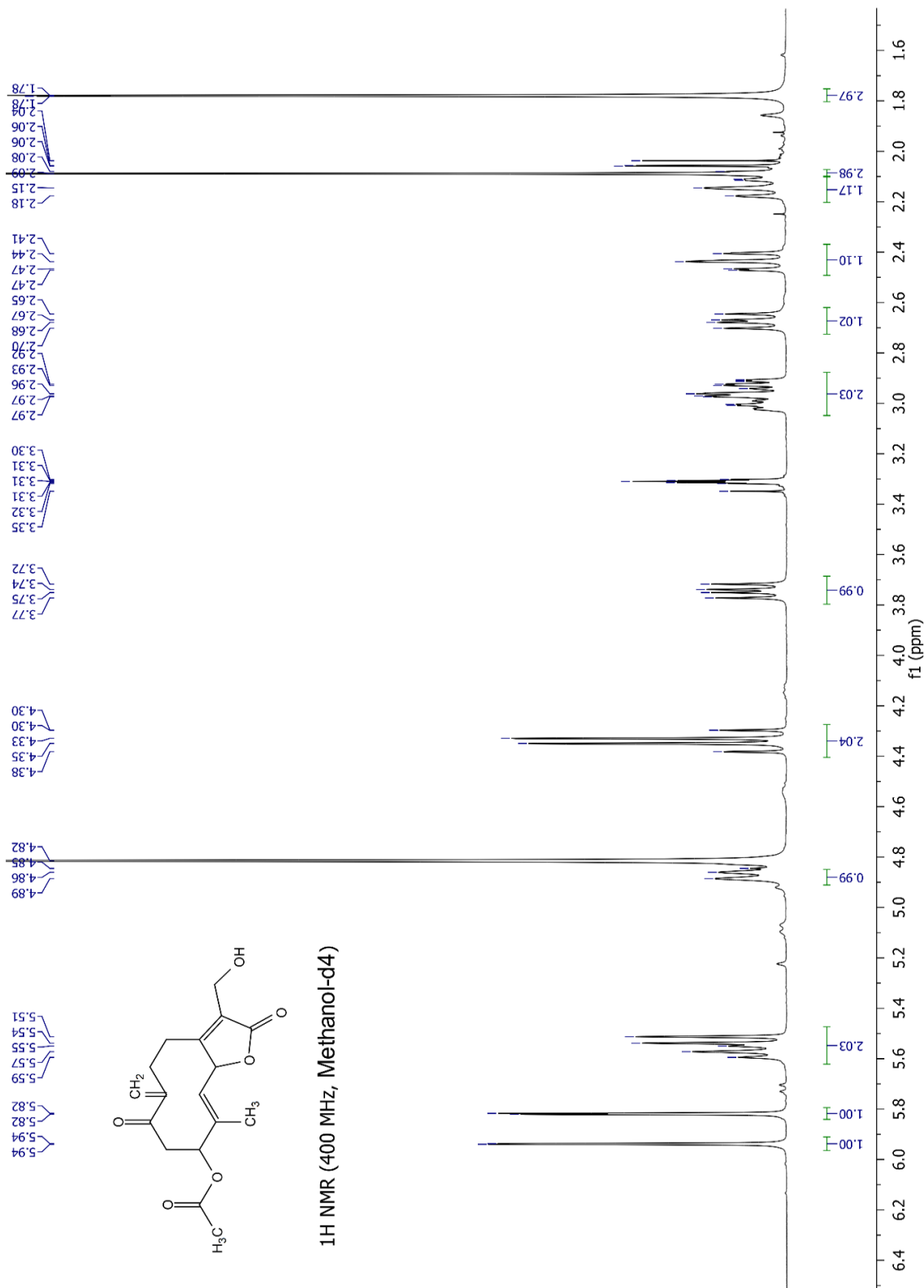


Fig. A 3 ¹H Spectrum of compound 2.

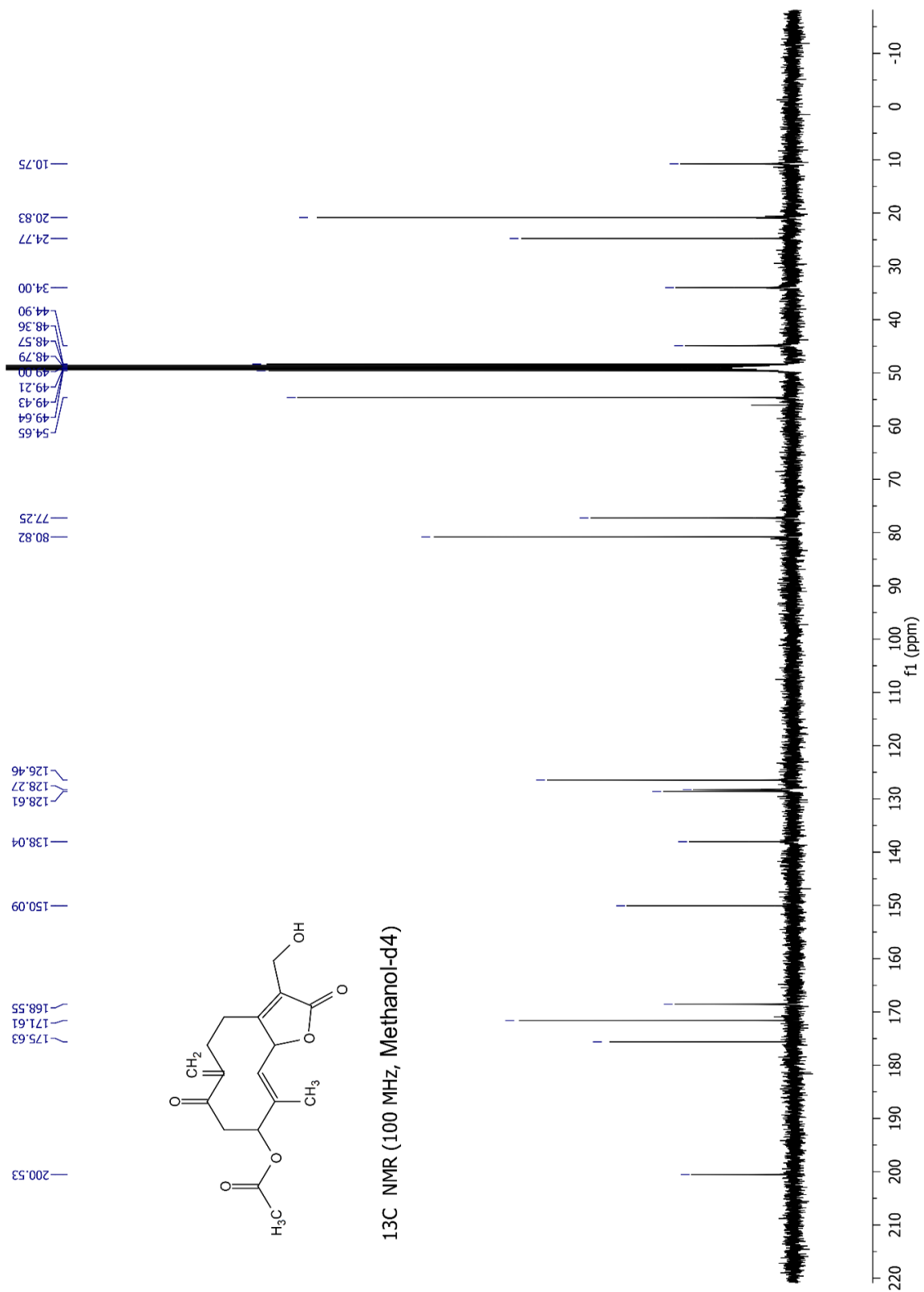
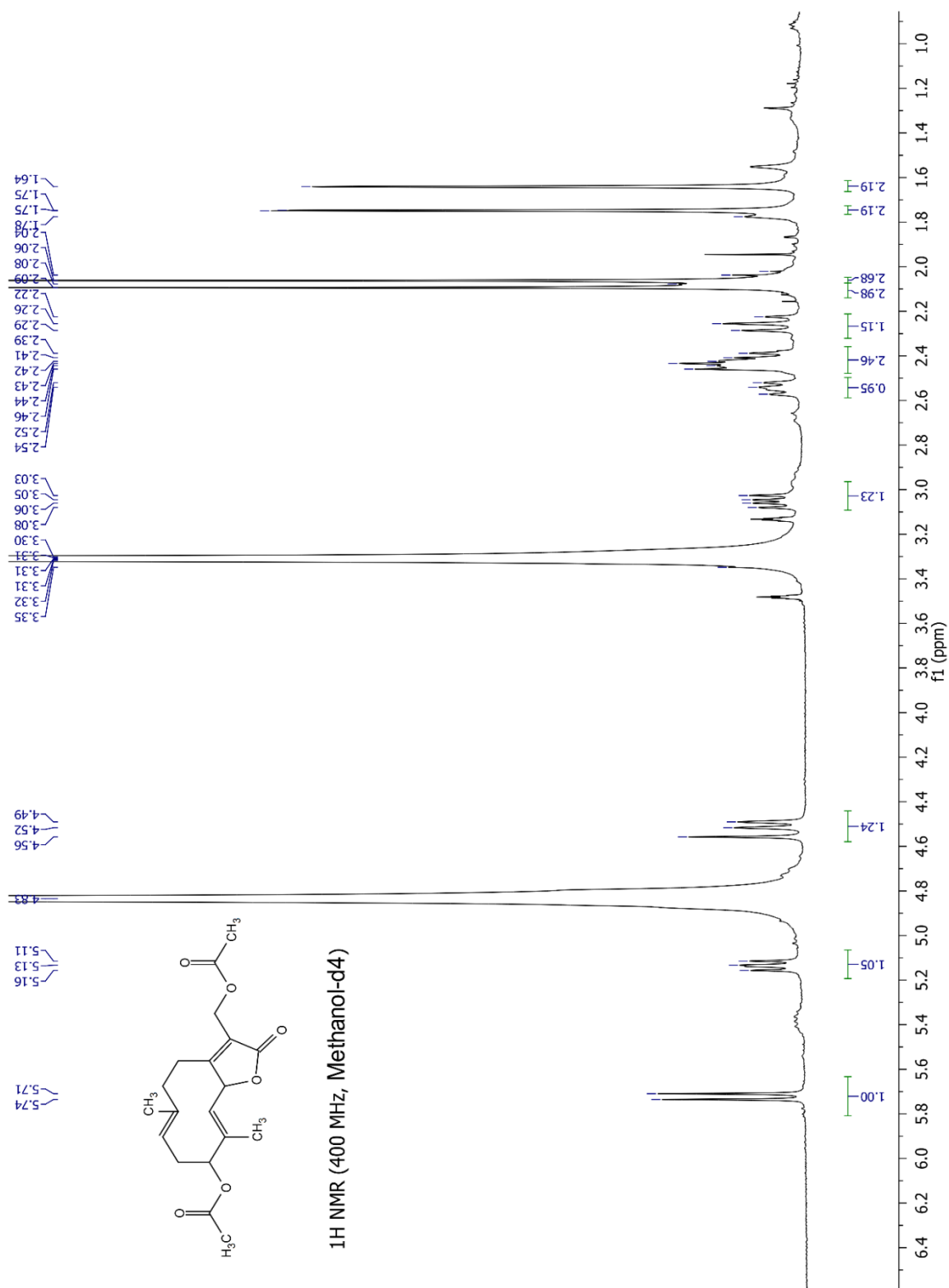


Fig. A 4 ¹³C Spectrum of compound 2.

Fig. A 5 ¹H Spectrum of compound 3.

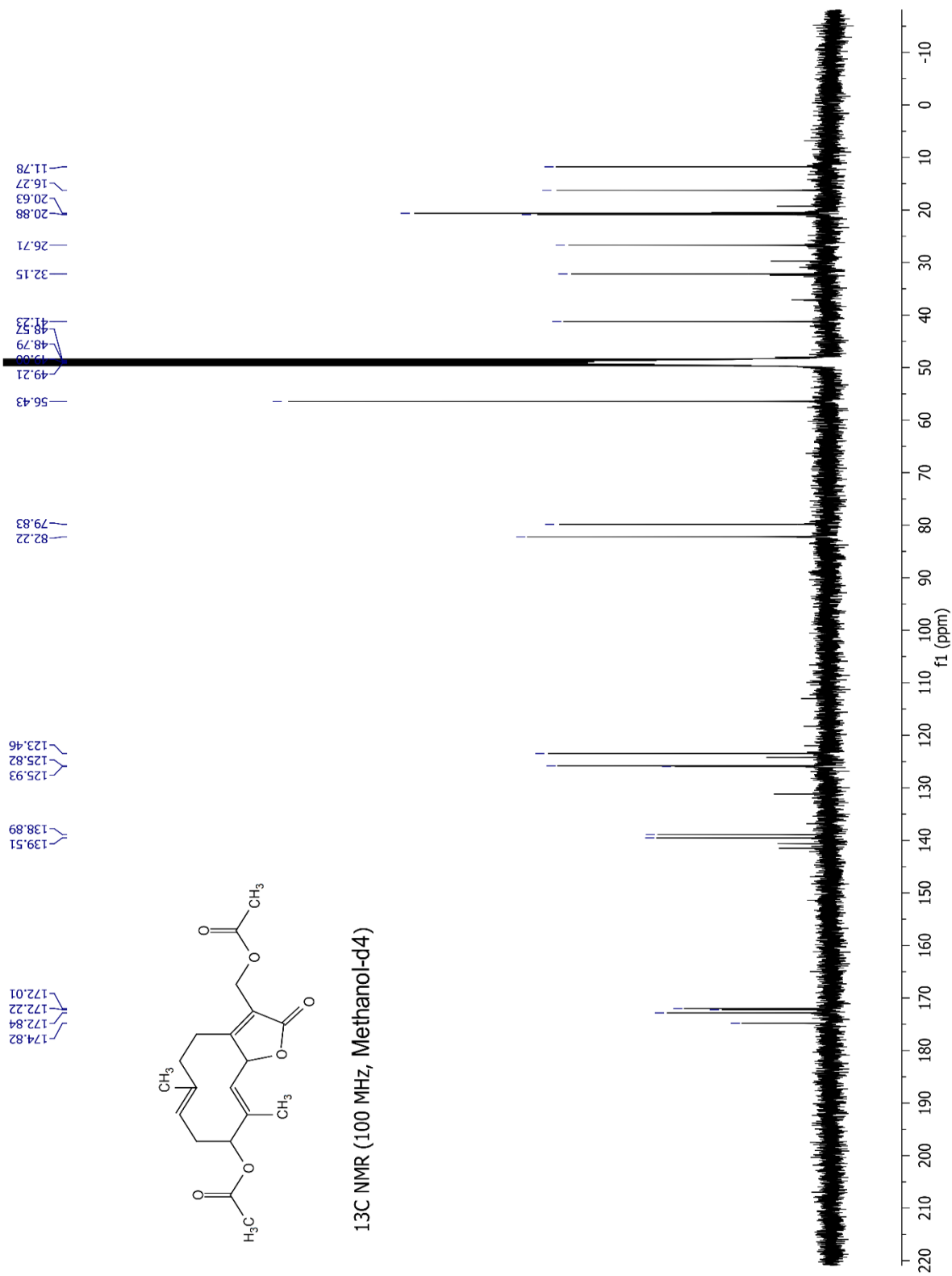
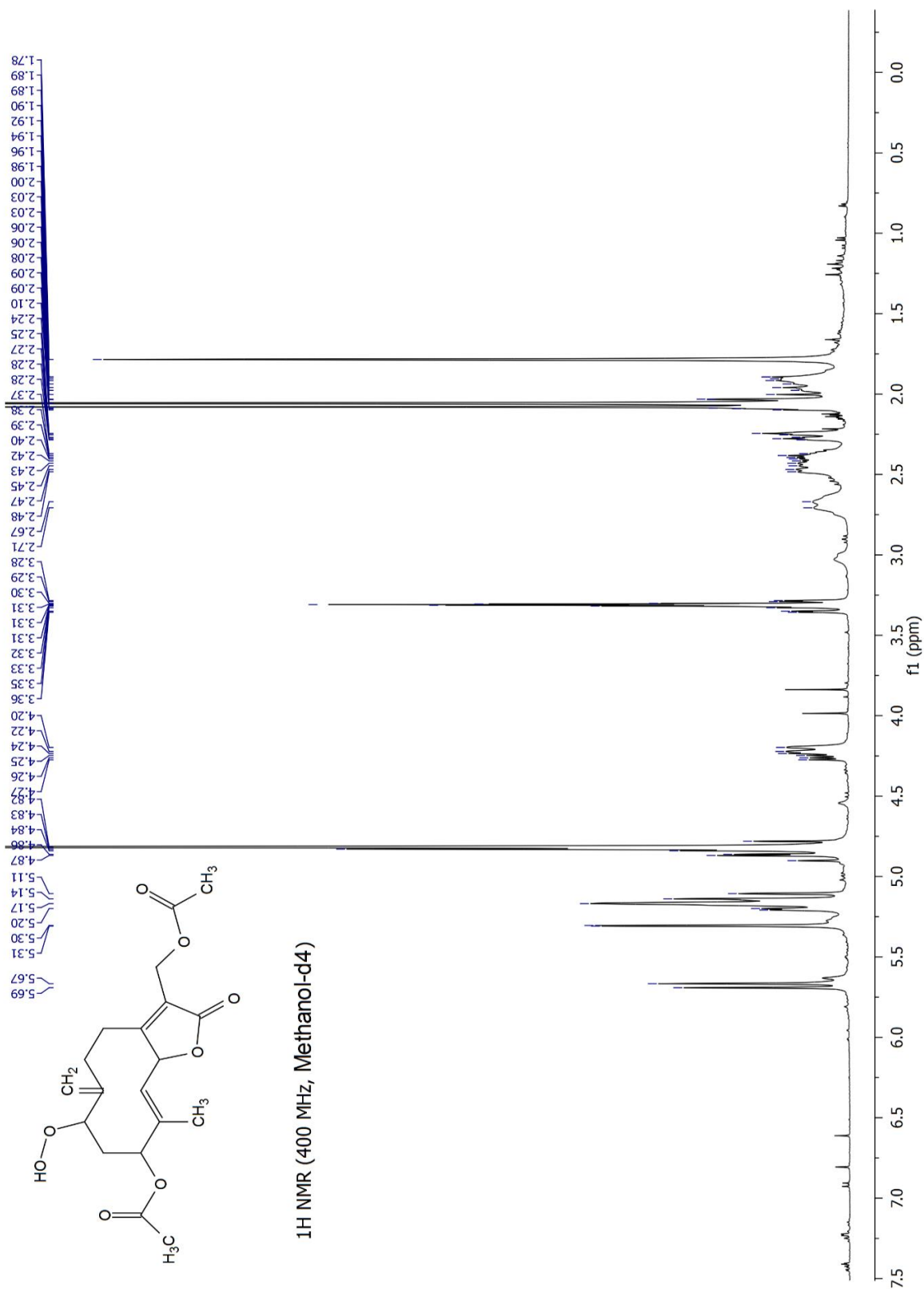


Fig. A 6 ¹³C Spectrum of compound 3.

Fig. A 7 ^1H Spectrum of compound 4.

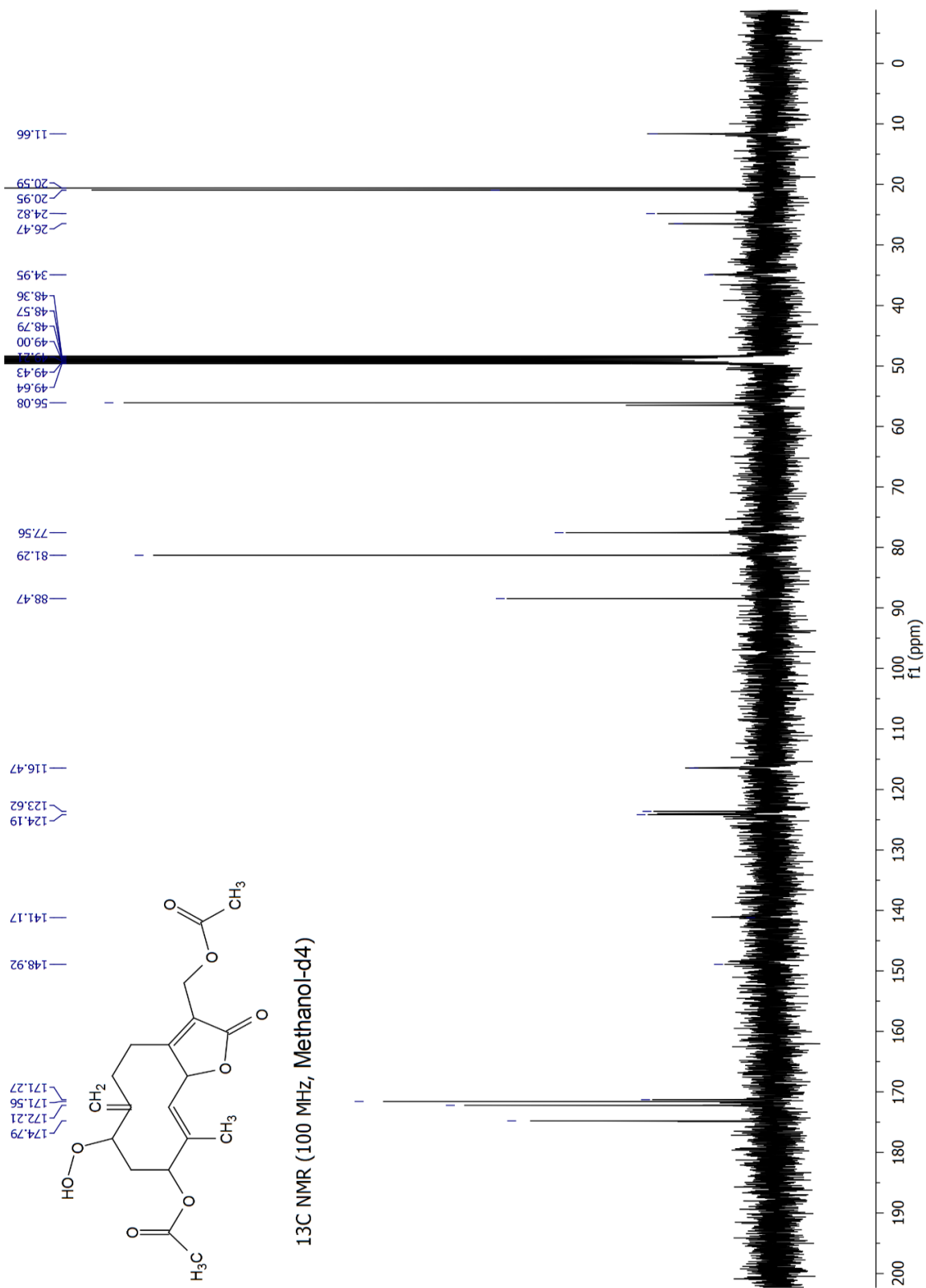


Fig. A 8 ¹³C Spectrum of compound 4.

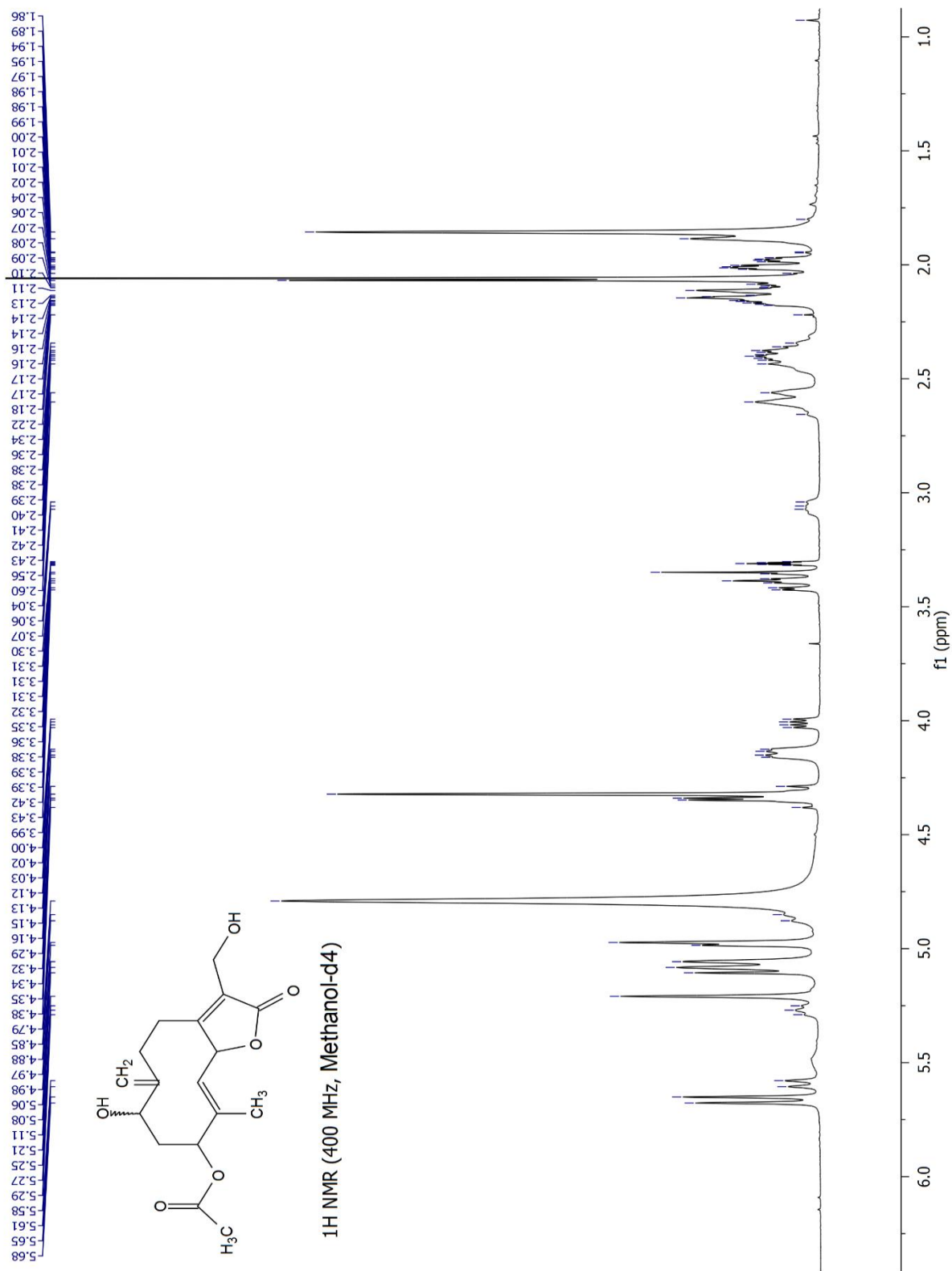
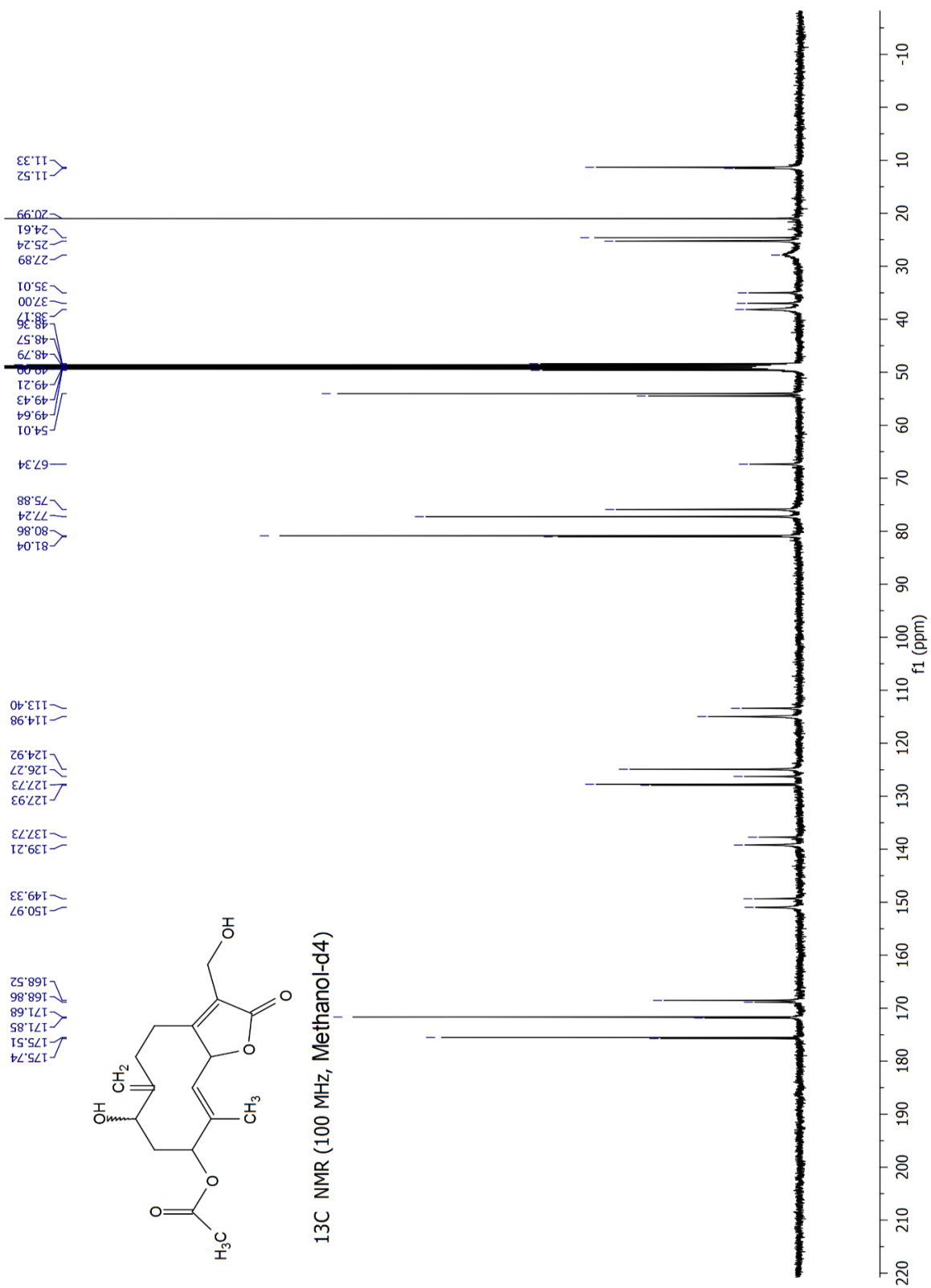
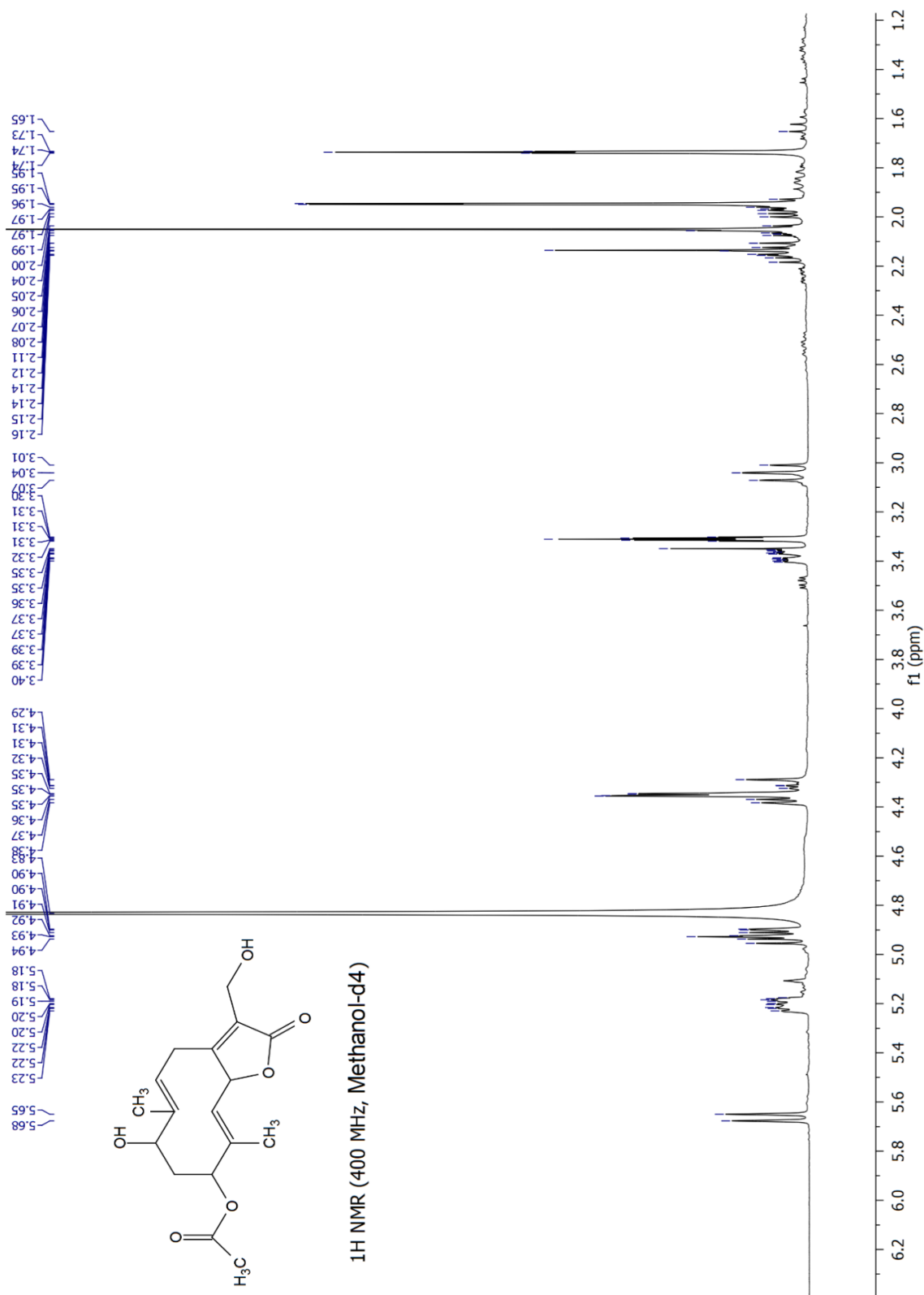


Fig. A 9 1H Spectrum of compounds 5+6.

Fig. A 10 ¹³C Spectrum of compounds 5+6.

Fig. A 11 ¹H Spectrum of compound 7.

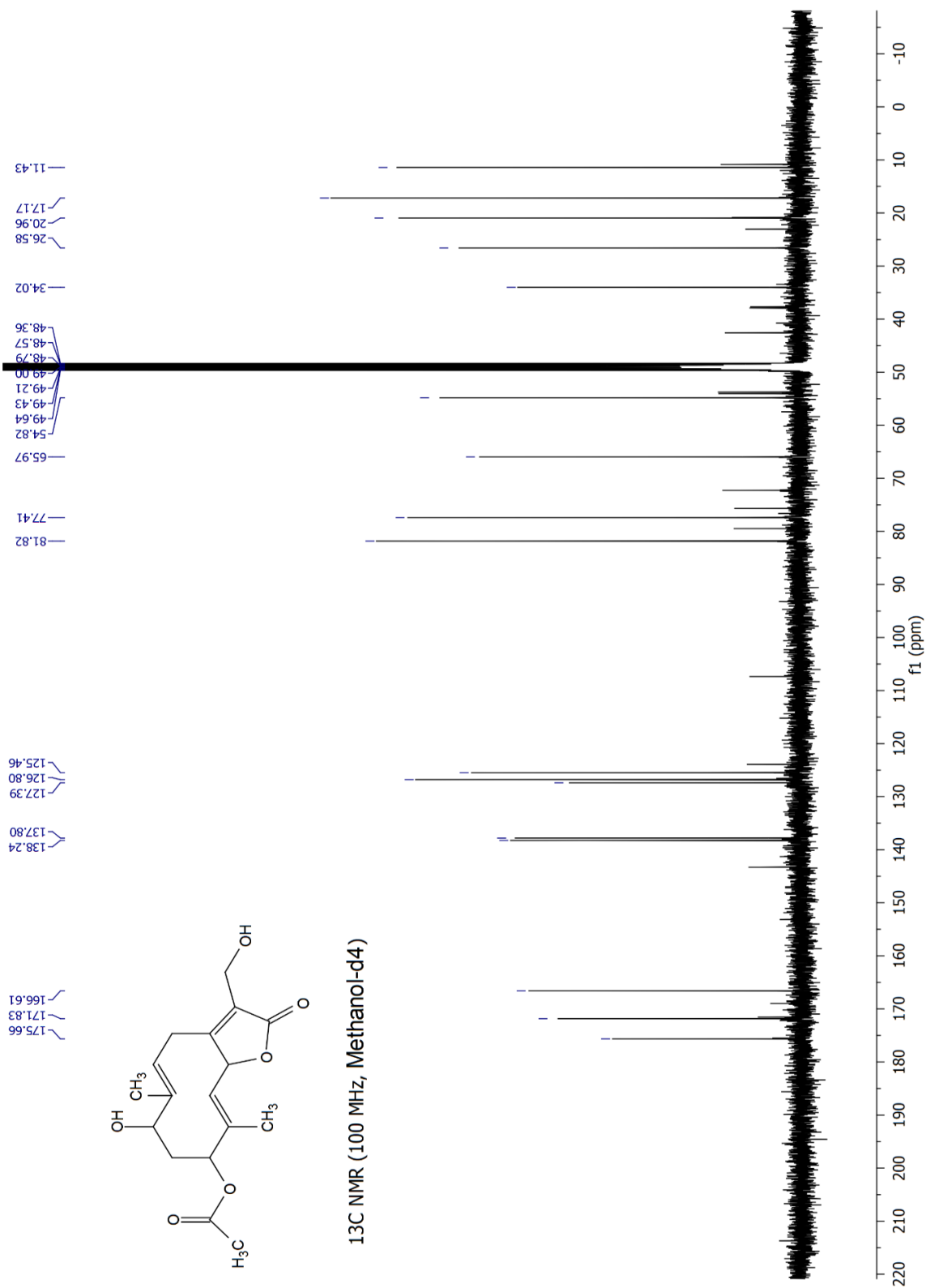
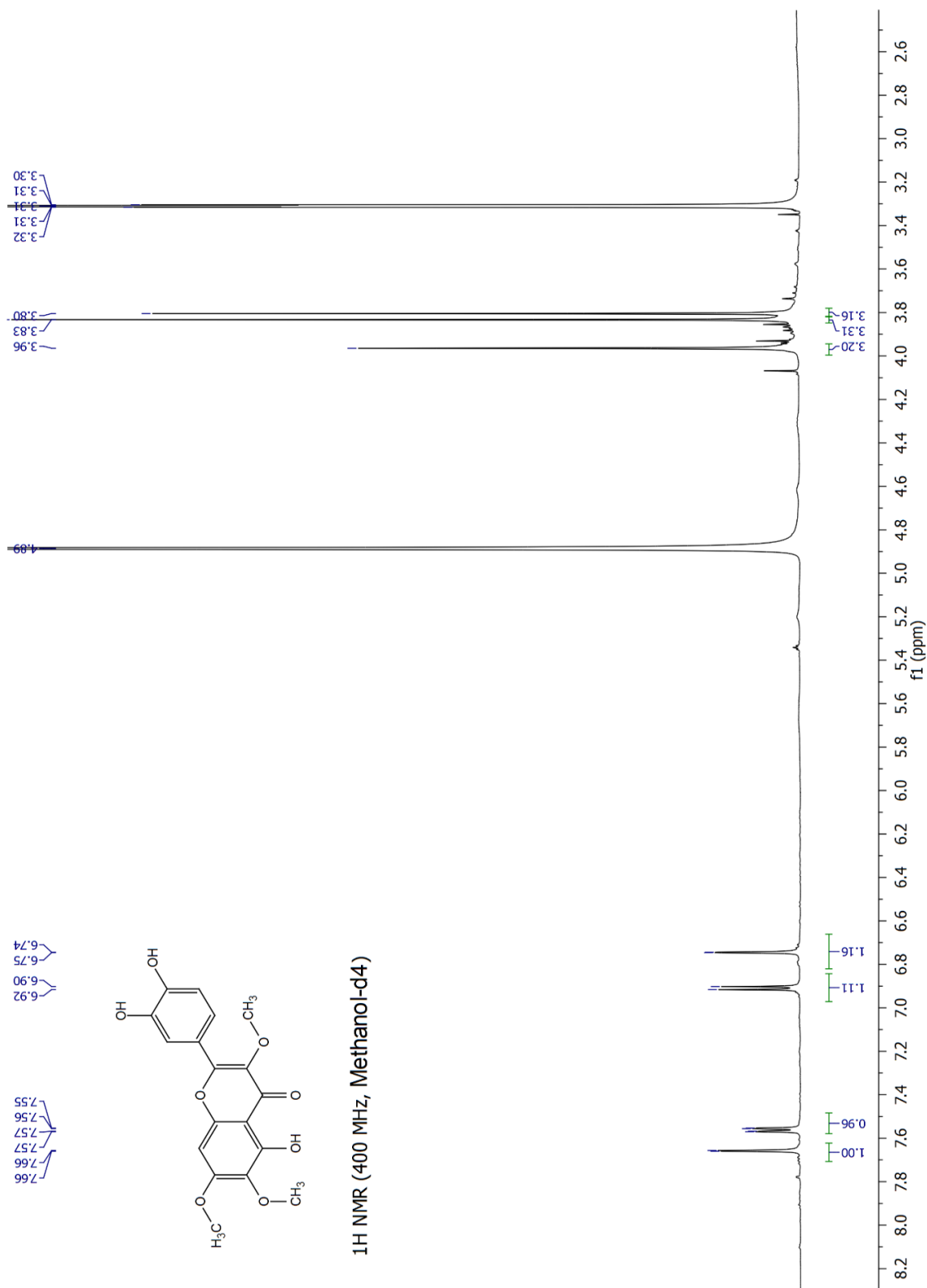


Fig. A 12 ¹³C Spectrum of compound 7.

Fig. A 13 ¹H Spectrum of compound 8.

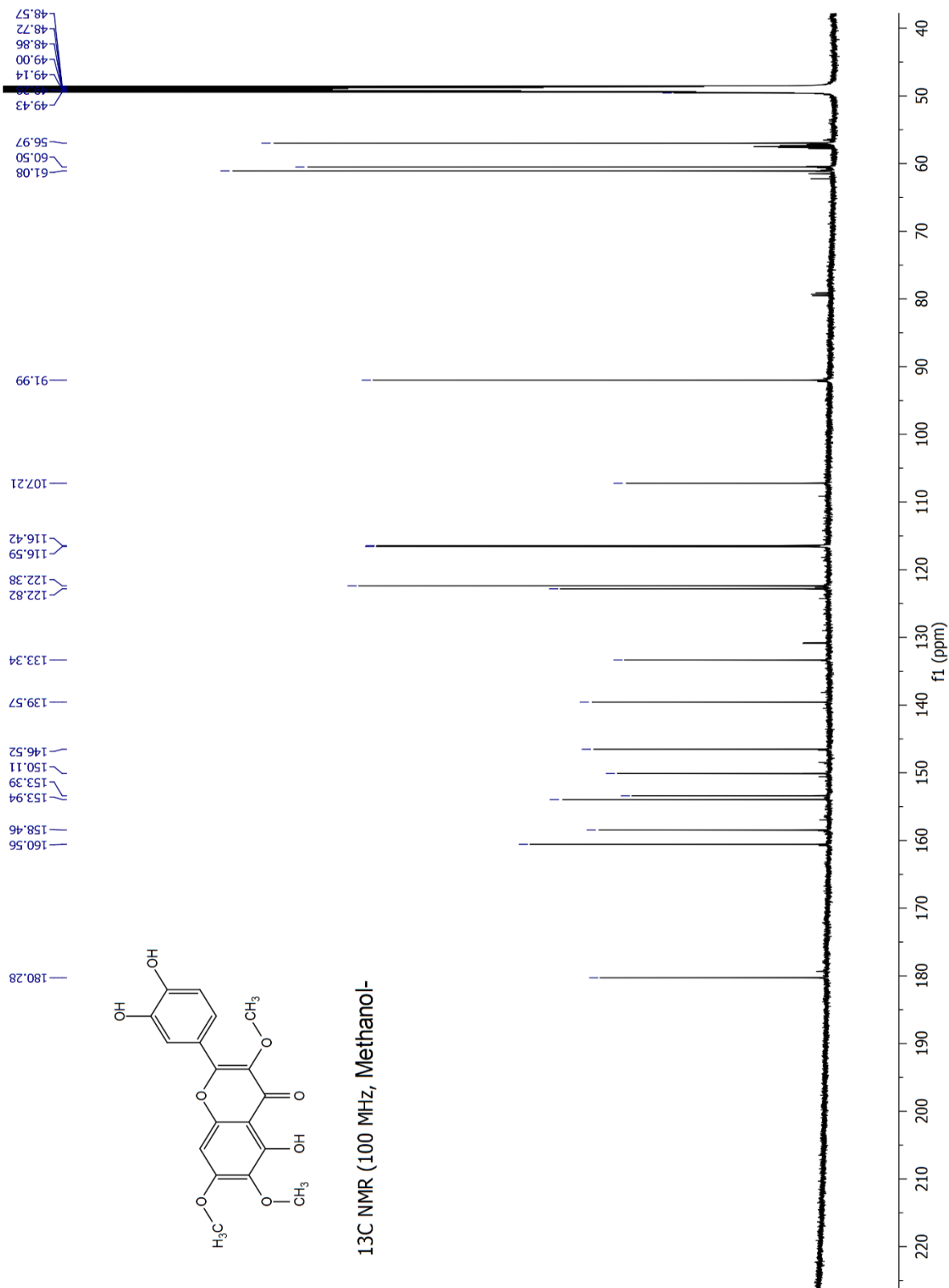
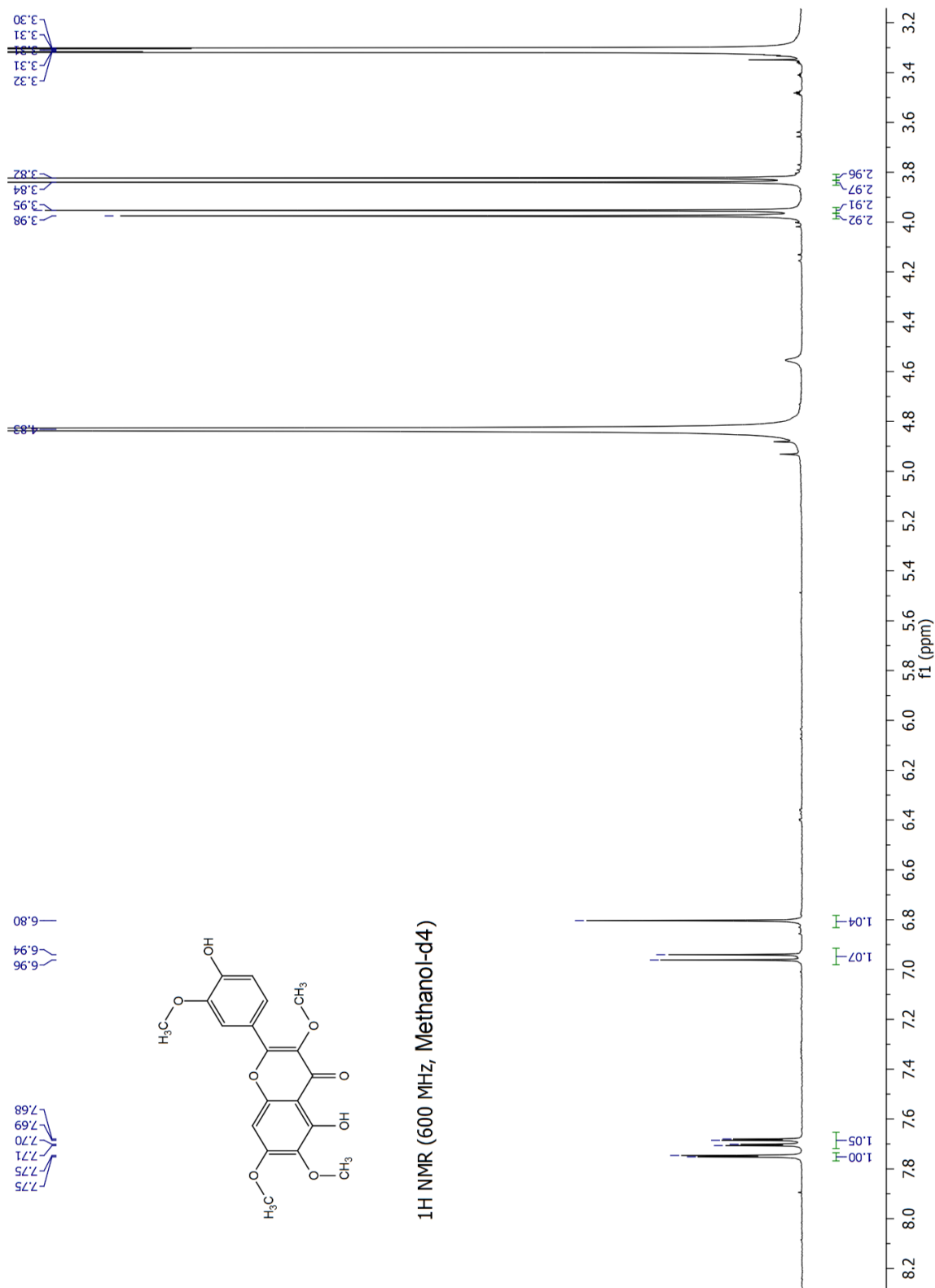


Fig. A 14 ^{13}C Spectrum of compound 8.

Fig. A 15 ¹H Spectrum of compound 9.

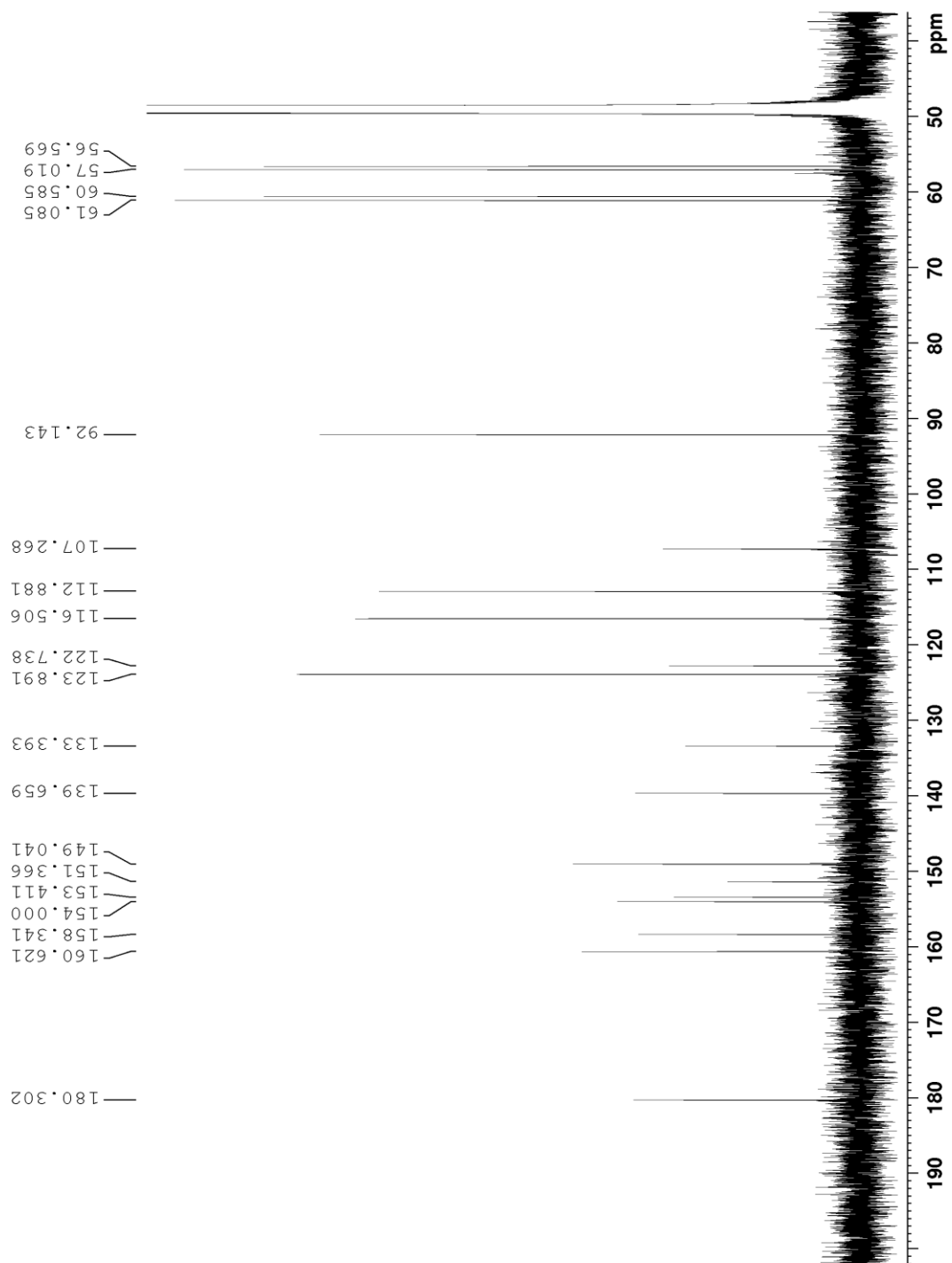
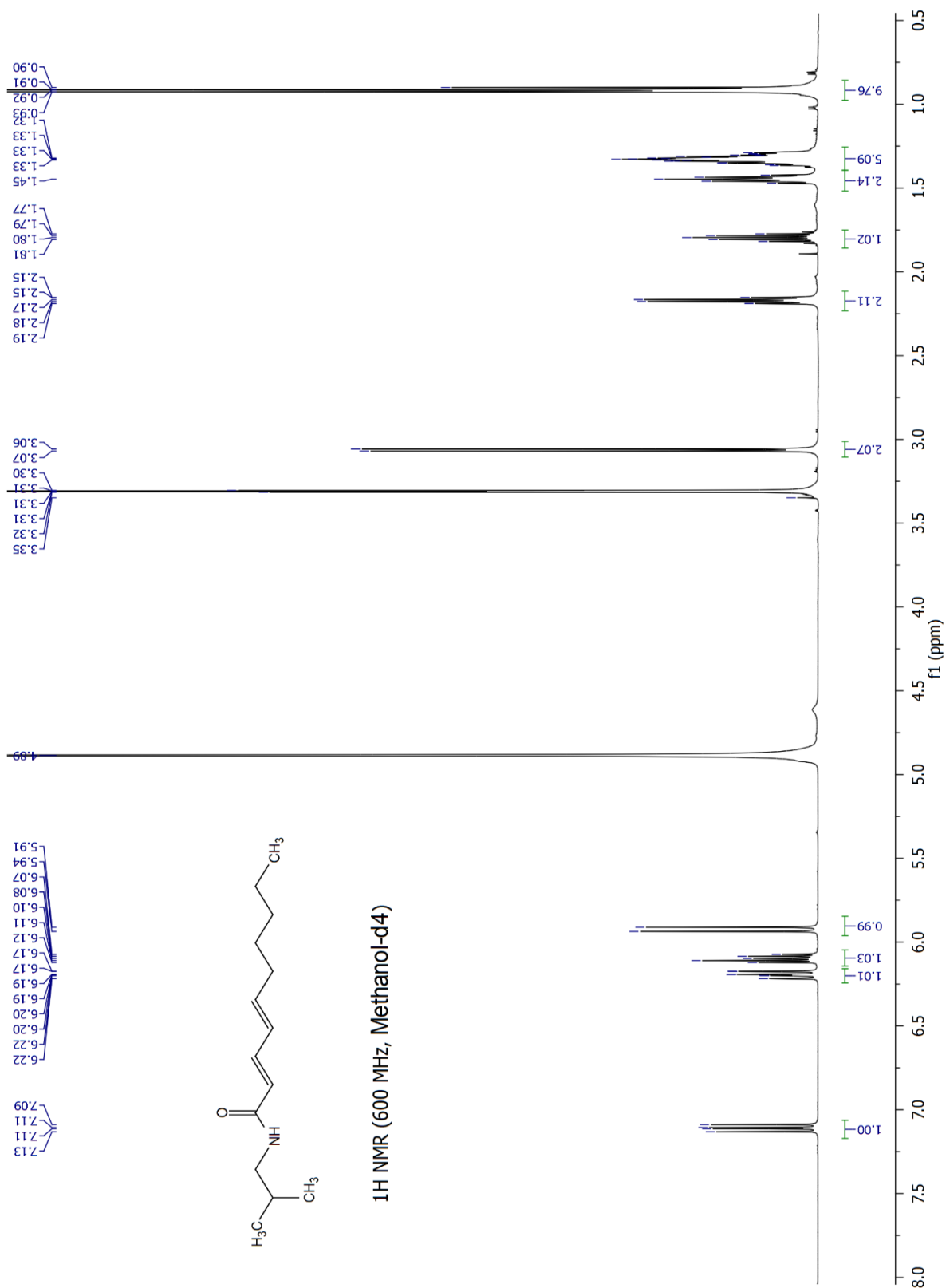
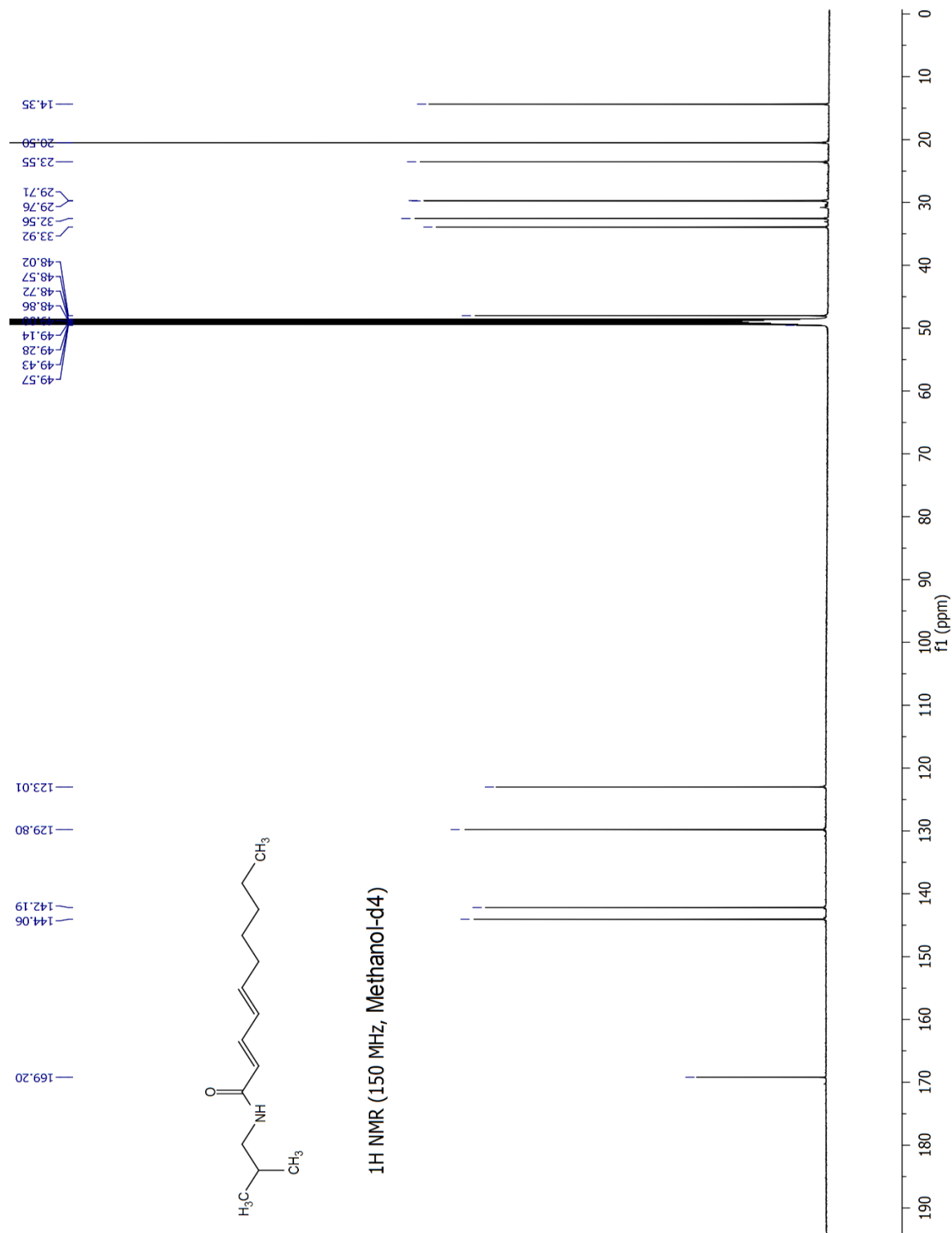
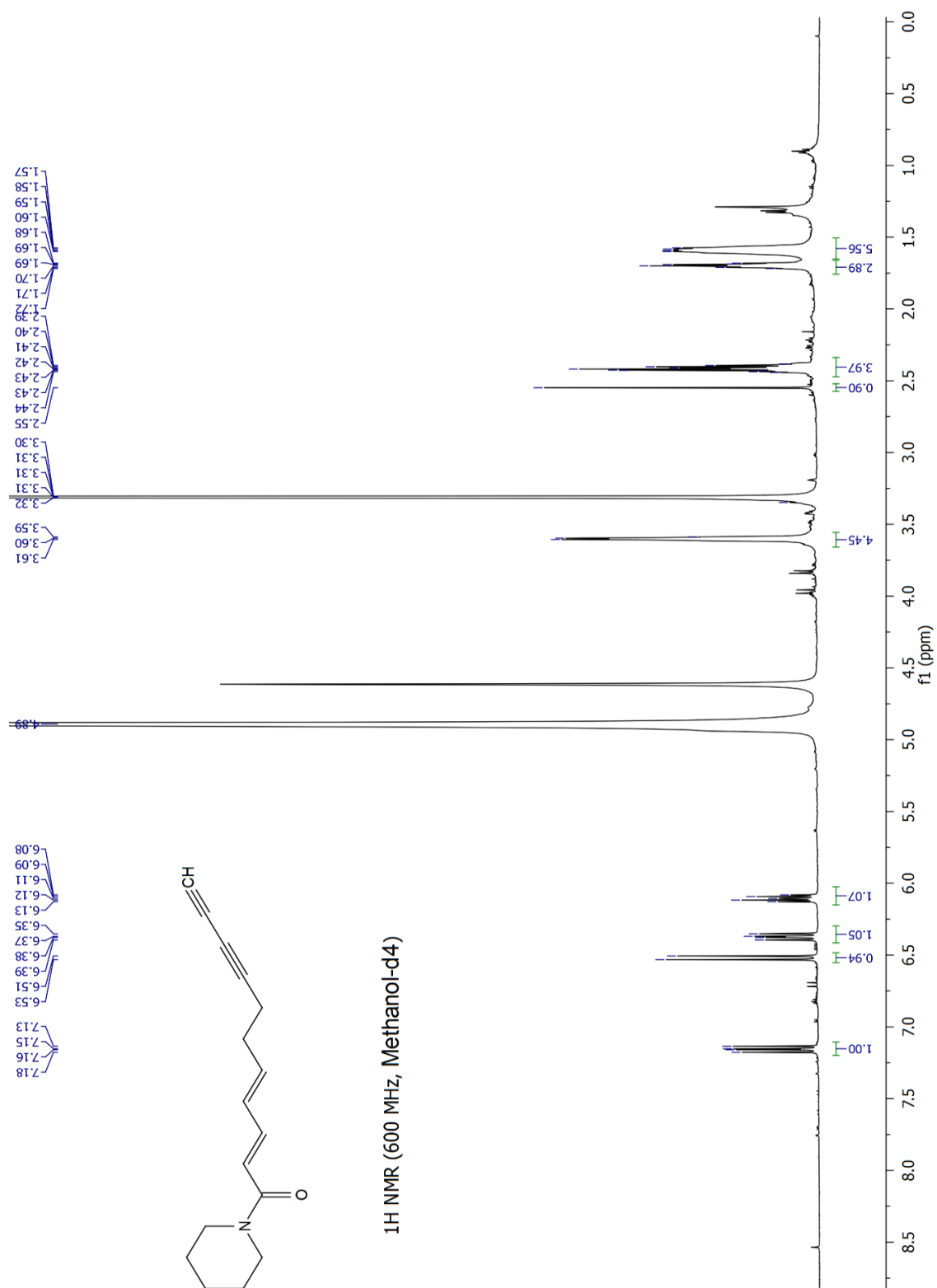
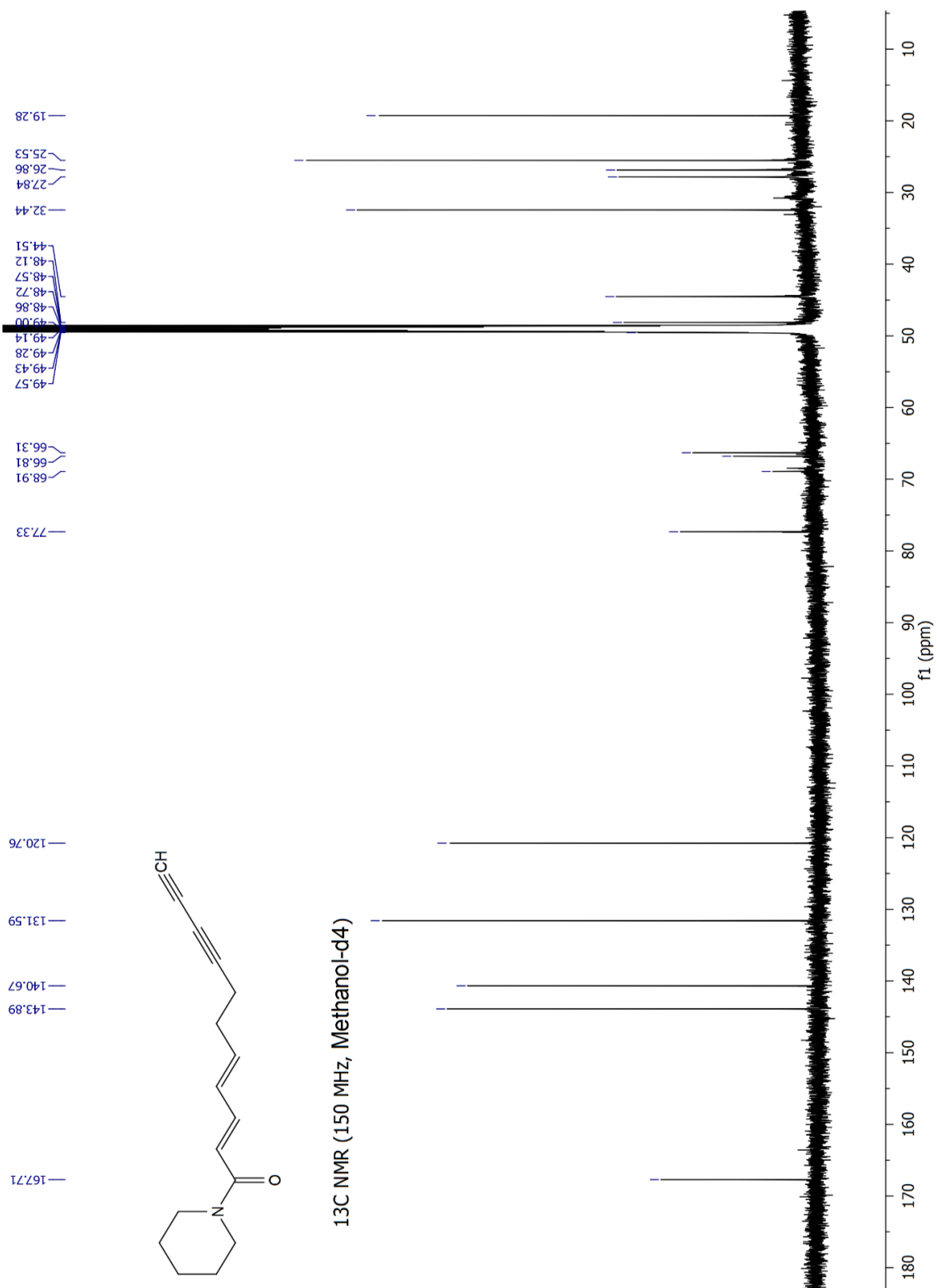


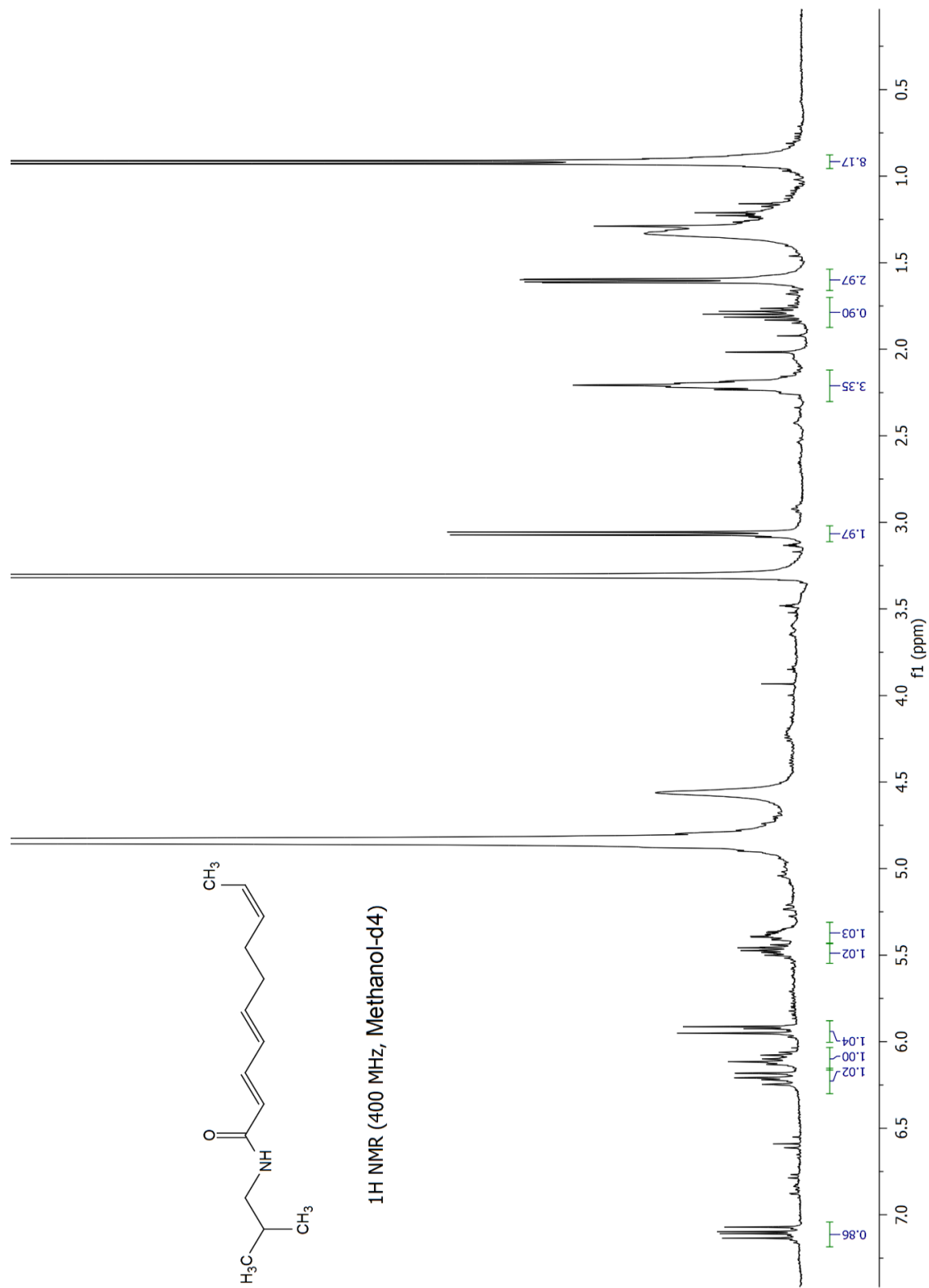
Fig. A ^{13}C Spectrum of compound 9.

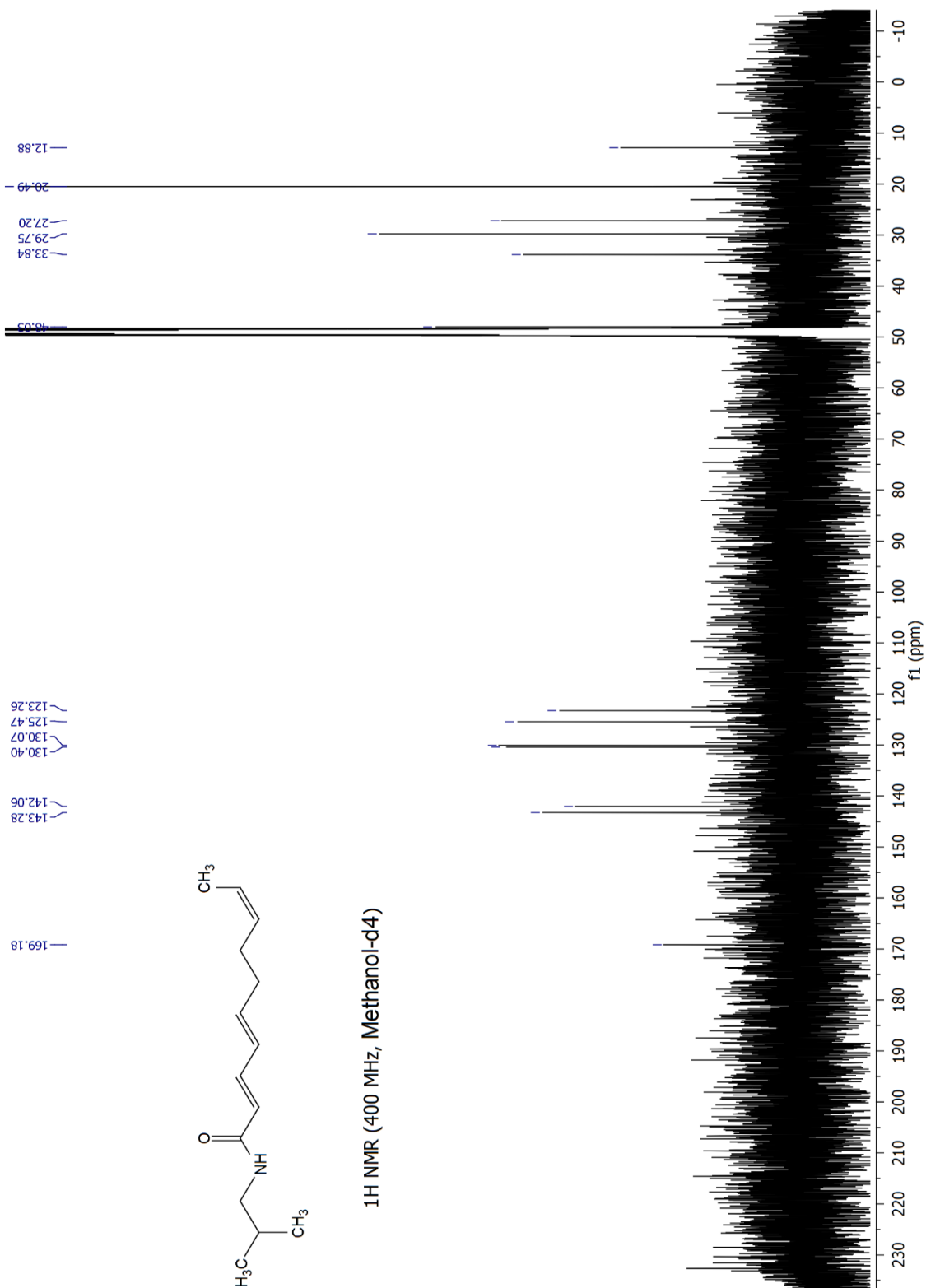
Fig. A 17 ¹H Spectrum of compound 10.

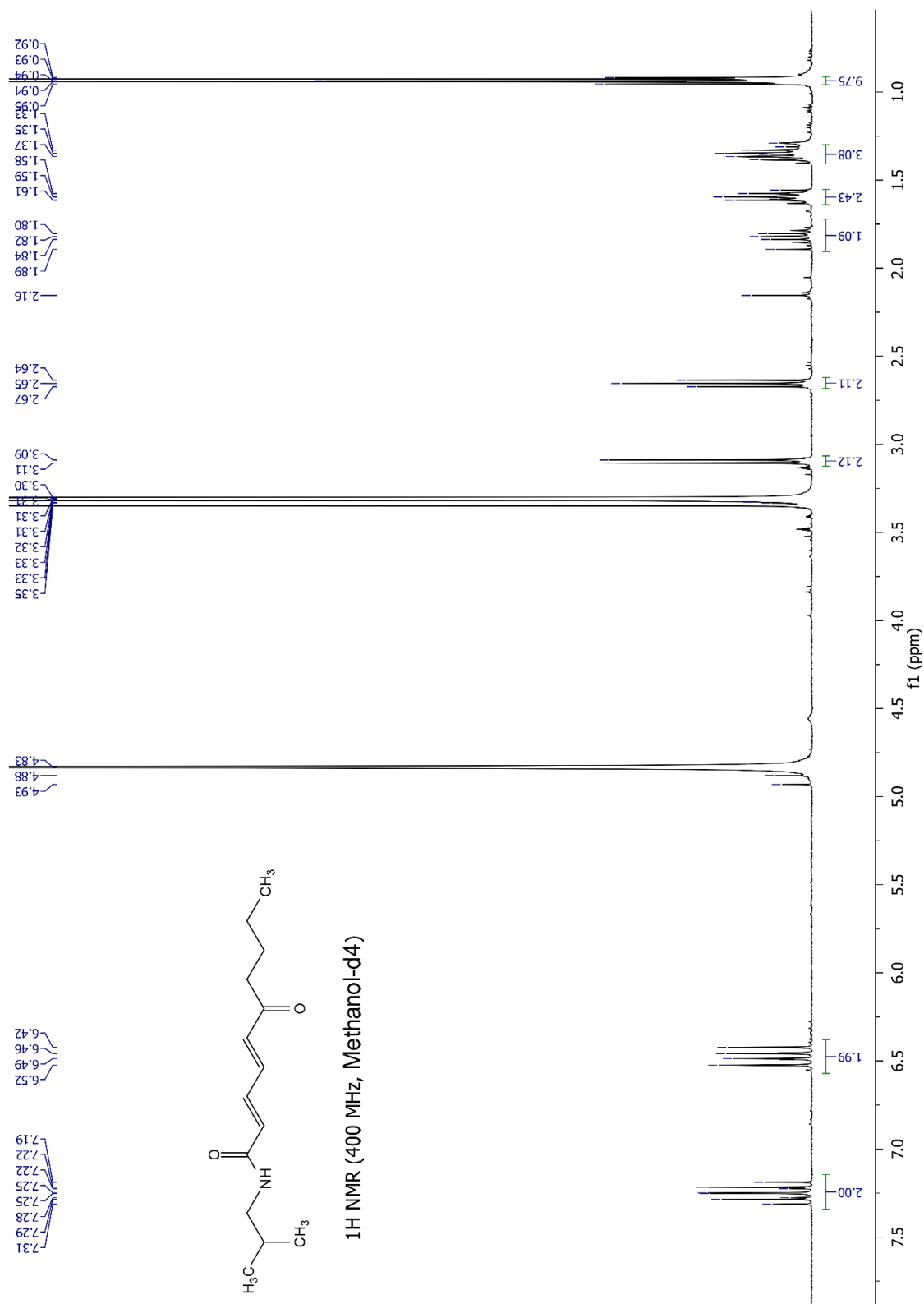
Fig. A 18 ¹³C Spectrum of compound 10.

Fig. A ¹H Spectrum of compound 11.

Fig. A 20 ¹³C Spectrum of compound 11.

Fig. A 21 ^1H Spectrum of compound 12.

Fig. A 22 ¹³C Spectrum of compound 12.

Fig. A 23 ¹H Spectrum of compound 13.

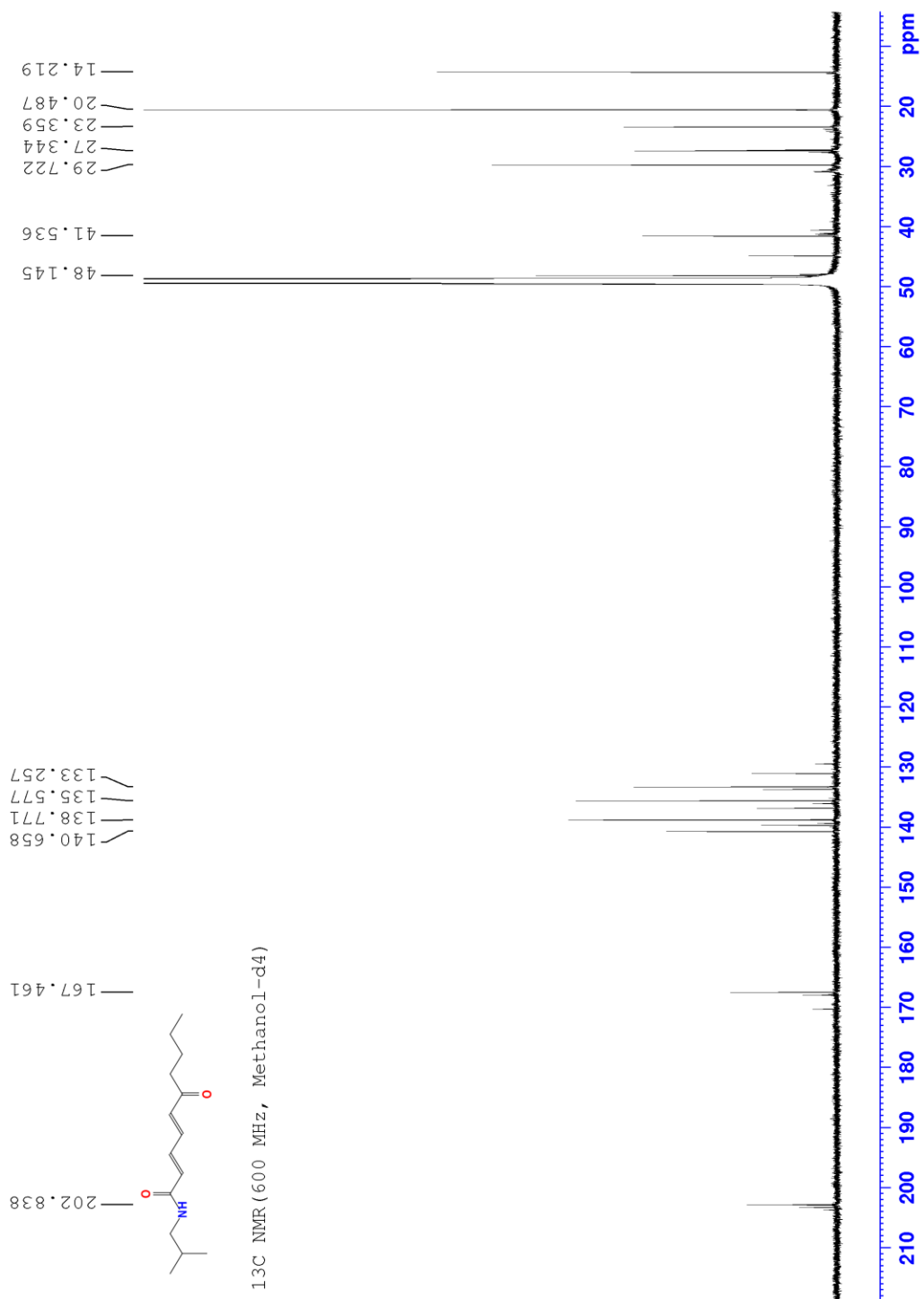


Fig. A 24 ¹³C Spectrum of compound 13.

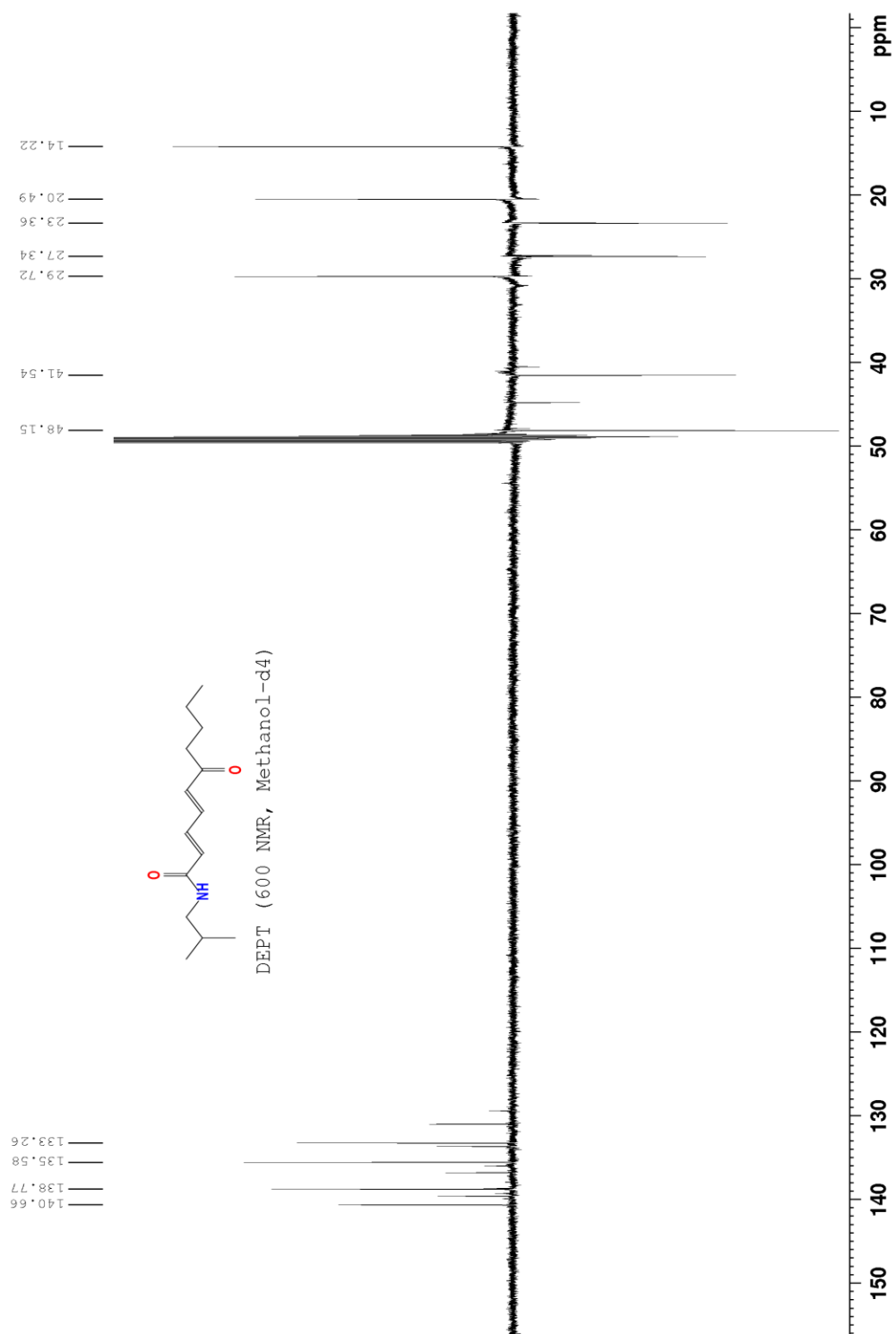
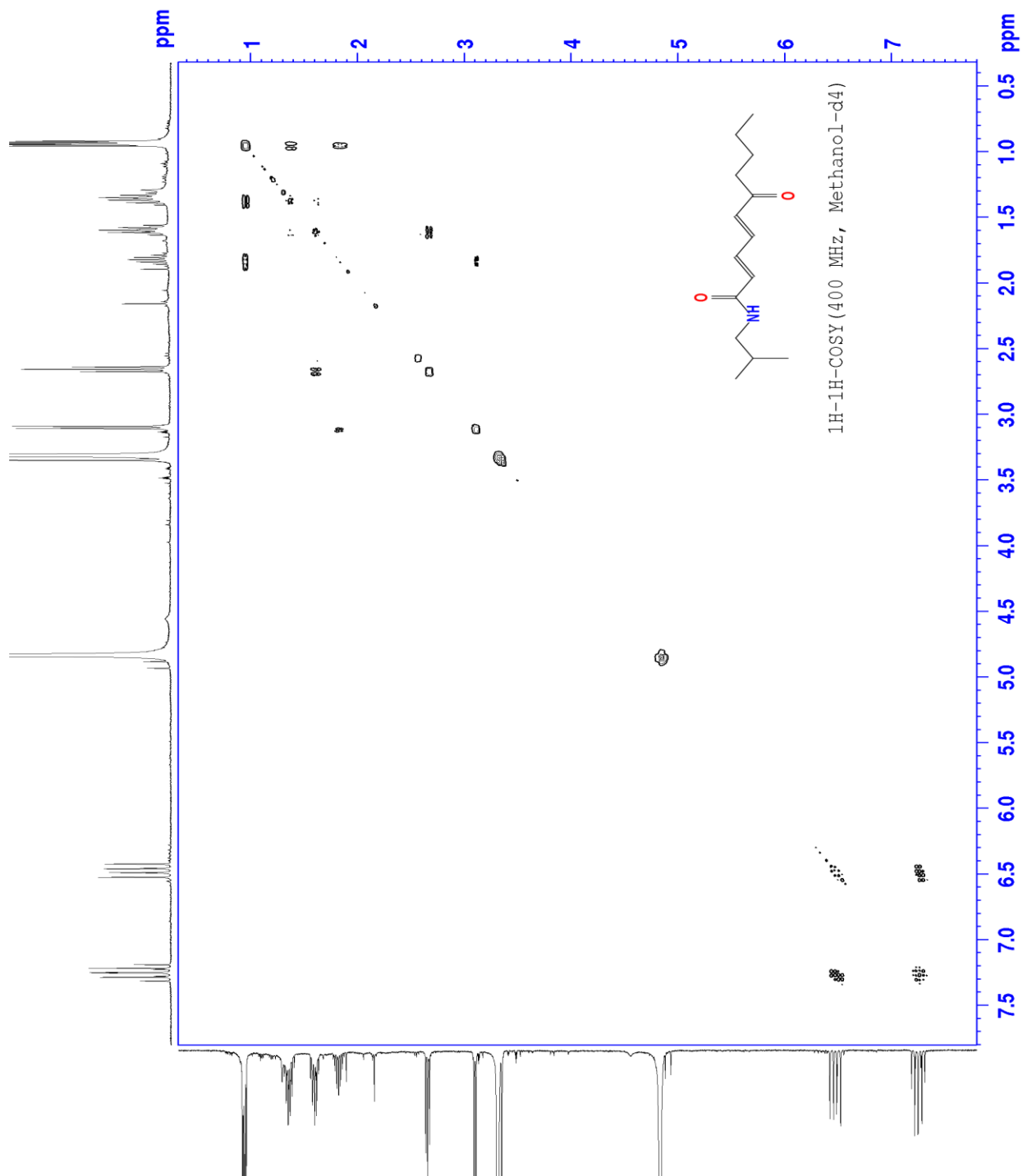


Fig. A 25 DEPT Spectrum of compound 13.

Fig. A 26 ^1H ^1H COSY Spectrum of compound 13.

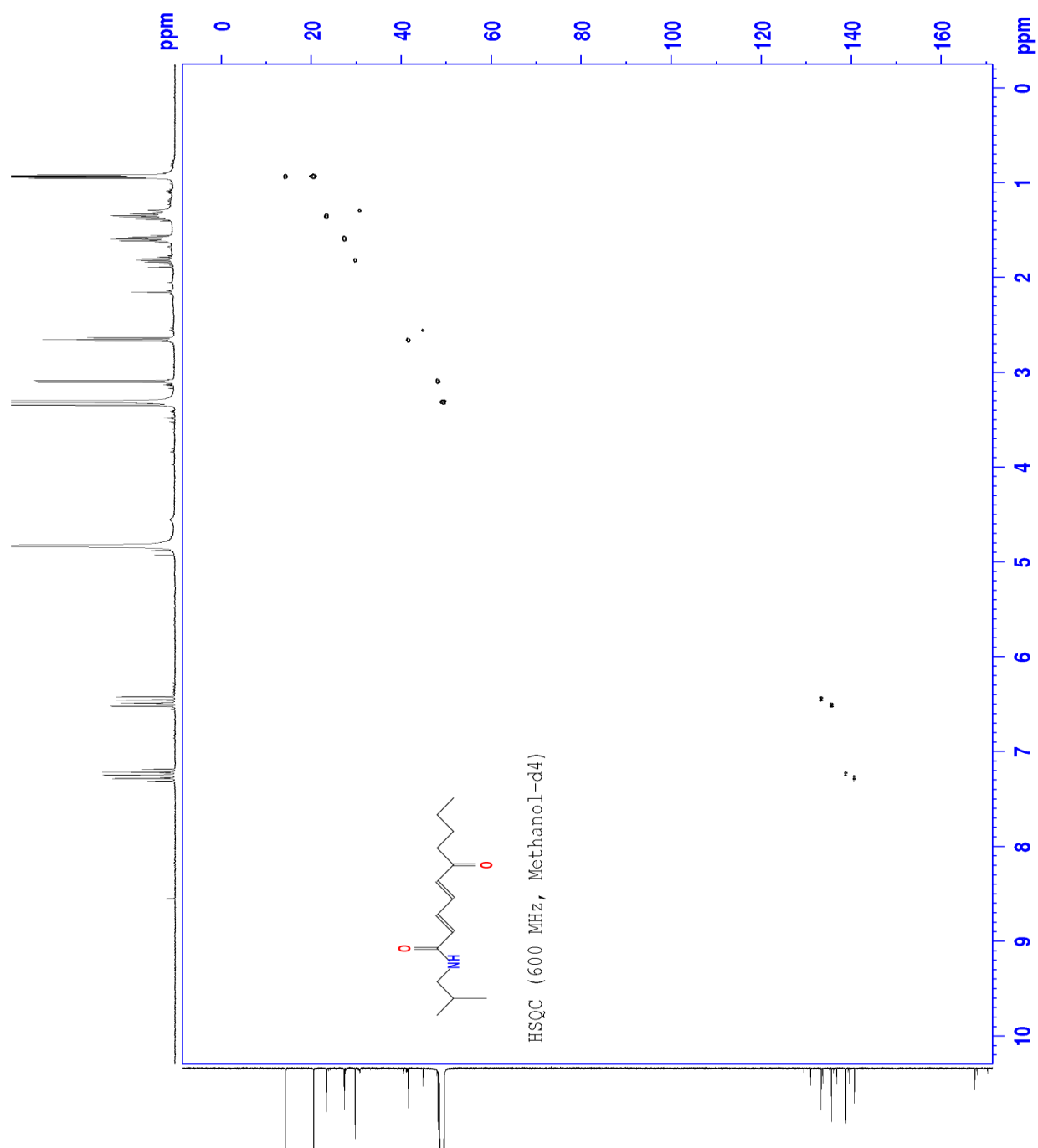


Fig. A 27 HSQC Spectrum of compound 13.

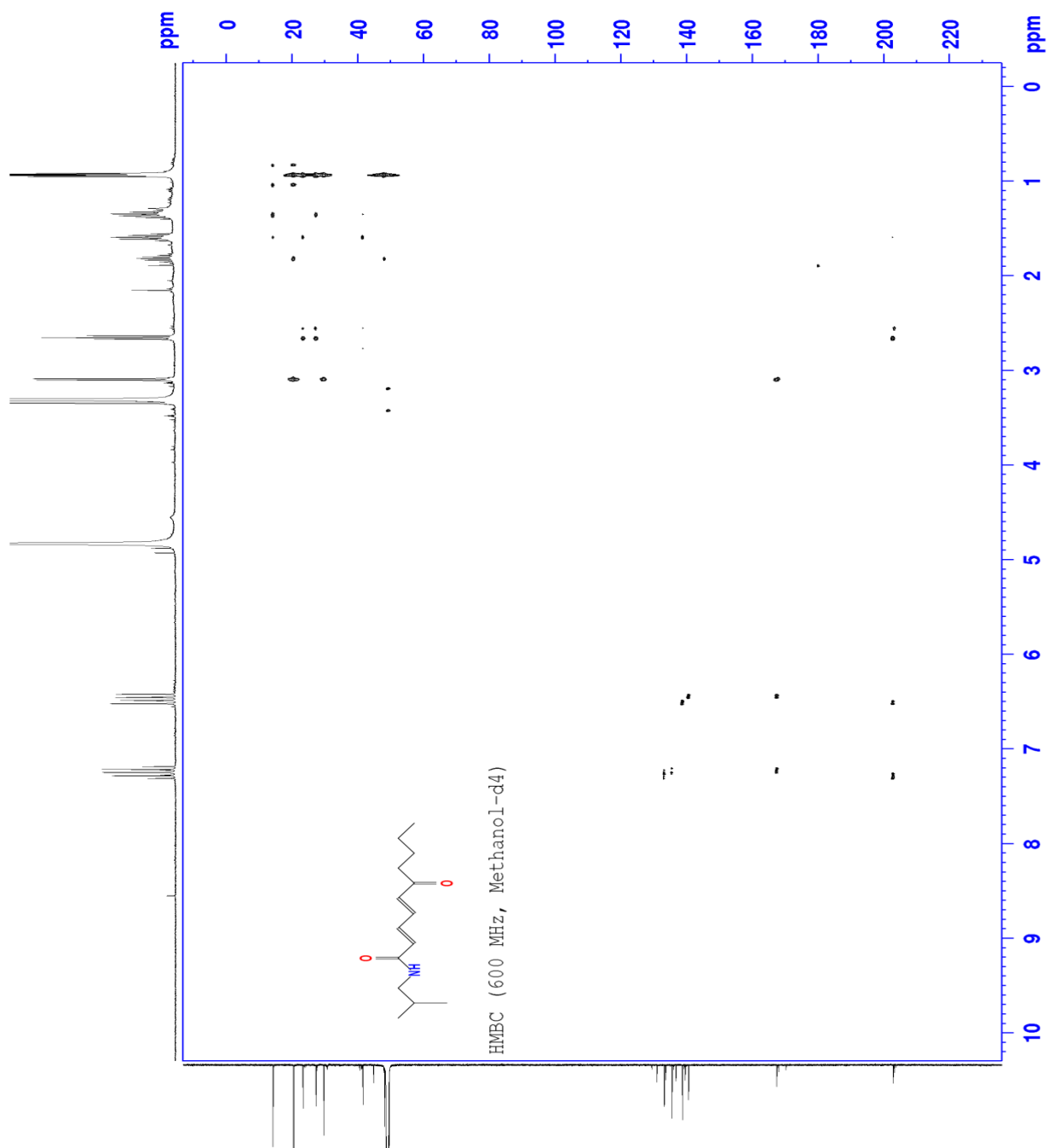
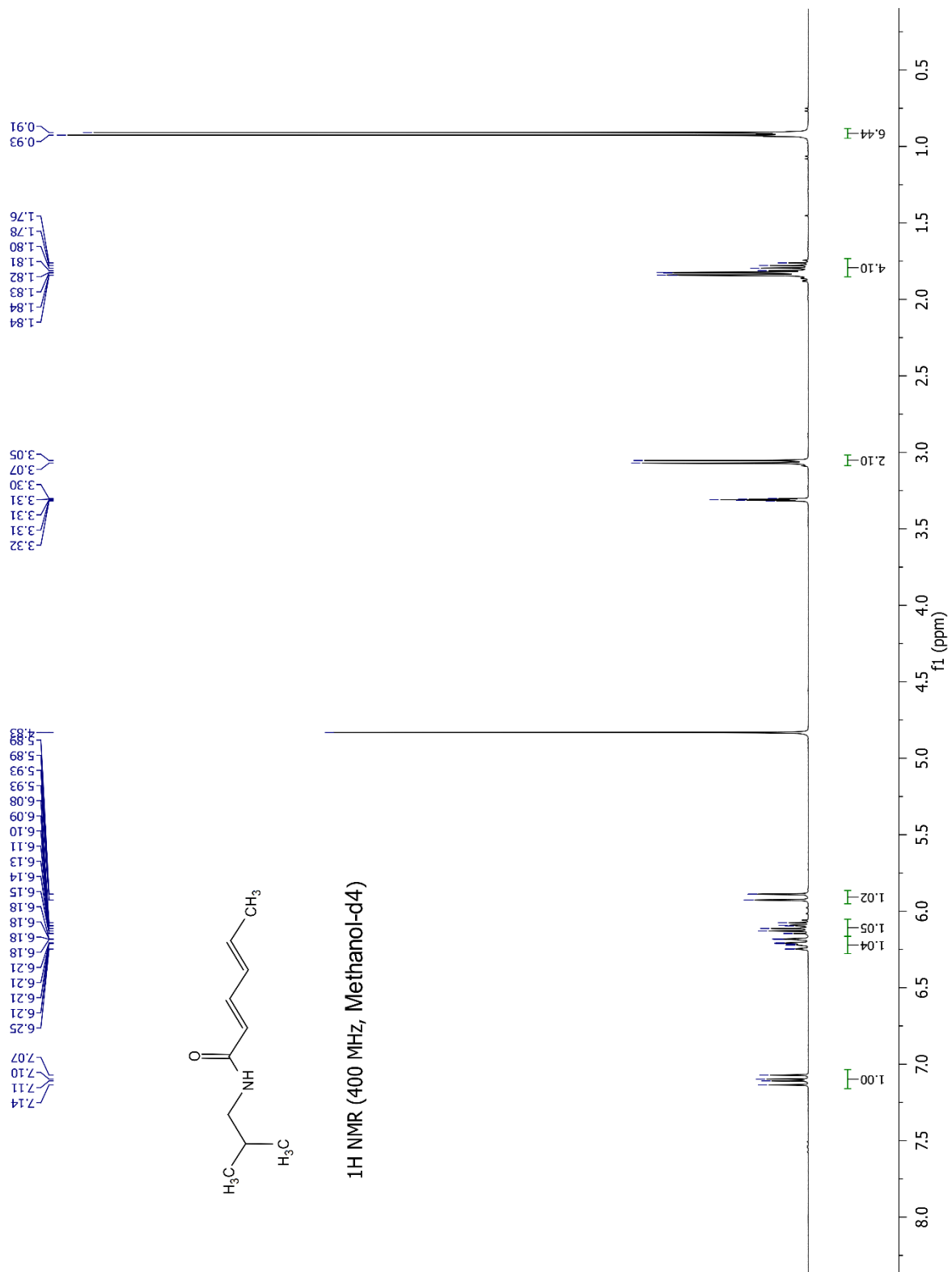
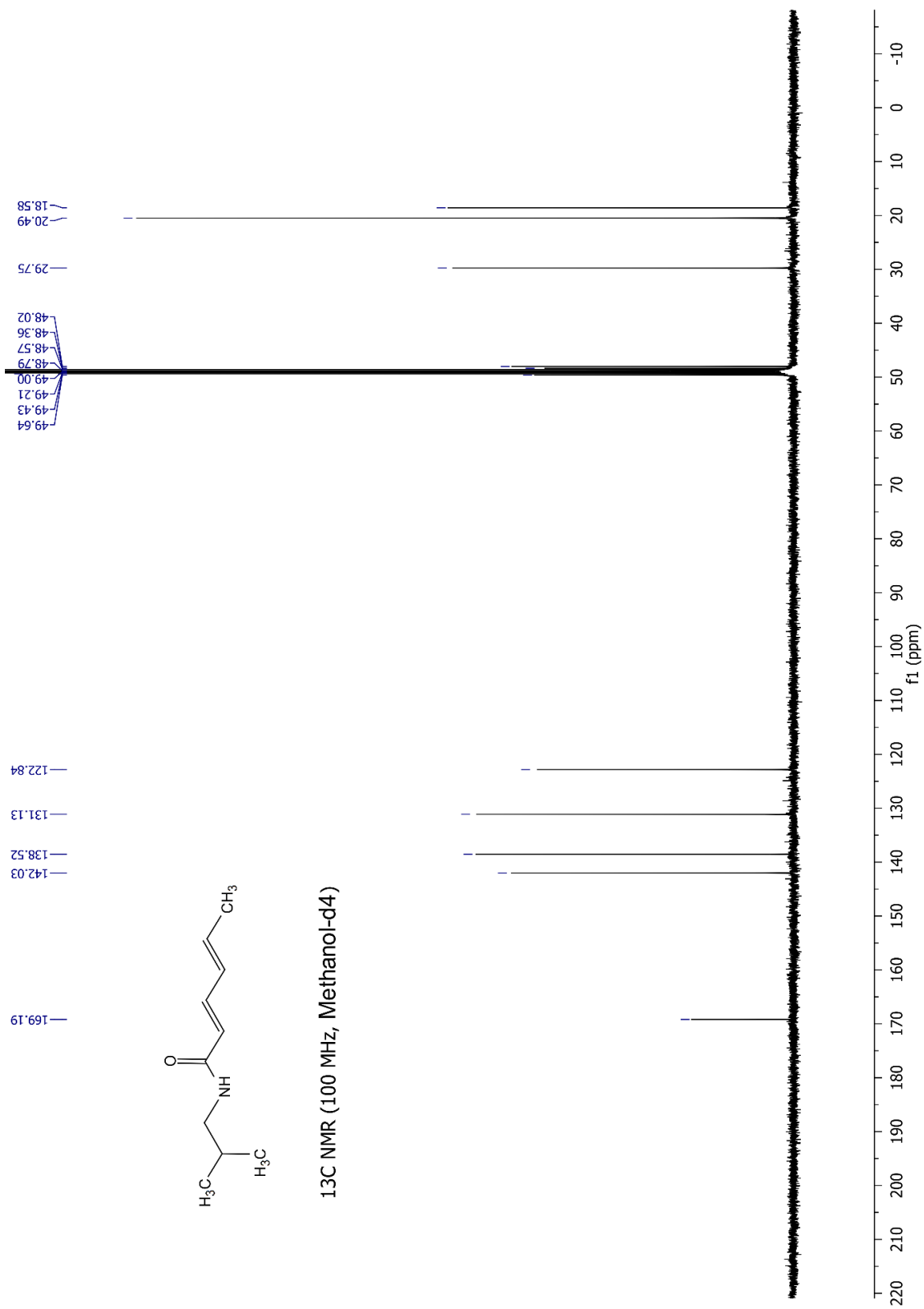


Fig. A 28 HMBC Spectrum of compound 13.

Fig. A 29 ¹H Spectrum of compound 14.

Fig. A 30 ^{13}C Spectrum of compound 14.

APPENDIX

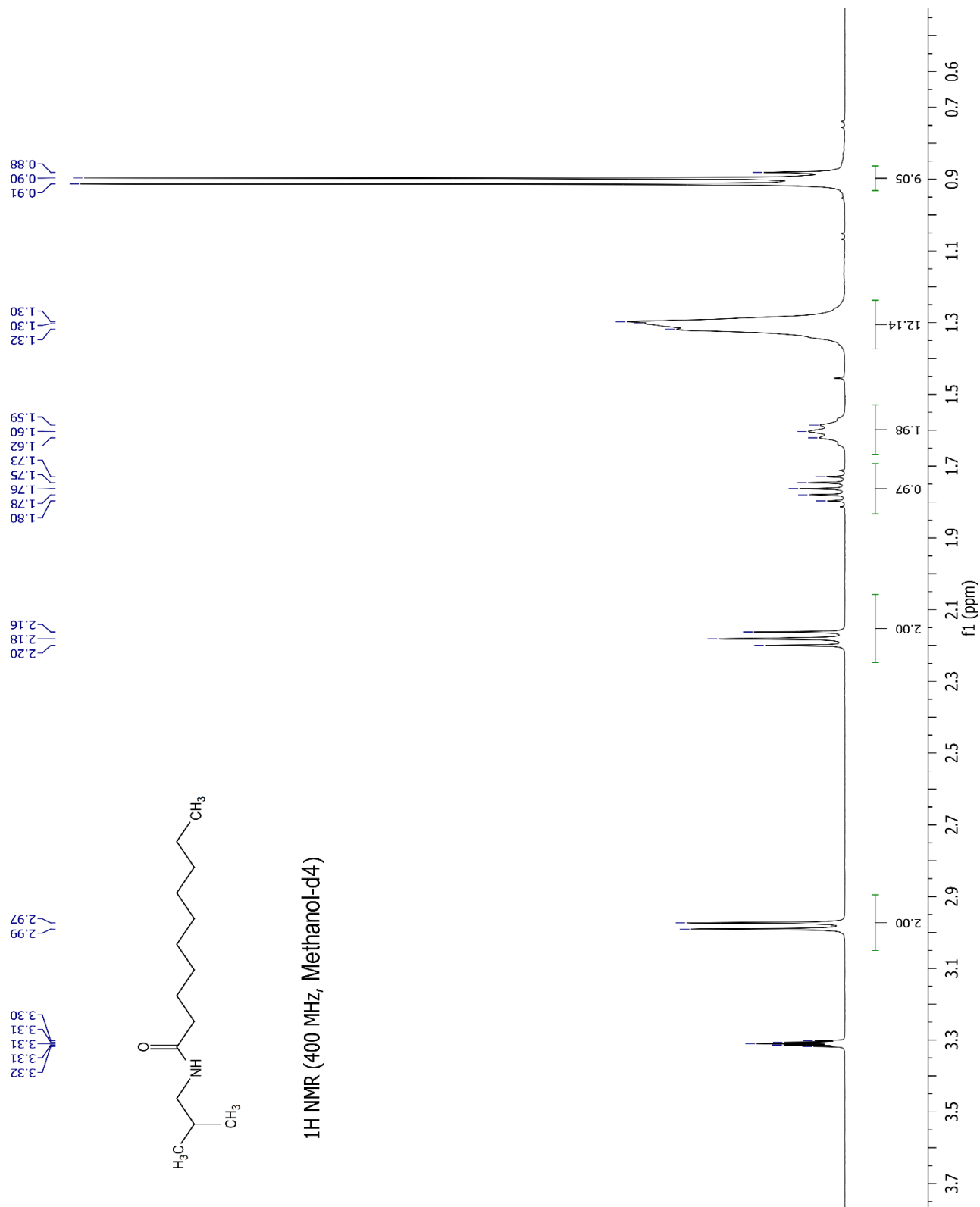
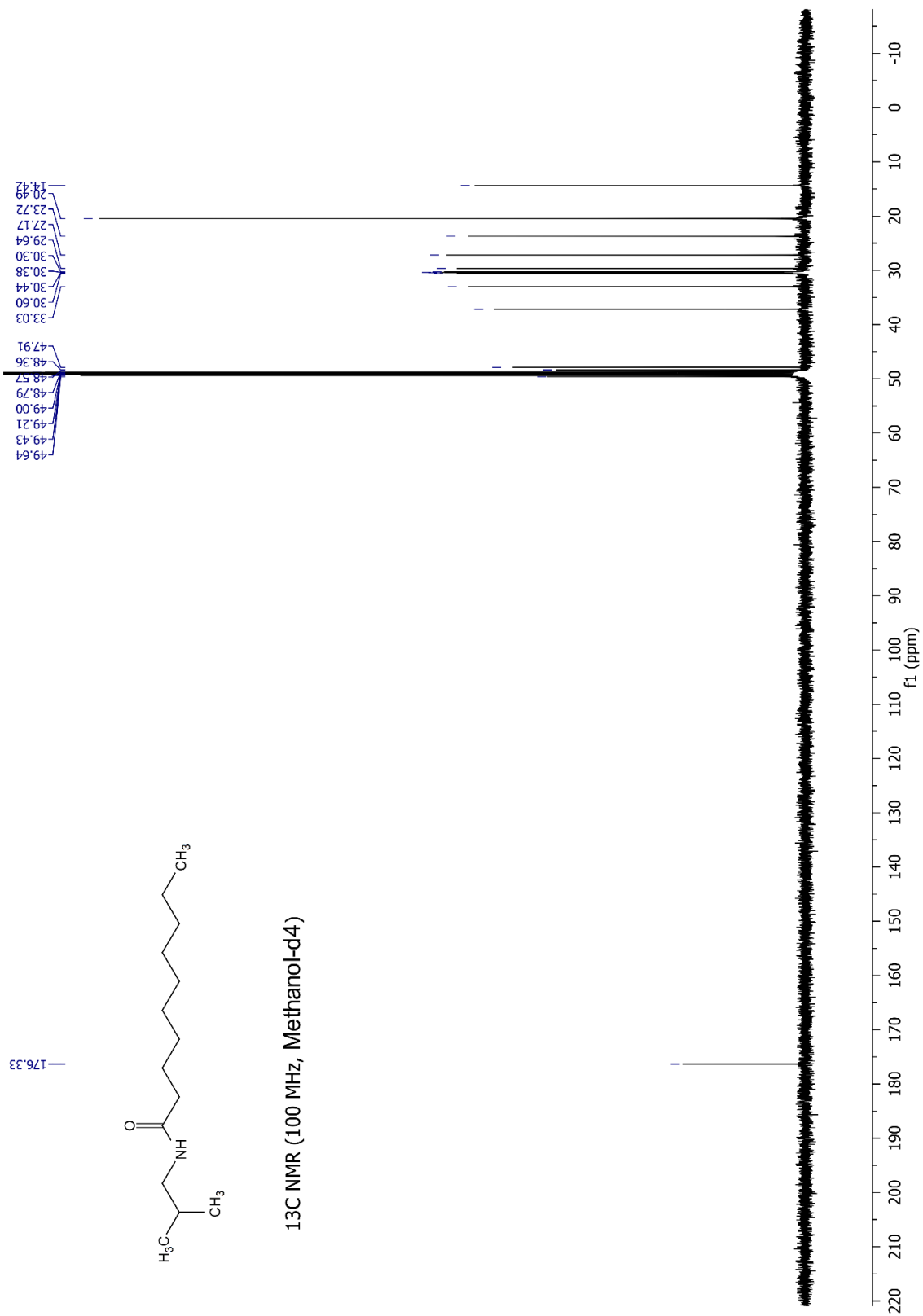
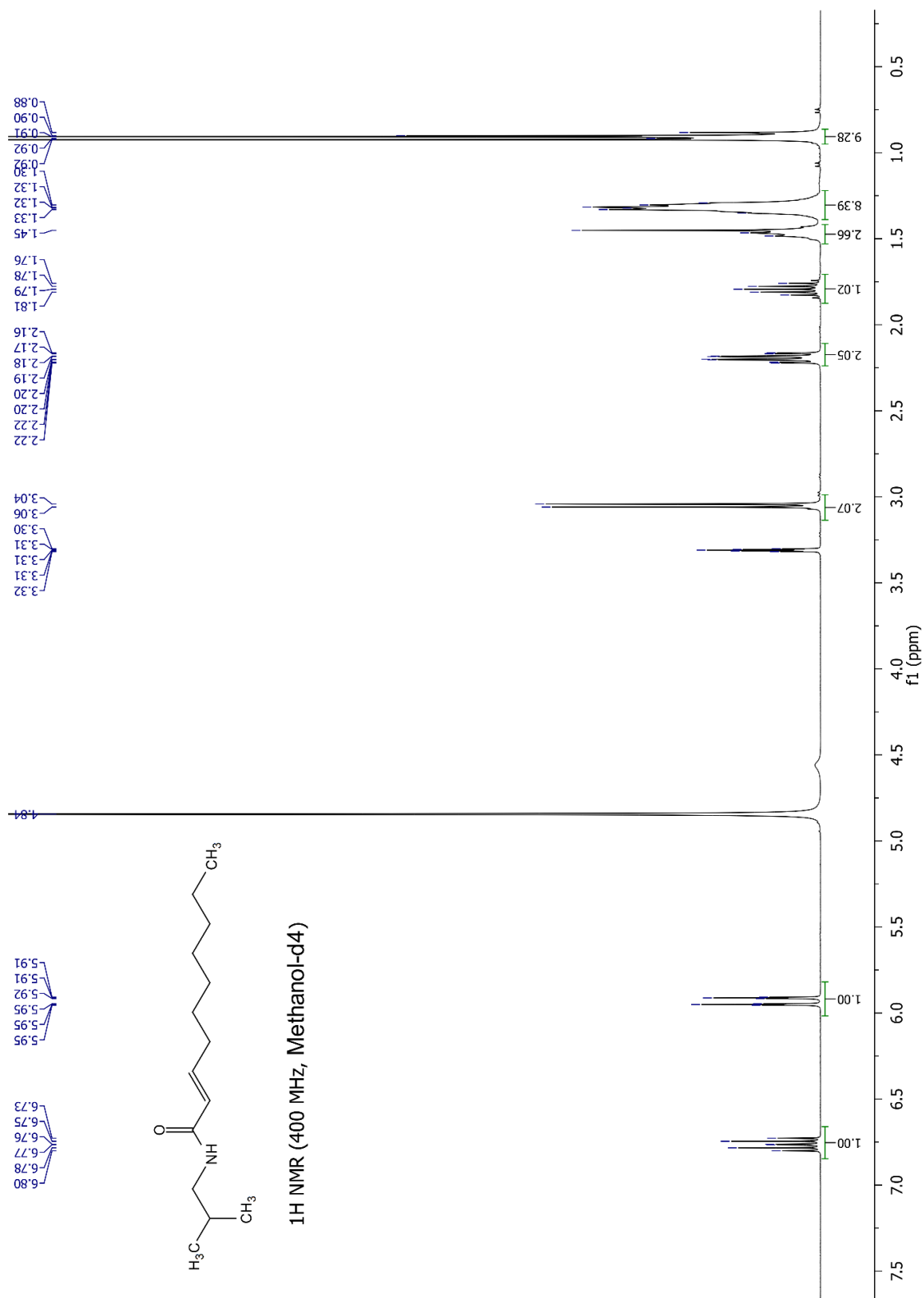
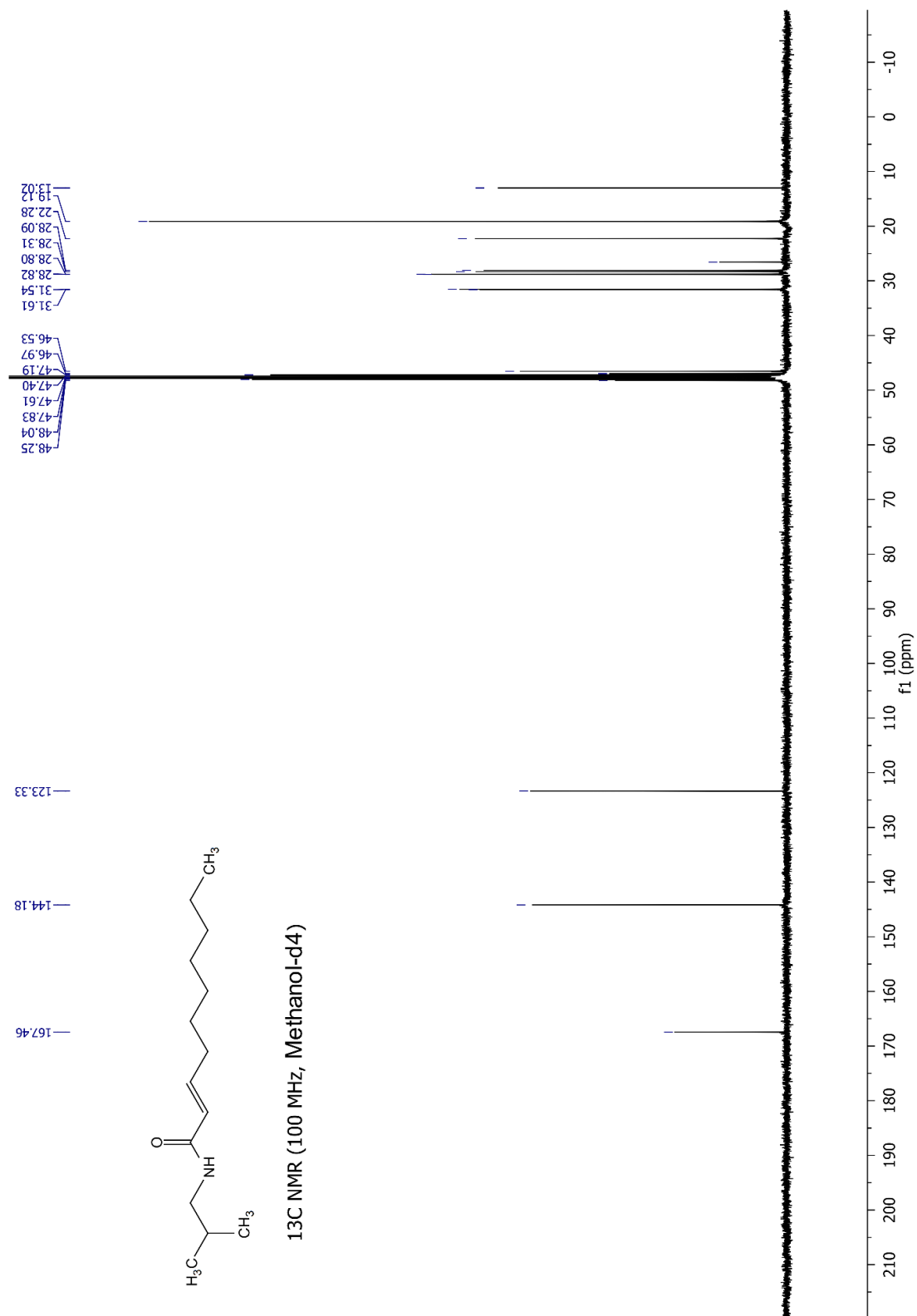
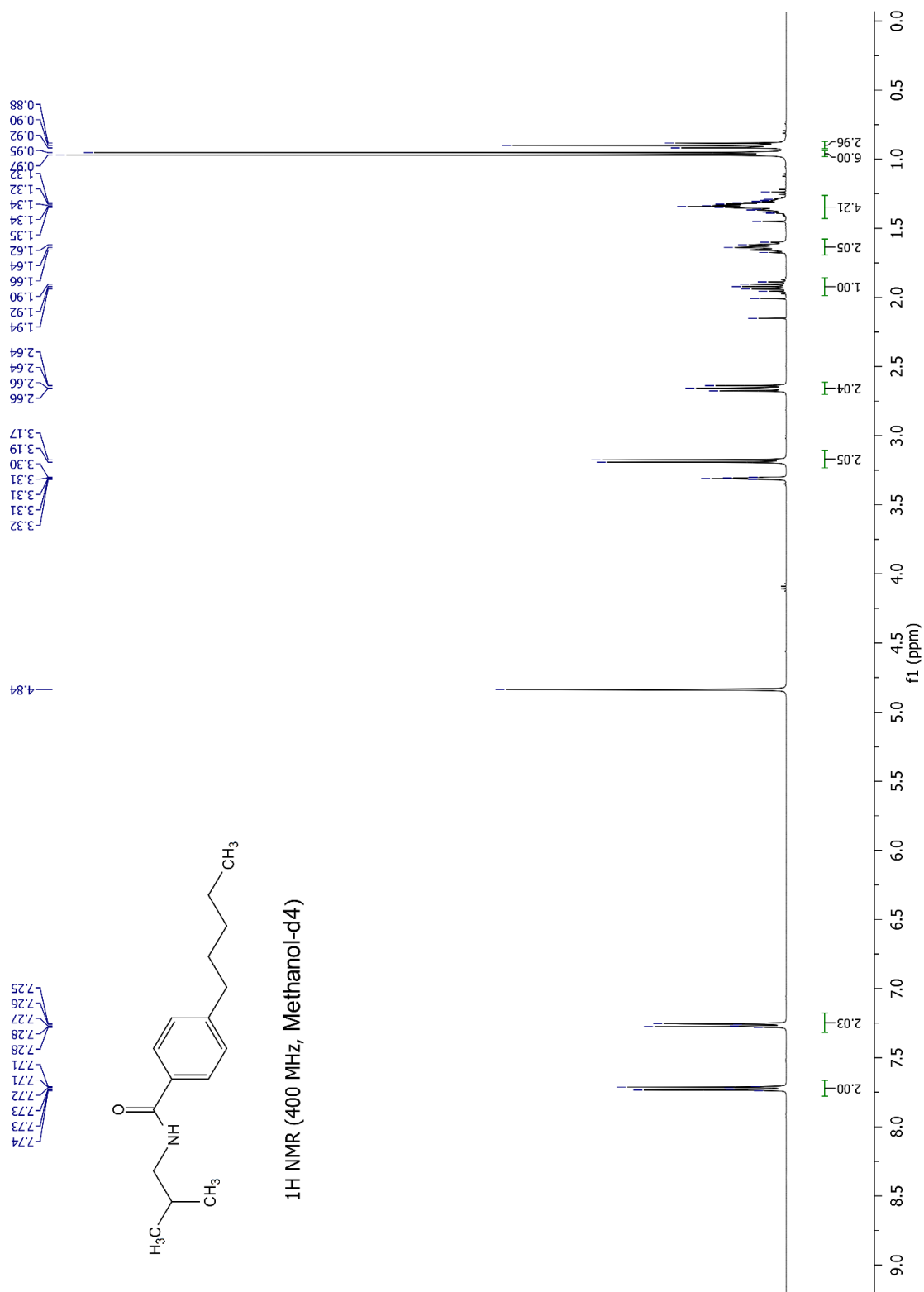


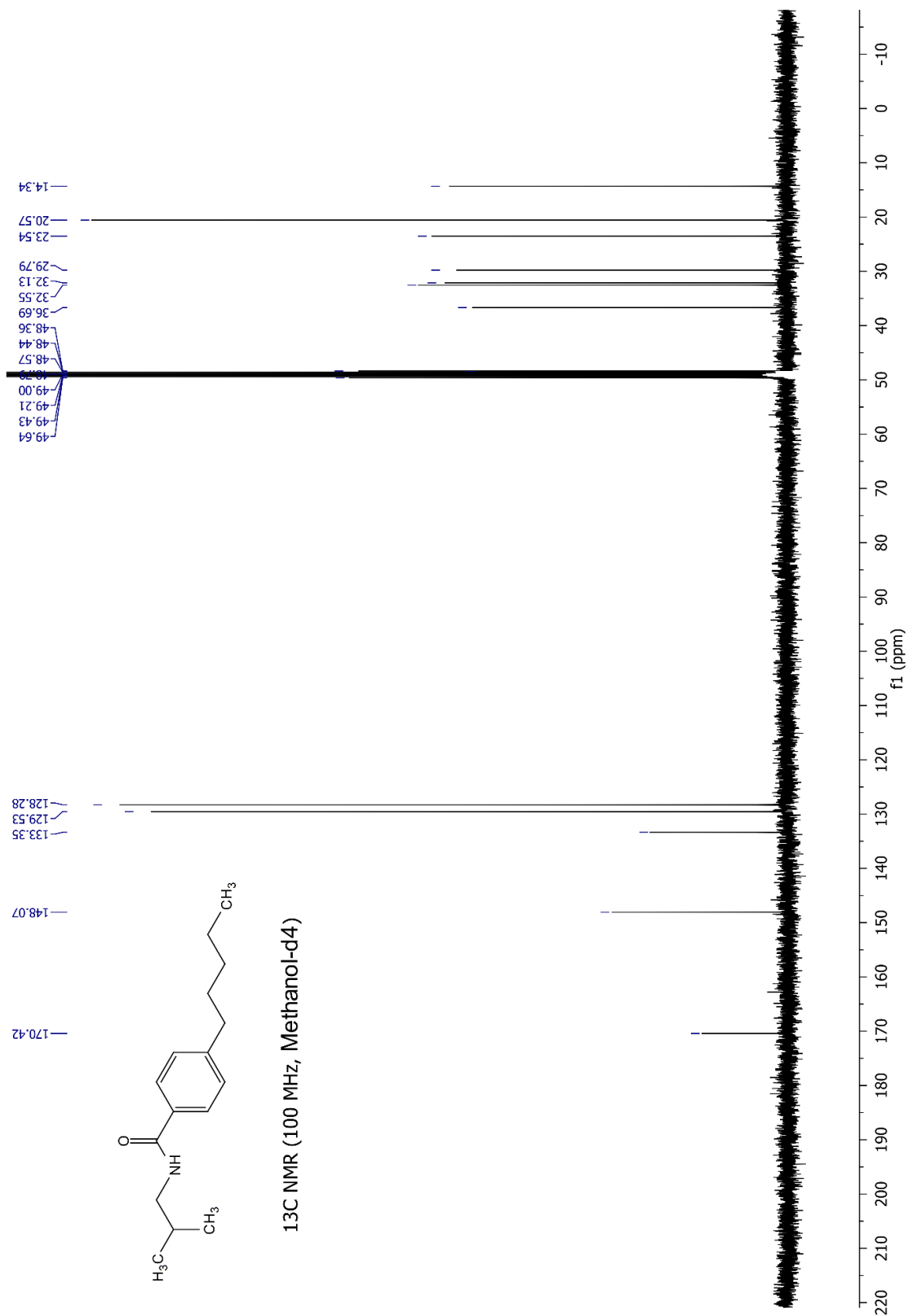
Fig. A 31 ¹H Spectrum of compound 15.

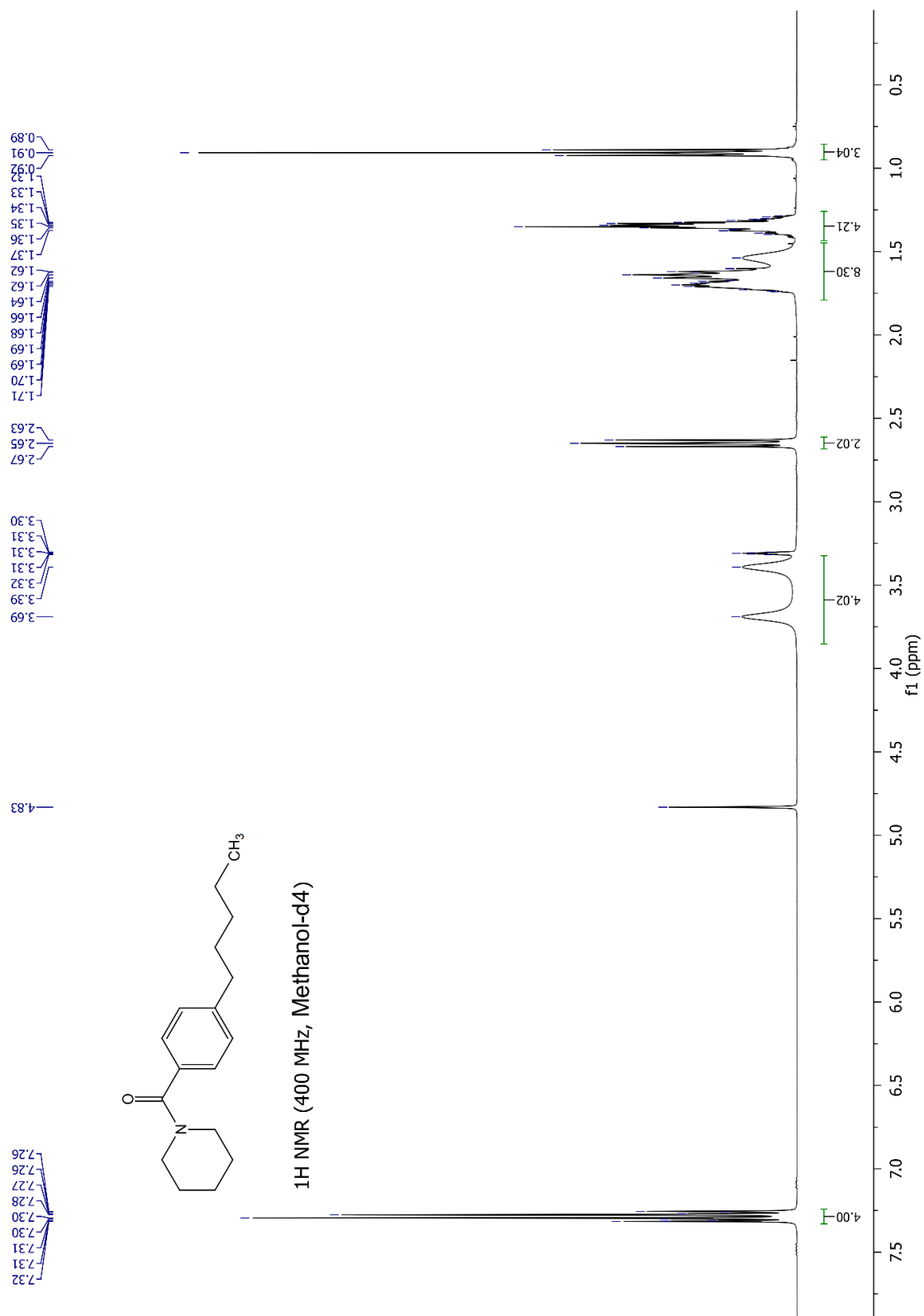
Fig. A 32 ^{13}C Spectrum of compound 15.

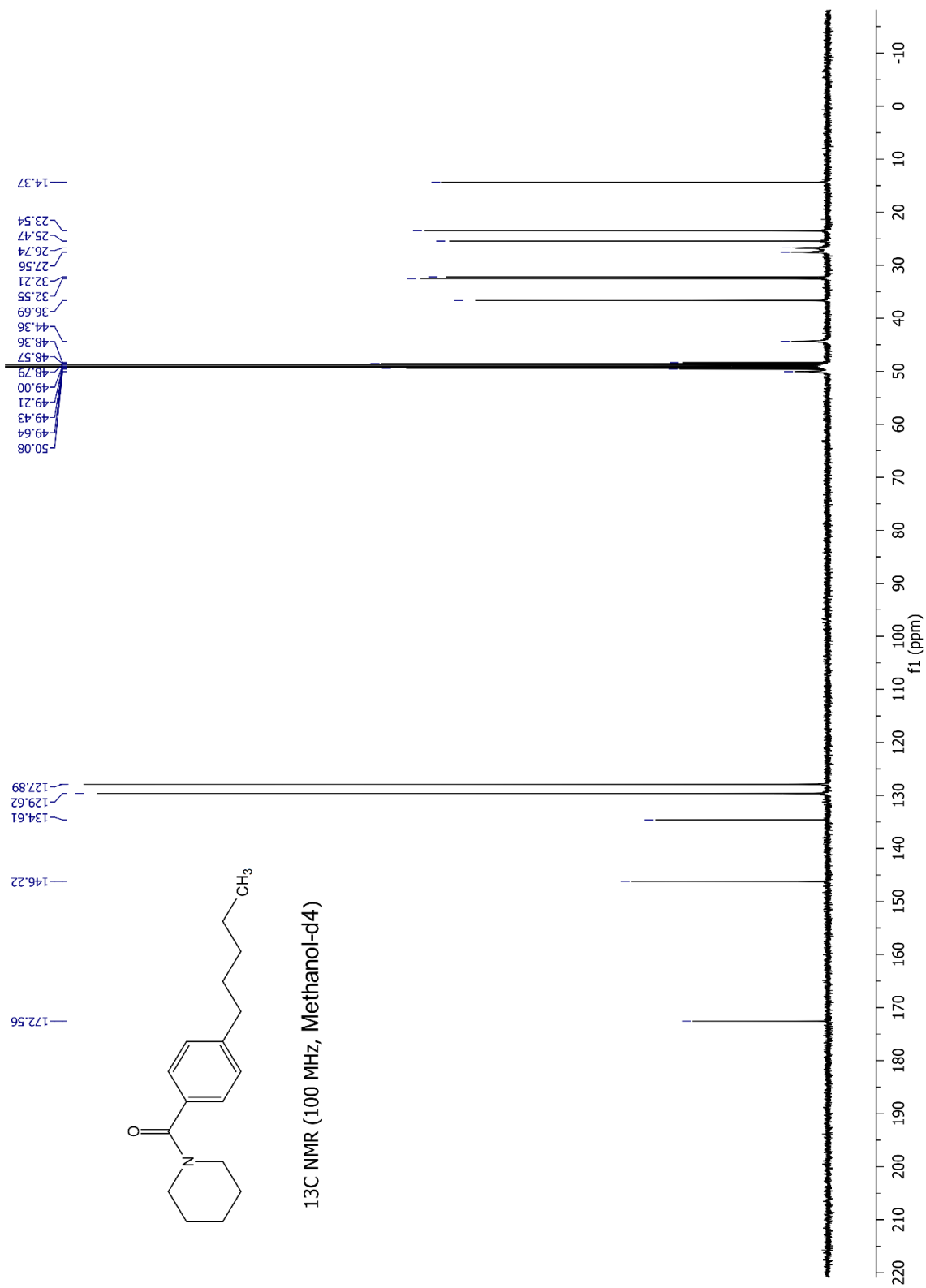
Fig. A 33 ¹H Spectrum of compound 16.

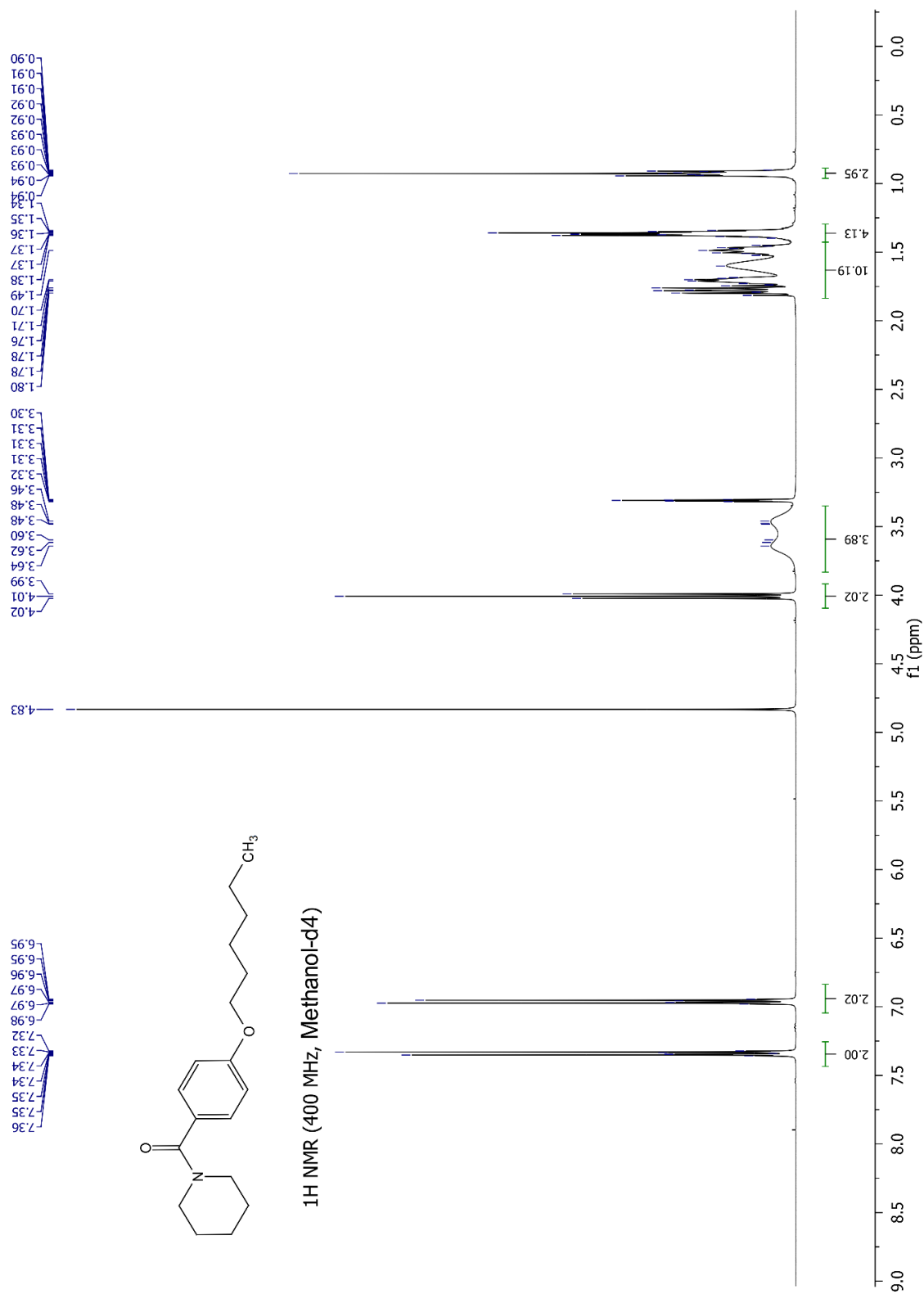
Fig. A 34 ^{13}C Spectrum of compound 16.

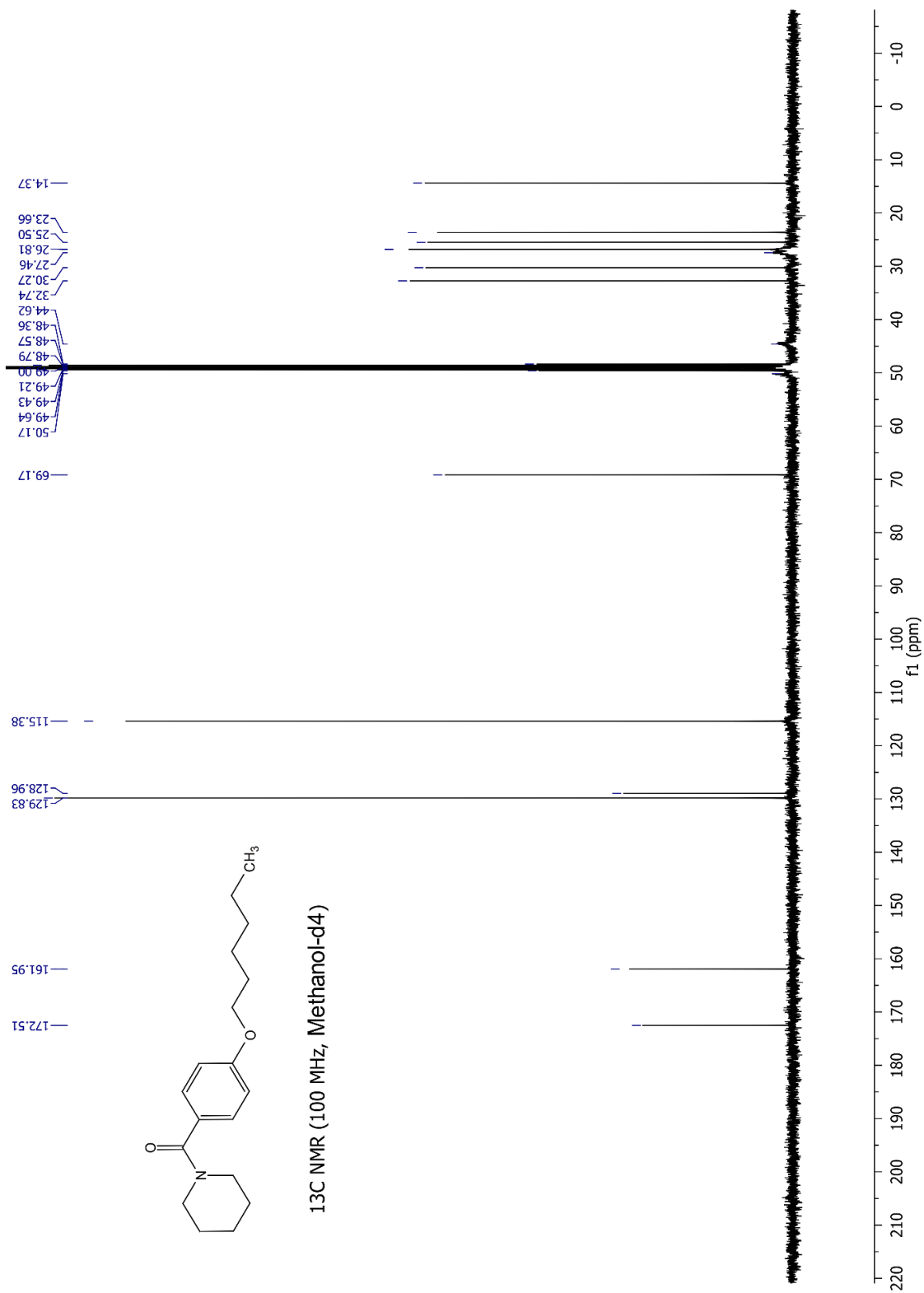
Fig. A 35 ¹H Spectrum of compound 17.

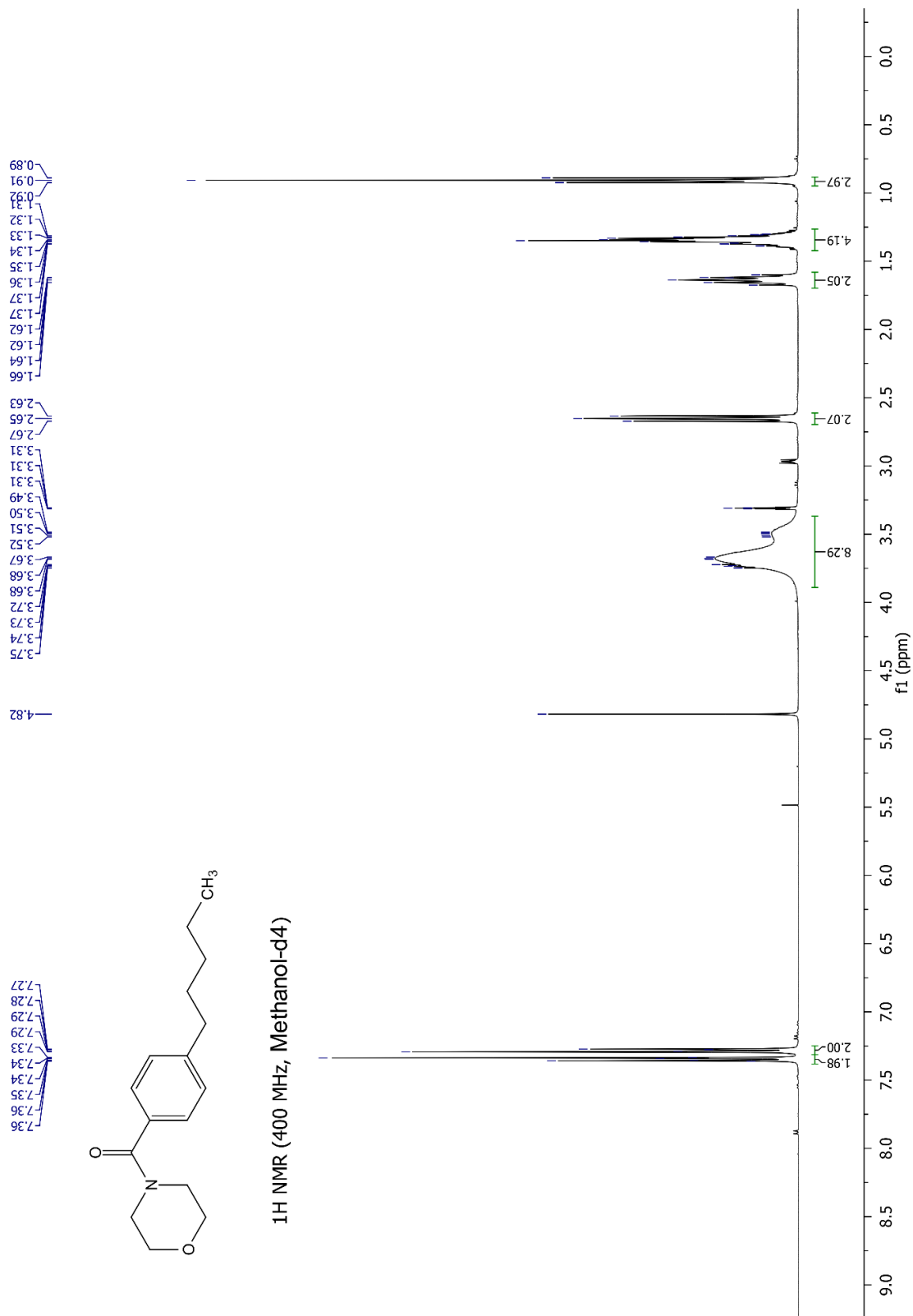
Fig. A 36 ^{13}C Spectrum of compound 17.

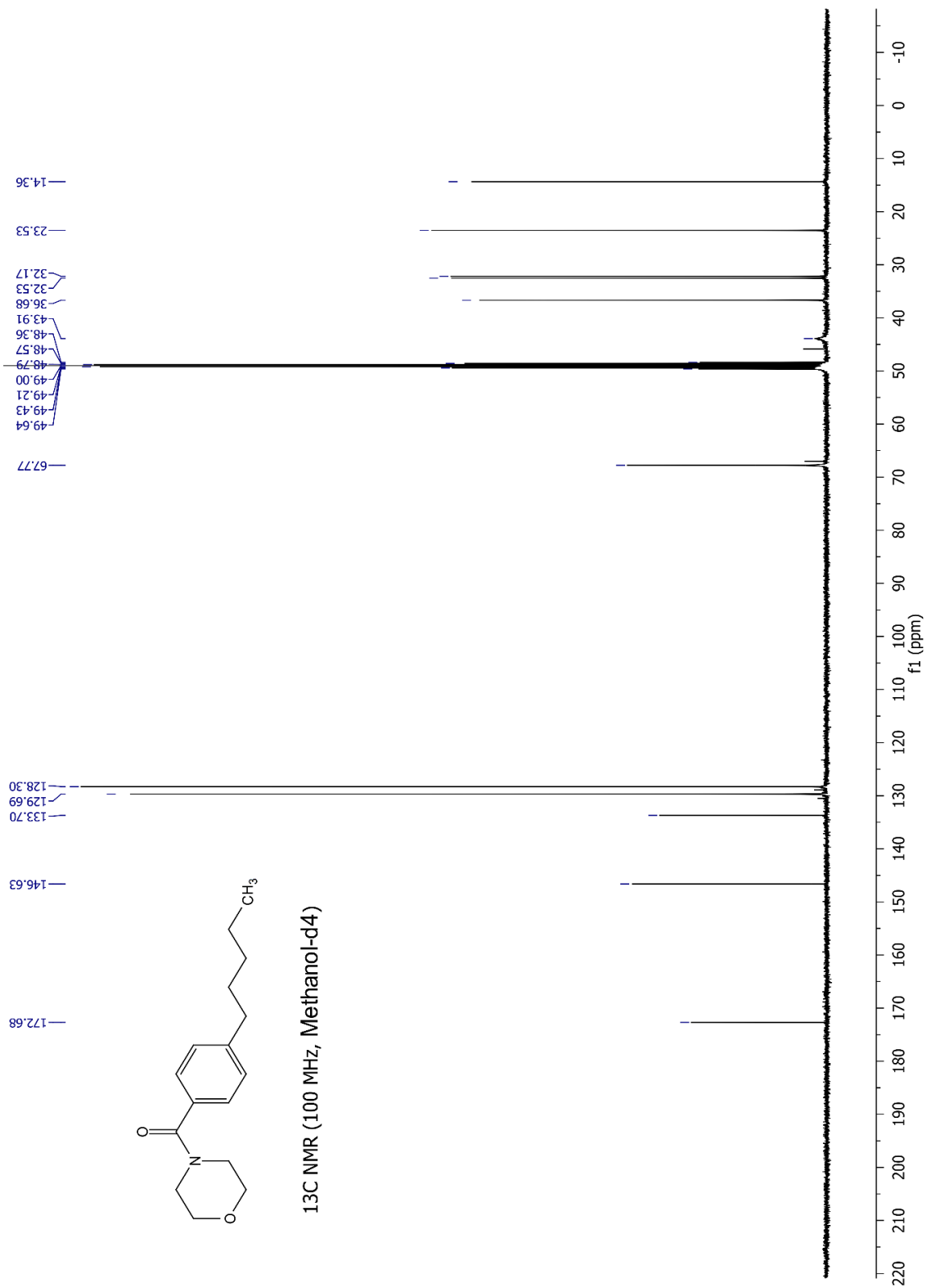
Fig. A 37 ^1H Spectrum of compound 18.

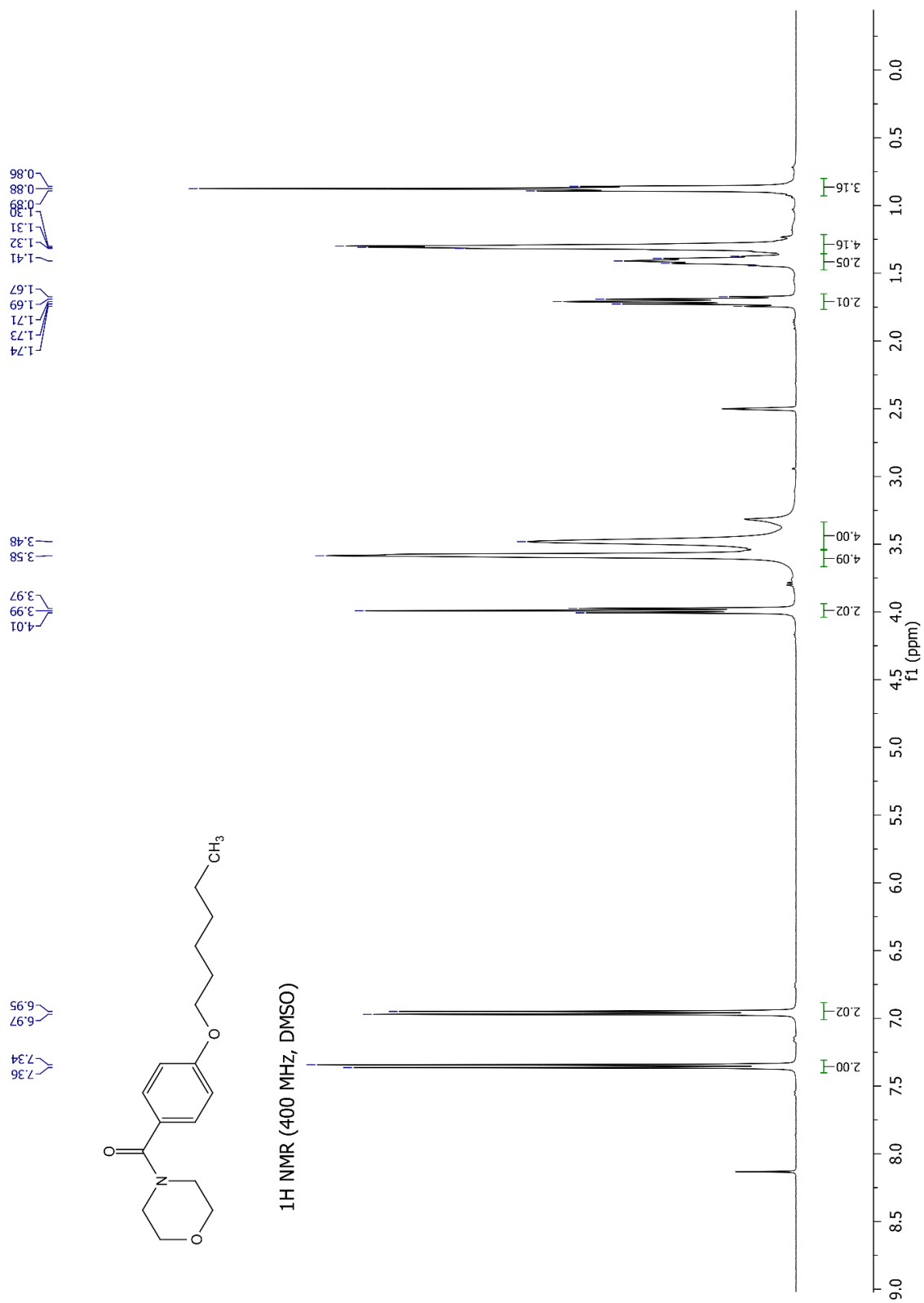
Fig. A 38 ^{13}C Spectrum of compound 18.

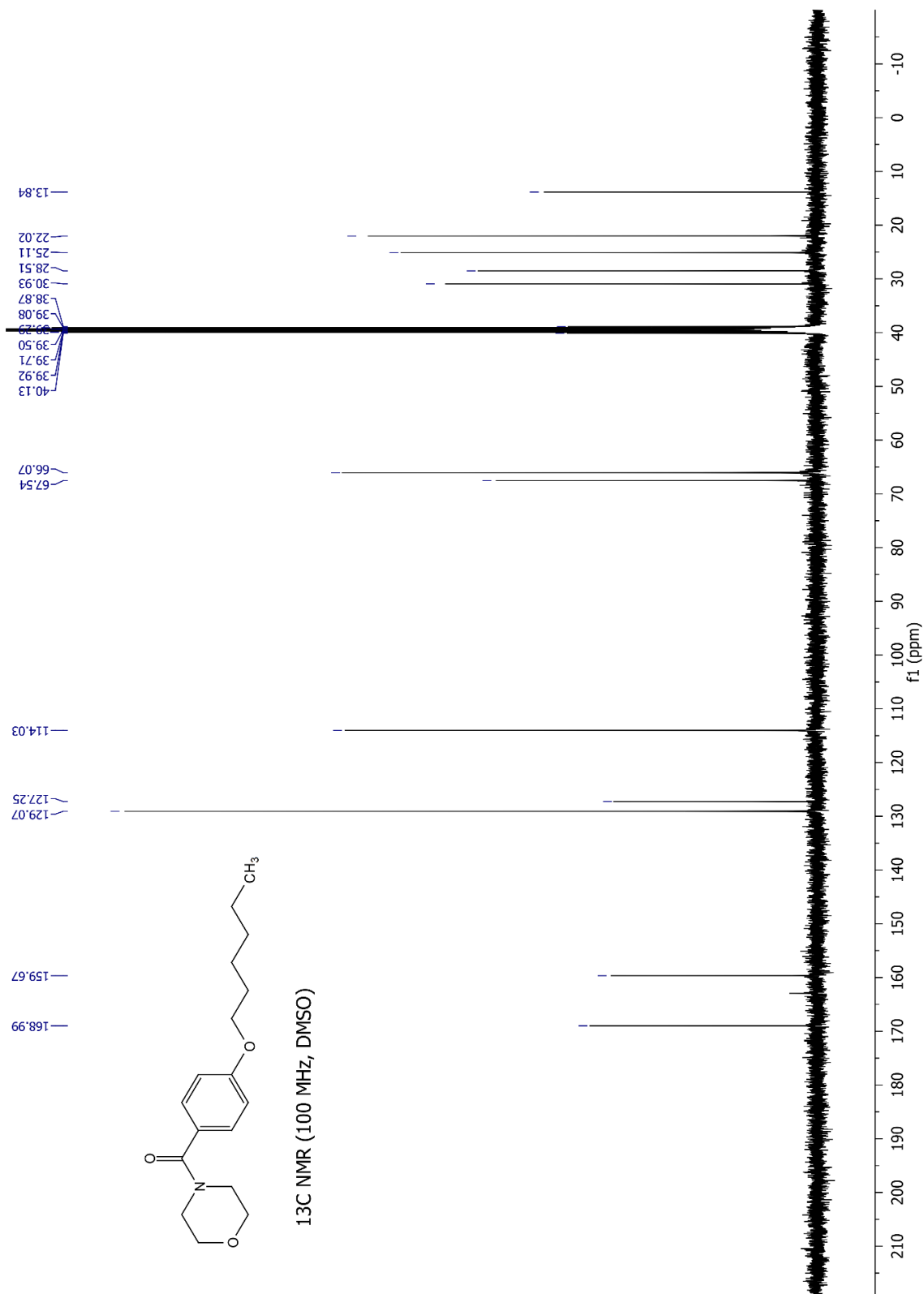
Fig. A 39 ¹H Spectrum of compound 19.

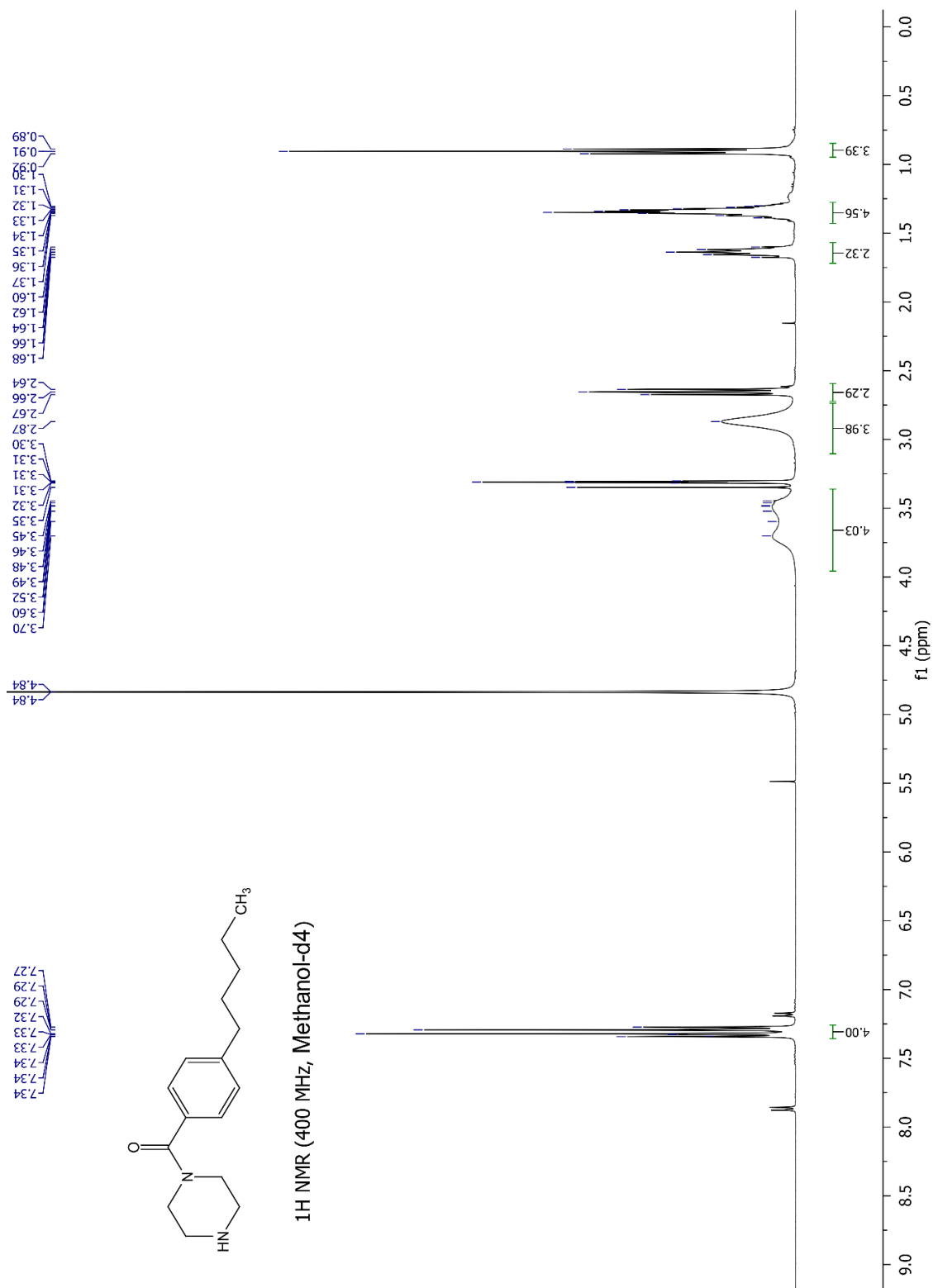
Fig. A 40 ¹³C Spectrum of compound 19.

Fig. A 41 ¹H Spectrum of compound 20.

Fig. A 42 ¹³C Spectrum of compound 20.

Fig. A 43 ¹H Spectrum of compound 21.

Fig. A 44 ^{13}C Spectrum of compound 21.

Fig. A 45 ¹H Spectrum of compound 22.

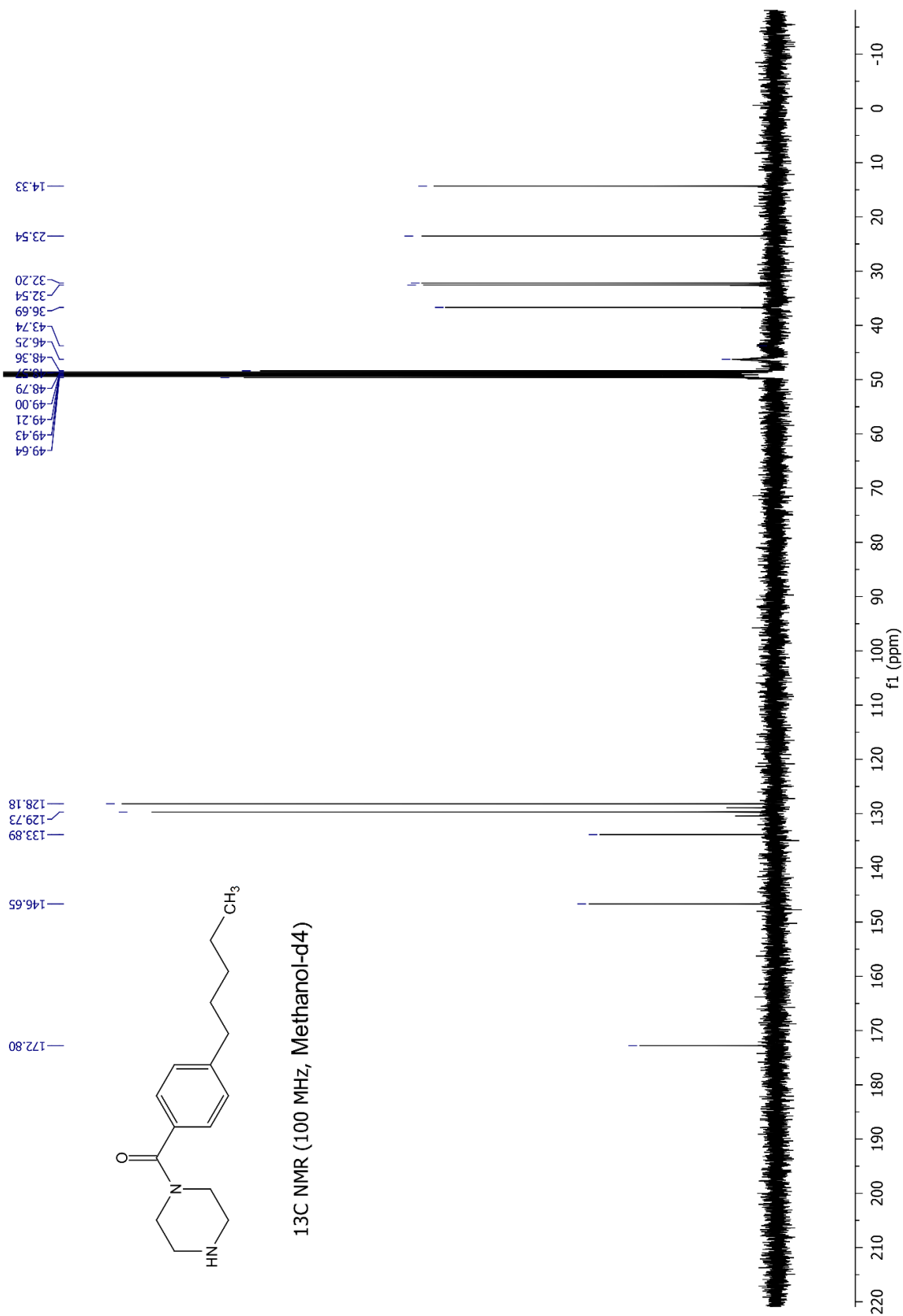
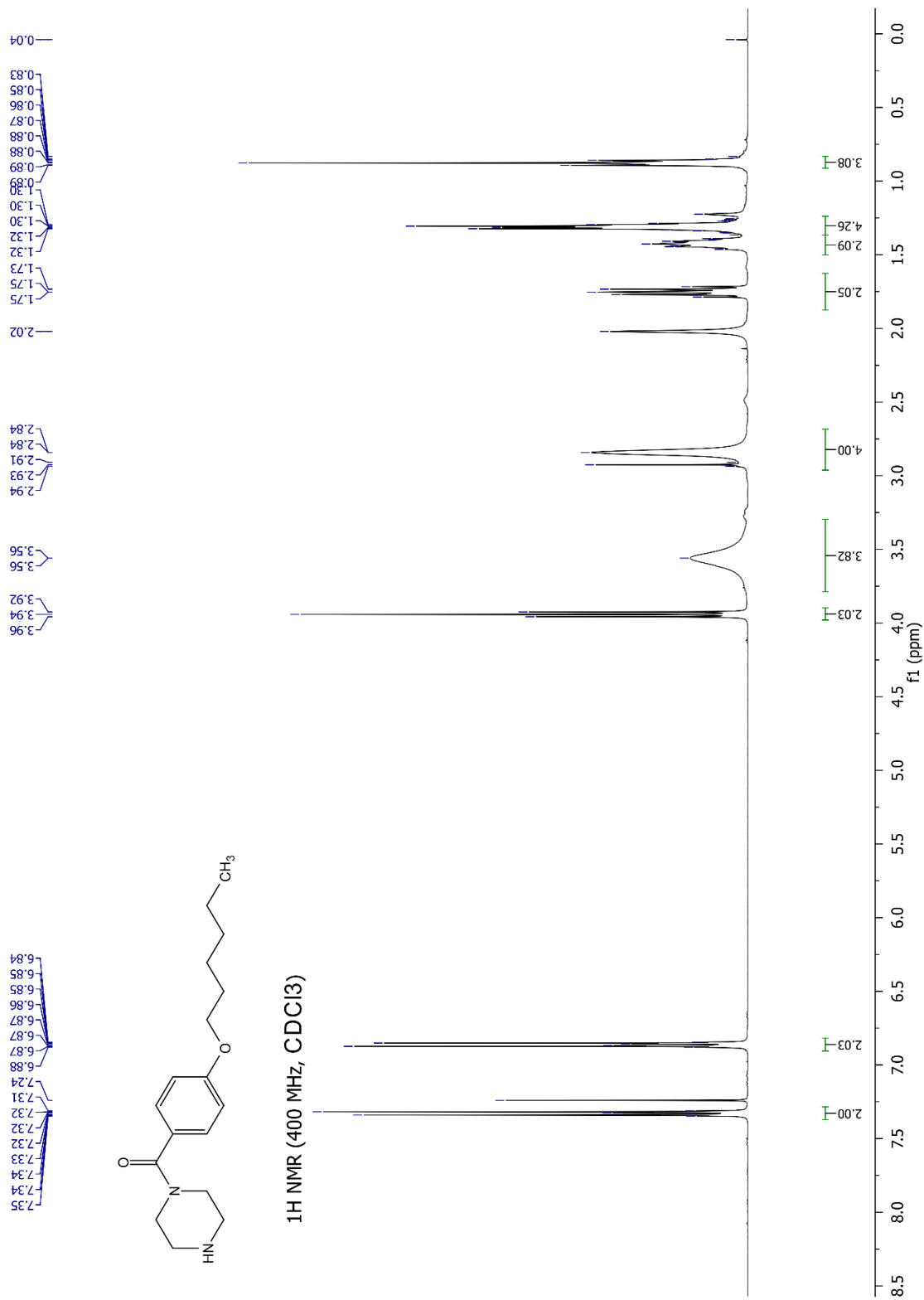
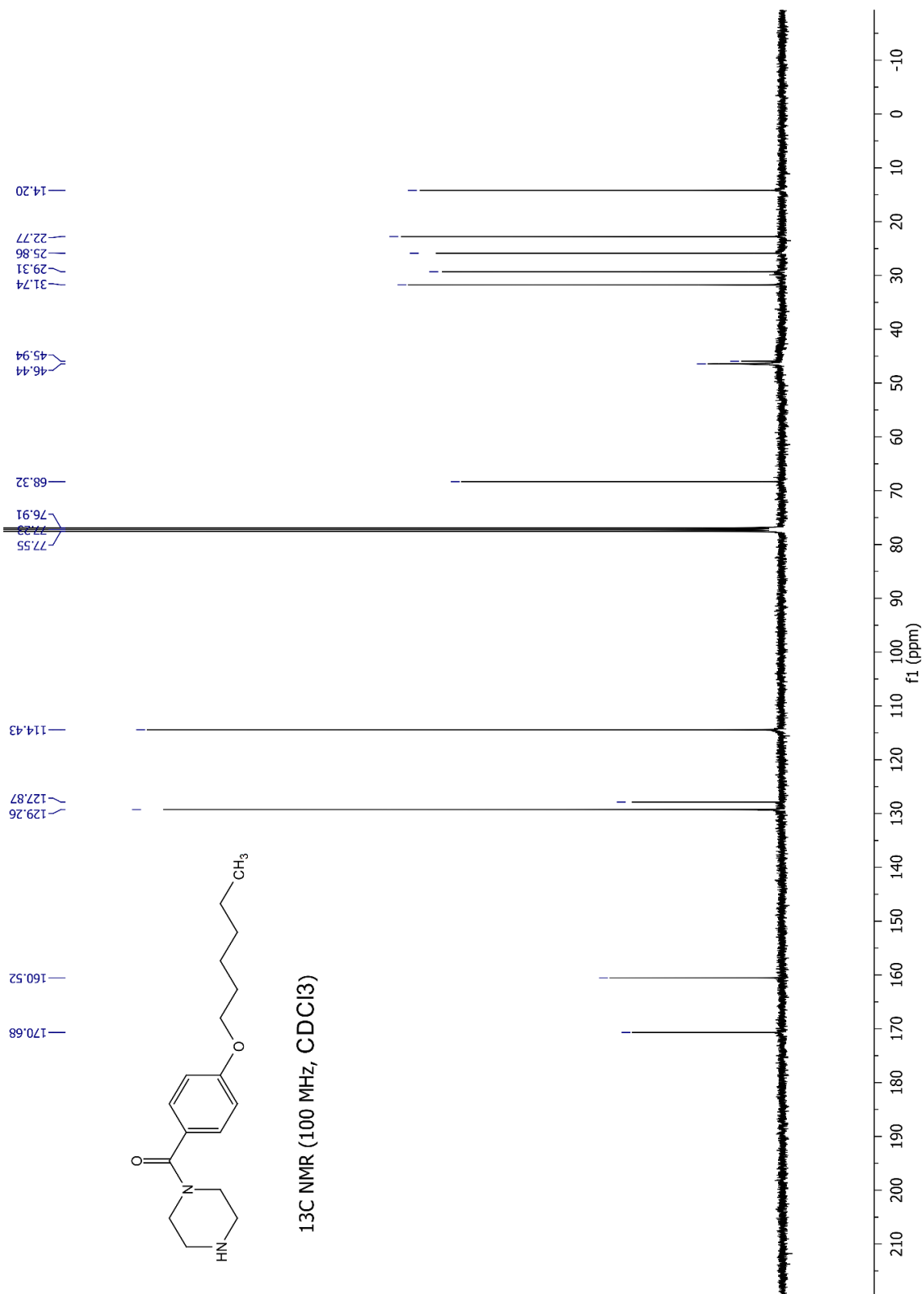
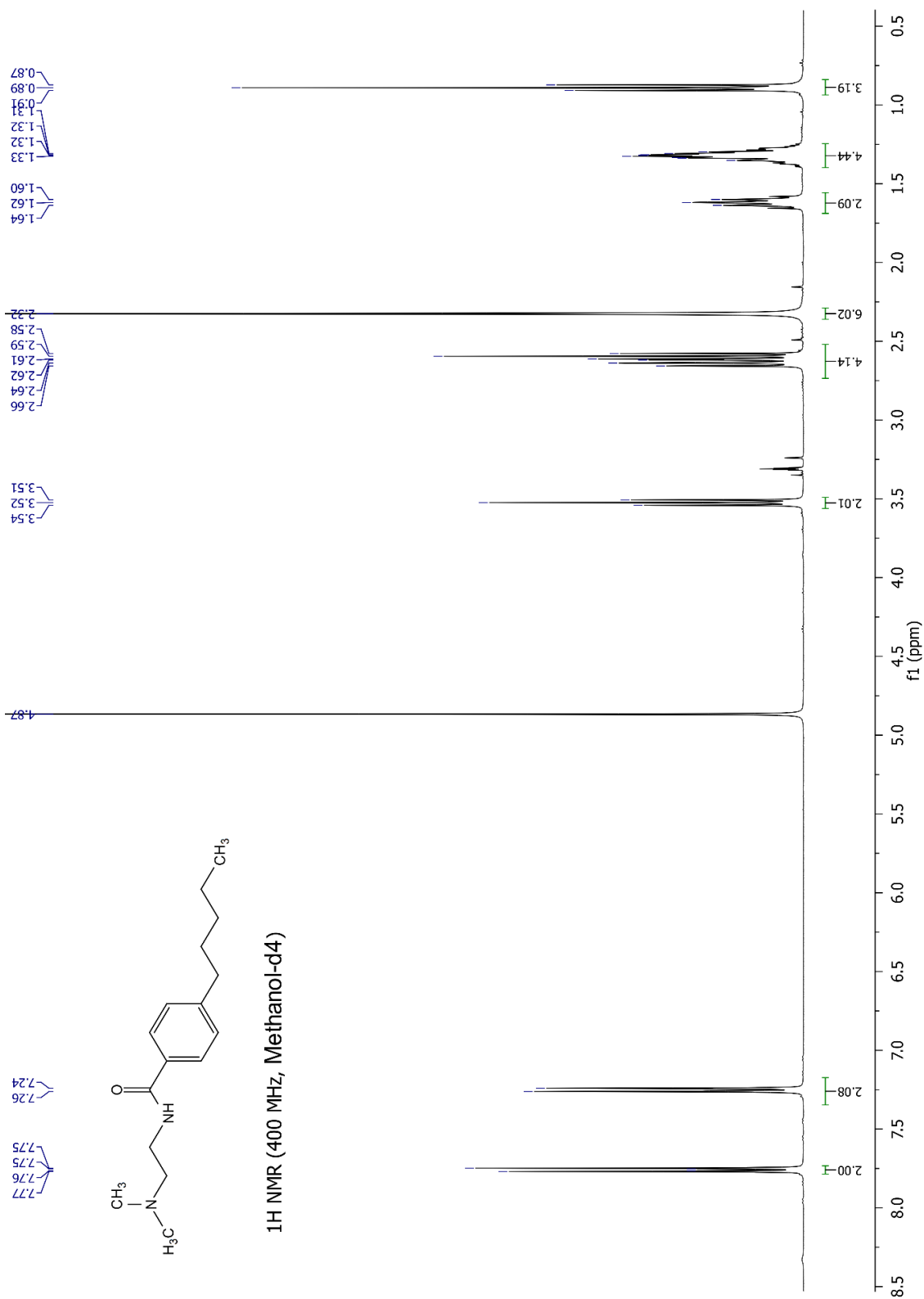
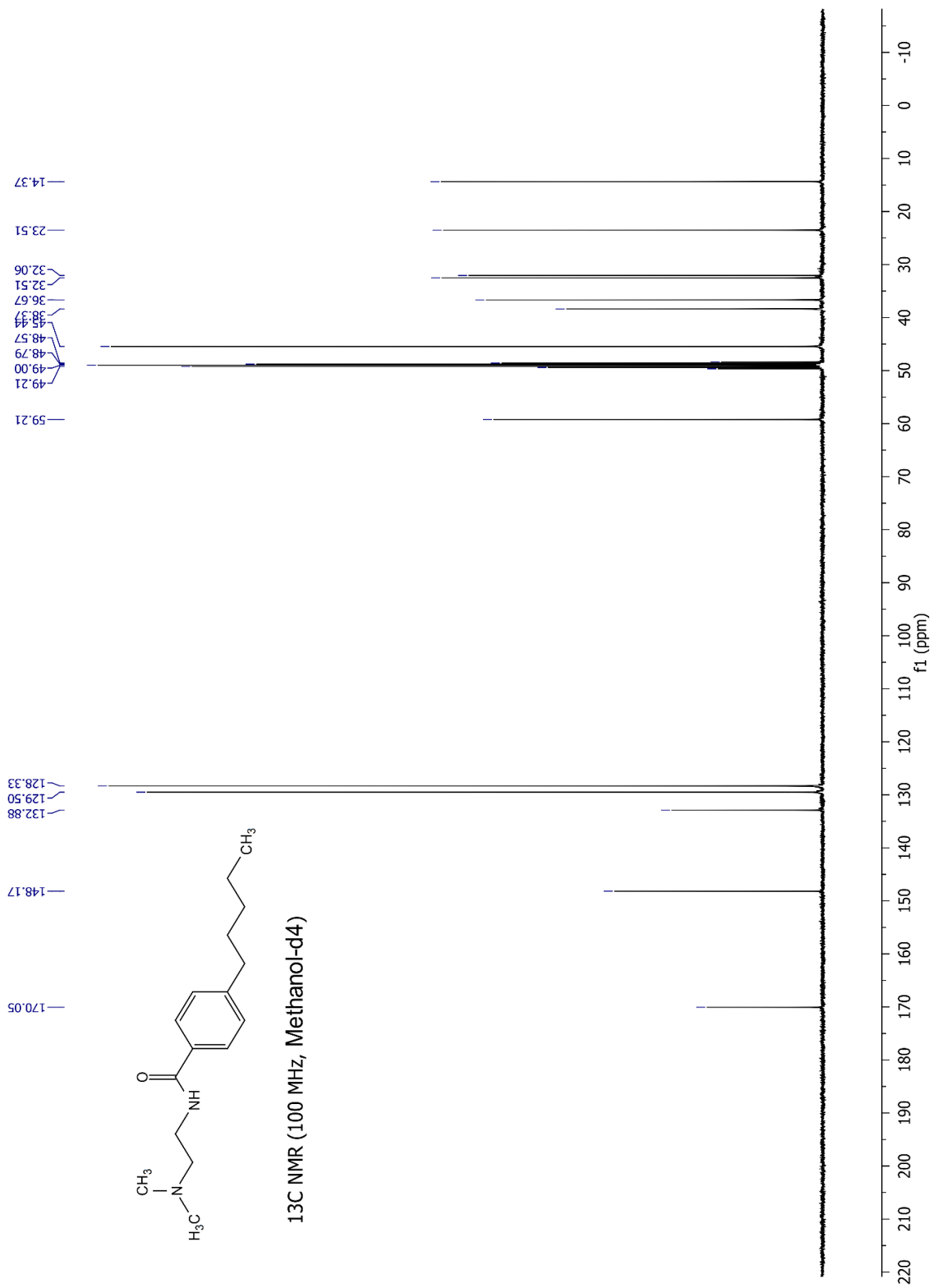


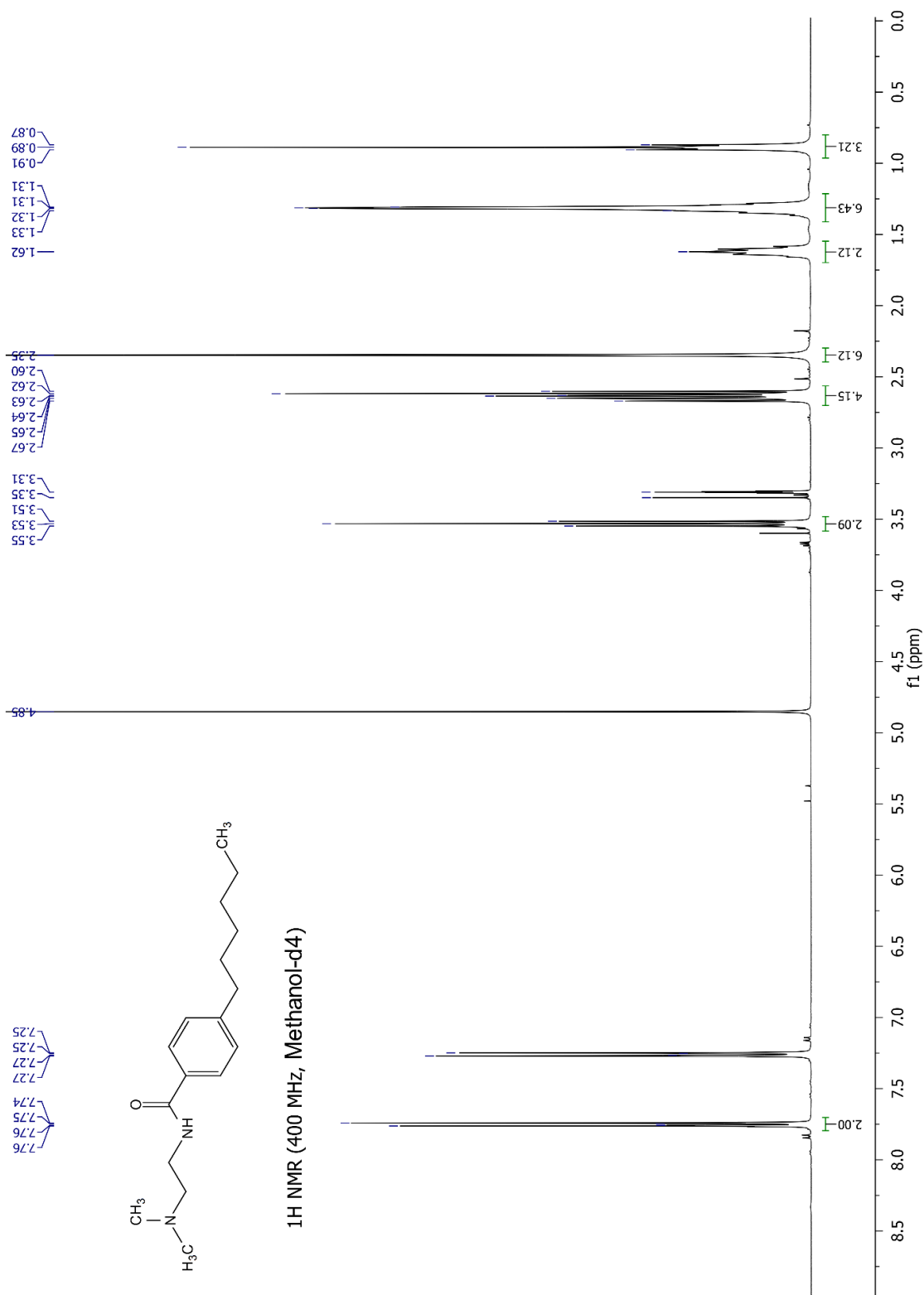
Fig. A 46 ¹³C Spectrum of compound 22.

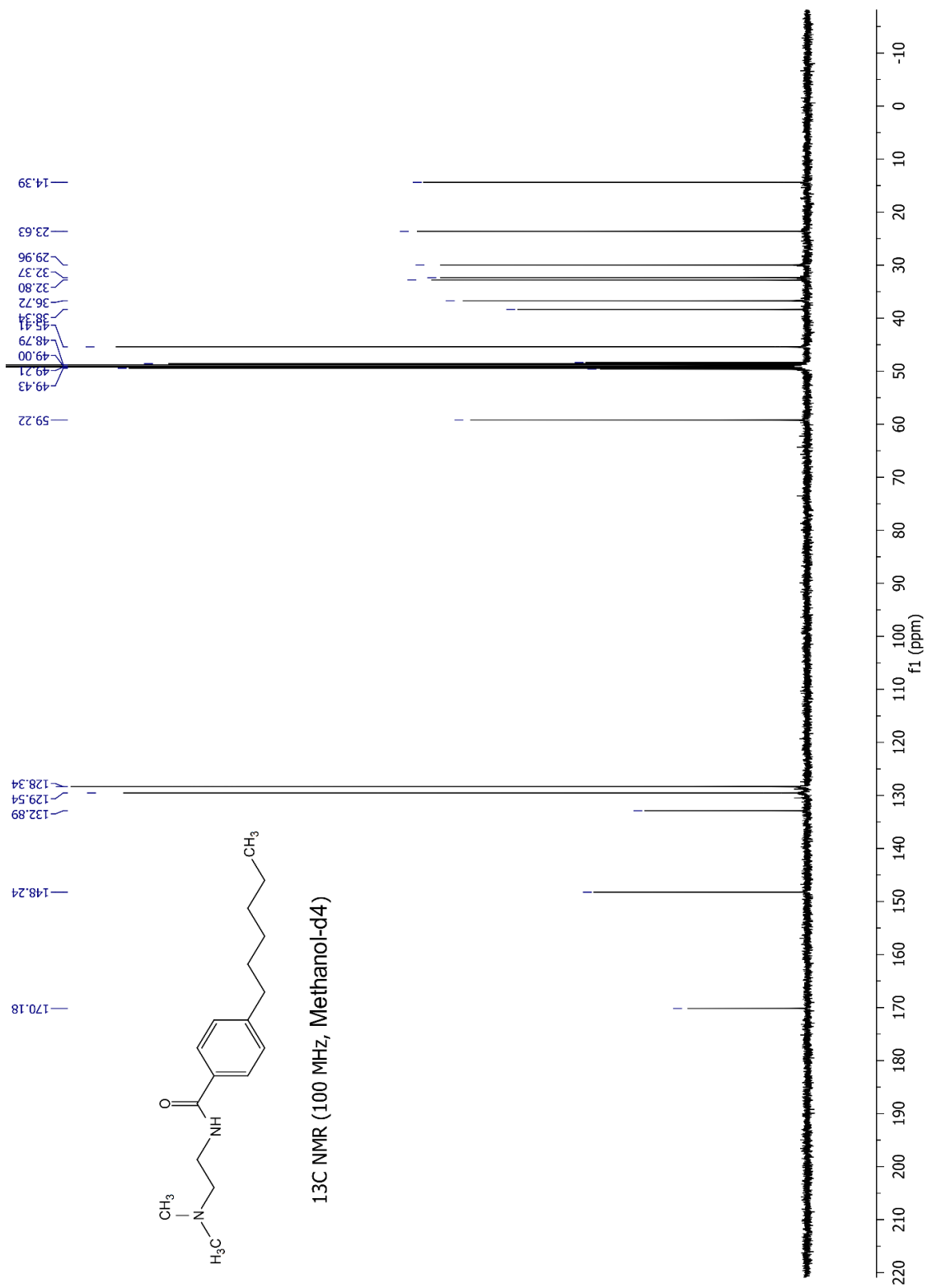
Fig. A 47 ¹H Spectrum of compound 23.

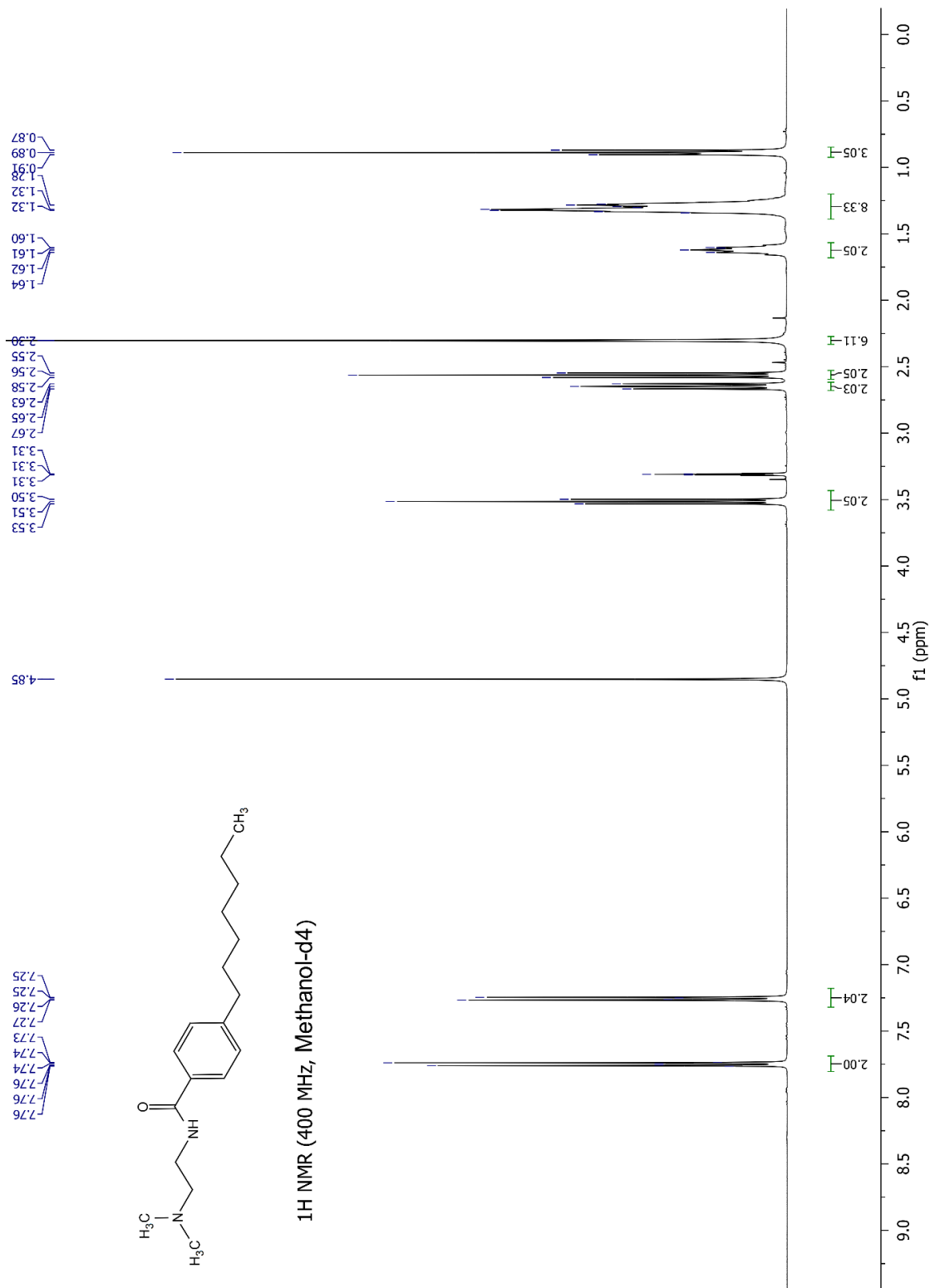
Fig. A 48 ¹³C Spectrum of compound 23.

Fig. A 49 ¹H Spectrum of compound 24.

Fig. A 50 ¹³C Spectrum of compound 24.

Fig. A 51 ¹H Spectrum of compound 25.

Fig. A 52 ¹³C Spectrum of compound 25.

Fig. A 53 ¹H Spectrum of compound 26.

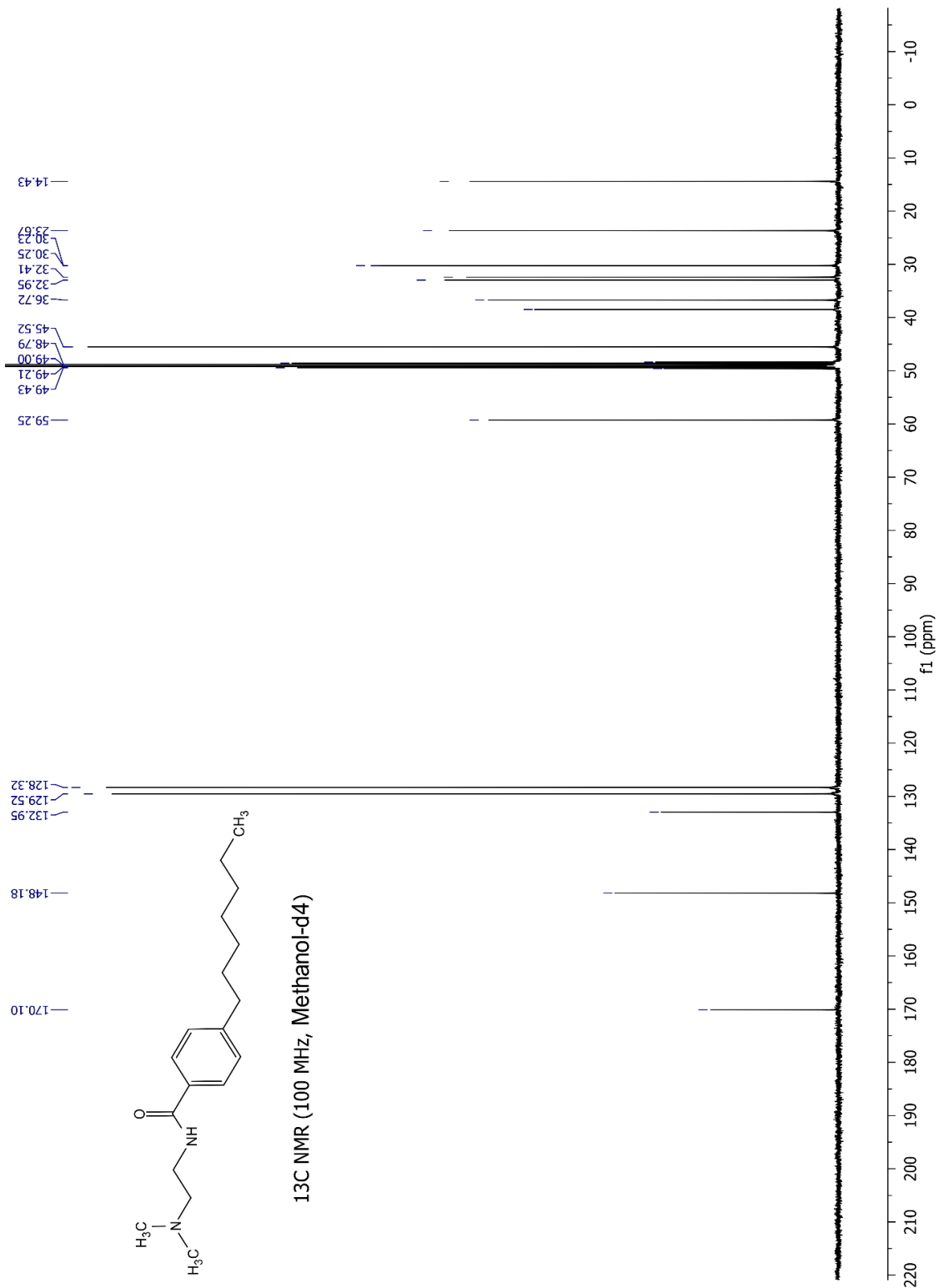
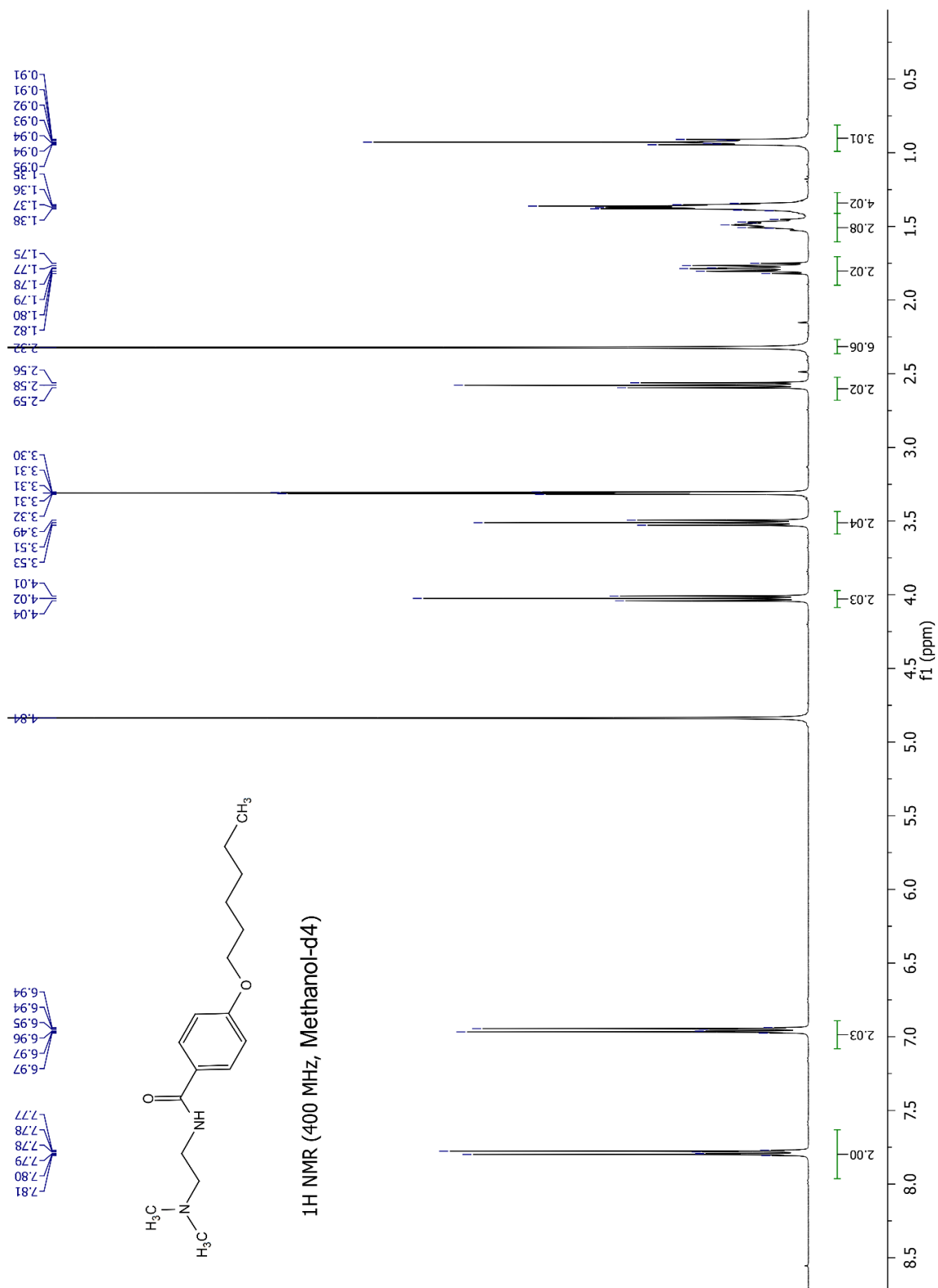
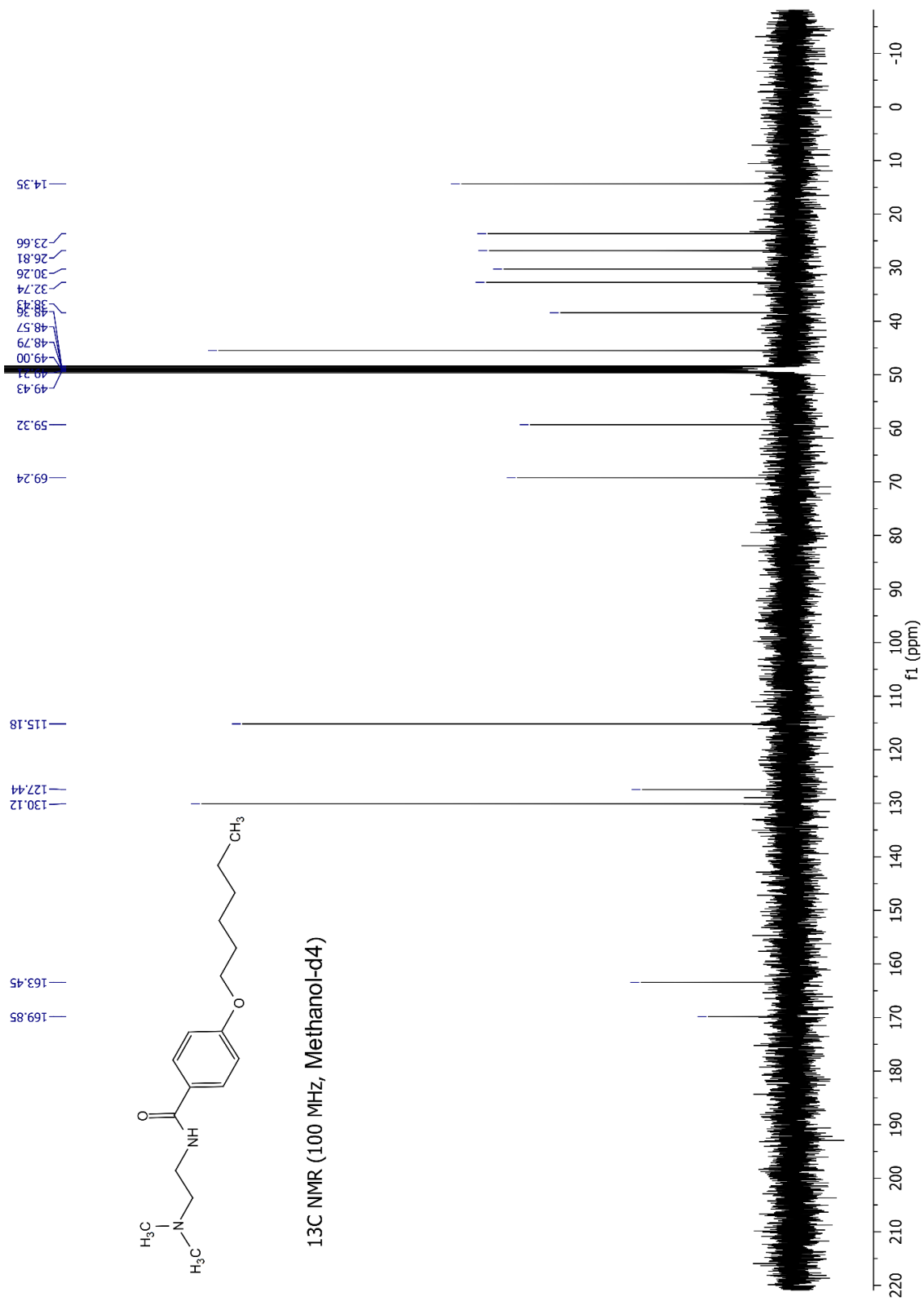
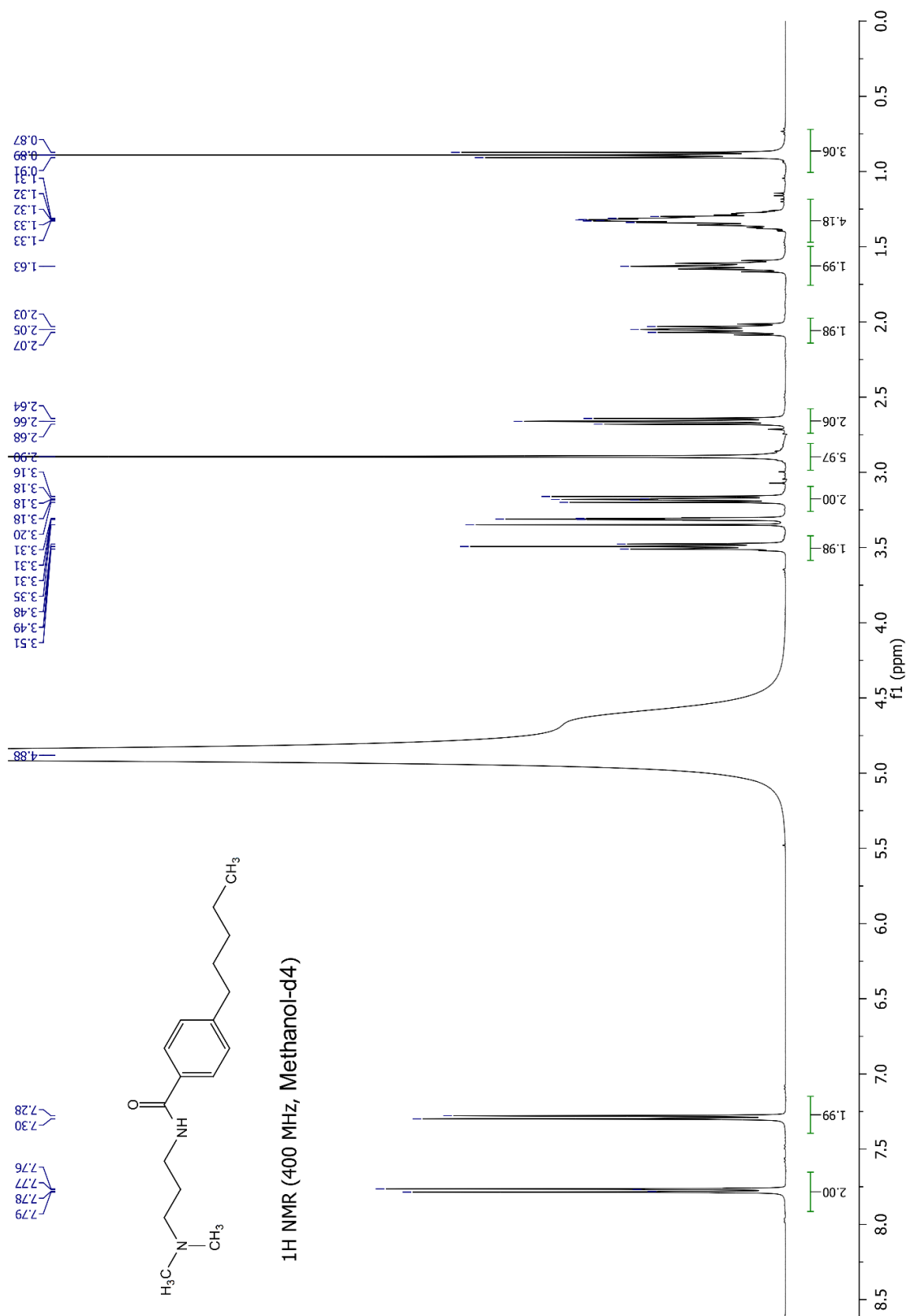
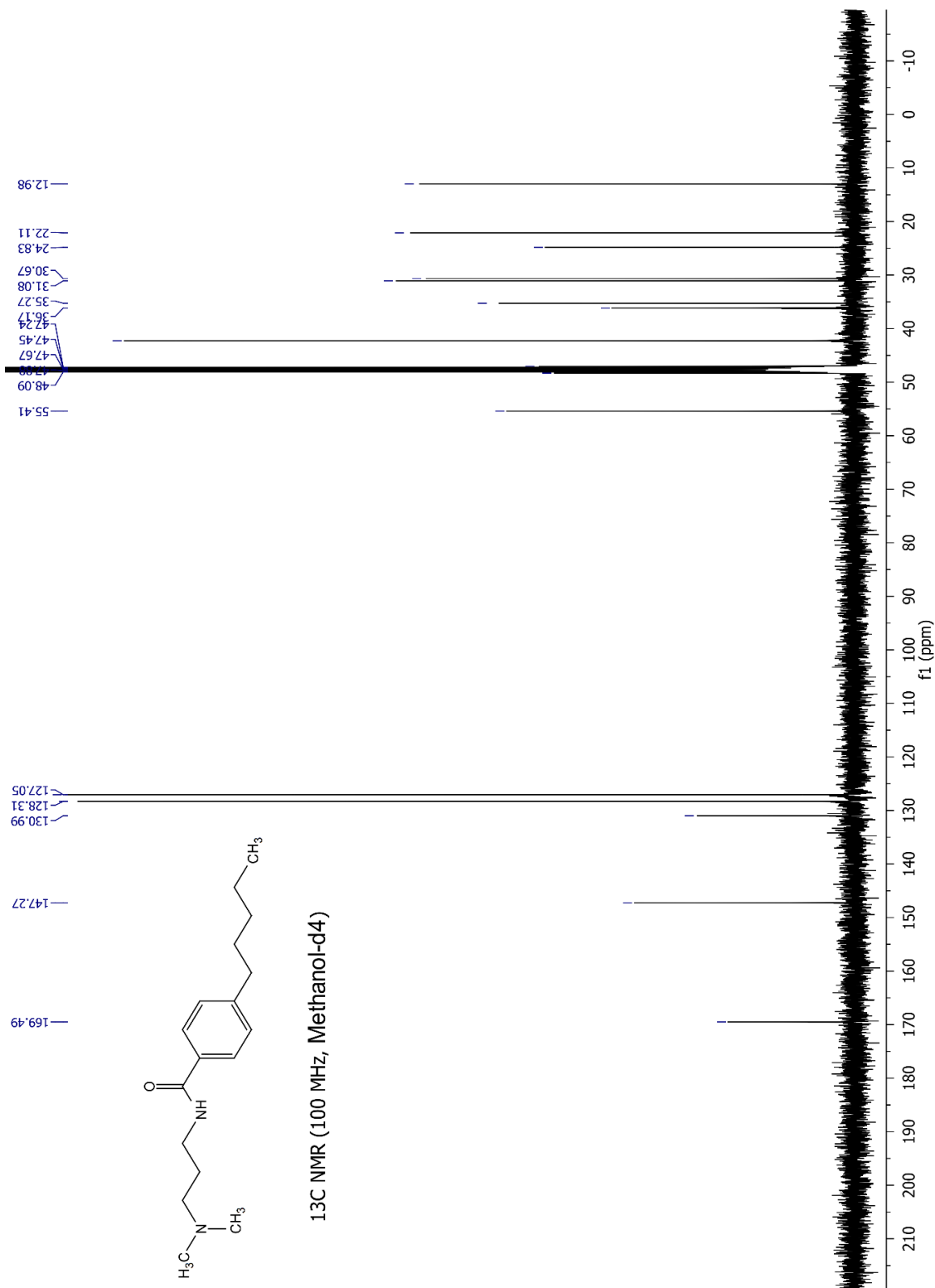


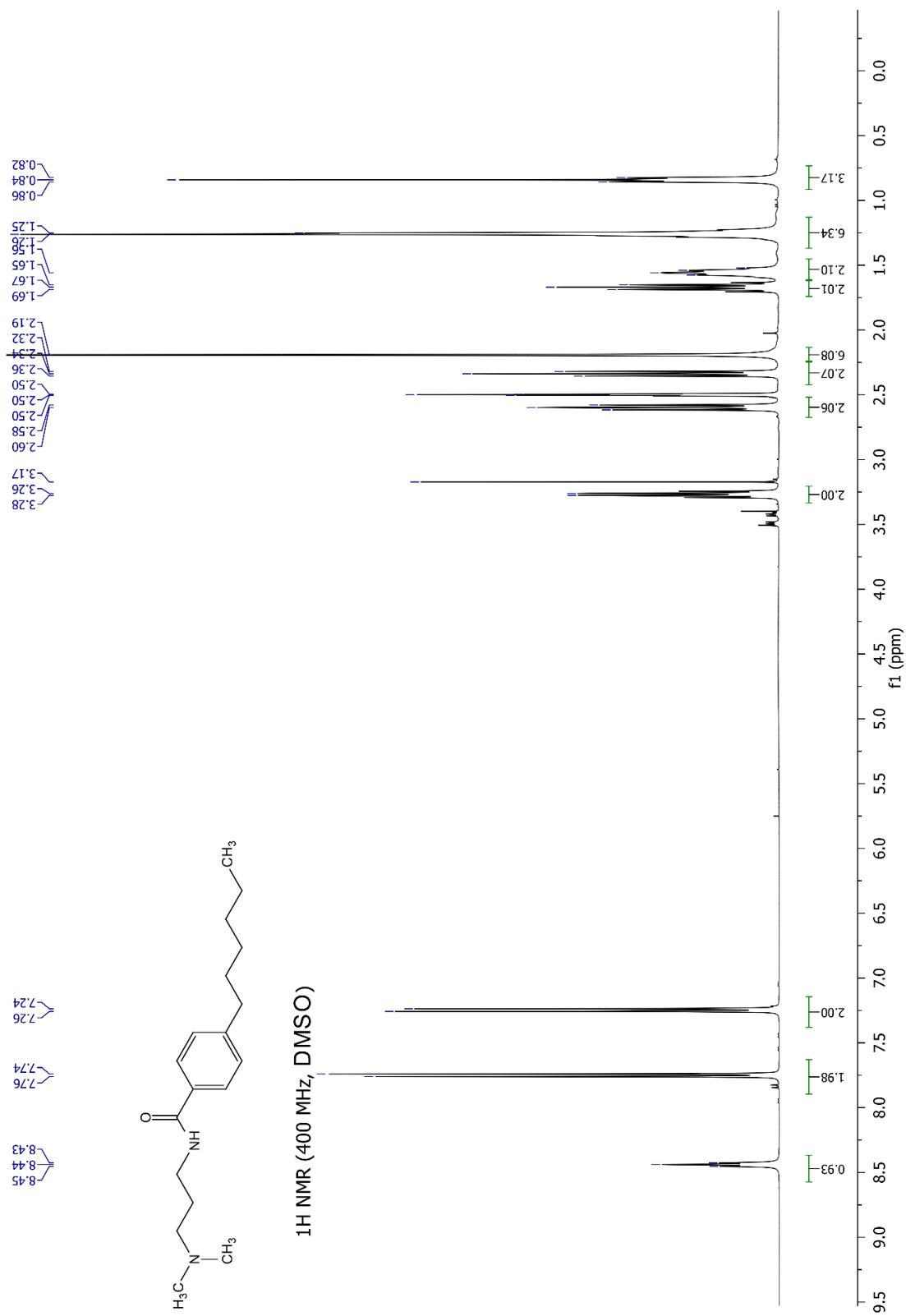
Fig. A 54 ¹³C Spectrum of compound 26.

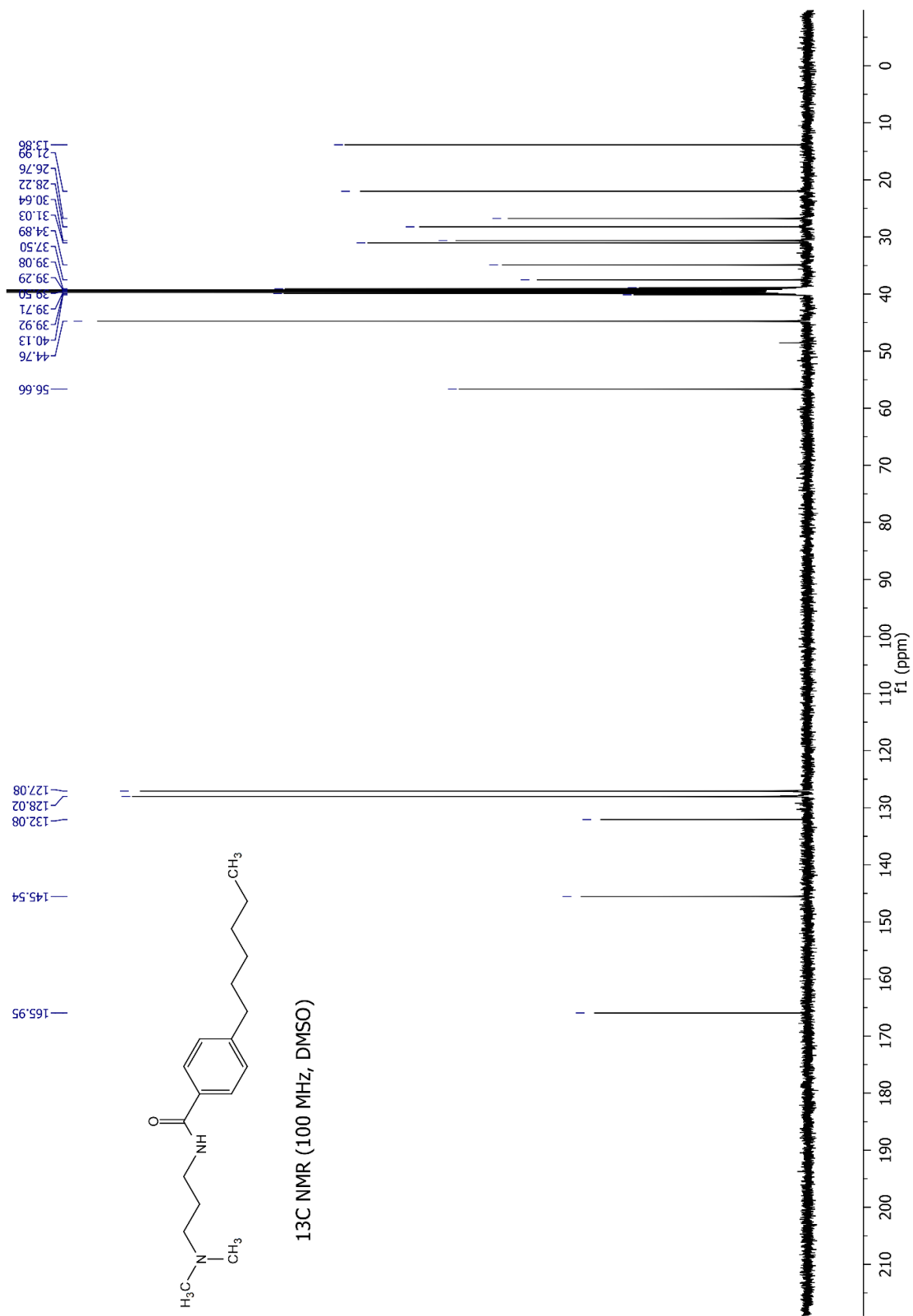
Fig. A 55 ¹H Spectrum of compound 27.

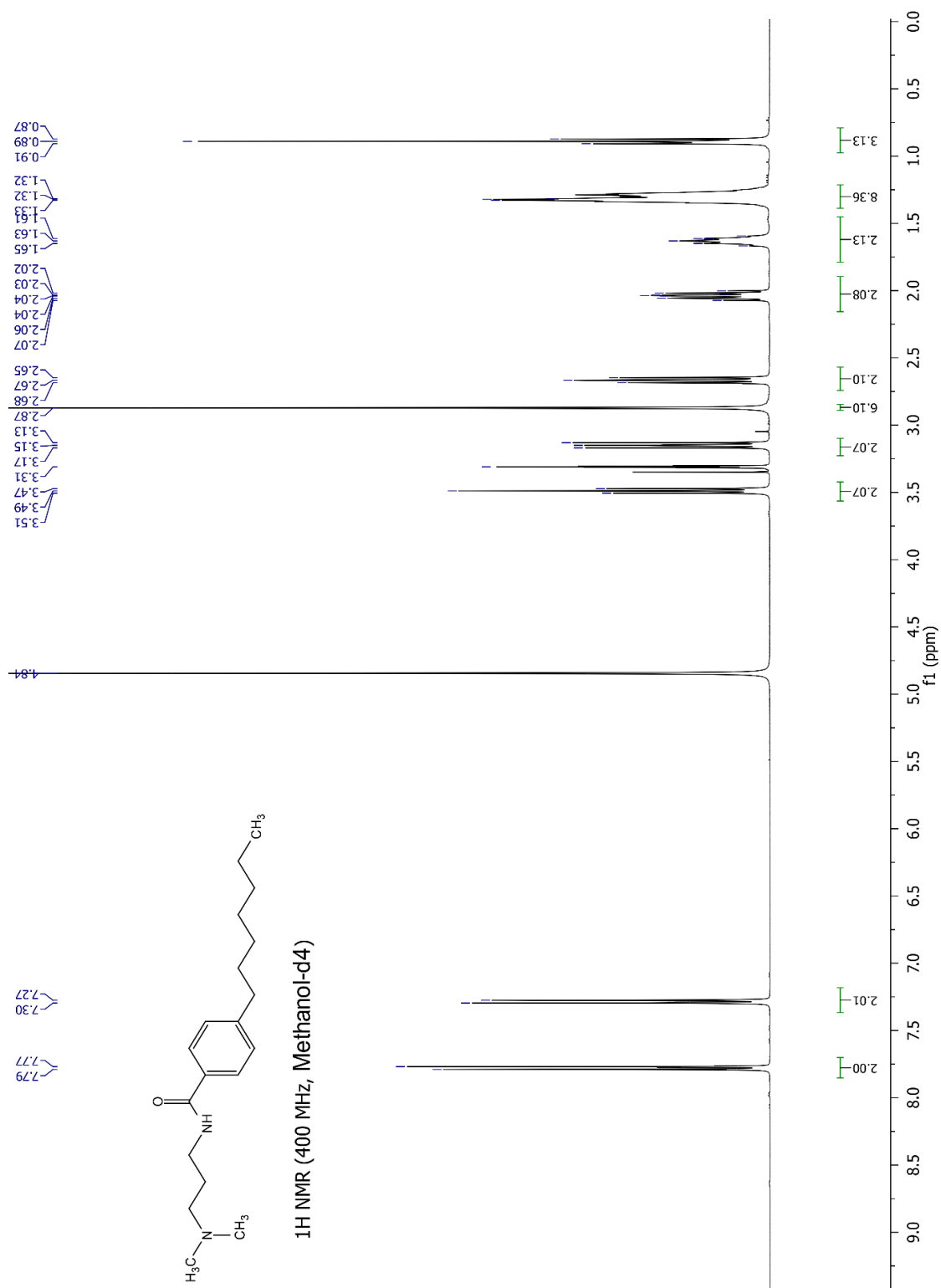
Fig. A 56 ¹³C Spectrum of compound 27.

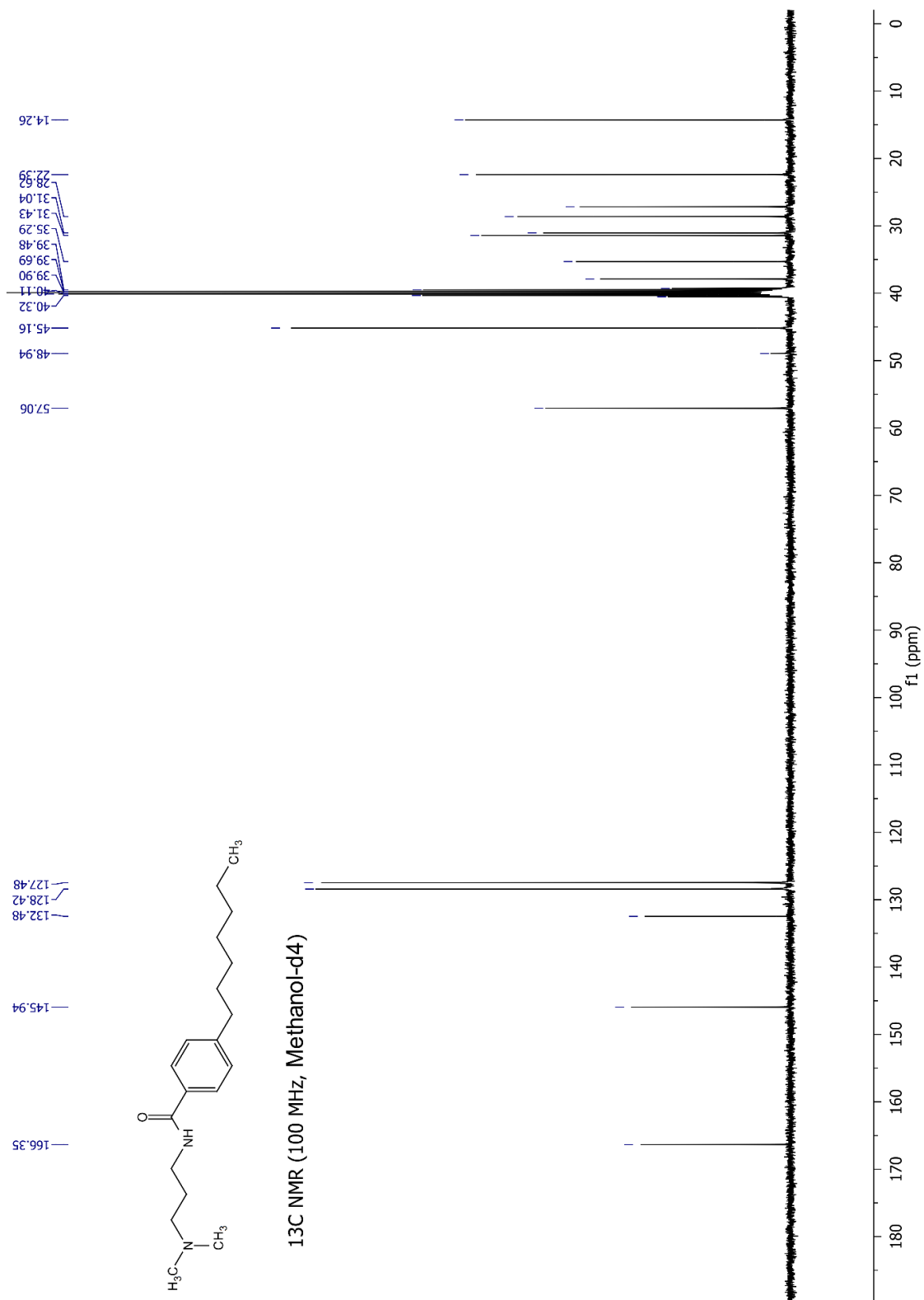
Fig. A 57 ¹H Spectrum of compound 28.

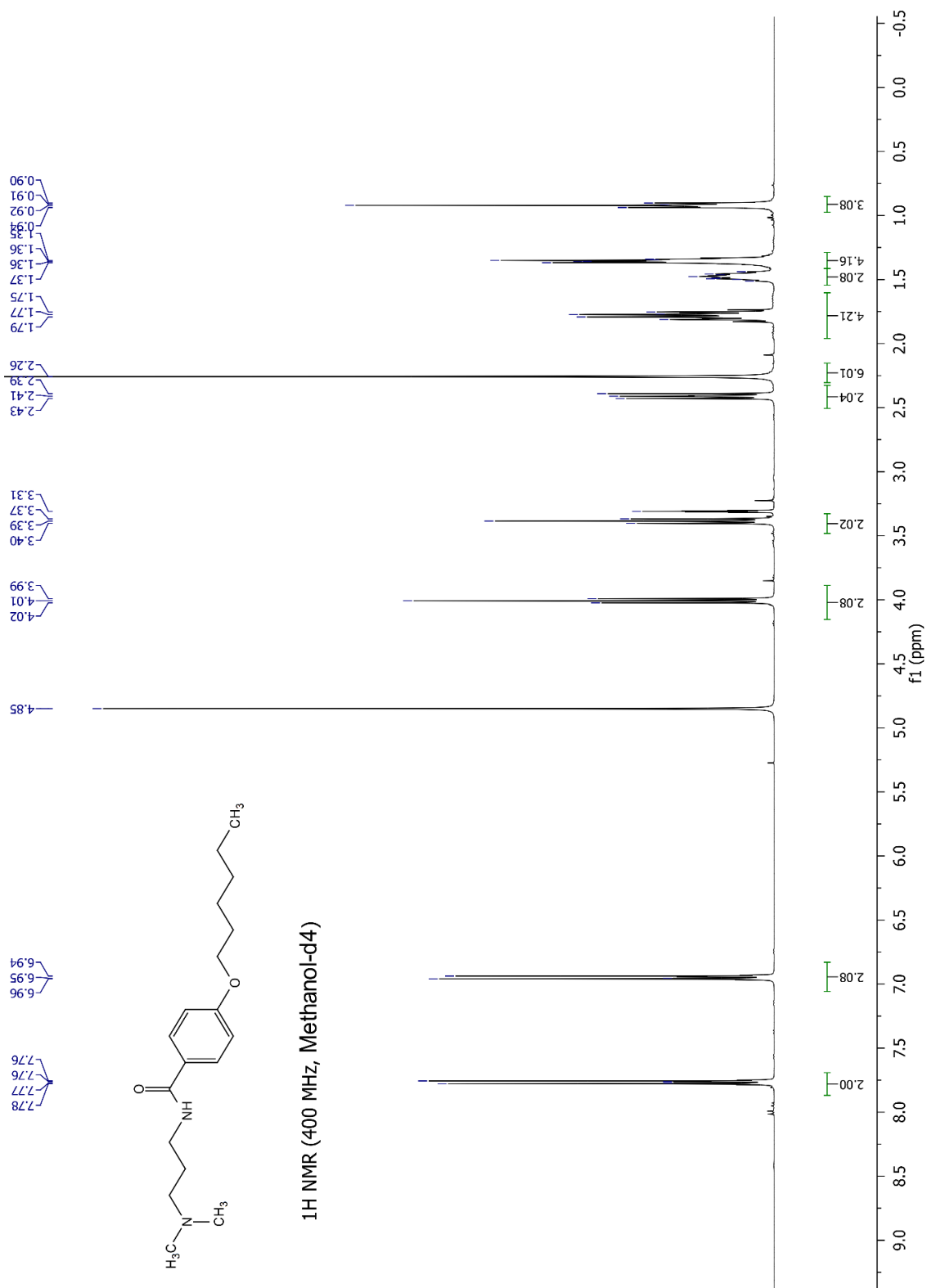
Fig. A 58 ¹³C Spectrum of compound 28.

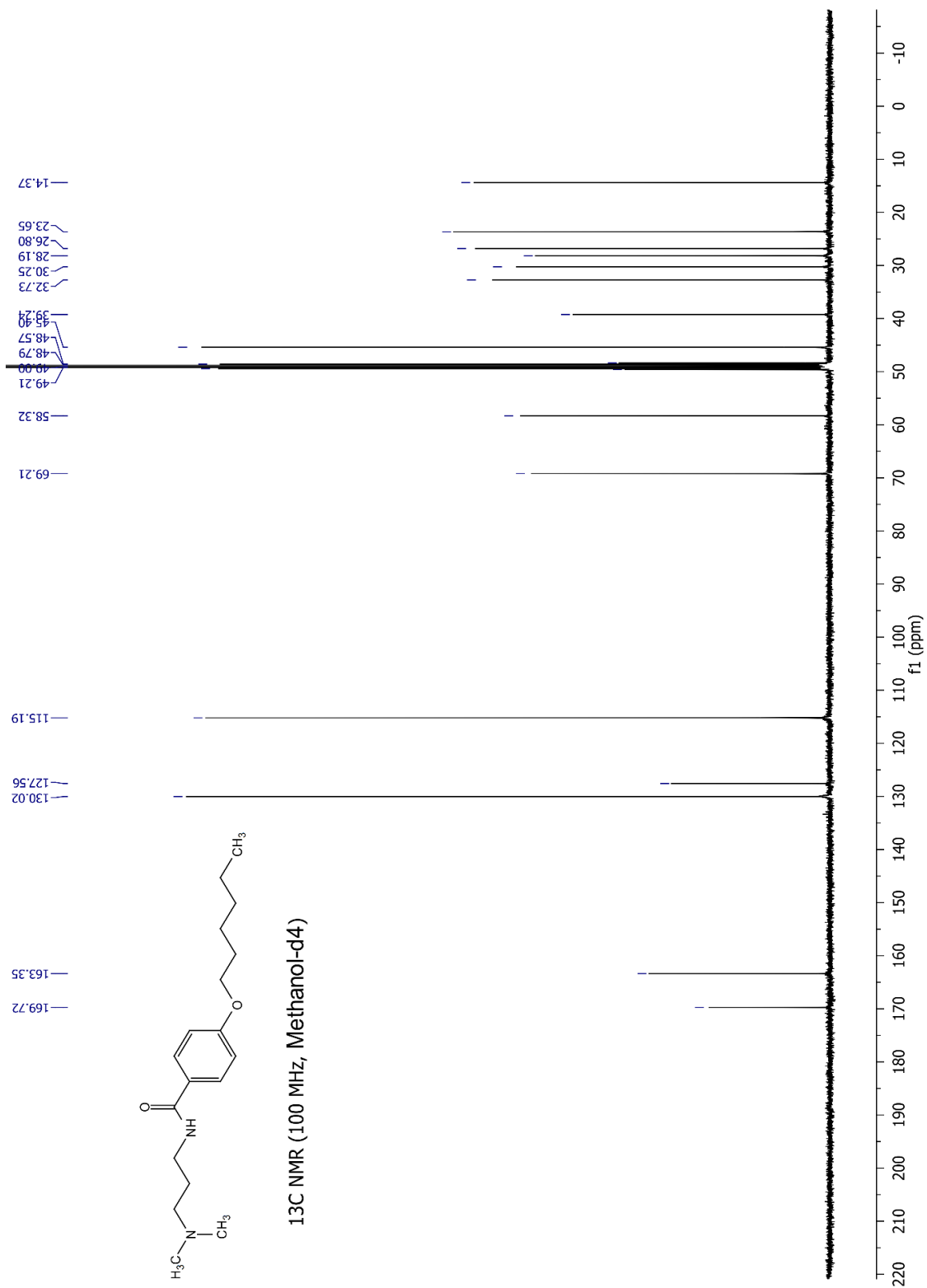
Fig. A 59 ¹H Spectrum of compound 29.

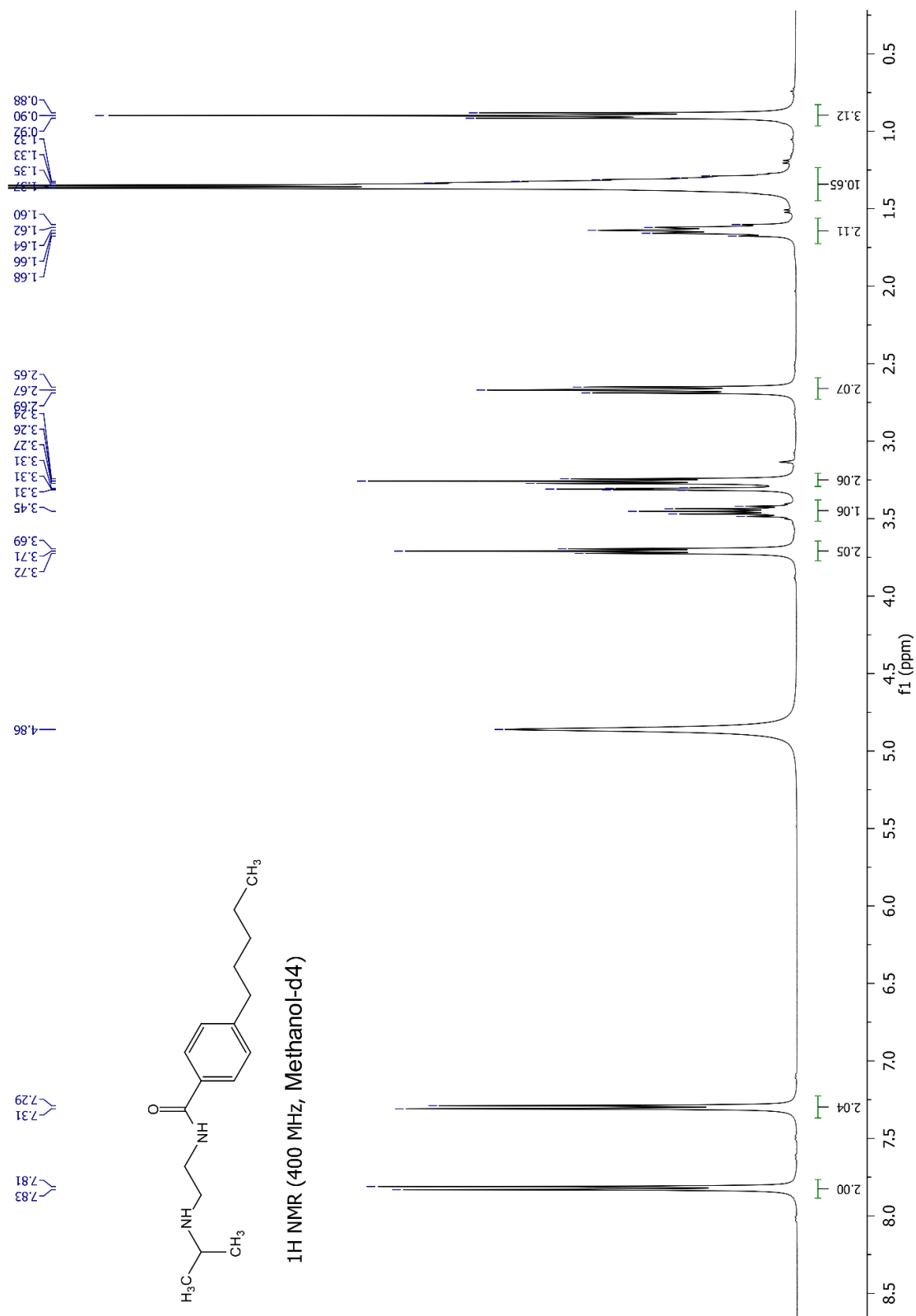
Fig. A 60 ¹³C Spectrum of compound 29.

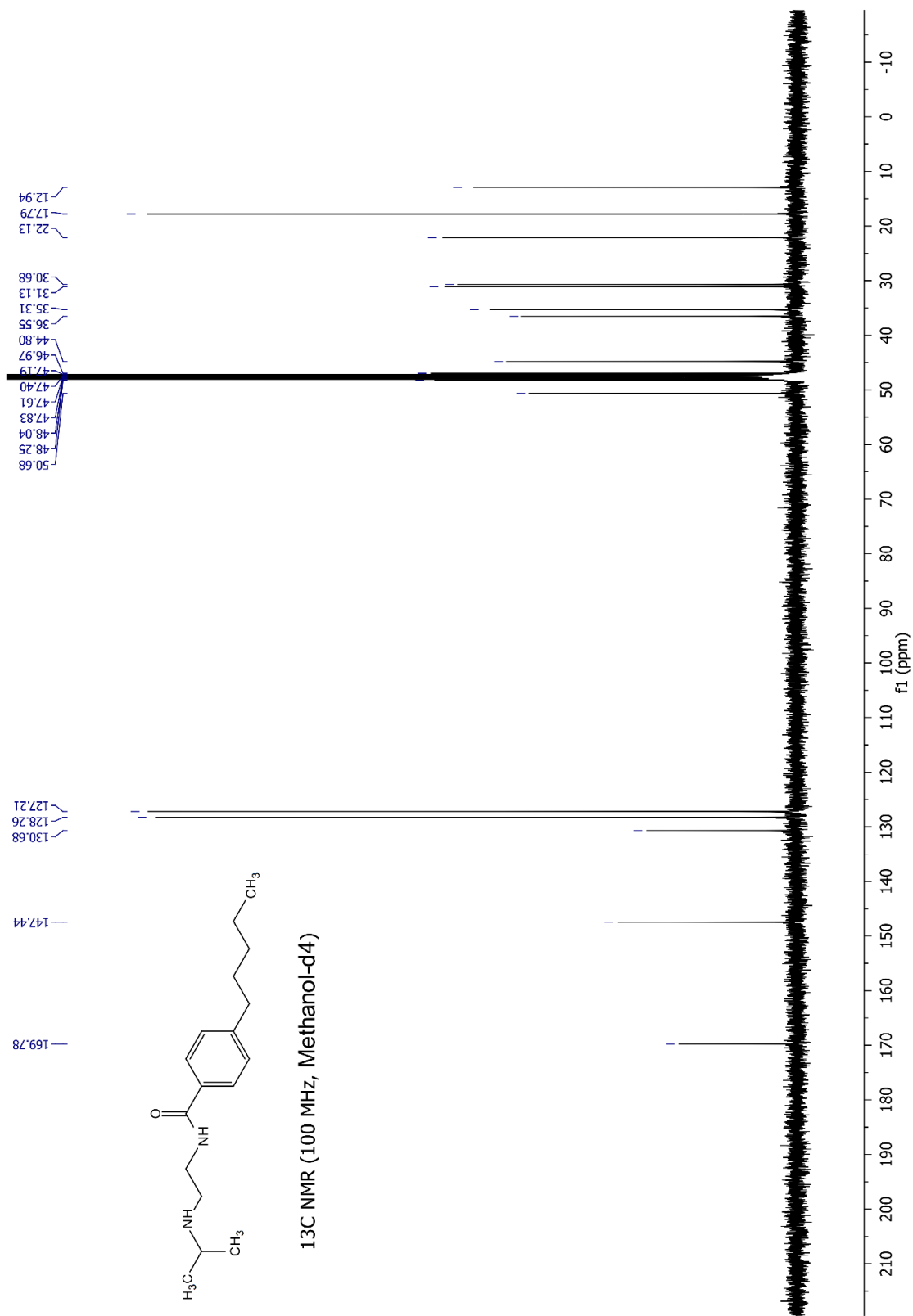
Fig. A 61 ^1H Spectrum of compound 30.

Fig. A 62 ¹³C Spectrum of compound 30.

Fig. A 63 ¹H Spectrum of compound 31.

Fig. A 64 ¹³C Spectrum of compound 31.

Fig. A 65 ¹H Spectrum of compound 32.

Fig. A 66 ¹³C Spectrum of compound 32.

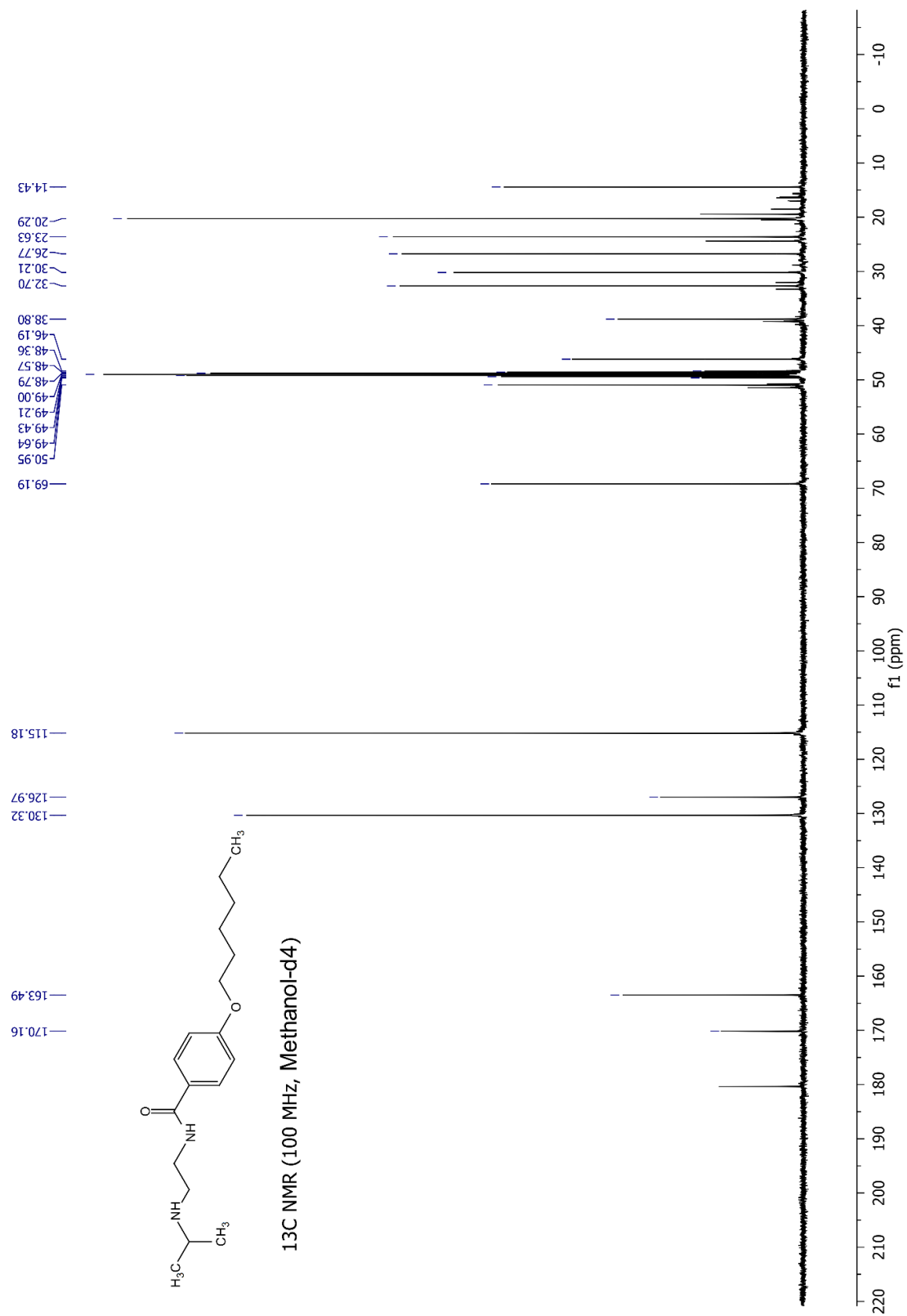
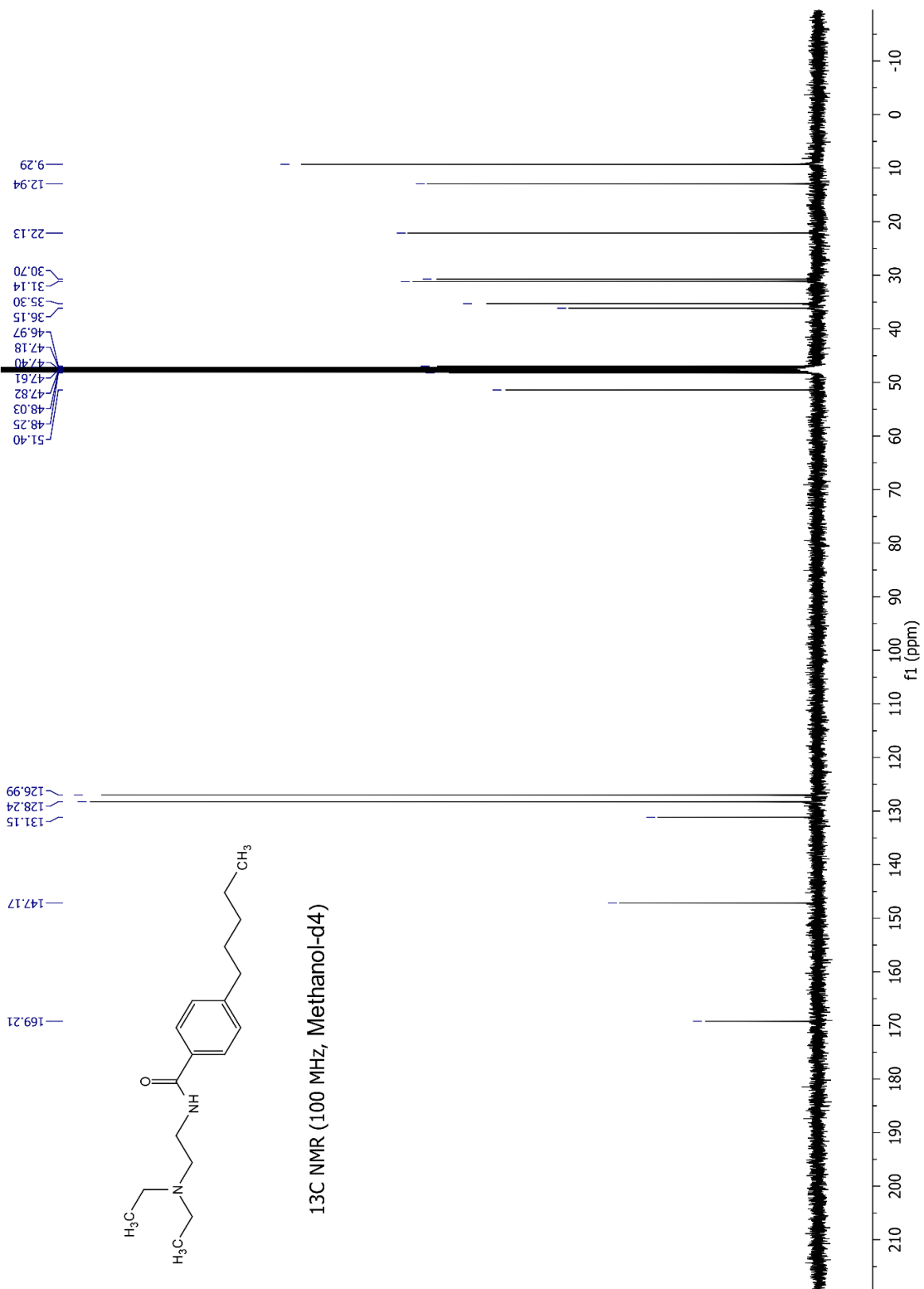
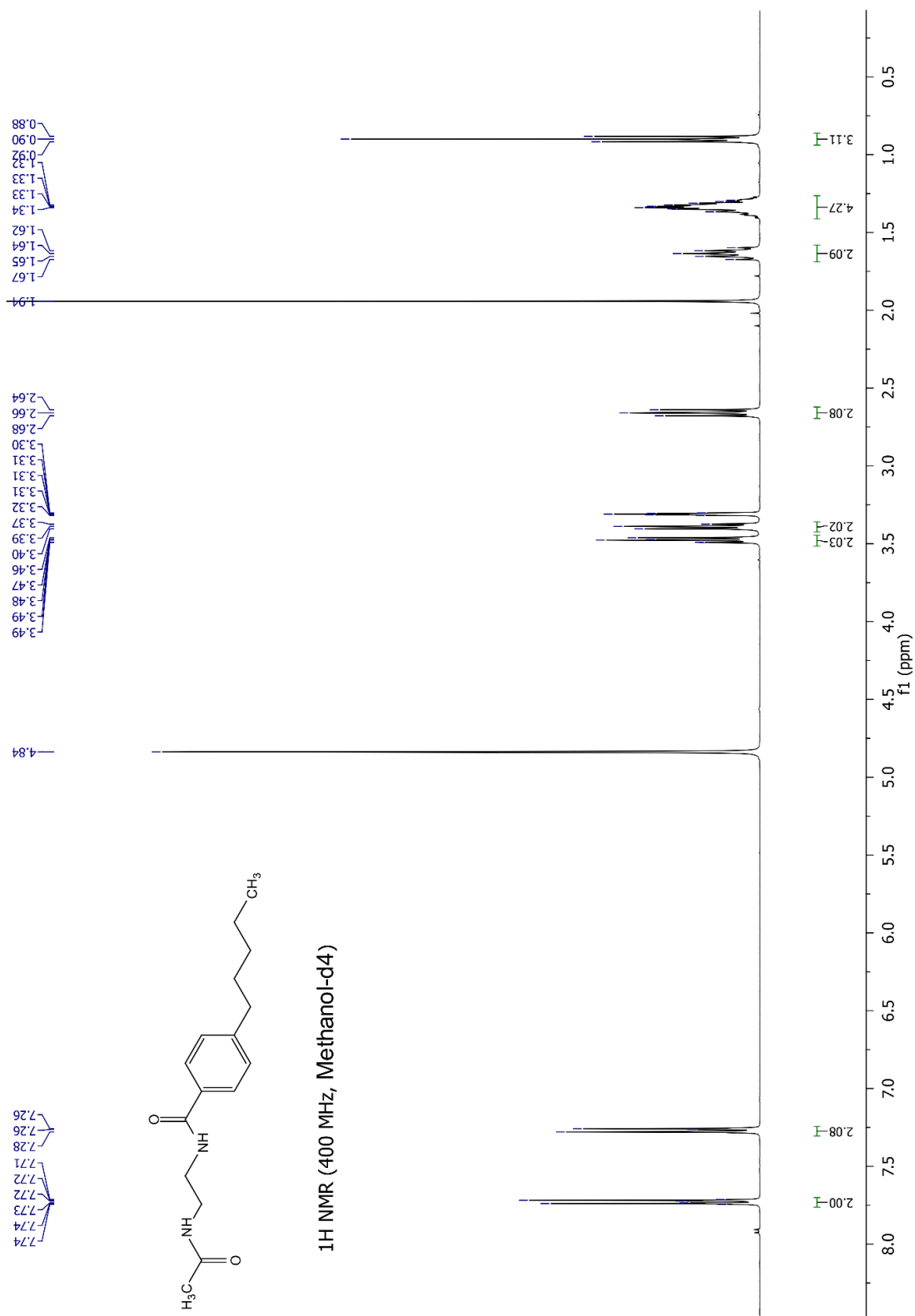
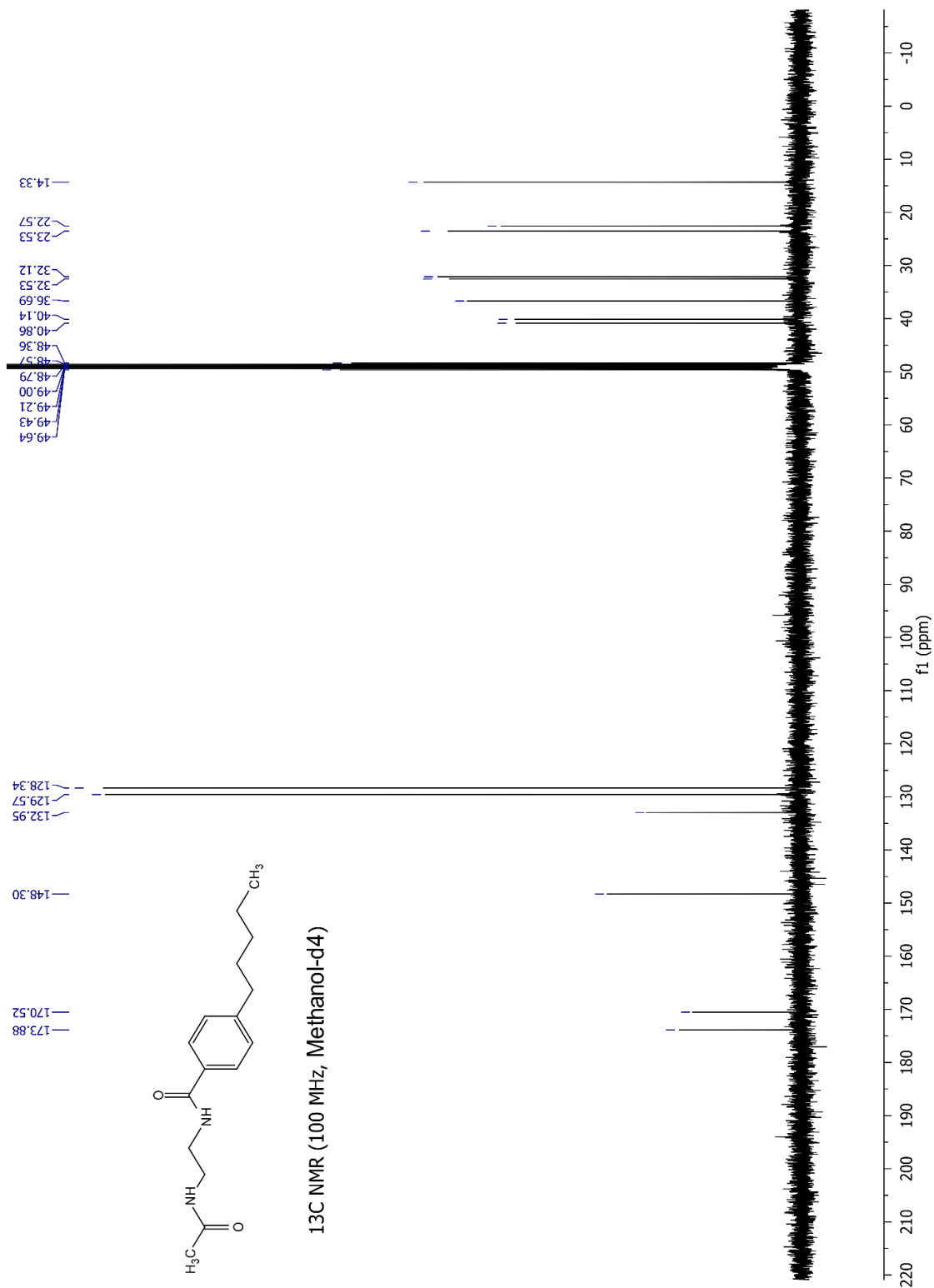
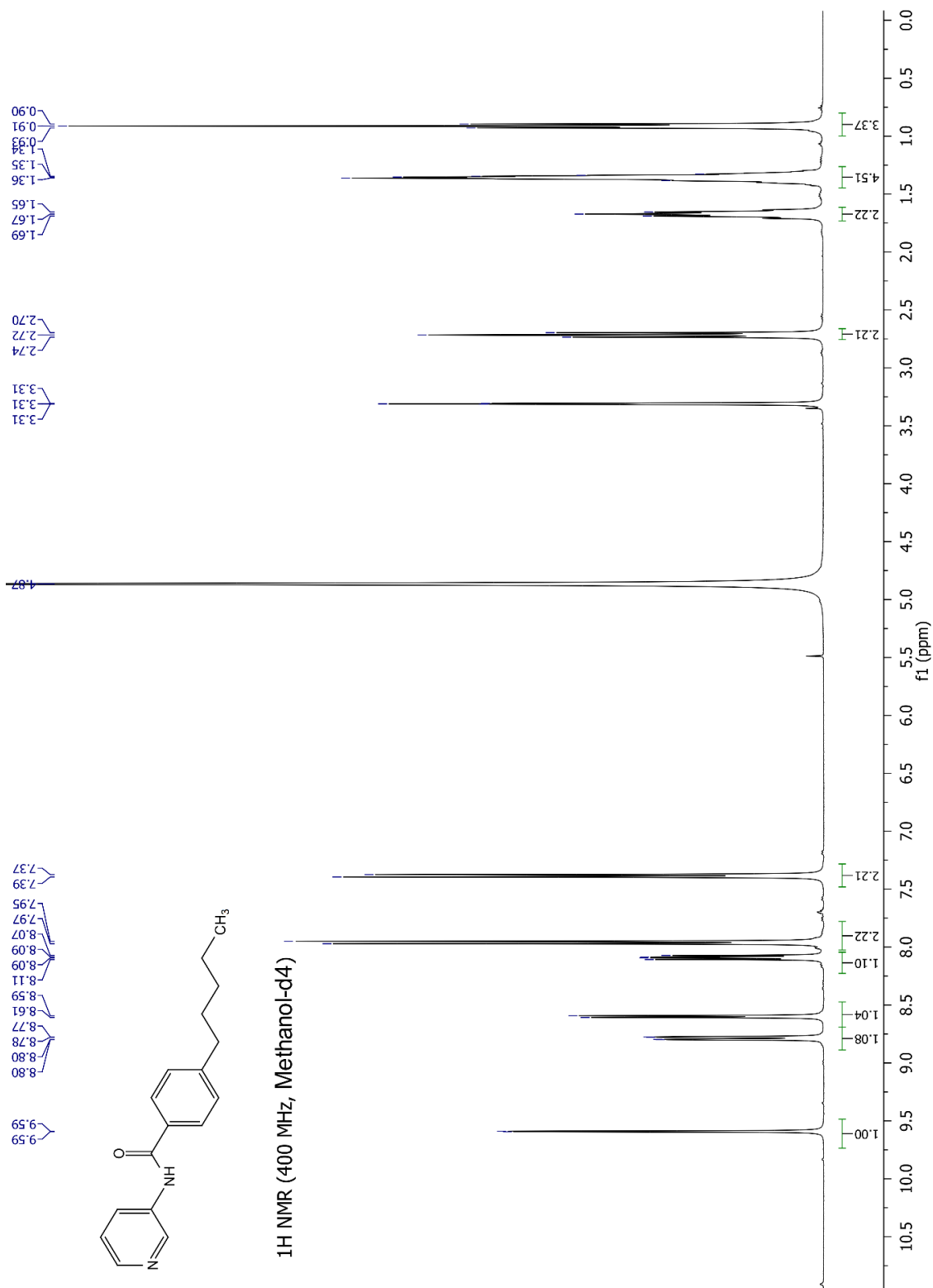


Fig. A 68 ¹³C Spectrum of compound 33.

Fig. A 70 ^{13}C Spectrum of compound 34.

Fig. A 71 ¹H Spectrum of compound 35.

Fig. A 72 ^{13}C Spectrum of compound 35.

Fig. A 73 ¹H Spectrum of compound 36.

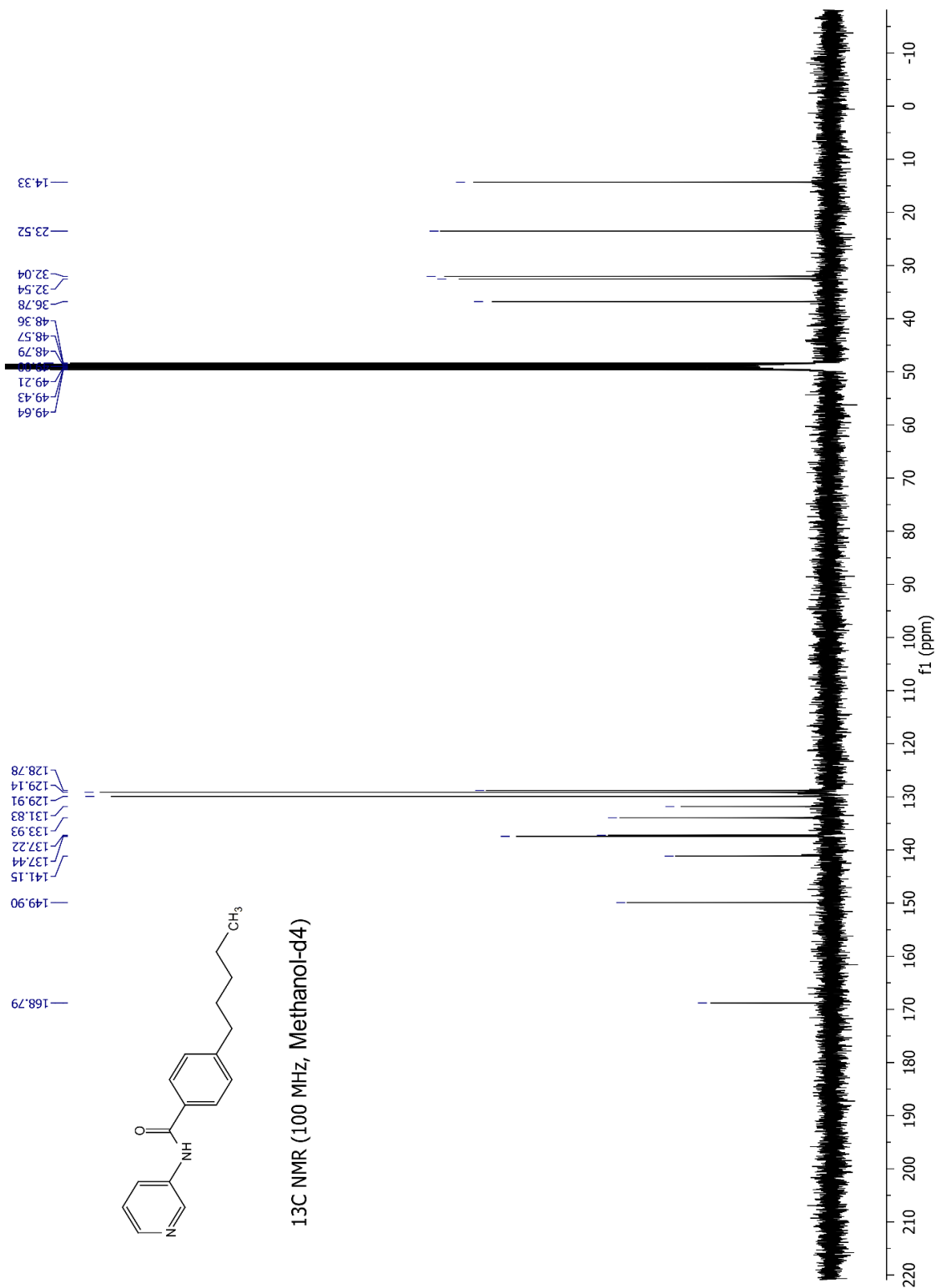
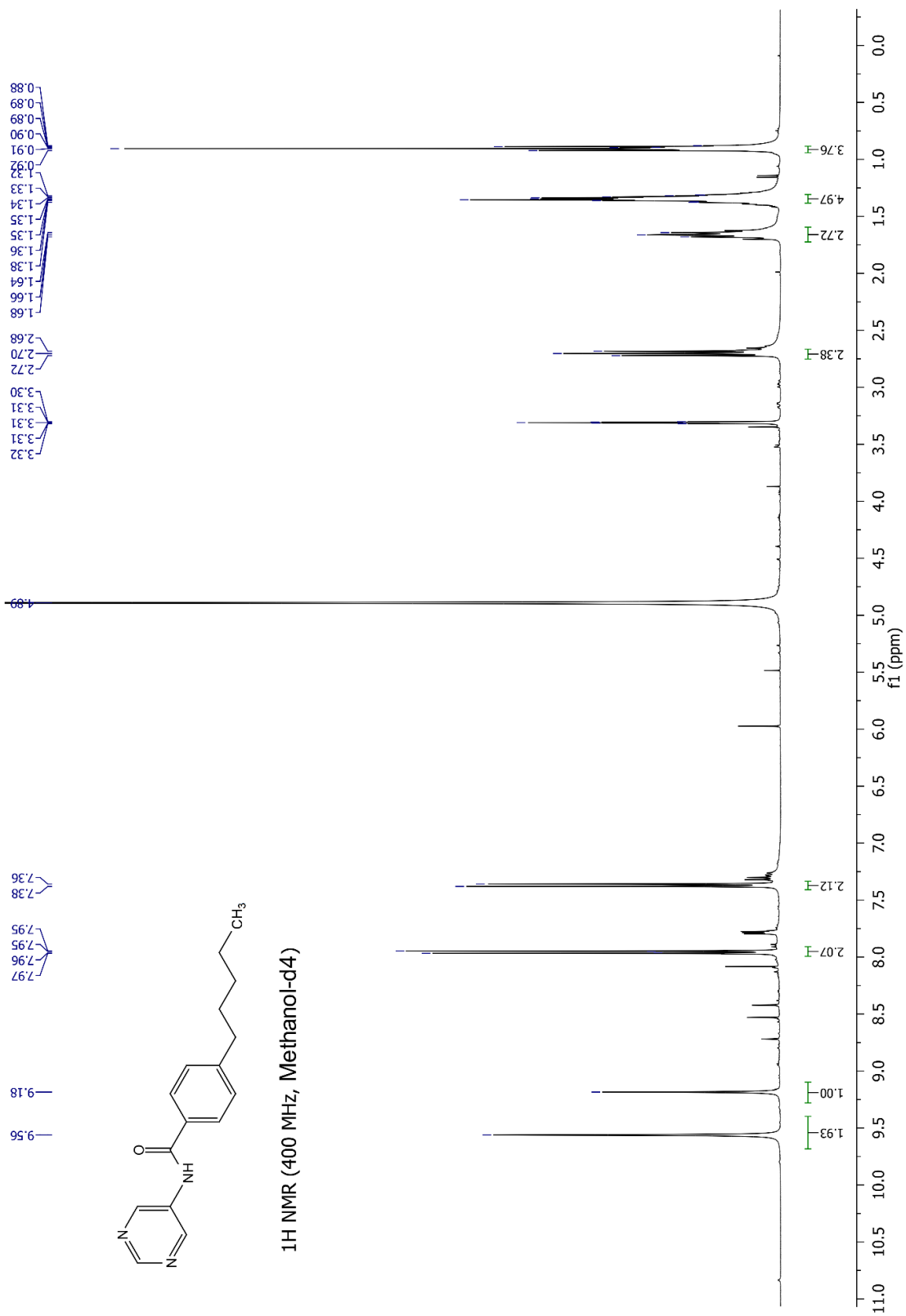
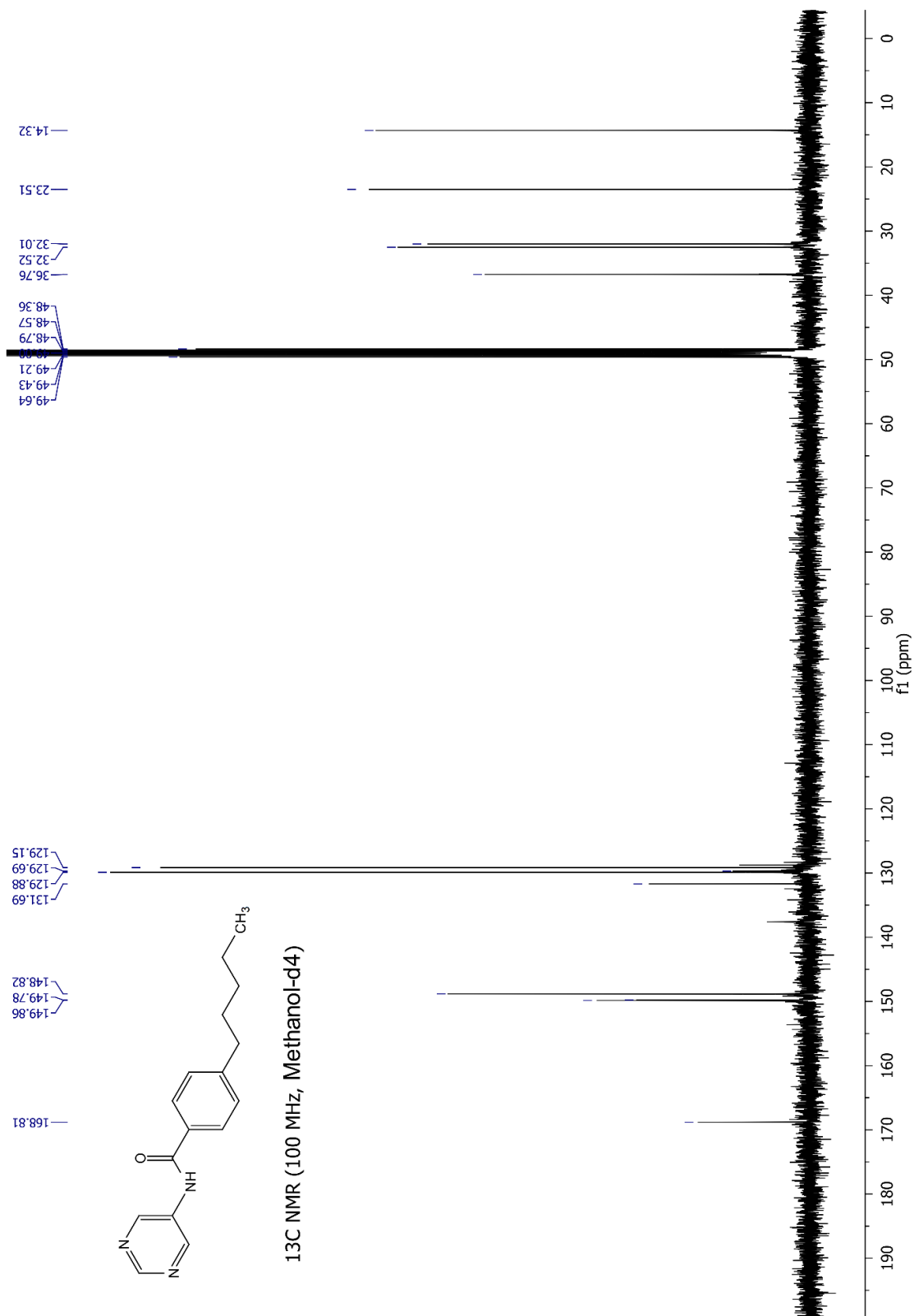
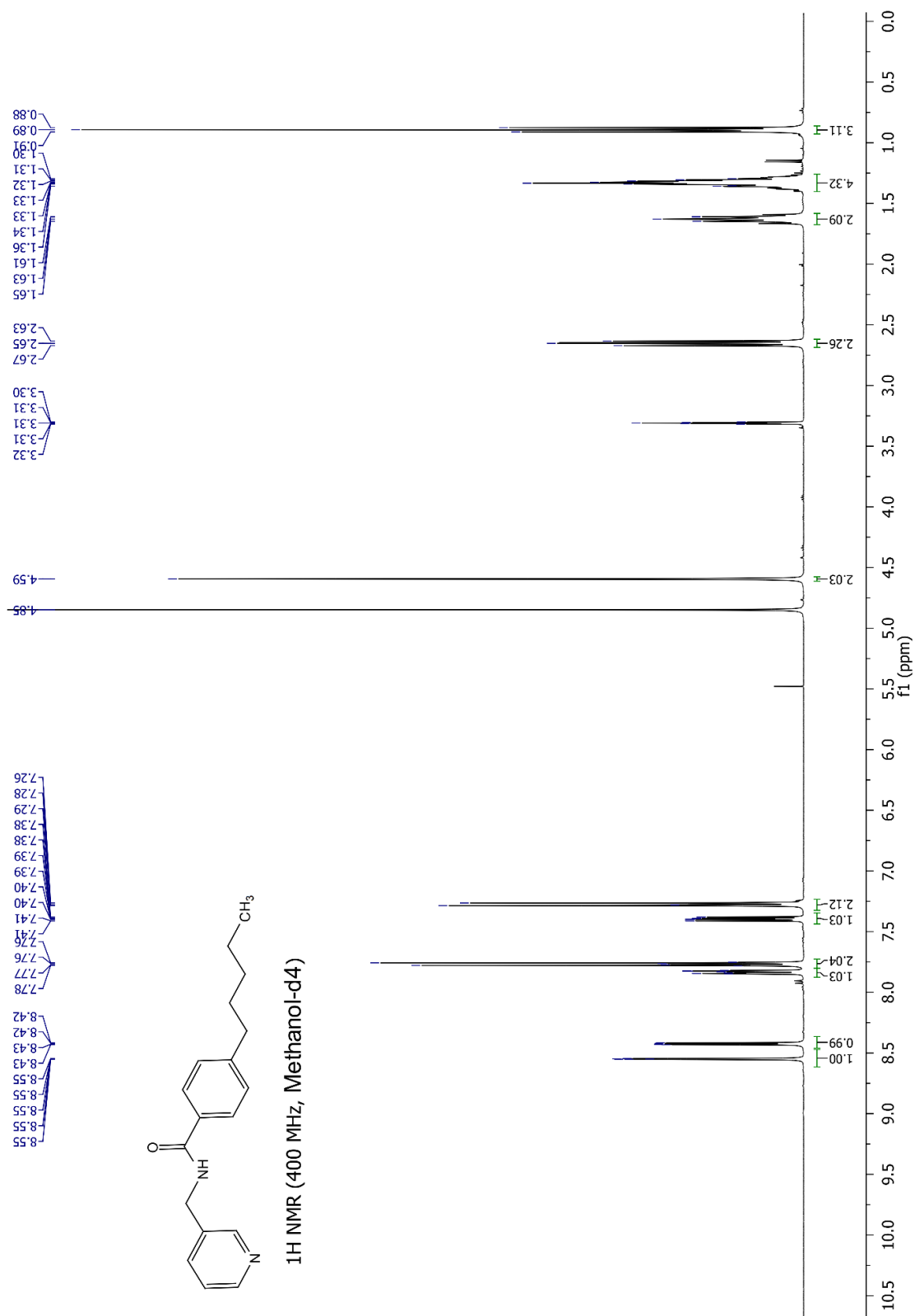
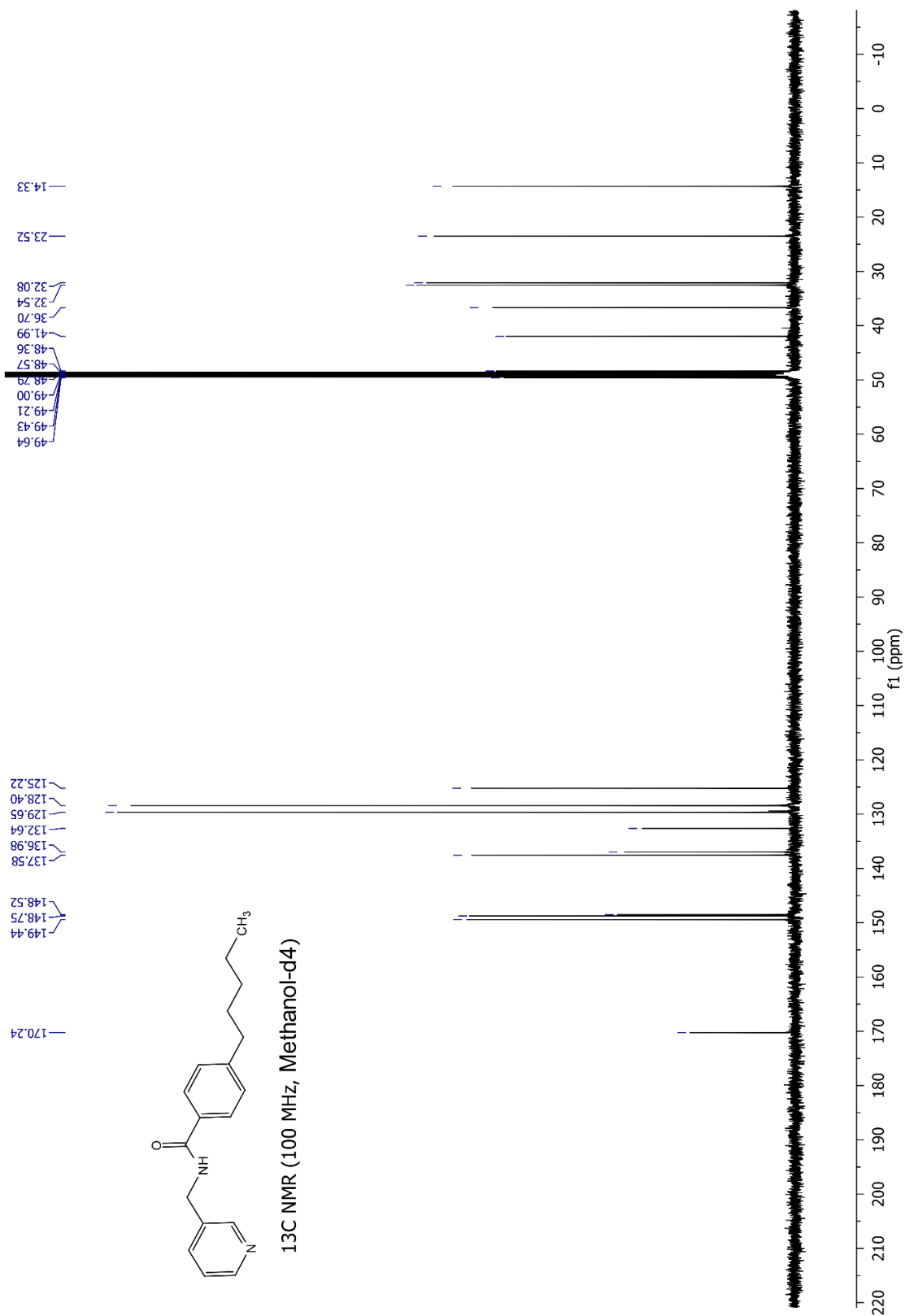


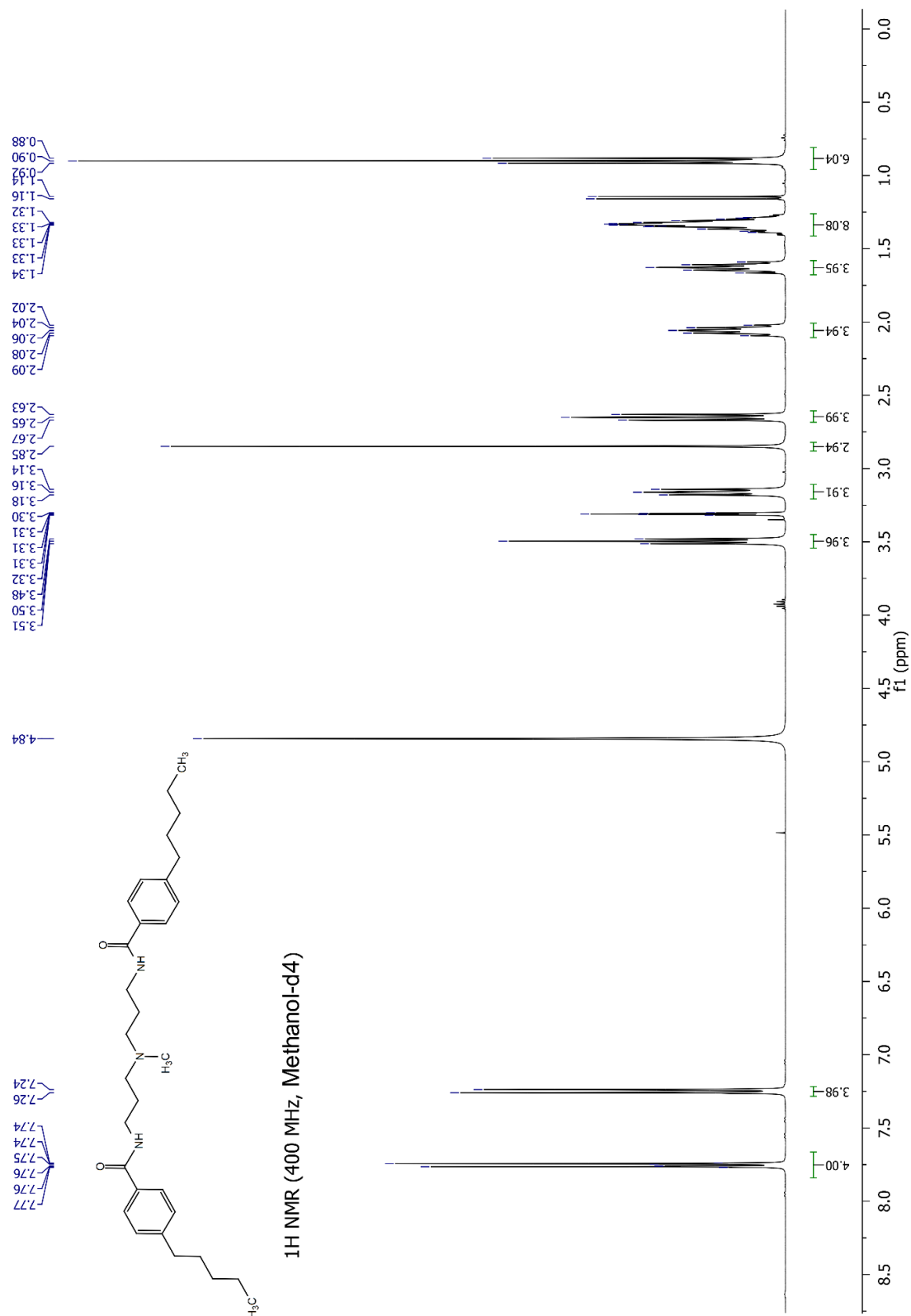
Fig. A 74 ¹³C Spectrum of compound 36.

Fig. A 75 ¹H Spectrum of compound 37.

Fig. A 76 ¹³C Spectrum of compound 37.

Fig. A 77 ¹H Spectrum of compound 38.

Fig. A 78 ^{13}C Spectrum of compound 38.

Fig. A 79 ¹H Spectrum of compound 39.

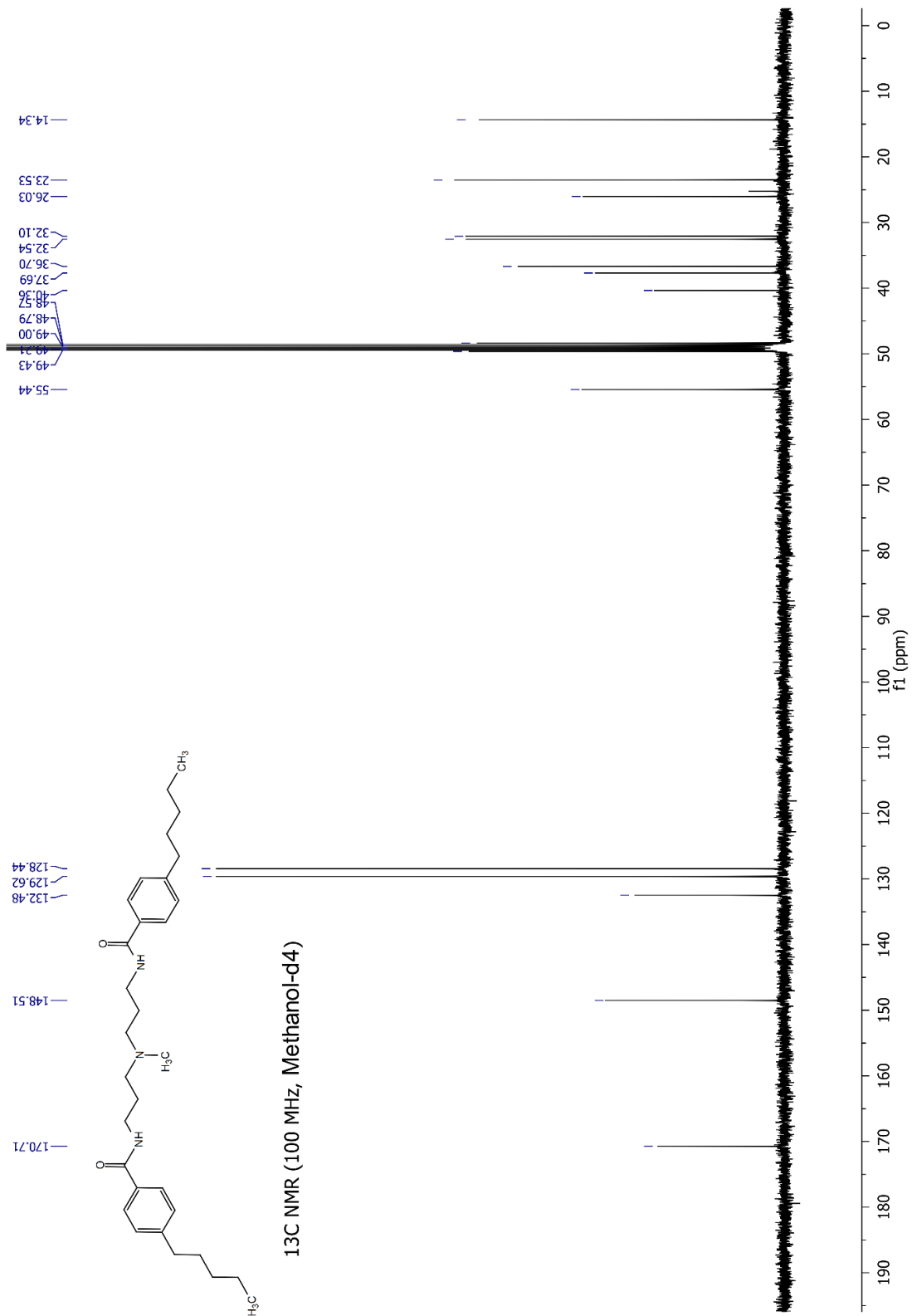
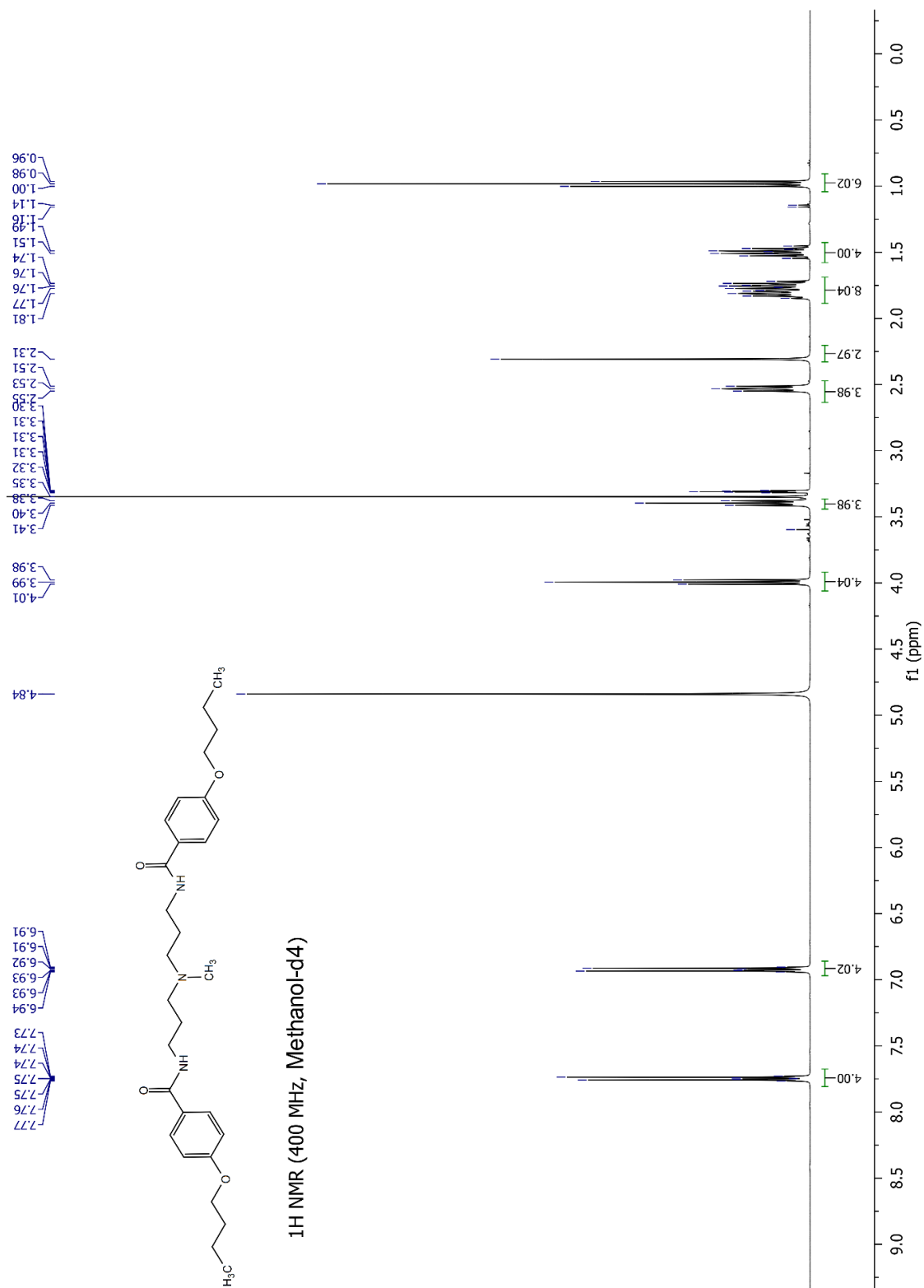
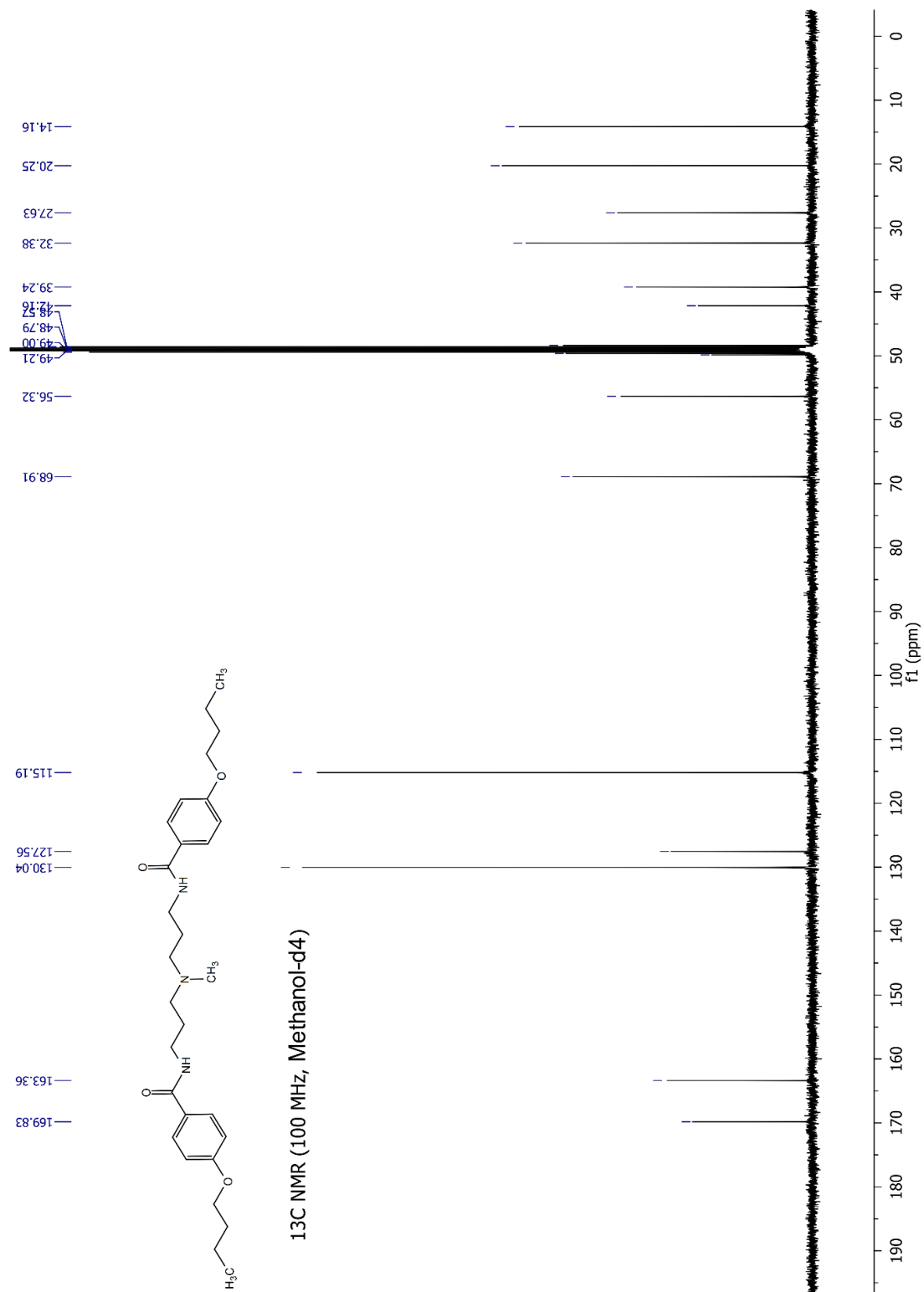
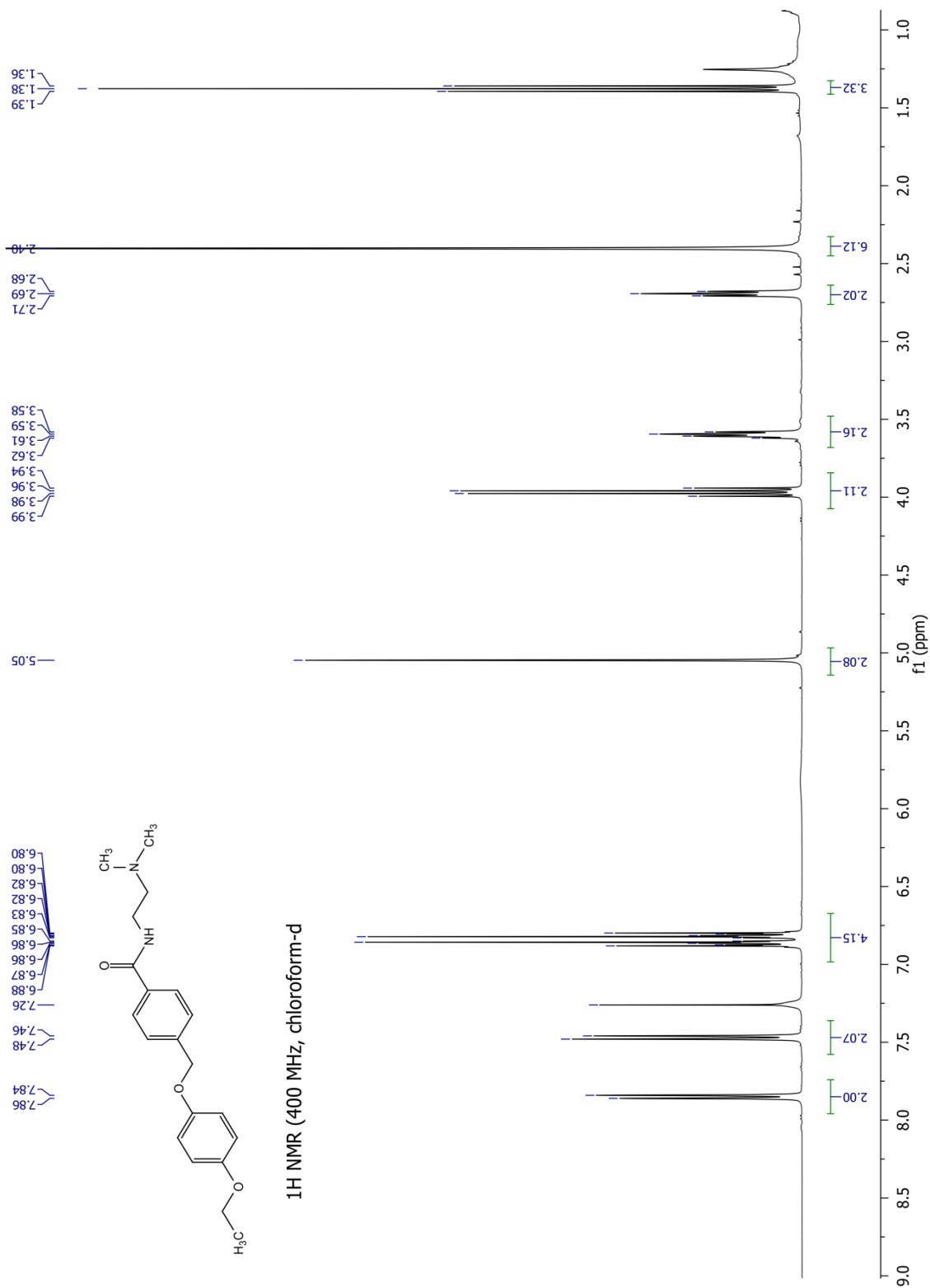
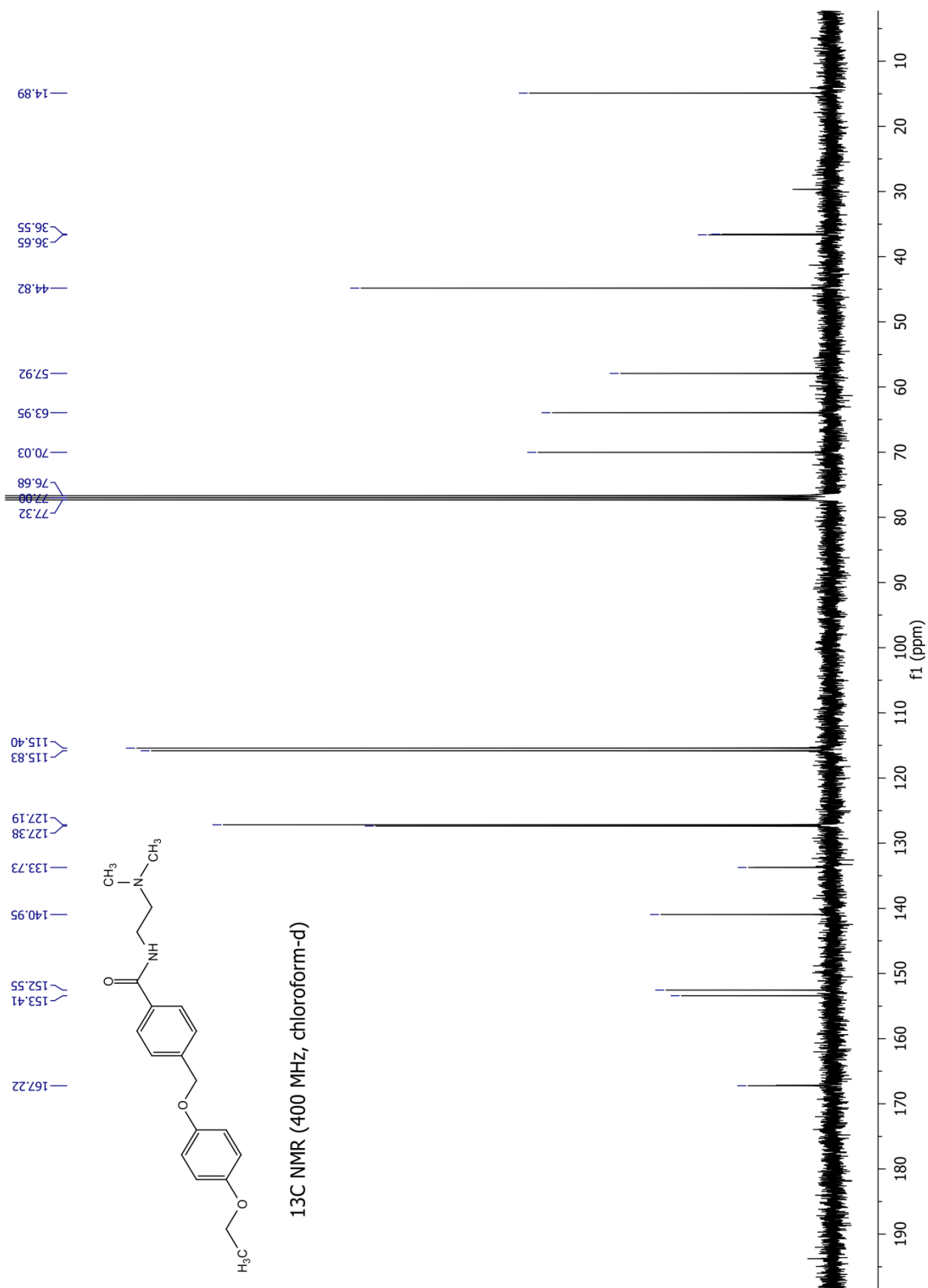


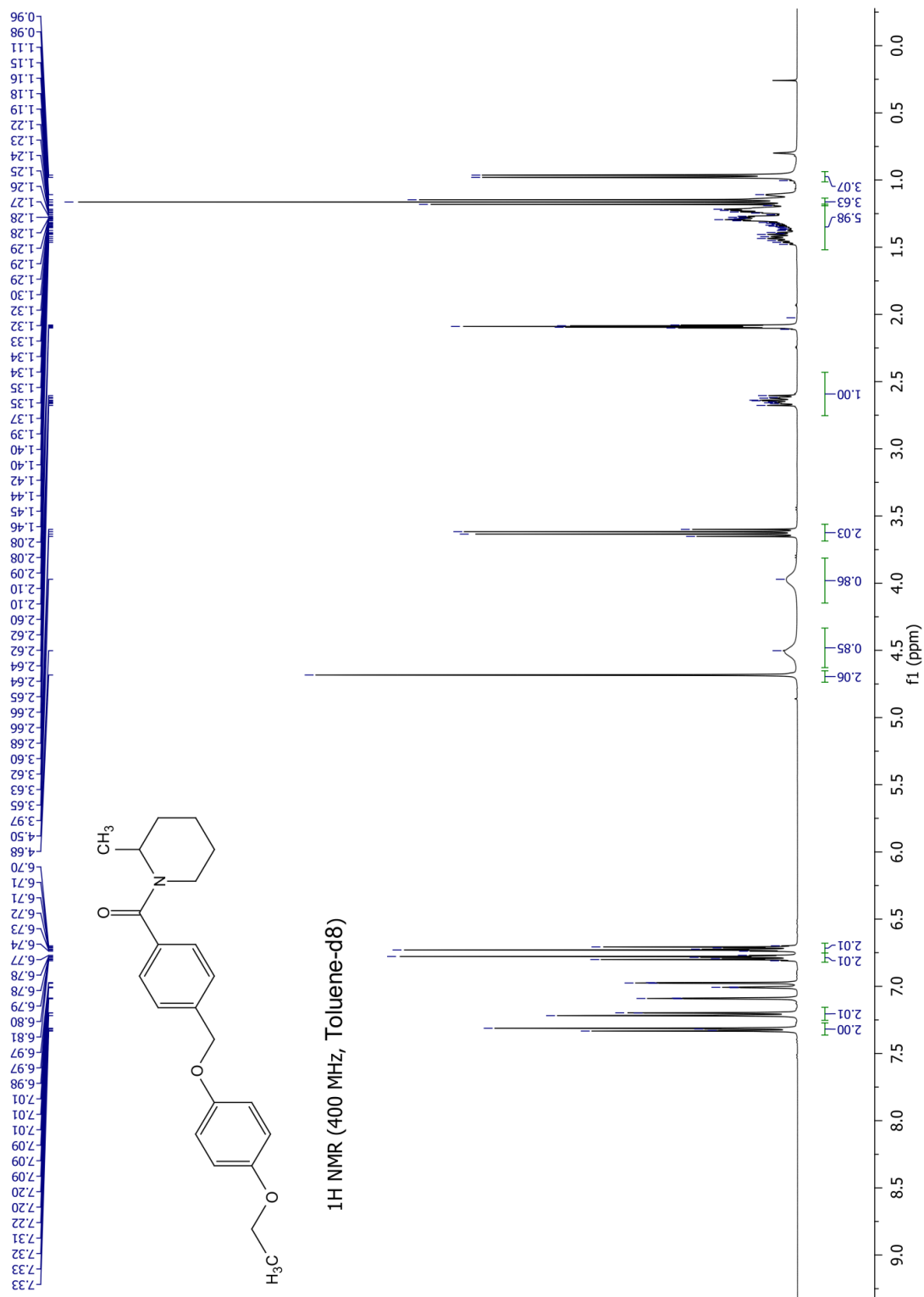
Fig. A 80 ¹³C Spectrum of compound 39.

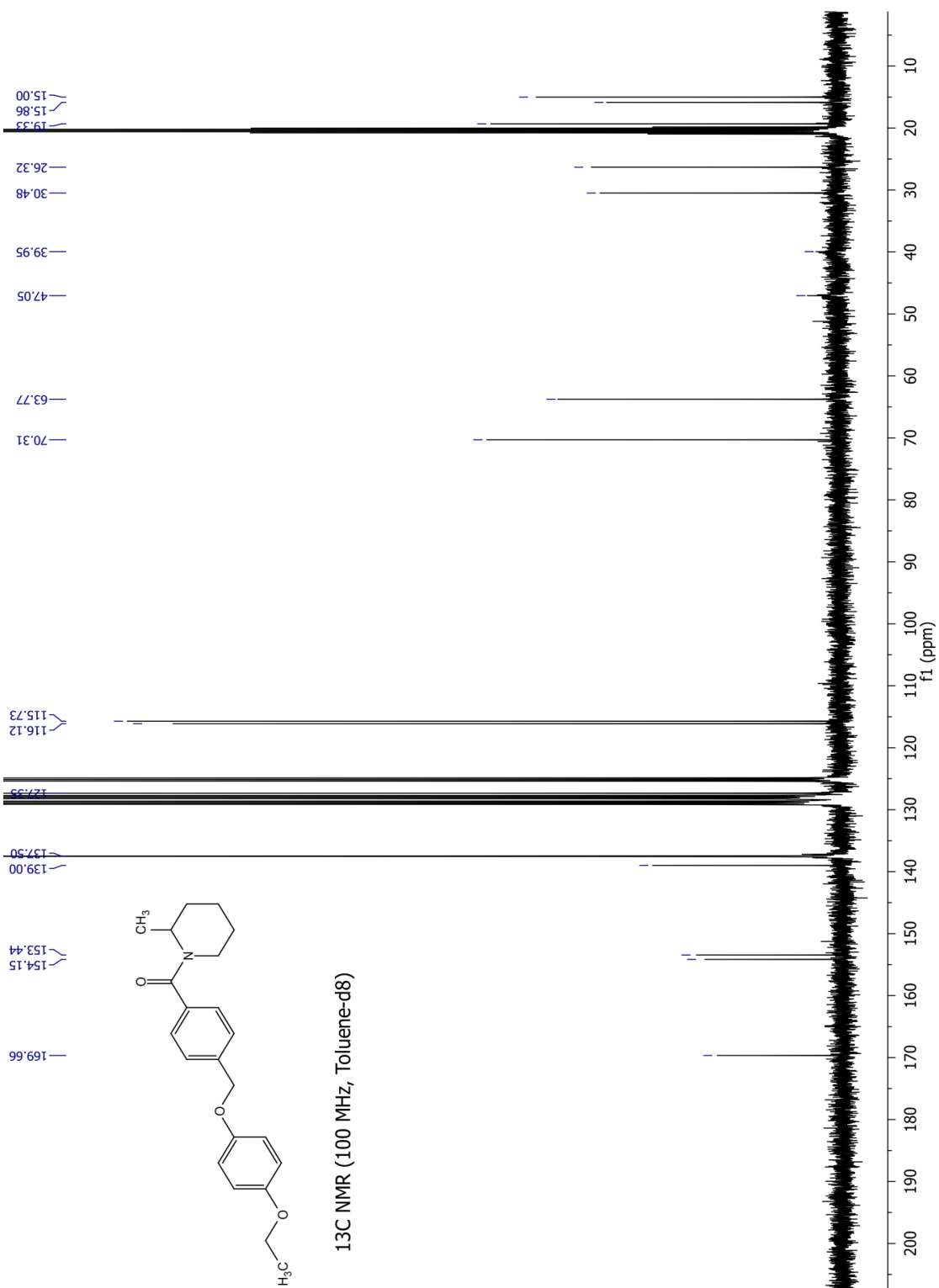
Fig. A 81 ¹H Spectrum of compound 40.

Fig. A 82 ¹³C Spectrum of compound 40.

Fig. A 83 ¹H Spectrum of compound 41.

Fig. A 84 ^{13}C Spectrum of compound 41.

Fig. A 85 ¹H Spectrum of compound 42.

Fig. A 86 ¹³C Spectrum of compound 42.

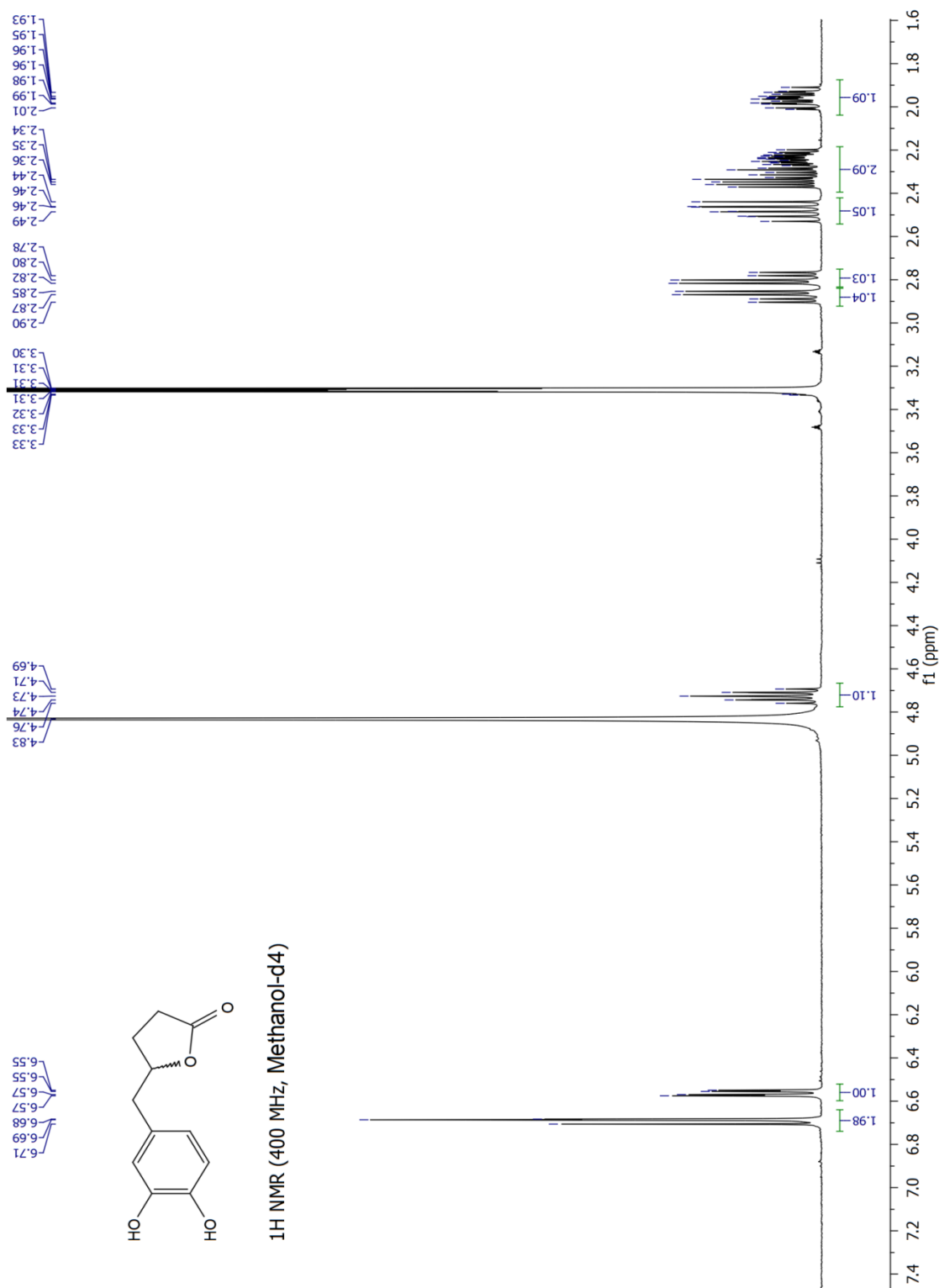


Fig. A 87 ¹H Spectrum of compound M1.

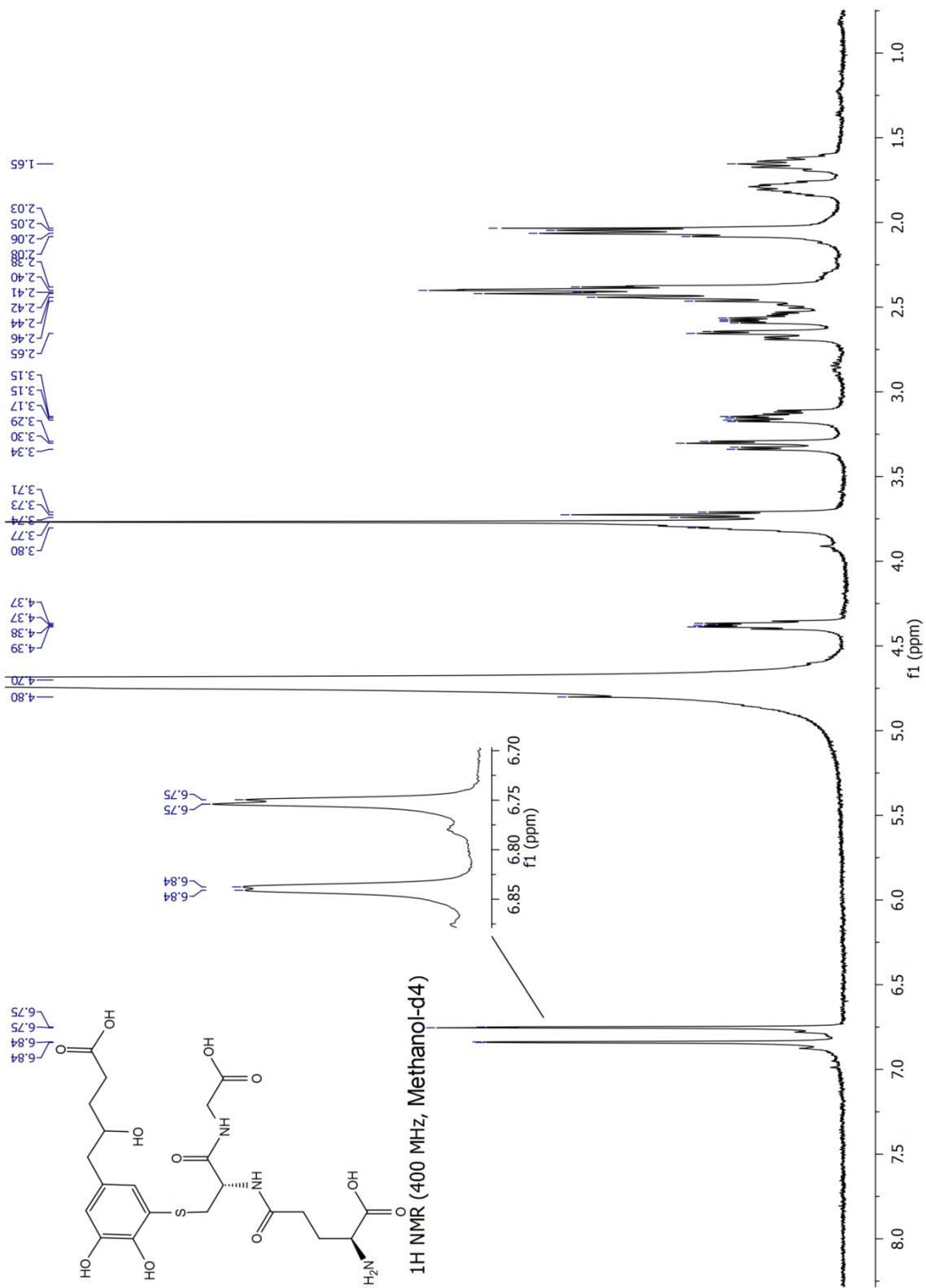


Fig. A 88 ¹H Spectrum of ring-opened lactone M1-GSH-Adduct.

